IntechOpen

Electrodeposition of Composite Materials

Edited by Adel M. A. Mohamed and Teresa D. Golden

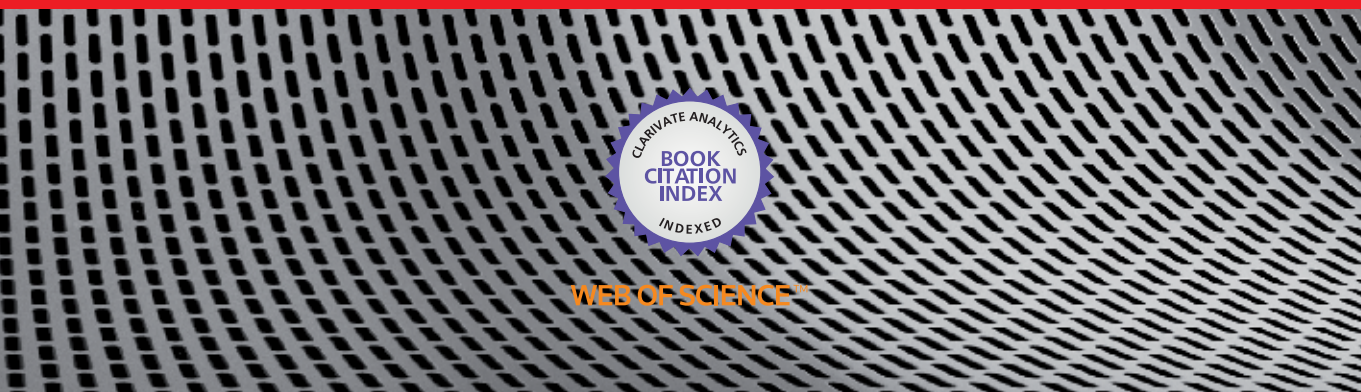

ELECTRODEPOSITION OF COMPOSITE MATERIALS

Edited by **Adel M. A. Mohamed**
and **Teresa D. Golden**

Electrodeposition of Composite Materials
http://dx.doi.org/10.5772/60892
Edited by Adel M. A. Mohamed and Teresa D. Golden

Contributors

Ashutosh Sharma, Siddhartha Das, Karabi Das, Ebru Saraloğlu Güler, Orkut Sancakoğlu, Trejo Gabriel, Mendez Alia, Torres Julieta, Ortega Raúl, Meas Yunny, Manríquez Federico, Martínez Alma, Jose De Jesus Perez-Bueno, Randa Abdel-Karim, Kavian Omar Cooke, W Gao, Yuxin Wang, Patricia Popoola, Nicholus Malatji, Lilian Senna, Thais Rezende, Deborah Cesar, Dalva Lago, A.M.A Mohamed, Casey R Thurber, Teresa Golden Golden, Peter Odetola, Olawale Popoola, David Delport

Notice

First published in Croatia, 2016 by INTECH d.o.o.
eBook (PDF) Published by IN TECH d.o.o.
Place and year of publication of eBook (PDF): Rijeka, 2019.
IntechOpen is the global imprint of IN TECH d.o.o.
Printed in Croatia

Legal deposit, Croatia: National and University Library in Zagreb

Additional hard and PDF copies can be obtained from orders@intechopen.com

Electrodeposition of Composite Materials
Edited by Adel M. A. Mohamed and Teresa D. Golden

p. cm.

ISBN 978-953-51-2270-8

eBook (PDF) ISBN 978-953-51-4205-8

Meet the editors

Dr. Adel M. A. Mohamed holds a Ph.D. degree in metallurgical engineering from Université du Québec à Chicoutimi (UQAC), Quebec, Canada, and MSc and BSc degrees in metallurgical engineering and materials from the Suez Canal University (SCU), Suez, Egypt. He has also completed postdoctoral studies at UQAC. He is working as Associate Professor at Faculty of Petroleum and Mining Engineering, SU, Egypt. He is also working as Research Professor at the University of North Texas (UNT), Texas, USA. His research focuses on the development of light metals for automotive applications and production of ceramic materials and nanotechnology of composite coatings for industrial applications. His accomplishments include around 70 publications in various international journals and conferences, and he has been Editor-in-Chief of a journal, Associate Editor of a journal, and a Reviewer for many international journals.

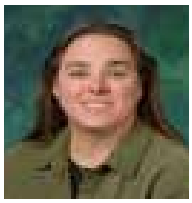

Dr. Teresa D. Golden holds a PhD degree in analytical chemistry from NMSU. She is a Full Professor in the chemistry department at the UNT, Texas. Her research focuses on the electrodeposition of nanomaterials for corrosion protection, deposition of metals and other materials using several techniques, and development of new coating for the oil and gas industry. She has published over 85 peer-reviewed journal articles and chapters.

Contents

Preface

Many books, journal articles, and conference proceedings have been published to address both theoretical and experimental aspects of various surface engineering and coating technologies, but a complete and comprehensive book that is solely devoted to the arts and sciences of *electrodeposition* of nanocomposite coatings that are intended for corrosion and wear applications has been missing. Therefore, this book is composed of 12 chapters written by experts in the field of electrodeposited surface coatings, the contents of which introduce the important basic electrodeposition parameters that affect the properties of composite coatings (e.g., corrosion and tribology).

The book begins with the chapters presenting an overview of the electrochemical methods used to deposit nanocomposites and the effects of the experimental parameters on nanocomposite deposition. The next chapters cover in detail specific nanocomposite coatings, Cu-Ni-nanoclay, and Ni-P/SiC composites, made electrochemically. Then, the following chapters review corrosion protection by nanocomposite coatings. Chapter 10 discusses the tribological performance of nanocomposite coatings. And the last two chapters (Chapters 11 and 12) cover the use of nanocomposites in specific technological areas (fuel cells and microelectronics).

This book is suitable for professional electrochemists, advanced undergraduate and postgraduate students, and also for electrodeposition specialists with a physical, technical, or chemical education. It can also be useful for engineers and specialists engaged in research on new electrodeposition technologies related to metallic objects. The scientific interest in this book is evident for many important centers of the research, laboratories and universities, as well as industry. Therefore, it is hoped this book will inspire and enthuse others to undertake research in the field of tribology and corrosion protection for nanocomposite surface coatings.

The Editor acknowledges InTech for this opportunity and for their enthusiastic and professional support. Finally, the editors thank the authors of each chapter for their availability for this work and also acknowledge the support of their respective institutions.

Adel M. A. Mohamed
Department of Metallurgical and Materials Engineering,
Faculty of Petroleum and Mining Engineering,
Suez University, Egypt

Center for Advanced Materials,
Qatar University, Doha, Qatar

Teresa D. Golden
Department of Chemistry,
University of North Texas, Denton,
Texas, USA

Chapter 1

Electrochemical Synthesis of Nanocomposites

Randa Abdel-Karim

Additional information is available at the end of the chapter

http://dx.doi.org/10.5772/62189

Abstract

This chapter presents an overview of research efforts focused on both fabrication and properties of nanocomposites prepared by electrodeposition. The nanoparticles can improve the base material in terms of wear resistance, damping properties, and mechanical strength as well as electrical properties. Different kinds of matrix, such as metals, polymers, and ceramic matrix, have been employed for the production of composites reinforced by nano-ceramic particles such as carbides, nitrides, and oxides as well as carbon nanotubes. Theoretical aspects and mechanisms related to the electrodeposition process of nanocomposite films, from aqueous solutions, are discussed.

Keywords: Nano-structured coatings, Electrocodeposition, Theoretical models, Characterization techniques, Applications

1. Introduction

Materials are considered nanosized when one of the components dimensions are in the nanometer scale, with typical dimensions smaller than 100 nm. Nanocomposites are composites in which one or more of the phases has dimensions in the nanoscale [1].

Nanocomposites are commonly known as materials consisting of two or more dissimilar materials with well-defined interfaces. Generally, one material forms a continuous matrix while the other provides the reinforcement [2].

They are reported to be the materials of 21st century in the view of possessing design uniqueness and property combinations that are not found in conventional composites. The general understanding of these properties is yet to be reached, even though the first inference on them was reported as early as 1992 [3]. Various techniques have been considered to prepare nanocomposite materials including thermal, plasma spraying and physical and chemical vapour deposition. Among these methods that is widely used, electrodeposition (ECD)), which offers several advantages when compared with other techniques [4]. Electrodeposition offers a lot of advantages over other surface modification techniques:

- Capability of manufacturing nanostructured multi-component films.
- High purity of deposited materials.
- Applicable to substrates of complex shape.
- Can be used for deposition of ceramics, glasses, polymers, composites.
- Rigid control of the composition and microstructure of deposit.
- Low cost of equipment and materials.
- Easy to be scaled up to industry level.
- This process avoids the problems associated with high temperature and high pressure processing.
- Reduction of waste often encountered in dipping or spraying techniques [5, 6].

Research into the preparation of nanocomposite coatings, by electrochemically co- deposition of fine particles with metal from electrolytic solutions, has been investigated by numerous authors [7-12].

As in the case of micro-composites, nanocomposite materials can be classified, according to their matrix materials, in three different categories;

- Metal Matrix Nanocomposites (MMNC) such as Cr/Al_2O_3 [13], Ni/Al_2O_3 [14], Co-TiO_2 [15], Zn-Ni/ TiO_2 [16], Al/CNT [17], Mg/CNT [18].
- Ceramic Matrix Nanocomposites (CMNC); such as Al_2O_3/ZrO_2 [19], ceramic/CNT [20],
- Polymer Matrix Nanocomposites (PMNC), such as Thermoplastic/thermoset polymer/ layered silicates [21], polyester/ Fe_2O_3 [22], polyester/TiO_2 [23].

Nanocomposite materials have been extensively investigated in bulk and thin film forms because of their wide range of applications, starting from traditional industries, such as general mechanics and automobiles, paper mills, textiles, and food industries, to high- technology industries, such as microelectronics and magnetoelectronics [24]. In addition, the applications of nanocomposite coatings include wear and abrasion-resistant surfaces, lubrication, high hardness tools, dispersion-strengthened alloys, and protection against oxidation and hot corrosion. It has been also used to produce high surface area cathodes that have been used as electro catalysts for hydrogen electrodes in industrial water electrolysis [25, 26].

2. Theoretical models of composites electrodeposition

2.1. Models neglecting the hydrodynamics of fluids

In 1972 Guglielmi [27] proposed the first mechanism on electrocodeposition of inert particles in the metal matrix, and later this mechanism has been adopted by various authors. The model proposed by Guglielmi does not consider mass transfer.

According to this mechanism the process involves a two-step mechanism, as follows;

- In the in the first step, when the particles approach the cathode they become weakly adsorbed at the cathode surface by Van der Waals forces.
- In the second step, particles are adsorbed strongly on the cathode surface by Coulomb forces and consequently are incorporated into the growing metal matrix.

The loose adsorption coverage, a ratio of the area covered by loosely adsorbed particles to the total electrode area, was expressed in terms of the concentration of suspended particles using the classical Langmuir adsorption isotherm. For the strong adsorption rate, the volume of particles strongly adsorbed was given by a Tafel-type exponential relationship at high over potentials that depended on kinetic constants. The volume of metal electrodeposited was obtained by Faraday's law. Thus, the volume fraction of incorporated particles was then formulated as a function of the bulk concentration and the electrode over potential. From this model the volume fraction of incorporated particles, α', can be mathematically expressed by:

$$\frac{\alpha'}{1-\alpha'} = \frac{zF\rho_m V_0}{M_m i_0} e^{(B-A)} \frac{KC_{P,b}}{1+KC_{p,b}} \tag{1}$$

where M_m is the atomic weight, ρ_m is and the density of electrodeposited metal respectively, i_0 the exchanging current density, z the valence of the electrodeposited metal, F the Faraday constant, η the electrode reaction over potential, $C_{p,b}$ the particle concentration in the bulk electrolyte. *k* is the Langmuir isotherm constant, which is mainly determined by the intensity of interaction between particles and cathode. The parameters V_0 and B are related to particle deposition, and they play a symmetrical role with the parameters. In addition, i_0 and A are related to metal deposition.

In 1987, in order to overcome the shortcoming in the Guglielmi's model Celis et al. [28] proposed another model. The model consists of five consecutive steps:

- The particles are surrounded by ionic clouds;
- Convection towards the cathode surface;
- Diffusion through the hydrodynamic boundary layer;
- Diffusion through the concentration boundary layer;
- Adsorption of particles at the cathode and particles are entrapped within the metal deposit by the reduction of the ionic cloud.

In Celis model, an equation relating weight of particle (W_p), with the weight increase per unit time and surface area (ΔW_p) due to particle incorporation. The weight fraction of particles embedded in percentage is;

$$\frac{\Delta W_p}{\Delta W_m + \Delta W_p} x100 \tag{2}$$

One of the limitations of this model is that the data needed for probability coefficient are not available [29].

In 1995, a theoretical model was proposed by Fransaer et al. [30] to describe the variations in the flow of current to disk electrodes caused by a finite number of spherical and probate particles. They developed a boundary collocation method to calculate the resistance variations and the influence on current in the presence of particles and in their absence. The increase in resistance to the flow of particles was measured as a function of the diameter of the particle. The resistance is increased by larger particles to a greater degree than smaller particles. The primary current distribution around a particle was plotted as a function of the aspect ratio of the particle. The position of the particle was also determined, from its influence on the current as it flows past the electrode.

2.2. Models including the hydrodynamics of fluids

In 1974 Foster and Kariapper et al. [31] performed adsorption studies on composite coatings. They proposed that if the particles in suspension acquire a positive surface charge, they could be incorporated into the metal film by electrostatic attraction. Their model is based on the following expression;

$$\frac{dVp}{dt} = \frac{N^* hC_v}{1 + hC_v} \tag{3}$$

where Vp is the volume fraction of the particles in the deposit, N* is the number of collisions of particles suitable for the co-deposition per second and C_v is volume percent of particles in the plating bath (%).

The parameter h was related to several parameters given by the following expression;

$$h = h^* \left(q\Delta E + L i^2 - ab \right) \tag{4}$$

where h* is a constant, q is the charge density on a particle, ΔE is the potential field at the cathode, I is the current density, L is the bond strength of the metal/particle per surface area, a is related to the shape and b depends on agitation.

In 1987, Valdes et al [32] reported a model for co-deposition on a rotating ring disk electrode (RRDE). The equation of continuity based on differential mass balance was chosen as a starting point where different mass transport processes (Brownian diffusion and convection) for particles have been considered. According to this model, the electrochemical rate of particle deposition can be written as;

$$r_p = K^0 (C_S^p) n \left[\exp\left(\frac{\alpha ZF}{RT} \right) \eta_a - \exp\left(\frac{1 - \alpha ZF}{RT} \right) \eta_a \right] \tag{5}$$

http://dx.doi.org/10.5772/62189

Where K^0 is an electrochemical rate constant which depends on C_S^P, the concentration of electroactive species (metal cations) adsorbed on the surface of the particels, n is valance and η_a is the activation overpotential.

In 1992, Fransaer et al. [33] proposed a trajectory model suggested for particle co-deposition on a rotating disk electrode (RDE). This particle is based on particles larger than 1 micrometer in size. In this model, Navier-Stocks equation for RDE was resolved by using Taylor expansion. The velocity of the particle that can reach towards the cathode is;

$$\frac{dz_p}{dt} = a_p^2 v_{stag} \frac{F_{stagn}^{'}}{F^{'}} - \frac{F_{ext}}{6\pi a_p F^{'}} \tag{6}$$

Where F_{ext} is the external force at any instant along the particle, $F_{stagn}^{'}$ is the force propelling the particle towards the electrode, $F^{'}$ is the resistance force felt by the particle while it is moving perpendicular towards electrode, a_p is the particle radius.

In 2000, according to the model of Vereecken et al. [34], the particles kinetics and residence time at the electrode surface have been considered. Convective-diffusion controls the transport of particles to the surface. The influence of particle gravitational force and hydrodynamics is accounted for various current densities. It is valid only when the particle size is smaller than the diffusion layer thickness. In their model they used Fick's first law and diffusion layer thickness. By combining both they got;

$$J_p = -1.554 v^{-\frac{1}{6}} D_p^{2/3} \left(C_{P,b} - C_{P,s}\right) w^{\frac{1}{2}} \tag{7}$$

where $C_{P,s}$, is the particle concentration at the surface, $C_{P,b}$ is particle concentration in the bulk, D_p is the diffusion coefficient, ν is the kinematic viscosity of the solution and ω is the rotation speed of the electrode.

The ratio of the number of moles of particles to the number of moles of metal atoms equals the ratio of their fluxes J_p / J_m.

J_p can be written as;

$$J_p = \frac{3V_{m,M}}{4\pi r^3 z F N_A} \frac{x_y}{1 - x_y} i \tag{8}$$

Where $V_{m,M}$ is the molar volume of metal film, N_A is the Avagadros number, x_y is the volume fraction of the particles in the film, r is the radius of the particles, F is Faradays constant, z is the charge of metal ions, i is the current density.

$$Jm = \frac{i}{zF} \tag{9}$$

Combining equations 7, 8, 9;

$$\frac{x_y}{1-x_y} = \frac{4\pi r^3 zFN_A}{3V_{m,M}} \left(1.554 v^{-\frac{1}{6}} D_p^{2l3} \right) \left(C_{P,b} - C_{P,s} \right) \frac{w^{\frac{1}{2}}}{i} \tag{10}$$

Where ν_p is the volume fraction of particles, ω is the rotation rate.

As indicated in Figure 1, the model of nanoparticles co-deposition suggested by Timoshkov et al. [35], is based on the following stages:

- Coagulation of ultra-fine particles in electrolytic bath,
- Formation of quasi-stable aggregates,
- Transport of the aggregates to the cathode surface by convection, migration and diffusion,
- Disintegration of the aggregates in the near-cathode surface,
- Weak adsorption of ultra-fine particles and aggregate fragments onto the cathode surface,
- Strong adsorption of dispersion fraction and embedment.

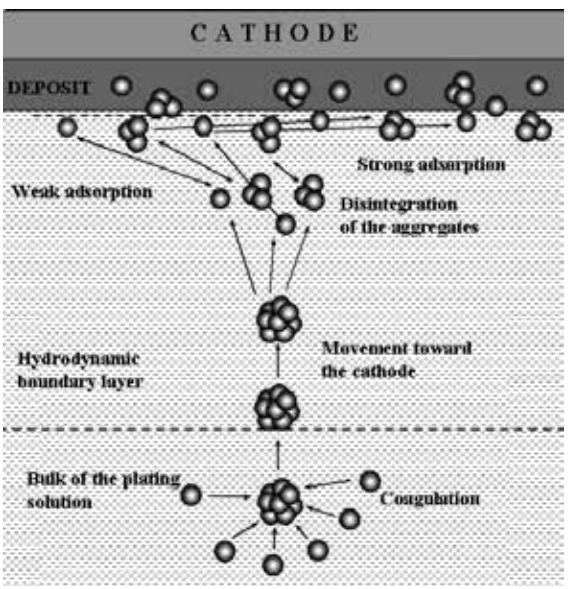

Figure 1. Model of nanoparticles co-deposition process [6, 35]

http://dx.doi.org/10.5772/62189

3. Particle interactions and suspension stability

3.1. The DLVO theory

The state of dispersion of particles in suspension can be controlled by careful manipulation of the inter-particle forces and their interactions. A quantitative description of the relationship between stability of suspension and energies of interactions between colloidal particles and other surfaces in a liquid has been given by the classical DLVO (Derjaguin-Landau-Verwey-Overbeek) theory. According to this theory, the stability of a colloidal system is determined by the total pair interaction between colloidal particles, which consists of coulombic double-layer repulsion and van der Waals' attraction. The total energy V_T of interaction of two

$$V_T = V_A + V_R \tag{11}$$

The attractive energy V_A of the London-van der Waals' interaction between two spherical particles can be expressed by:

$$V_A = -\frac{A}{6}\left(\frac{2}{S^2-4}+\frac{2}{S^2}\right) \tag{12}$$

where A is the Hamaker constant and S = 2 + H/a, with H the shortest distance between the two spheres and a the particle radius. If H << a, Equation (2) can be simplified to:

$$V_A = -A\frac{a}{12H} \tag{13}$$

The repulsive energy V_R is:

$$V_R = 2\pi\varepsilon\varepsilon_0 a\Psi lin\left[1+e^{-kH}\right] \tag{14}$$

where ε is the dielectric constant of the solvent, ε^0 is the vacuum dielectric permittivity, Ψ is the surface potential, l/k is the Debye length:

$$k = \left(\frac{e^2\sum n_i z_i}{\varepsilon\varepsilon_0 kT}\right)^{\frac{1}{2}} \tag{15}$$

where e is the electron charge, k is the Boltzmann constant, T is the absolute temperature, n_i is the concentration of ions with valence z_i [6].

3.2. Particle charging

The charge on the particles can be developed according to the following mechanisms:

a. Ions are selectively adsorbed onto the solid particle from the electrolyte.

b. Ions are dissociated from the solid phase into the electrolyte.

c. Dipolar molecules are adsorbed or orientated at the particles surface.

d. Electrons are transferred between the solid and liquid phase due to differences in work function.

Charged particle in a suspension is surrounded by oppositely charged ions. In the so-called boundary layer, the concentration of these ions is higher than their concentration in the bulk electrolyte. These ions and the particle should move in opposite directions when an electric field is applied. At the same time, the ions are also attracted by the particle, and as a result, a fraction of the ions surrounding the particle will not move in the opposite direction but move along with the particle. Accordingly, the speed of a particle is not determined by the surface charge but by the net charge enclosed in the liquid sphere, which moves along with the particle [6, 29].

3.3. Particle transport

The particle transfer toward the cathode surface occurs by four mechanisms, namely convection, migration, diffusion, and Brownian movement.

Convection: It includes thermal and stirring effects, which can be increased extensively by applying vibration, shock, and other stirring types and temperature gradients.

Migration: It is the movement of positive ions and negative ions, or charged particles, through the electrolyte under the effect of applied potential between the electrodes immersed in that electrolyte. The migration process occurs only for charged particles.

Diffusion: Electrode reaction decreases the concentration of oxidant or reductant at the electrode surface, producing a concentration gradient. Thus, the species movement from the higher to the lower concentration is enhanced. The diffusion process occurs for both charged and uncharged particles.

Brownian's movement: It is dependent on the particle size and may be ignored for particle size larger than 1 μm [24].

3.4. Other interparticle forces

During the electrodeposition process of nanocomposites, the following forces are taken into consideration:

- Mechanical forces, resulting from interaction with the fluid flow and other particles, gravity and buoyancy.
- Electrical forces, due to the electric field presented in the electrolyte.
- Molecular forces working on the particle in the vicinity of the cathode electrodes surface [24].

http://dx.doi.org/10.5772/62189

4. Effect of deposition parameters on ECD

The electrodeposition process and thus the resulted microstructure of composite coating can be affected by many parameters, such as:

- The electrolyte condition: chemical composition of the electrolyte bath, presence of additives, pH, temperature, and electrolyte stirring.
- Current conditions: current density and type of applied current (pulse or DC).
- The properties of the reinforcing particles: particle size, surface properties, concentration, and type of dispersion in the electrolyte [23, 36].

a. Current Density

Current density plays an important role in controlling the deposition rate which will in turn affect the concentration, composition and morphology of incorporated particles in the coatings. It also influences the thickness of the composite films, such that as the current density increases the thickness of the coatings increases. Low current density produces films with large surface irregularities. When the current density is increased, the amount of particle incorporation obtained has been found to increase for the Ni-TiO_2 system with a relatively slow agitation, decrease for natural or synthetic diamond in Ni and for Cr particles co-deposited in Ni and to be unaffected when co-depositing alumina in Ni [24].

Particles reinforcement in the composite coatings varies with current density. At first, incorporation increases sharply at the beginning with increase in current density till it reaches maximum value followed by sharp decrease. Therefore, hardness of composite coatings mainly increases due to the combined effect of both grain refining as well as of dispersive strengthening. When electroplating at lower current densities, metal ions dissolved from anode are transported at low rate and hence there is insufficient time for these ions to absorb on particles resulting in weak Coulomb force between anions adsorbed on particles leading to lower concentration of electrodeposited particles in the composite coatings. On the other hand, at higher current densities, metal ions dissolved from anode are transported faster than particles by the mechanical agitation which causes a decrease in co-deposition of particles as well as hardness of composite coatings. Therefore, selection of optimum current density is important to enhance the concentration of particles in the composite coatings [37]. The maximum current density for preparing nanocomposite coatings is limited by the limiting current density.

The DC electrodeposition methods are often associated with slower deposition rates and coating defects such as surface roughness, porosity, poor adhesion, undesirable microstructure, etc. Recently, pulse current (PC) and pulse reverse current (PRC). ECD methods have attracted significant attention to improve deposition rates and microstructure of the coatings for improved mechanical and corrosion properties [24, 25].

b. Bath Temperature

According to Akarapu [25], two contrary behaviors were observed regarding the effect of temperature on the obtained crystallization size. This discrepancy was due to the two contra-

dictory effects of temperature increase on the thermodynamic and kinetic driving force of nucleation process. As the electrolyte's temperature increases, the thermodynamic driving force of crystallization decreases and the critical size of the nucleus will increase. This will lead to lower nucleus densities and formation of coarse grain. On the other hand, the increase in temperature leads to enhancement of the kinetic driving force. This results in an increase in the rate of nucleation and thus fine grains formation [25].

c. Bath Agitation

Agitation of the plating solution is important in determining particle incorporation. There are various methods of agitation employed include circulation by pumping, purging, of air, ultrasonic agitation, and the plate pumper technique. In general, if the agitation is too slow (laminar flow), the particles in the bath may not disperse completely, except when their density is low. If the agitation is too high (turbulent), particles will not have sufficient time to get attached to the surface, and this results in poor particles incorporation [25].

Increase in the bath agitation in the parallel plate electrode setup has been found to increase the amount of particles co-deposited within the electroplated film for the Ni-Al_2O_3 and Ni-TiO_2 systems. When the agitation is increases, a greater number of particles arrive at the electrode surface and the amount of particle incorporation in the metal film increases. However, if the agitation is too intense, the residence time for the particles at the electrode surface is insufficient and the particles are swept away before they can be incorporated into the growing metal film [25]. The amount of co-deposition has also been observed to decrease in the Cu-SiC and Cu-CrB_2 systems with increasing agitation [24].

d. Particle Characteristics

Particles can be characterized by their composition and crystallographic phase, as well as by their size, density, and shape. The particle composition can have a dramatic impact on the amount of incorporation obtained for a particular bath composition. For instance three times more TiO_2 than $A1_2O_3$ has reportedly been incorporated into a Ni matrix, under the same deposition conditions. The particle size also effects on the amount of co-deposited particles in the composite coatings. For example when the particle size in the electrolyte increases then amount of adsorbed ions on the surface increases, which leads to the increase in the migration velocity of the particles and also results in a higher columbic force of attraction, leads to increase in the amount of the particles. But the density of particles in the coating decreases as the particle size in the electrolyte increases [25].

The electrode/particle interaction will be affected by the particle properties, such as material type, shape, size, surface charge, concentration, and dispersion in the bath. The co-deposition of nano-sized particles produces a composite coating with a much higher hardness than that achieved with micron-sized particles. The smaller the particle, the more difficult the co-deposition into the metal matrix due to the high tendency of agglomeration. In addition, the smaller the particle size, the greater the effect of colloidal properties (van der Waals, electro-static, and solvent interaction forces) [24].

e. Bath composition

The composition of the co-deposition bath is not only defined by the concentration and type of electrolyte used for depositing the matrix metal, but also by the particle loading in suspension, the pH, and the additives used. A variety of electrolytes have been used for the electro co-deposition process to form metal matrix of copper include acid copper sulphate bath, alkaline pyrophosphate bath. Electrolyte concentrations typically range between 100-600 g/l and the particle loading in suspension has ranged from 2-200 g/l [25].

According to Narasimman et al. [38], various additives can be used for preventing the agglomeration of particles, increasing the volume fraction of reinforcing particles in the deposit, and providing good dispersion and thus high hardness. The addition of surfactants plays a role in modifying the surface charge and reducing the particle agglomeration, thus improving their electrostatic adsorption on the cathode surface. As a result of decreasing the agglomeration of particles, the amount of effective particles would be significantly increased, resulting in higher amounts of the reinforcing particles. The addition of surfactants changes the zeta potential of the particles.

The effect of additives in the plating bath on the microstructure and physical properties of deposits was reported by many researchers. For example, the addition of saccharin to plating electrolyte was found to improve the ductility and brightness. The role of additives on a grain refining can be summarized as follows:

- As refiner, blocking the surface by complexation, decreasing the adsorbed ions diffusion on cathode, and thus inhibiting the growth of crystals.
- Controlling the evolution rate of hydrogen on cathode.
- Changing the cathodic overpotential [38].

5. Types of Nanocomposites

5.1. Metal matrix nanocomposites

Various processes are used to manufacture MMCs which are described here. These processes are classified on the basis of temperature of the metallic matrix during processing. Accordingly, the processes can be classified into five categories: (1) liquid-phase processes, (2) solid–liquid processes, (3) two- phase (solid–liquid) processes and (4) in situ processes. (5) deposition techniques [39-40].

5.1.1. Electrodeposition of nickel nanocomposites

Nickel nanocomposite coatings are used in a wide variety of industrial and engineering applications, such as consumer electronics, chemical, computer and telecommunications industries in order to improve corrosion and wear resistance, modify magnetic and other properties. For nickel matrix electrodeposits, a great variety of particles have been used such

as oxides i.e. TiO_2 [41, 42], Al_2O_3 [43], CeO_2 [44, 45], ZrO_2 [46], graphene oxide GO [47], carbon nanotubes CNT; Al_2O_3/Y_2O_3/CNT [48], carbides like SiC [49- 51], WC [52] and nitrides such as TiN [53] and Si_3N_4 [54].

The Ni-TiO_2 system was selected because nickel is an industrially important coating for corrosion protection [42]. Generally the volume fraction of co-deposited particles is limited for nanoparticles and usually it is inversely proportional to their size. For example, Shao et al. [43] studied the rate of incorporation of two different sizes of Al_2O_3 nanoparticles (50 nm and 300 nm) into a nickel deposit. Using similar operating parameters (1000 rpm, 20 mA cm^{-2}), it was found that the percentage volume fraction of the 300 nm Al_2O_3 in the nickel deposit was much higher compared to the 50 nm Al_2O_3. The presence of nanosized particles in a metal deposit may induce changes in the crystalline structure of the metallic coating.

Ni–CeO_2 nanocomposite coatings were prepared by co--deposition of Ni and CeO_2 nanoparticles with an average particle size of 7 nm onto pure Ni surfaces from a nickel sulphate. The as-codeposited Ni–CeO_2 nanocomposite coatings showed a superior oxidation resistance compared with the electrodeposited pure Ni coating at 800 °C. The co-deposited CeO_2 nanoparticles blocked the outward diffusion of nickel along the grain boundaries. However, the effects of CeO_2 particles on the oxidation resistance significantly decrease at 1050 °C and 1150 °C due to the outward-volume diffusion of nickel controlling the oxidation growth mechanism [45].

According to Zeng et al [46], increasing concentration of the CeO_2 nanoparticles in the bath increased the weight percent of CeO_2 particles in the nanocomposite coatings, and improved the micro- hardness, and the friction, corrosion, and wear behaviour of the coatings. However, excessive CeO_2 nano-particle loadings were detrimental to the coating properties.

Ni–Al_2O_3–SiC hybrid composite films with an acceptable homogeneity and granular structure having 9.2 and 7.7 % vol. Al_2O_3 and SiC nanoparticles, respectively were developed successfully by M. Masoudi et al [50]. Both micro hardness and wear resistance increased owing to dispersion and grain-refinement strengthening of nanoparticles. The oxidation resistance of the Ni–Al_2O_3–SiC hybrid composite coatings was measured to be approximately 41 % greater than the unreinforced Ni deposit and almost 30 % better than the Ni–Al_2O_3 composite coatings.

Ni-SiC nanocomposite coatings were applied on AZ91 magnesium alloy from Watts bath with different SiC content. Micro-hardness of specimens was measured and the results revealed a significant enhancement: from 74 Vickers for bare AZ91 magnesium alloy to 523 Vickers for coated specimen. The obtained data showed the superior corrosion resistance for the coated AZ91 magnesium alloy [51].

The effect of incorporation of Si_3N_4 particles in the Ni nanocomposite coating on the micro hardness, corrosion behaviour has been evaluated by Kasturibai et al. [54]. The micro hardness of the composite coatings (720 HV) was higher than that of pure nickel (310 HV) due to dispersion-strengthening and matrix grain refining and increased with the increase of incorporated Si_3N_4 particle content. The corrosion potential (E_{corr}) in the case of Ni–Si_3N_4 nano-composite had shown a negative shift, confirming the cathodic protective nature of the coating [54].

According to R. Abdel-Karim et al. [55], Ni–Mo nanocomposite coatings were prepared using a nickel salt bath containing suspended Mo nanoparticles using direct current. The crystallite size (18–32 nm) and the surface roughness increased by raising the current density. A remarkable deterioration in the corrosion resistance of Ni–Mo composites was observed with the increase of Mo content. This could be due to crystallite size-refining and surface roughness effect and correspondingly a large surface area. Resulted high surface roughness lead to improved electrocatalytic effect for hydrogen evolution.

5.1.2. Electrodeposition of copper nanocomposites

The conventionally used reinforcements in the Cu matrix such as oxides, carbide nanoparticles etc., have resulted in considerable improvement in the mechanical properties. Copper- TiO_2 nano composites were deposited from an acidic copper sulphate bath. Due to relation of optical properties and photo responsively of TiO_2 nanoparticles to nanoparticle size, surface area and morphology, optimization of these parameters in order to having efficient response have crucial importance. Good quality deposits (finer grain size and more homogeneous) were obtained at rather low pH [56].

According to Quayum et al. [57], Cu-NPs /ZnO / ITO composite film electrode has been prepared by electrodeposition of Cu nanoparticles (NPs), ZnO nanorods on indium tin oxide (ITO). Cu-NPs/ZnO composite electrode had high sensitivity and stability and showed higher catalytic current for glucose oxidation in the field of biosensors.

According to Li et al. [58], Cu/C composites were successfully fabricated by three step electrodeposition. The effects of hot pressure temperature and alloy element Fe on the interface characteristic of Cu/C composite were investigated. The addition of alloy element Fe not only improves the tensile strength and the lateral shear strength of the Cu/C composite, but also changes the interface bond type from the physical bond type to the chemical bond type.

The Cu/ZnO nanocomposite films have been synthesized by cathodic electrodeposition [59]. The SEM and TEM images reveal the formation of hexagonal two-dimensional ZnO sheets and Cu nanoparticles. The Cu/ZnO nanocomposite film showed good emission current stability.

Chrobak.et al. [60], studied both elastic and magnetic properties of the Cu+ Ni nanocomposite coatings with dispersed Ni nanopowder particles obtained by applying the electrolytic deposition method. The magnetization curves M (T) showed a superparamagnetic effect at T<50 K which depends on dispersion of magnetic particles in a nonmagnetic matrix. It was also shown that the observed decrease of the apparent Young's modulus due to an increase of coating roughness.

Pavithra et al. [61], demonstrated the synthesis of very hard Cu-Graphene composite foils by a simple, scalable and economical pulse reverse electrodeposition method with a well-designed pulse profile. Carbon as a reinforcement material, in the form of fibres, nanotubes etc., will result in superior mechanical, electrical properties and an extremely high thermal conductivity. The improved strength of metal matrix composites is due to its excellent mechanical properties of Graphene. In addition, graphene is also shown to block dislocation motion in a nanolayered metal-graphene composites resulting in ultrahigh strength [62].

5.1.3. Electrodeposition of cobalt nanocomposites

Nanocrystalline cobalt and cobalt-based alloys are good candidates for the replacement of the highly toxic electroplated hexavalent chromium. They have excellent mechanical and wear-resistant properties, high saturation magnetization, and good thermal stability. Nanocrystalline cobalt and its alloys have higher hardness over the polycrystalline counterparts. Electrochemically prepared Co nanodeposits have three to five times higher coercivity (Hc) than conventional polycrystalline Co [63].

Cobalt composites containing incorporated TiO_2 particles are interesting materials, due to the semiconducting properties of TiO_2, with applications as photocatalysts, particularly in the treatment of polluted water, but, in the same time, due to magnetic properties of Co matrix. More attention has been focused on ferromagnetism in Co-doped TiO_2 anatase films, nanocrystals, nanorods and nanotubes, with potential applications in spintronics. The inclusion of TiO_2 in a nanocomposite layer with increasing current density causes the decrease of saturation magnetization from 279.5 (a.u.) to 76.0 (a.u). Magnetic anisotropy of nanocomposite films depends on the concentration on morphology and magnetic properties of Co-TiO_2 electrodeposited nanocomposite films [63]. According to Sivaraman et al. [64], the electrodeposited the composites exhibited a partially amorphous/nanocrystalline character, with the crystalline fractions originating from the hexagonal-close packed structure of Co. A refinement of the Co crystallite size was observed in deposits containing higher weight percentage of yttrium compounds. The hardness increased with the yttrium content.

5.1.4. Electrodeposition of chromium nanocomposites

Deposition of thick Cr from Cr (III) bath is cumbersome and thin Cr does not have enough wear resistance. The electrodeposition of Cr–Al_2O_3 nanocomposite from Cr (III) bath appears a feasible way for improvement of wear resistance, hardness, lubricity and high temperature resistance of the deposited layer [65].

Cr-TiO_2 nano-composites were prepared by electrodeposition. The addition of TiO_2 in the coating led to improvement corrosion resistance of the composite coating as compared to the pure chromium coating. This improvement is due to the physical barriers produced by TiO_2 to the corrosion process by filling crevices, gaps and micron holes on the surface of the chromium coating. This excellent corrosion resistance of the composite coatings provides wide applications in modern industry [66].

Juneghani et al. [67] examined Cr–SiC nanocomposite coatings with various contents of SiC nanoparticles prepared by electrodeposition in optimized Cr plating bath containing different concentrations of SiC nanoparticles. The co-deposited SiC nanoparticles are uniformly distributed into the Cr matrix which improves the corrosion and wear performance of coating.

5.1.5. Electrodeposition of zinc nanocomposites

Zinc deposits provide good protection to iron and steel components due to its sacrificial nature, low cost and ease of application. Nanocrystalline zinc shows improved properties such as

hardness, ductility, corrosion and wear resistance. The graphene based metal materials have been widely reported that the graphene as a support material for metal nanoparticles to obtain catalytic, optoelectronic and magnetic properties. The GO sheets were reduced to be rGO sheets after electrodeposition process while Zn^{2+} also reduced on the surface of rGO sheets. Due to the greatly increasing in the specific surface area, the Zn/rGO film may be used as efficient catalyst for the reaction of methanol generated by carbon dioxide and hydrogen (Figure 2) [68].

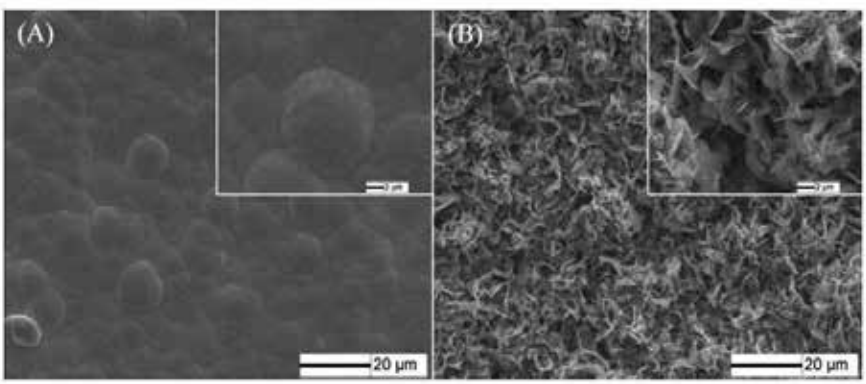

Figure 2. Representative SEM images of (A) Zn film and (B) Zn/rGO film. The insets are the corresponding high-resolution images [68].

Indeed, pure zinc coatings suffer from poor mechanical properties and the incorporation of a second hard phase during the electrodeposition process (e.g. ceramic nanoparticles such as ceria (Figure 3) [69], SiO_2 [70] or Al_2O_3 [71], is of great importance.

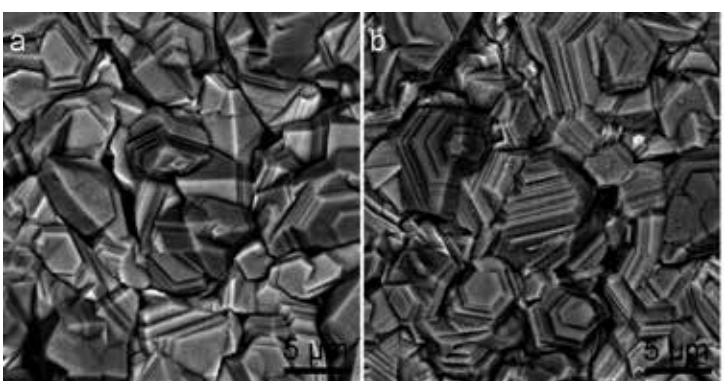

Figure 3. Surface SEM image of (a) pure zinc and (b) zinc-ceria nanocomposite coatings [69].

According to Gomes et al. [72], Zn-TiO_2 coatings were successfully prepared by co-deposition method. The film's surface is rough and the TiO_2 agglomerates are randomly distributed on

the metallic matrix formed by staked hexagonal plates oriented in different direction. These unique characteristics are essential for the thermal conversion of Zn to ZnO. The photo-electrochemical degradation of organic molecules was achieved with this type of Ti/ZnO-TiO_2 photoanodes (Figure 4).

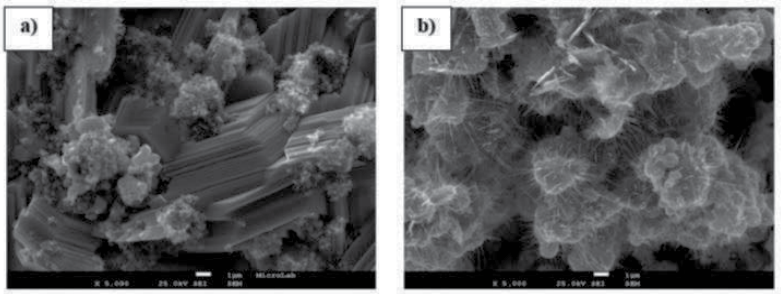

Figure 4. FEG-SEM images for (a) as-deposited and (b) annealed Zn-TiO2 nanocomposite films [72].

5.2. Ceramic Matrix Nanocomposites

Ceramic matrix composites (CMCs) can extensively overcome the intrinsic brittleness and lack or mechanical reliability of monolithic ceramics, which are otherwise attractive for their high stiffness and strength. In addition to mechanical effects, the reinforcing phase can improve electrical conductivity, thermal expansion coefficient, hardness and thermal shock resistance. The combination of these characteristics with intrinsic advantages of ceramic materials such as high-temperature stability, high corrosion resistance, light weight and electrical insulation, makes CMCs very attractive functional and structural materials for a variety of applications. A wide range of reinforcing fibers have been investigated, including those based on SiC, carbon, alumina, and mullite. However, carbon fibers are among the highest performance toughening elements investigated [73, 74].

Electrodeposition of ceramic films employing electrochemical methods is a fast evolving field. The methods for electrodeposition may be divided into two: electrophoretic and electrolytic deposition. Electrolytic deposition can be driven using cathodic currents by either reducing the metal ions, which causes their deposition, e.g., Cu_2O, or by driving a proton dependent reducing process, leading to an increase of the pH on the electrode surface and the subsequent metal hydroxide deposition. The deposition of ceramic nanocomposite materials is of utmost importance in different fields spanning from supercapacitors to anticorrosion films and from coatings of medical implants to advanced lubricant materials [75].

5.3. Polymeric matrix nanocomposites PNCs

Cathodic electrodeposition of polymer-metal and polymer-ceramic materials is an area of intense interest. Such materials exhibit interesting mechanical, thermal, electrical, optical and magnetic properties whose applications have motivated the development of electrochemical

techniques [76, 77]. PNCs are among the most promising class of new materials because they are light weight, flexible, low cost, anti-corrosive, and have good process ability and mechanical properties. Most polymers are electrical insulators and are used for a variety of insulating applications in industry. However, the inherent electrical insulation means polymers tend to hold the electrostatic charges, and allow the electromagnetic frequency interference (EMI) to travel through without loss [78].

Some polymer/nanoparticle (NP) composites have already been reported in the literatures, such as polyaniline/metal oxide NP composites, PPy/TiO_2, PPy/Ti, PPy/Au, PPy/Ag, PPy/Pt, and PPy/Pd, prepared by electrodeposition [79]. The incorporation of metal nanoparticles into the conducting polymer offers improved performance for both the host and the guest. They can be applied in application in electronics because incorporation of metal clusters is known to increase the conductivity of the polymer. The applications of these composites have also been extended to various fields such as, sensors, photovoltaic cells, memory devices, protective coatings against corrosion, and supercapacitors. The application of these composites in catalysis is of particular interest. The polymer allows the control of the environment around the metal center, thus influencing selectivity of the chemical reactions [80].

Conducting polymer/inorganic oxide nanocomposites have recently attracted great attention due to their unique microstructure, physiochemical and electro-optical properties, and a wide range of their potential usage in battery cathodes and in the construction of nanoscopic assemblies in sensors and microelectronics. Conductive polymer/ZnO nanocomposites coating were prepared on type-304 austenitic stainless steel (SS) using H_2SO_4 acid as electrolyte by potentiostatic methods. It was found that ZnO nanoparticles improve the barrier and electrochemical anticorrosive properties of polymer [81].

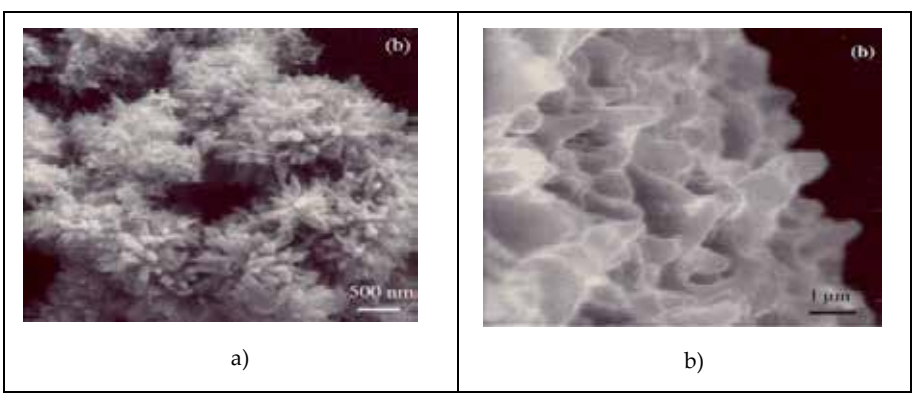

Figure 5. SEM micrographs of the deposits; (a) ZnO NPs, (b) ZnO NPs [81].

Electrically conducting polypyrrole (PPy)–iron group (Ni, Co, Fe and their alloys) composite films have been electrodeposited at cathodic process to give ''tailored'' soft and hard magnetism. The composites of the PPy doped with dodecylsulfate (DS) (PPy–DS) with NiFe alloy showed soft magnetism with coercivity HC, k <9 Oe, while the PPy–DS with CoMnP alloy

showed hard magnetism with HC, k>1085 Oe. These results indicated the possibility conducting polymer–magnetic metals composites fabrication by electrodeposition [82].

The incorporation of metal nanoparticles into the conducting polymer offers enhanced performance for both the host and the guest. They have diverse application potentials in electronics because incorporation of metal clusters is known to increase the conductivity of the polymer. The applications of these composites have also been extended to various fields such as, sensors, photovoltaic cells, memory devices, protective coatings against corrosion, and supercapacitors. Of particular interest is the application of these composites in catalysis. The polymer allows the control of the environment around the metal center, thus influencing selectivity of the chemical reactions [83].

Y. Lattach et al. [84] stated that nanocomposite anode materials for water oxidation have been readily synthesized by electrodeposition of iridium oxide nanoparticles into poly (pyrrole-alkylammonium) films. Electroanalytical investigations have shown that the electrocatalytic activity of iridium oxide nanoparticles is fully maintained when they are incorporated in the polymer matrix.

Electrodeposition process was carried out by dispersing UHMWPE powders in an electrolytic solution of cobalt sulphate/cobalt chloride solution to obtain Co/UHMWPE composite coating on stainless steel substrate (304L). UHMWPE was selected as surface modifier element, due to its high biocompatibility and low coefficient of friction. This material can be used in many biomedical applications [85].

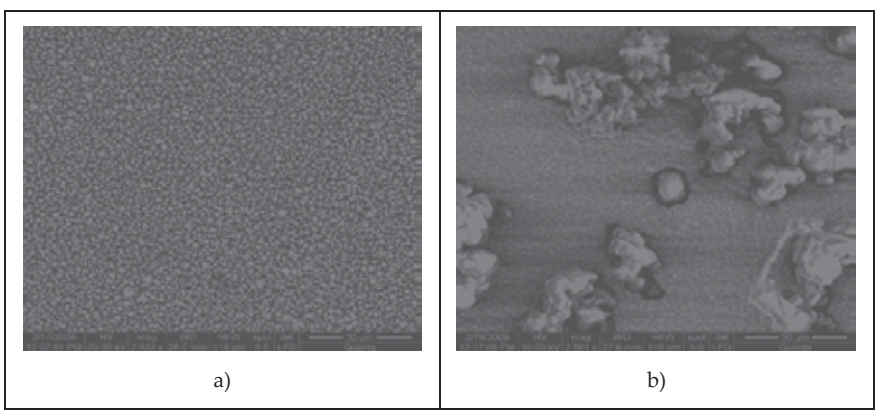

Figure 6. SEM surface morphology of coatings obtained at current density of 48 mA/cm^2 and deposition time of 30 min: (a) Pure Co; (b) Co/UHMWPE Composite Coatings with 30g/L [85].

6. Conclusions

In conclusion, materials science and engineering has experienced a tremendous growth in the field of nanocomposite development with enhanced chemical, mechanical, and physical

properties. The progress in nanocomposites is varied and covers many industries. Nanocomposites with a variety of enhanced physical, thermal and other unique properties can be manufactured. They have properties that are superior to conventional microscale composites and can be synthesized using simple and inexpensive techniques. Theoretical aspects and mechanisms related to the electrodeposition process of nanocomposite films, from aqueous solutions, were discussed. The three types of matrix (metal, ceramic, polymers) nanocomposites were presented, underlining the needs for these materials and some recent results on structure, properties and potential applications.

Author details

Randa Abdel-Karim*

Address all correspondence to: randaabdelkarim@gmail.com

Faculty of Engineering, Cairo University, Egypt

References

[1] A. Gomes, I. Pereira, B. Fernandez and R. Pereiro, Advances in Nanocomposites - Synthesis, Characterization and Industrial Applications, (edit. B. S. R. Reddy) chapter 21, Electrodeposition of Metal Matrix Nanocomposites: Improvement of the Chemical Characterization Techniques, INTECH, 2011.

[2] V. B. Singh and D. K. Singh, An Overview on the Preparation, Characterization and Properties of Electrodeposited-Metal Matrix Nanocomposites, Nanosci. Technol. 2014, 1(3), 1-20.

[3] P. Henrique C. Camargo, K. G. Satyanarayan. F. Wypych, Synthesis, Structure, Properties and New Application Opportunities, Materials Research 2009, 12(1), 1-39.

[4] V. Viswanathan, T. Laha, K. Balani, A. Agarwal, S. Seal, Challenges and Advances in Nanocomposite Processing Techniques, Materials Science and Engineering 2006, R 54 121–285.

[5] R. Abdel-Karim and A.F. Waheed, Modern Surface Engineering Treatments, (edit. M. Aliofkhazraei), Chapter 6: Nanocoatings, INTECH, 2013.

[6] X. Pang, Fabrication of Advanced Organic-Inorganic Nanocomposite Coatings for Biomedical Applications by Electrodeposition, Ph. D. thesis, McMaster University, Canada, 2008.

[7] Riccardo Casati and Maurizio Vedani, Metal Matrix Composites Reinforced by Nano-Particles—A Review, Metals 2014, 4, 65-83.

[8] .A. Avidko, Metal-Graphene Nanocomposite with Enhanced Mechanical Properties: A Review, Rev. Adv. Mater. Sci. 2014, 38, 190-200.

[9] C. Cai and Y. Wang, Novel Nanocomposite Materials for Advanced Li-Ion Rechargeable Batteries, Materials 2009, 2, 1205-1238.

[10] N. Silvestre, State-of-the-art Review on Carbon Nanotube Reinforced Metal Matrix Composites, International Journal of Composite Materials 2013, 3(6A), 28-44.

[11] U. Erb, K. T. Aust, and G. Palumbo, Nanostructured Materials, (Edit: C. C. Koch), Chapter 6: Electrodeposited Nanocrystalline Materials, (Second Edition), Elsevier, 2006.

[12] T. Ohgai, Electrodeposited Nanowires and Their Applications, (edit: N. Lupu), Chapter 3: Fabrication of Functional Metallic Nanowires Using Electrodeposition Technique, INTECH, 2011.

[13] M. S. Doolabi, S. K. Sadrnezhaad, D. S. Doolabi and M. Asadirad, Influence of Pulse Parameters on Electrocodeposition of Cr–Al_2O_3 Nanocomposite Coatings from Trivalent Chromium Bath, International Heat Treatment and Surface Engineering 2012, 6 (4), 178-184.

[14] E. Beltowska-Lehman, A. Goral, P. Indyka, Electrodeposition and Characterization of Ni/Al_2O_3 Nanocomposite Coatings, Archives of Metallurgy and Materials 2011, 56(4), 919-931.

[15] S. Mahdavi, S.R. Allahkaram, Composition, Characteristics and Tribological Behaviour of Cr, Co–Cr and Co–Cr/TiO_2 Nano-composite Coatings Electrodeposited from Trivalent Chromium Based Baths, Journal of Alloys and Compounds 2015, 635(25), 150–157.

[16] B. M. Praveen and T. V. Venkatesha, Electrodeposition and Corrosion Resistance Properties of Zn-Ni/TiO_2 Nano composite Coatings, International Journal of Electrochemistry 2011, 2011, Article ID 261407, 4 pages.

[17] A. Agarwal, S. R. Bakshi, D. Lahiri Carbon Nanotubes: Reinforced Metal Matrix Composites, Chapter 4: Metal-Carbon nanotube systems, CRC, 2011.

[18] A. Sommers, Q. Wang, X. Han, C. T' Joen, Y. Parkd, A. Jacobi, Ceramics and Ceramic Matrix Composites for Heat Exchangers in Advanced Thermal Systems A review, Applied Thermal Engineering 2010, 30 (11), 1277-1291.

[19] M. Abdullah, J. Ahmad, M. Mehmood, and M. Mujahid, Effect of CTAB Addition on Improvement of Properties of Al_2O_3 (w)–Al_2O_3 (n)–ZrO_2 (n) (3mole% Yttria Stabilized Tetragonal Zirconia) Nanocomposite. International Journal of Information and Education Technology 2012, 2(5), 543-546.

[20] M. Sathish Kumar, K. Manonmani, B. Parasuram, S. Karthikeyan, Composites Reinforced with Carbon Nanotubes - A Review, J. Environ. Nanotechnol. 2013, 2(3), 67-80.

[21] L. Wei, N. Hu and Y. Zhang, Synthesis of Polymer—Mesoporous Silica Nanocomposites, Materials 2010, 3, 4066-4079.

[22] G. Naveen Kumar, Y.V. Mohana Reddy, K. Hemachandra Reddy, Synthesis and Characterization of Iron Oxide Nanoparticles Reinforced Polyester/nanocomposites, International Journal of Scientific and Research Publications 2015, 5(8), 1-13.

[23] K Nam, Y Tsutsumi, C Yoshikawa, Y Tanaka, R Fukaya, T Kimura, H Kobayashi, T Hanawa, and A Kishida, Preparation of Novel Polymer–Metal Oxide Nanocomposites with Nanophase Separated Hierarchical Structure, Bull. Mater. Sci. 2011, 34(7), 1289–1296.

[24] Y. H. Ahmad and A. M. A. Mohamed, Electrodeposition of Nanostructured Nickel-Ceramic Composite Coatings: A review, Int. J. Electrochem. Sci. 2014, 9, 1942 – 1963.

[25] A. Akarapu, Surface Property Modification of Copper by Nanocomposite Coating, Master thesis, National Institute of Technology Rourkela, India, 2011.

[26] N. Saheb, N. Ul Qadir, M. U. Siddiqui, A. M. Arif, S. S. Akhtar and N. Al-Aqeeli Characterization of Nano-reinforcement Dispersion in Inorganic Nanocomposites: A Review, Materials 2014, 7, 4148- 4181.

[27] N. Guglielmi, Kinetics of the Deposition of Inert Particles from Electrolytic Baths, J. Electrochem. Soc. 1972, 119, 1009-1012.

[28] P. Celis, J.R. Roos, C. Buelens, A Mathematical Model For the Electrolytic Codeposition of Particle with a Metallic Matrix, J. Electrochem. Soc. 1987, 13, 1402- 1408.

[29] T. R. Khan, Nanocomposite Coating: Codeposition of SiO_2 Particles During Electrogalvanizing, Ph. D Thesis, Bochum University, Germany, 2011.

[30] J. Fransaer, V. Bouet, J. P. Celis, C. Gabrielli, F. Huet and G. Maurin, Perturbation of the Flow of Current to a Disk Electrode by an Insulating Sphere, J. Electrochem. Soc. 1995, 142(12), 4181-4189.

[31] J. Foster and A.M.J. Kariapper, Study of Mechanism of Formation of Electrodeposited Coatings, Trans. Inst. Met. Finish. 1973, 51, 27–31.

[32] J. L. Valdes, Electrodeposition of Colloidal Particles, J. Electrochem. Soc. 1987, 134(4), 223C-225C.

[33] J. Fransaer, J. P. Celis and J. R. Roos, Analysis of the Electrolytic Codeposition of Non-Brownian Particles with Metals, J. Electrochem. Soc. 1992, 139(2), 413-425.

[34] P. M. Vereecken, I. Shao and P. C. Searson, Particle Codeposition in Nanocomposite Films, J. Electrochem. Soc. 2000, 147(7), 2572-2575.

[35] I. Timoshkov, V. Kurmashev and V. Timoshkov, Advances in Nanocomposite Technology, (Edit. by Dr. A. Hashim), Chapter 3: Electroplated Nanocomposites of High Wear Resistance for Advanced Systems Application, INTECH, 2011.

[36] Z. Abdel Hamid, Review Article: Composite and Nanocomposite Coatings, Journal of Metallurgical Engineering (ME) 2014, 3(1), 29-42.

[37] T. Borkar, Electrodeposition of Nickel Composites Coatings, Mumbai University, India, 2007.

[38] P. Narasimman, M. Pushpavanam and V.M. Periasamy, Effect of Surfactants on the Electrodeposition of Ni-SiC Composites, Portugaliae Electrochimica Acta 2012, 30(1), 1-14.

[39] B. C. Kandpal, J. Kumar, H. Singh, Production Technologies of Metal Matrix Composite: A Review, IJRMET 2014, 4 (2), 27-32.

[40] F. C. Walsh and C. Ponce de Leon, A Review of the Electrodeposition of Metal Matrix Composite Coatings by Inclusion of Particles in a Metal Layer: an Established and Diversifying Technology, Transactions of the IMF 2014, 92 (2), 83-98.

[41] A. I. Palvlov, L. Benea, J. P. Celis, L. Vazouez, Influence of Nano-TiO_2 Co-deposition on the Morphology, Microtopography and Cryttallinity of Ni/Nano-TiO_2 Electrosynthesis Nanocomposite Coatings, Digest Journal of Nanomaterials and Biostructures 2013, 8(3), 1043 – 1050.

[42] Y. Li, X. Sun, J. Qiao, Mechanical and Corrosion-Resistance Performance of Electrodeposited Titania–Nickel Nanocomposite Coatings, Surf. Coat. Technol. 2005, 192, 331– 335.

[43] I. Shao, P.M. Vereecken, R.C. Cammarata, P.C. Searson, Kinetics of Particle Codeposition of Nanocomposites, J. Electrochem. Soc. 2002, 149, C610- C614.

[44] H. Zhang, Y. Zhou, J. Sun, Preparation and Oxidation Behavior of Electrodeposited Ni–CeO_2 Nanocomposite Coatings, Trans. Nonferrous Met. Soc. China 2013, 23, 2011−2020.

[45] Y.B. Zeng, N.S. Qu and X.Y. Hu, Preparation and Characterization of Electrodeposited Ni-CeO_2 Nano-composite Coatings with High Current Density, Int. J. Electrochem. Sci. 2014, 9, 8145 – 8154.

[46] I. Zhitomirsky, M. Niewczas, and A. Petric, Synthesis and Magnetic Properties of Ni-Zirconia Composites, Materials and Manufacturing Processes 2003, 18(5), 719–730.

[47] L. You, W. Guofeng, L. Qi, and Y. Mo, Ni/GO Nanocomposites and its Plasticity, Manufacturing Rev. 2015, 2, 8-13.

[48] S. Mirzamohammadi, M. Kh. Aliov, A. R. Sabur, A. Hassanzahdeh-Tabrizi, Study of Wear resistance and Nanostructure of Tertiary Al_2O_3/Y_2O_3/CNT Pulsed Eectrodeposited Ni-Based Nanocomposite, Physicochemical Mechanics of Materials 2010, 1, 67-75.

[49] M. H. Fini, A. Amadeh, Nanomaterials: Applications and Properties (NAP-2011). Vol. 1, Part I, 2011.

[50] M. Masoudi, M. Hashim, H. M. Kamari, Characterization of Novel Ni–Al_2O_3–SiC Nano-composite Coatings Synthesized by Co-electrodeposition, Appl Nanosci. 2014, 4, 649–656.

[51] L. Shi, C. Sun, P. Gao, F. Zhou, W. Liu, Mechanical Properties and Wear and Corrosion Resistance of Electrodeposited Ni–Co/SiC Nanocomposite Coating, Applied Surface Science 2006, 252, 3591–3599.

[52] D. k. Singh, M. K. Tripathi, V. B. Singh, Electrodeposition and Characterization of Ni-WC Composite Coating from Non – aqueous Bath, International Journal of Materials Science and Applications 2013, 2(2), 68-73.

[53] J. Wang, F. Xia and M. Huang, Preparation and Mechanical Properties of Ni-TiN Composite Layers by Ultrasonic Electrode Position, Research Journal of Applied Sciences, Engineering and Technology 2013, 6(7), 1303-1308.

[54] S. Kasturibai and G. P. Kaliagnan, Pulse Electrodeposition and Corrosion Properties of Ni–Si_3N_4 Nanocomposite Coatings, Bull. Mater. Sci. 2014, 37, 721–728.

[55] R. Abdel-Karim, J. Halim, S. El-Raghy, M. Nabil, A. Waheed, Surface Morphology and Electrochemical Characterization of Electrodeposited Ni–Mo Nano-composites as Cathodes for Hydrogen Evolution, Journal of Alloys and Compounds 2012, 530, 85–90.

[56] S. M. Delgosha, S. Sharifi, Influence of pH on the Electrochemical Deposition of Composite Coatings in Copper Matrix with TiO_2 Nanoparticles, Optics 2014, 3(1), 1-4.

[57] M. E. Quayum, B. Biswas and M. D. Khairul, H. Bhuiyan, Electro-synthesis of Cu / ZnO Nanocomposite Electrode on Ito Electrode and Its Application in Oxidation of Ascorbic Acid and Glicose, J. Asiat. Soc. Bangladesh, Sci. 2013, 39(2), 183-190.

[58] Y. Li, P. Bai, Y. Li, Fabrication and Fibre Matrix Interface Characteristics of Cu/C (Fe) Composite, Science of Sintering 2009, 41, 193-198.

[59] F. J. Sheini, J. Singh, O.N. Srivasatva, D. S. Joag, M. A. More, Electrochemical Synthesis of Cu/ZnO Nanocomposite Films and Their Efficient Field Emission Behavior, Applied Surface Science 2010, 256, 2110–2114.

[60] A. Chrobak, M. Kubisztal, J. Kubisztal, E. Chrobak, G. Haneczok, Microstructure, Magnetic and Elastic Properties of Electrodeposited Cu+ Ni Nanocomposites Coatings, Journal of Achievements in Materials and Manufacturing Engineering 2011, 49(1), 17-26.

[61] C. L. P. Pavithra, B. V. Sarada, K. V. Rajulapati, T. N. Rao & G. Sundararajan, A New Electrochemical Approach for the Synthesis of Copper-Graphene Nanocomposite Foils with High Hardness, Scientific Reports 2014, 4:4049, 1- 7.

[62] M. Poiana, L. Vlad, P. Pascariu, A. V. Sandu, V. Nica, V. Georgescu, Effects of Current Density on Morphology and Magnetic Properties of Co-TiO_2 Electrodeposited

Nanocomposite Films, Optoelectronics and Advanced Materials– Rapid Communications 2012, 6 (3-4), 434 - 440.

[63] R. Abdel-Karim, Handbook of Nanoelectrochemistry, (Edit.M.Aliofkhazraei, A.H. Makhlouf), Chapter 2: Electrochemical Fabrication of Nanostructures,Springer International Publishing, Switzerland, 2016.

[64] K. M. Sivaraman, O. Ergeneman, S.Pané, E. Pellicer, J. Sort, K. Shou, S. Surinach, M.D. Baró, B.J. Nelson, Electrodeposition of Cobalt–yttrium Hydroxide/oxide Nanocomposite Films From Particle-free Aqueous Baths Containing Chloride Salts, Electrochimica Acta 2011, 56, 5142–5150.

[65] M. S. Doolabi, S. K. Sadrnezhaad, D. Salehi Doolabi and M. Asadirad, Influence of Pulse Parameters on Electrocodeposition of Cr–Al_2O_3 Nanocomposite Coatings From Trivalent Chromium Bath, International Heat Treatment and Surface Engineering 2012, 6 (4), 178- 184.

[66] M. Noroozifar, M. Khorasani-Motlagh, Z. Yavari, Effect of Nano-TiO_2 Particles on the Corrosion Behavior of Chromium-Based Coatings, Int. J. Nanosci. Nanotechnol. 2013, 9(2), 85-94.

[67] M. A. Juneghani, M. Farzam, H. Zohdirad, Wear and Corrosion Resistance and Electroplating Characteristics of Electrodeposited Cr–SiC Nano-composite Coatings Trans. Nonferrous Met. Soc. China 2013, 23, 1993–2001.

[68] H. Wenting, Z. Liqun, N. Haiyang, L. Huicong, and L. Weiping, Thin Film of Zn/rGO Nanocomposites Fabricated by Electrodeposition, International Journal of Materials Science and Engineering 2013, 1(1), 32-35.

[69] L. Exbrayat, E. Calvi, T. Douillard, G. Marcos, C. Savall, C. Berziou, J. Creus, and P. Steyer, Role of Ceria Nanoparticles on the Electrodeposited Zinc Coating's Growth: Interest of a TEM-Scale Investigation, ECS Electrochemistry Letters 2014, 3 (9), D33-D35.

[70] Y. Ullal, A. Chitharanjan Hegde, Corrosion Protection of Electrodeposited Multilayer Nanocomposite Zn-Ni-SiO_2 Coatings, Электроннаяобработкаматериалов, 2013, 49(2), 73–79.

[71] I. Constantinescu, F. Oprea, O. Mitoseriu, A Comparative Study of the Properties of Zinc-SiO_2 and Zinc-Al_2O_3 Composite Layers, The 4th International Conference Advanced Composite Materials Engineering COMAT 2012, 18- 20 October 2012, Brasov, Romania.

[72] A. Gomes, T. Frade and I. D. Nogueira, Morphological Characterization of Zn-Based Nanostructured Thin Films, Current Microscopy Contributions to Advances in Science and Technology, (Edit.A. Méndez-Vilas,), Formatex Research Center-Spain, 2014.

[73] J. Cho, A. R Boccaccini, M. SP Shaffer, Ceramic Matrix Composites Containing Carbon Nanotubes, Journal of Materials Science 2009, 44(8), 1934-1951.

[74] M. Rosso, "Ceramic and Metal Matrix Composites: Routes and Properties", Journal of Materials Processing Technology 2006, 175, 364–375.

[75] R. Toledano, R. Okner and D. Mandler, Electrochemical Codeposition of Ceramic Nanocomposite Films, ENS'07 Paris, France, 3-4 December 2007.

[76] I. Zhitomirsky and X. Pang, Electrodeposition of Polymer-metal and Polymer-ceramic Nanocomposites, 207th ECS Meeting, 2006.

[77] M. Oliveira and A.V. Machado, Nanocomposites: Synthesis, Characterization and Applications, (Edit. X. Wang), Chapter 4. Preparation of Polymer-Based Nanocomposites by Different Routes, Nova Science Publisher, 2013.

[78] X. Luo, Electrically Conductive Metal Nanowire Polymer Nanocomposites, Ph. D. thesis, University of Alberta, USA, 2013.

[79] A. B. Moghaddam, T. Nazari, J. Badraghi, M. Kazemzad, Synthesis of ZnO Nanoparticles and Electrodeposition of Polypyrrole/ZnO Nanocomposite Film, Int. J. Electrochem. Sci., 2009, 4, 247 – 257.

[80] P. Satyananda, K. Balasubramanian, V. Thirukkallam, K. Varadarajan, Synthesis and Characterization of Metal Nanoparticle Embedded Conducting Polymer–Polyoxometalate Composites, Nanoscale Res Lett 2008, 3, 14–20.

[81] A. Ganash, Anticorrosive Properties of Poly (o-phenylenediamine)/ZnO Nanocomposites Coated Stainless Steel, Journal of Nanomaterials 2014, (2014), Article ID 540276, 8 pages.

[82] C. A. Ferreira, S.C. Domench and P.C. Lacaze, Synthesis and Characterization of Polypyrrole/TiO_2 Composites on Mild Steel, Journal of Applied Electrochemistry 2001, 31, 49-56.

[83] J. M. Ko, D.Y. Park, N.V. Myunga, J.S. Chungb, K. Nobe, Electrodeposited Conducting Polymer–magnetic Metal Composite Films, Synthetic Metals 2002, 128, 47–50.

[84] Y. Lattach, J. F. Rivera, T. Bamine, A. Deronzier, and J. Moutet, Iridium Oxide–Polymer Nanocomposite Electrode Materials for Water Oxidation, ACS Appl. Mater. Interfaces 2014, 6, 12852−12859.

[85] L. Benea, M. Mardare-Pralea, Electrodeposition of UHMWPE Particles with Cobalt for Biomedical Applications, Digest Journal of Nanomaterials and Biostructures 2011, 6(3), 1025-1034.

Chapter 2

Effects of Electroplating Characteristics on the Coating Properties

Ebru Saraloğlu Güler

Additional information is available at the end of the chapter

http://dx.doi.org/10.5772/61745

Abstract

Electroplating parameters that can be listed as bath temperature, pH of the bath, current density, surfactant addition or type, coating thickness must be controlled during the deposition process since they determine the properties of the coating. However, it is difficult to manage the effects of this high number of parameters including their interaction effects. At this point, fractional factorial design that is a statistical method steps in that have the advantage of evaluating the influences and the complex variable interactions of parameters with a plausible number of experiments. In the design low and high values must be attributed to the parameters before the experiments and these values are selected according to the solution used. There are suitable plating conditions (written in handbooks) for each bath without particle addition and low – high values can be chosen between these ranges or just below or above them. For instance, the temperature range is 40-60°C, current density range is 2-7 A/dm^2 and pH range is 3.5-4.0 for nickel electroplating [36]. Besides the coating property, the electroplating parameters influence the hydrogen evolution reaction that is a side reaction that takes place at the cathode and may lead to morphological problems on the coated surface. The aim of this chapter is to provide information about how the parameters affect the amount of particles in the deposit. Because the reason of adding the particles to the bath is to improve the matrix properties by the particles emerged. So the more particles present and disperse in the coating, the more they will contribute to the coating property. Another important effect is the internal stress that led to departure of the deposit.

Keywords: Electroplating parameters, coating properties, composite deposition, electrocodeposition, particle concentration

1. Introduction

The electroplating method can be used to produce composite coatings by adding particles in the metal plating bath. The particles are trapped in the coating during deposition. Composite

coatings are composed of an electrodeposited metal matrix and dispersed solid particles. The metal powders, metal alloy powders and metal oxide powders of Al, Co, Cu, In, Mg, Ni, Si, Sn, V, Zn and nitrides of Al, B, Si and C (graphite or diamond) and carbides of B, Bi, Si, W and MoS_2 and organic materials such as polytetrafluoroethylene (PTFE) and polymer spheres are used as the particles [40].

The main application areas of the composite deposition are electronic, biomedical, telecommunication, automotive, space and consumer applications where high strength, equiaxed micro-components are required.

The electroplating parameters must be controlled during electrodeposition since they have significant effect on the coating properties, deposition efficiency and hydrogen evolution. Besides the current density, pH of the bath, bath temperature that places among the main electroplating parameters [36], there are more parameters including the type, the size, the concentration of the particles [37] and the addition of surfactants and their types [20]. The main properties of the coating can be listed as the corrosion resistance in TiO_2 – nickel coating [38], tribological properties in MoS_2 – nickel coating [4], mechanical properties in TiO_2 – nickel coating [38], internal stress in MoS_2 – nickel coating [9], texture in chromium – carbon deposit [39], particle content of the deposit [24] are severely affected by the electroplating parameters.

The aim of this chapter is to emphasize on the electroplating parameters, their effects and interaction effect on the coating properties. Particle incorporation in the deposit is an important property that must be analysed since composite electroplating aroused in order to improve the matrix properties with particle addition. Another important property is the internal stress that must kept at minimum levels not to disrupt the deposit.

2. Electroplating parameters

2.1. Current density

Electrodeposition process consists of two steps that are nucleation, growth mechanisms and thickening of the primary layer. The nucleation is enhanced by high current density unlike the growth process [1]. Thus, smaller grain sizes are observed at higher current densities due to the increase in the nucleation rate [2]. On the other hand, high current density increases pH in the vicinity of the electrode during the reduction process that creates a competition between metal deposition and hydrogen gas [6] [3]. Hydrogen evolution contributes to the internal stress in the deposit [4][5]. Therefore, it is important to figure out the current density values at which hydrogen evolution does not occur together with metal deposition [4].

The current density also affects the particle content in the deposit. The particle (WC) content of the coating increases linearly with an increase in the current density from 0.1 to 0.5 A/dm^2 regardless of the particle diameters [7]. On the other hand, Kuo [6] claims that the particle (MoS_2) content in the deposit decreases when the current density increases from 4 to 8 A/dm^2. According to the results of Hu and Bai [41], increasing current density generally increased the particle content but the effect of current density depends on pH. Figure 1 shows that when

http://dx.doi.org/10.5772/61745

the current density (B) is increased, the particle content is increasedwhen pH (C) is 1 and decreased when pH is 5 [41].

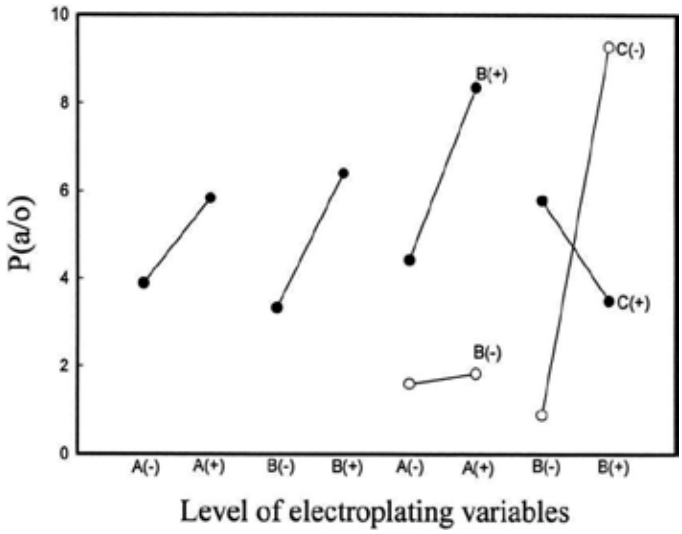

Figure 1. The effects and interaction effects of parameters on the atomic percent of phosphorus in the deposit. A: main effect of temperature, B: main effect of current density, BxC: current density – pH interaction effect, AxB: temperature – current density interaction effect [41]

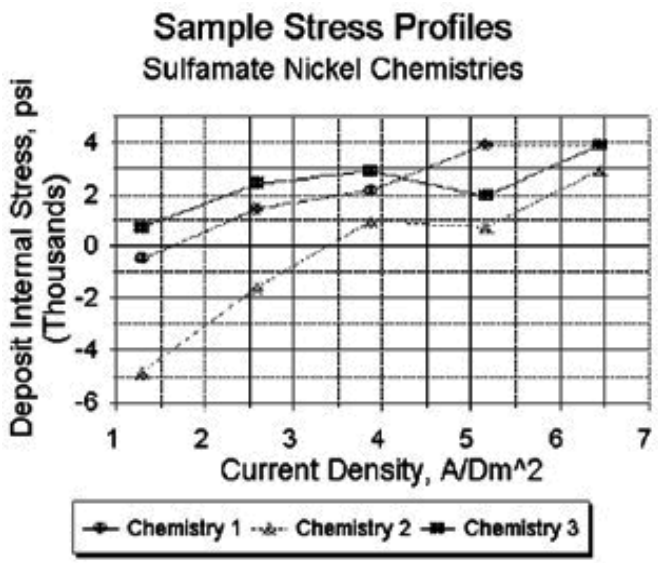

Figure 2. Stress behaviour for sulfamate nickel electrolytes with three different chemistries [42]

Another effect of increasing current density from 0.15 to 5 A/dm^2 is increasing the internal stress [8] since the stress stems from the residual stresses. However significant effect cannot be detected when the current density increased from 1.2 to 4.8 A/dm^2 [9] because the effect of current density on the internal stress depends on the electroplating solution composition. Figure 2 shows the effect of changing only one component amount of the solution on the current density dependence of the internal stress [42]. Moreover the effect of the current density depends on pH.

2.2. pH of the bath

The effect of pH on particle incorporation is dependent on the nature of the particles. For instance, when MoS_2 particles are used as the incorporate particles, the effect of pH value on the particle content in deposit was insignificant. Nevertheless it can be concluded that increasing pH decreased the amount of particles present in the coating [6]. However, incorporated particles are significantly decreased when pH is below 2 in Al_2O_3-Ni coating pair [11]. In addition, decreasing pH is preferred to manage the internal stress. Low pH values, less than 5, are selected to obtain acceptable stress levels [10]. Increase in pH of the solution may lead to discharge of hydroxyl ions instead of nickel dissolution and oxygen evolution [10] resulted in high internal stresses. It is also concluded that the internal stress was increased when the pH was increased from 2 to 4 in MoS_2 – Ni system [12].

3. Bath temperature

The effect of the temperature on the particle content in the deposit depends on the type of the particle. There is a small increase in the particle (MoS_2) content in coating with increasing the temperature 30, 40, 50 respectively [6]. It was mentioned that the temperature has an insignificant effect. For instance, no effect of temperature was detected in $BaCr_2O_4$-Ni [13] and Al_2O_3-Ni [14] coating couples. Because, the applied voltage is the main parameter that directly affects the activity of the reaction. In addition, Ni deposits more efficiently with increase in temperature. On the other hand, the influence of the temperature was reported as positive up to certain point. After that point, the amount of particles decreases with increasing the temperature.

General trend on the effect of the bath temperature on the internal stress is positive, meaning that increasing temperature decreases the internal stress. On the other hand, according to some of the studies the stress is more influenced by the current density regardless of the temperature [10].

Another advantage of the high temperature is the polarization effect. It is known that concentration polarization is the component of the polarization which is due to the change in the electrolyte concentration that stems from the current flow through the electrode – solution interface. So, the electrochemical cell potential difference deviates from its equilibrium value. Concentration polarization is decreased by increasing temperature because diffusion layer thickness gets smaller and ionic diffusion increases.

http://dx.doi.org/10.5772/61745

On the other hand, high temperature values increases energy consumption and supply heat for bath evaporation. Furthermore, thermal stresses will arrive at high processing temperatures and can become a serious problem especially when the coating and substrate have different thermal expansion coefficients. Therefore, an optimum plating temperature must be preferred to satisfy energy consumption and the coating quality.

4. Particle type

It is a common fact that if the amount of the particles in the solution is increased, the particle content in the deposit will also increase up to a certain point. However the type of the particle also acts as an important parameter. Both of the conductive and non-conductive particles have their own advantages against each other. Because conducting particles (molybdenum disulfide, chromium carbide, zirconium diboride, graphite) attracted to the cathode then act as depositing sites which resulted in dendritic growth [15]. Despite the advantage of easily attraction of conducting particles to the cathode, selective deposition on the conducting sites led to increased surface roughness.

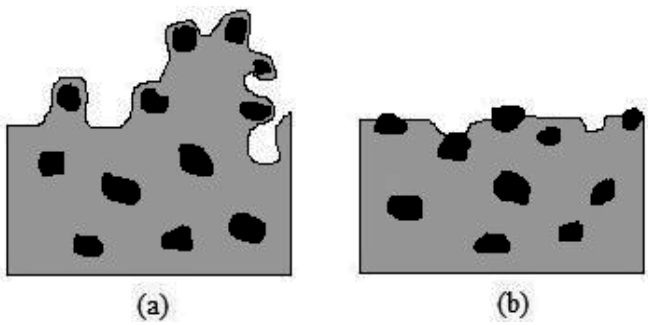

Figure 3. Schematic view of the composite coating including a) conducting and b)non-conducting particles

On the other hand, non-conductive particles end up with smoother deposit surfaces with low porosity [15].

Mechanical properties can be changed by the type of the incorporated particles. For instance, PTFE in Ni matrix increases wear resistance [16], MoS_2 incorporated with Ni decreased the coefficient of friction [9], Al_2O_3 and SiC dispersed in Cu increased the microhardness of the coatings [17]. Moreover, wear and corrosion resistance can be improved by the addition of silicon carbide nano-particles [18] [19].

5. Particle size

Small particle sizes can be agitated easily and led to an increase in the particle concentration in the deposit during composite electroplating. For example, the amount of particles is

increased by decreasing the particle size in Ni/SiC system [21]. Furthermore, the effect of particles in decreasing the friction coefficient is more effective when the particle size is decreased in Ni-MoS_2 system [9].

6. Particle concentration

Generally, increasing the particle concentration in the bath increases the weight percentage of particles in the deposit up to a certain point [9] [22] [23]. That point can be thought like the saturation point. There is a rapid increase in the particle amount in the low particle concentration regions whereas a slight increase occurs in the high concentration regions. The collisions between particles and cathode determine the codeposition of the particles and they are diminished in the high MoS_2 concentration region resulting in slight increase or decreased particle amount in the growing metal deposit [6].

7. Surfactant addition / type

Coating performance can be developed by the addition of the surfactants like (cetyltrimethylammonium bromide (CTAB), sodyumdodecyl sulfate (SDS), and saccharine [20]. The advantage of adding surfactants is their dispersing effect of particles. Thus the property of the particles will be uniform on the surface. Surfactants adsorb on the particles and favor the distribution of the particles [24].

Surfactants are indispensable especially for the hydrophobic particles (fluorographite, MoS_2) to be dispersed in the electroplating solution. Surfactants like sodium lauryl sulphate enhanced the electrostatic adsorption of suspended particles on cathode surface by increasing their positive charges [25]. Similarly, azobenzene (AZTAB) promoted particle deposition into the nickel matrix by their more positive reduction potential than that of nickel [26]. Another surfactant, cetyl trimethyl ammonium bromide (CTAB) has an advantage of increasing the volume percentage of SiC in the deposit besides homogeneous and non-agglomerated distribution of particles in SiC-nickel composite coatings [27].

Further advantage of the surfactants is suppressing the hydrogen evolution reaction. For example, saccharin which is an anionic surfactant is an effective way to overcome the hydrogen evolution problem [34].

The surfactants can be grouped under two main headings which are anionic and cationic surfactants according to their charges. Cationic surfactants increased the particle incorporation in the coating [28] [29] [30] [31]. Anionic surfactants may have positive or negative effect on the codeposition efficiency of the particles depending on the particle type and bath solution. For instance, SDS which is an anionic surfactant did not affect the codeposiston of particles [31]. On the other hand, cationic surfactants have the advantage of adsorbing

http://dx.doi.org/10.5772/61745

on the particles that have negative surface charge [29]. Therefore, a net positive charge was formed by the adsorption of cationic surfactants that inhibited the formation of particle clusters and led to more stable particle suspension in the bath. Moreover, this positive charge improved the tendency of particles to move towards cathode and increased the amount of particles in the deposit [29] [30]. For instance, addition of cationic surfactant benzyl ammonium salts (BAS), increased the amount of MoS_2 codeposition [32]. In addition, BAS adsorbed on MoS_2 particles decreased the conductivity of the particles and resulted in homogeneous deposition of nickel and MoS_2 particles [32] [15]. On the other hand, it was stated that anionic surfactants in the electrolyte can give particles a negative charge and make them to move towards the substrate [35].

The disadvantage of the surfactants may occur if there are unabsorbed free surfactants, because they could lead to stress development and brittleness in the deposit [33]. Since the amount of incorporated surfactant is generally very small, their undesirable effects may be ignored [33]. However, increasing surfactant (CTAB) amount caused an increase in the internal stress due to the high possibilty of embedded CTAB in the nickel matrix [32].

8. Fractional factorial design

2^{n-1} fractional factorial design is a statistical design that can be used to identify the effects of n electrodeposition variables on the coating properties with the reasonable number of experiments. In addition, the interaction effects of the parameters can be analyzed by the help of fractional factorial. The property of the coating in other words the response value in the program is generally taken as the amount of particles in the deposit during composite coatings. For instance, in the study of Hu and Bai [41], phosphorus content in the deposit was taken as the response value and temperature, current density pH, NaH_2PO_2 H_2O concentration of the solution and agitation rate were taken as the electroplating parameters. Another most commonly used response value during composite coating is internal stress. Electroplating parameters were MoS_2 particle concentration, temperature, pH, current density and coating thickness where the response value is the internal stress in the study of Saraloglu Guler et. al. [9]. Other response values can be listed as friction coefficient, corrosion resistance, wear resistance, hardness which are the properties obtained by particle addition so increased amount of particle content in the deposit will have a positive effect on these values. The hydrogen evolution reaction must also be considered during this selection. The effects of the electroplating parameters on hydrogen evolution reaction can be studied before the composite deposition in order to determine the current density range where H_2 is not simultaneously discharged with Ni plating [12].

Fixed limit values that are said to be low (-1) and high (1) levels are selected for the electroplating parameters in fractional factorial design. Table 1 shows the parameters and their low and high fixed limit values for levels of fractional factorial design.

Electroplating Characteristics	Properties of the Coating
Current density	The coefficient of friction
pH of the bath	Wear resistance
Bath temperature	Corrosion resistance
Particle concentration of the bath	Mechanical Properties
Particle size	Internal Stress
Particle type	Texture formation
Surfactant addition/ type	Particle content of the deposit
	Grain size
	Electrodeposition/ particle uniformity

Table 1. The electroplating parameters and the properties of the deposit

Author details

Ebru Saraloğlu Güler

Address all correspondence to: esaraloglu@gmail.com

Baskent University, Ankara, Turkey

References

[1] Pletcher D.. Industrial Electrochemistry. Springer Netherlands; 1984. 325 p.

[2] Bockris J.O'M., Conway B.E., White R.E., editors. Modern Aspects of Electrochemistry. New York: Springer; 1992. 551 p.

[3] Schlesinger M., Paunovic M., editors. Modern Electroplating. 5th ed. John Wiley & Sons; 2010. 736 p.

[4] SaralogluGulerE..Electrocodeposition of molibdenum disulfide particles in nickel [thesis]. Turkey: Middle East Technical University; 2013. 94 p.

[5] Mizushima I., Tang P.T., Hansen H.N., Somers M.A.J.. Residual stress in Ni - W electrodeposits. Electrochim. Acta. 2006;51(27):6128.

[6] Kuo S.L.. The Influence of Process Parameters on the MoS2 Content of Ni-MoS2 Composite Coating by the Robust Design Method. Journal of the Chinese Institute of Engineers. 2004;27(2):243-251.

[7] Nunez M., editor. Metal Electrodeposition. New York: Nova Science; 2005.

[8] Pathak S., Guinard M., Vernooij M.G.C., Cousin B., Wang Z., Michler J., Philippe V.. Influence of lower current densities on the residual stress and structure of thick nickel electrodeposits. Surface Coating Technology. 2011;205(12):3651.

[9] SaralogluGuler E., Karakayaİ., KoncaE.. Effects of current density, coating thickness,temperature, pH and particle concentration on internal stress during Ni–MoS2 electrocodeposition. SurfaceEngineering. 2014;30(2):109-114.

[10] Lowenheim F. A., editor. Modern Electroplating. 3rd ed. NewYork: Wiley; 1974. 801 p.

[11] Alkire R.C., Kolb D. M., editors. Advances in Electrochemical Science and Engineering. Germany: Wiley; 2002.

[12] Saraloglu Guler E., Konca E., Karakaya İ.. Effect of Electrodeposition Parameters on the Current Density of Hydrogen Evolution Reaction in Ni and Ni-MoS2 Composite Coatings. International Journal of Electrochemical Science. 2013;8:5496 - 5505.

[13] Quyang J.H., Liang X.S., Wen J., Liu Z.G., Yang Z. L.. Electrodeposition and Tribological Properties of Self-lubricating Ni–BaCr2O4 Composite Coatings. Wear. 2011;271(9-10)

[14] Alkire R.C., Kolb D.M., editors. Advances in Electrochemical Science and Engineering. 7th ed. Verlag: Wiley; 2001. 193-223 p.

[15] Abi-Akar H., Riley C.. Electrocodeposition of Nickel-Diamond and Cobalt-Chromium Carbide in Low Gravity. Chemistry of Materials. 1996;8(11):2601–2610.

[16] You Y., Gu C., Wang X., Tu J.. Electrochemical Preparation and Characterization of Ni–PTFE Composite Coatings from a Non-Aqueous Solution Without Additives. Int. J. Electrochem. Sci.. 2012;7:12440 - 12455.

[17] Stankovic V.D., Gojo M.. Electrodeposited composite coatings of copper with inert, semiconductive and conductive particles. Surface and Coatings Technology. 1996;81(2-3):225–232.

[18] Shi L., Sun C., Gao P., Zhou F., Liu W.. Mechanical properties and wear and corrosion resistance of electrodeposited Ni–Co/SiC nanocomposite coating. Applied Surface Science. 2006;252(10):3591–3599.

[19] Yao Y., Yao S., Zhang L., Wang H.. Electrodeposition and mechanical and corrosion resistance properties of Ni–W/SiC nanocomposite coatings. Materials Letters. 2007;61(1):67–70.

[20] Fahami A., Nasiri-Tabrizi B, Rostami M., Ebrahimi-Kahrizsangi R.. Influence of Surfactants on the Characteristics of Nickel Matrix Nanocomposite Coatings. ISRN Electrochemistry. 2013;2013

[21] Garcia I., Fransaer J., Celis J.P.. "Electrodeposition and sliding wear resistance of nickel composite coatings containing micron and submicron SiC particles. Surface and Coatings Technology. 2001;148(2-3):171–178.

[22] Chang Y.C., Chang Y.Y, Lin C.I.. Process Aspects of the Electrolytic Codeposition of Molybdenum Disulfide with Nickel. Electrochimicia Acta. 1998;43(3-4):315-324.

[23] Huang Z.J., Xiong D.J.. MoS2 Coated with Al2O3 for Ni-MoS2 / Al2O3 Composite Coatings by Pulse Electrodeposition. Surface Coatings Technology. 2008;202(14): 3208–3214.

[24] Walsh F.C., Ponce de Leon C.. A review of the electrodeposition of metal matrix composite coatings by inclusion of particles in a metal layer: an established and diversifying technology. Transactions of the IMF. 2014;92(2):83-98.

[25] Sharma G., Yadava Y.K., Sharma V.K.. Characteristics of Electrocodeposited Ni–Co–SiC Composite Coating. Bulletin of Materials Science. 2006;29(5):491-496.

[26] Shrestha N.K., Kawai M., Saji T.. Co-deposition of B4C particles and nickel under the influence of a redox-active surfactant and anti-wear property of the coatings. Surface & Coatings Technology. 2005;200:2414–2419.

[27] Hou K.H., Ger M.D., Wang L.M, Ke S.T.. The wear behaviour of electro-codeposited Ni–SiC composites. Wear. 2002;253(9-10):994–1003.

[28] Ouyang J., Liang X., Wen J., Liu Z., Yang Z.. Electrodeposition and tribological properties of self-lubricating Ni—BaCr2O4 composite coatings. Wear. 2011;271(9-10): 2037–2045.

[29] Shrestha N.K., Sakurada K., Masuko M., Saji T.. Composite coatings of nickel and ceramic particles prepared in two steps. N. K. Shrestha, K. Sakurada, M. Masuko and T. Saji,. 2001;140(2):175–181.

[30] Shrestha N.K., Masukob M., Saji T.. Composite Plating of Ni/SiC Using Azo-cationic Surfactants and Wear Resistance of Coatings. Wear. 2003;254(5-6):555–564.

[31] García-Lecina E., García-Urrutia C., Díez J.A., Fornell J., Pellicer E., Sort J.. Codeposition of inorganic fullerene-like WS2 nanoparticles in an electrodeposited nickel matrix under the influence of ultrasonic agitation. Electrochimica Acta. 2013;114:859–867.

[32] Wang L.M.. Journal of Applied Electrochemistry. Effect of surfactant BAS on MoS2 codeposition behaviour. 2008;38(2):245-249.

[33] Hovestad A., Jansen L.J.J.. Electrochemical codeposition of inert particles in a metallic matrix. Journal of Applied Electrochemistry. 1995;25(6):519-527.

[34] Popov B.N., Yin K., White R.E.. Galvanostatic Pulse and Pulse Reverse Plating of Nickel-Iron Alloys from Electrolytes Containing Organic Compounds on a Rotating Disk Electrode. Journal of The Electrochemical Society. 1993;140(5): 1321-1330.

[35] Wünsche F., Bund A., Plieth W.. Investigations on the electrochemical preparation of gold-nanoparticle composites. J. Solid State Electrochem. 2004;8:209-213

[36] Nickel Institute. http://www.nickelinstitute.org/ [Internet]. 2013. Available from: http://www.nickelinstitute.org/~/Media/Files/TechnicalLiterature/NPH_141015.pdf

[37] Ahmad Y H., Mohamed M.A.. Electrodeposition of Nanostructured Nickel-Ceramic Composite Coatings: A review. Int. J. Electrochem. Sci.. 2014;9:1942 - 1963.

[38] Shao W., Nabb D., Renevier N., Sherrington I., Luo J.K.. Materials Science and Engineering. Mechanical and corrosion resistance properties of TiO2 nanoparticles reinforced Ni coating by. 2012;40

[39] Yar-Mukhamedova G.S.. Investigation of the Texture of Composite Electrodeposited Chromium–Carbon Coatings. Materials Science. 2000;36(5):752-754.

[40] Palumbo G., Brooks I., Mccrea J., Hibbard G.D., Gonzales F., Tomantschger K.. Process for Electroplating Metallic and Metal MAtrix Composite Foils, Coatings and Microcomponents. European PAtent Specification. 2008;EP 1 516 076 B1

[41] Hu C., Bai A.. Composition control of electroplated nickel]phosphorus. Surface and Coatings Technology. 2001;137:181]187.

[42] Stein B.. A Practical Guide to Understanding, Measuring and Controlling Stress in Electroformed Metals. In: ESF Electroforming Symposium; Las Vegas. Las Vegas: 1996.

Chapter 3

Parametric Variables in Electro-deposition of Composite Coatings

Peter Odetola, Patricia Popoola, Olawale Popoola and David Delport

Additional information is available at the end of the chapter

http://dx.doi.org/10.5772/62010

Abstract

Nowadays, synergy of the attractive properties of materials while avoiding limitations of their use in isolation is a major driver for flexibility in design and manufacture. This allows tailoring of materials' properties to meet specifications. Composite technology utilizes an excellent combination of properties: strength, stiffness, light weight, wear, chemical, corrosion, and temperature resistance, which transcend those of the constituent materials. Engineering structures, equipment, and vessels in key industries that are material-dependent are susceptible to deterioration process and damage over time in their service conditions. Composite coatings through electro-deposition offer a reliable cost-effective means of impacting special surface properties for corrosion protection, better appearance, and mechanical properties' enhancement. The properties of the composite coatings can be optimized by varying the type, size, amount and distribution of the particles content incorporated among others.

Keywords: Co-deposition, Nano-particles, Current density, Micro-hardness, Agglomeration, Metal deposit and Microstructure

1. Introduction

1.1. Composite coating

A composite coating is a multi-phase coating with well-controlled phase distribution and geometry to optimize the properties of the matrix phase and reinforcement co-deposited phase or phases. Composite coatings have been used to achieve combination of specific properties of corrosion and wear resistance, corrosion inhibition and electrical conductivity, tribological control and self-lubrication. At times, two apparently opposed properties are specified such as high tensile strength and at the same time high ductility. The most common applications

include controlling corrosion of various structures like steel, bridges, offshore platforms, underground pipelines, and mechanical driving equipment.

1.2. Nanotechnology applications in composite coating

Based on the principles that govern material behavior, it has been established that a material or device with particles size less than 100 nm length is in the nanotechnology domain. These particles primarily promote the mechanical and metallurgical properties of composite coatings in the areas of micro-hardness, corrosion resistance and tribological control and frictional and wear properties. Therefore, nanotechnology helps in characterizing the co-deposit of composite coatings to enhance specific features in the coating formulation.

Nanotechnology applications in coatings have gained tremendous ground in research and developments in recent years. This is a result of two factors:

- Increased availability of different types of nanoparticles of metal oxides, metal carbides and clays
- Advancements in technologies that can handle inert particles of a different material in the metal matrix coating structure at the nano-scale

1.3. Electro-deposition

Electro-deposition is a deposition technique that applies metallic coatings to metallic or other conductive surfaces through electrochemical processes. It is an excellent means of producing a composite coating successfully on metal surfaces. In this method, the distribution of particles is uniform, the rate of deposition is high, and the temperature of operation is low (i.e., < 100^0C). Compared to high-temperature methods such as pyrometallurgy and powder metallurgy, control of the microstructure and composition is easier.

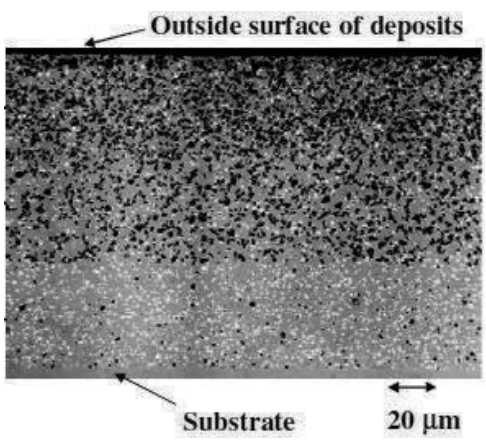

Figure 1. Co-deposition of nanoparticles on metal substrate (Low et., al) [1]

http://dx.doi.org/10.5772/62010

1.4. Purpose of electroplating

- **Functional applications:** It is used principally to apply metal coatings that impart specific surface properties such as wear and abrasion resistance, tribology control and self-lubricating property, reflectivity, and conductivity.
- **Decorative and protective applications:** Metals such as tin, zinc, and steel, which are not really attractive in appearance, are plated to give them an aesthetic look and protective outer layer. Chromium, nickel, brass, copper, and precious metals such as gold, platinum and titanium are common metals applied to variety of items.
- **Corrosion control applications:** Electroplating is applied on metal to enhance materials' surface properties and also impart corrosion resistance. For instance, tin-plated food containers are highly resistant to corrosion and so can preserve their content well.

1.5. Electro-deposition parameters

The structure and properties of composite coatings depend on many parameters, including:

- Particle characteristics (type, shape, size, particle concentration, surface charge)
- Electrolyte composition (electrolyte concentration, additives, temperature, pH, surfactant type and concentration)
- Current density (direct current, pulsed current, pulse time, duty cycle, potentiostatic control)
- Hydrodynamics (laminar, mixed, turbulent regimes)
- Electrode geometry (rotating disk electrode, rotating cylinder electrode, plate-in-tanks, parallel plate electrodes, and many variations).

Owing to their high surface energy, reinforcement particles can be easily agglomerated. Subsequently, obtaining uniform distribution of these particles is an important aim that can be achieved in optimum parameters.

1.5.1. Particle type and concentration

Particle size influences the rate of incorporation into the metal deposit. The rate of incorporation of metal deposit per unit volume is inversely proportional to the nanoparticles size. The volume fraction of nanoparticles in the metal deposit increases substantially when the amount of nanoparticles concentration in the solution increases. A saturation state of particles in the deposit is reached at high nanoparticle concentration in the solution.

1.5.2. Pulse frequency

Micro-hardness as well as co-deposition of particles increases on variation of frequency from 0.1Hz to 10Hz and is followed by sharp decrease from 10Hz to 100Hz frequency. For frequencies below 10Hz, reduction rate of metal ions is higher as compared to ions adsorbed on nanoparticles, which reduce the nanoparticles content in the composite coating. At very high

frequency, the content of nanoparticles in composite reduced because the shorter OFF time is not enough to remove concentration gradient of nanoparticles adjacent to the cathode. Wear loss and micro-hardness of composites significantly decreases when pulse frequency increases from 10Hz to 1000Hz. Significant adhesive wear is observed at higher frequencies.

1.5.3. Current density

By definition, current density is the current per unit surface area of the cathode. It is expressed in mA/cm^2 of surface of the electrode.

Current density actively governs metal deposition and co-deposition process. An increase in current density results in more rapid deposition of the metal matrix and fewer particles are embedded in the coating. To obtain uniform deposition, the current density must be minimal, so that the rate of particles' incorporation into the growing metal will exceed the adsorption on the cathode. Reinforcement of nanoparticles into metal matrix not only restrains the grain growth but also reduces the plastic deformation of metal matrix by combined effect of grain refining and dispersion strengthening, resulting in significant increase in hardness of composite coatings.

The current density can be measured in the following terms:

- Direct current
- Pulsed direct current
- Pulsed reverse current.

Direct current technique is based on the concept that the incorporation of nanoparticles occurs simultaneously with the reduction reaction of an ionic species to form the metal surface. **Pulsed direct current** works on the concept of alternating two or more direct cathodic currents for various deposition times. This allows the incorporation of higher concentrations of nanoparticles as well as producing a wider range of deposit compositions and properties. **Pulsed reverse current** technique, as the name connotes, has similar characteristics but imposes a cathodic current during the ON time and an anodic current during the OFF time. This method has been the most successful for incorporating higher concentrations of nanoparticles because it helps to eliminate a fraction of the electrodeposited metal during the OFF time. Pulse reverse current technique ensures refine surface microstructure, increased incorporation rate of nanoparticles into the metal deposit and uniform size selective entrapment of particles. During the anodic period, larger sizes of nanoparticles dissolve, whereas smaller nano-particles continue to be entrapped.

1.5.4. Duty cycle

As duty cycle increases from 10 to 100%, micro-hardness as well as incorporated particles decrease significantly. Lower duty cycle gives longer OFF time for arrival of nanoparticles at the double layer. Therefore, more nanoparticles are reinforced in composite coatings at lower duty cycle and coatings become harder. The improvement in hardness at lower duty cycle is mainly due to grain refinement at pulse OFF-time longer than ON-time.

http://dx.doi.org/10.5772/62010

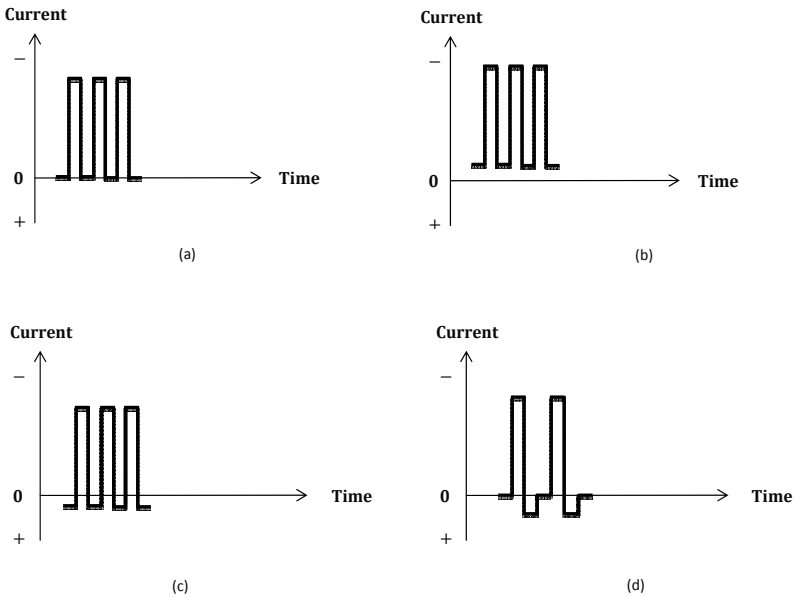

Figure 2. Showing different phases of current density during deposition (a) Pulse direct current with zero current during off time; (b) Superimposed pulse direct current with cathodic current during off-time; (c) Pulse reverse current with anodic current during off time; (d) Pulsed reverse current with combination of zero and anodic current during off time.

1.5.5. Bath agitation

Electrolyte agitation increases convection of bath contents and therefore enhances the flux of the particles reaching the cathode surface. Intensive agitation may cause adverse effect by disconnection and removal of the particles by turbulent streams of the electrolyte.

Bath agitation serves the purposes of keeping the particles evenly distributed, well suspended in the electrolyte and effectively transported to the cathode surface. Excessive agitation has tendency of removing particles from cathode surface before they can be embedded in the metal deposit. This is due to turbulence initiated by the electrolyte in the bath.

For industrial applications, the popular methods used in open tanks include the overhead blade stirrer, the reciprocating plate plunger or a pumped recycle loop of the electrolyte. For laboratory investigations, magnetic stirrers, rotating disk or cylinder electrodes and parallel plate channel flow can be employed. In contrast, the commonly used plate-in-tank geometry provides poorly defined fluid flow conditions.

1.6. Nano-composite Coatings

The backbone of composite coating is multi-phase union of matrix and second-phase particles in correct ratio. Matrix plays the role of continuous phase and the solvent to disperse the second phase.

Types	Chemical Compositions	Concentrations
Watts Bath	*Nickel sulphate:* $NiSO_4 \cdot 7H_2O$	$240g/l$
	Nickel chloride: $NiCl_2 \cdot 6H_2O$	$20g/l$
	Boric acid: H_3BO_3	$30g/l$
Sulphate Bath	*Nickel sulphamate:* $Ni(SO_3 \cdot NH_2)_2$	$300-450g/l$
	Nickel chloride: $NiCl_2 \cdot 6H_2O$	$0-30g/l$
	Boric acid: H_3BO_3	$30-45g/l$
Chloride Bath	*Nickel sulphate:* $NiSO_4 \cdot 7H_2O$	$50-75g/l$
	Nickel chloride: $NiCl_2 \cdot 6H_2O$	$100-130g/l$
	Boric acid: H_3BO_3	$50-55g/l$

Table 1. Different types of electrolytic baths

Composite coating can be classified on the basis of the matrix and the reinforcing co-deposited particles. The matrix phase on a broader scale can be grouped into:

- Metal matrix
- Ceramic matrix
- Polymer matrix

The common metals used as matrices for electrolytic co-deposition are: Silver (Ag), Chromium (Cr), Cobalt (Co), Iron (Fe), Zinc (Zn), Nickel (Ni), Copper (Cu) and Gold (Au).

A variety of composite coatings can be deposited by reinforcing different nanoparticles. Reinforcement particles can be carbides (TiC, SiC, WC,Cr_2C_3)[2,3,4,5,6,7], borides [8], oxides (ZnO, In_2O_3, ZrO_2, CeO_2, Al_2O_3,Cr_2O_3,SiO_2,TiO_2) [9,10,11.12], graphite, diamond, or solid lubricants, such as polyethylene and polytetrafluoroethylene [13,14]. Variable amounts of these particles in the coatings become precipitated to impart special properties to the deposited layers. These properties mainly depend on the microstructure of the matrix phase of a composite coating and the amount and distribution of co-deposited particles (non-metallic inclusions) which are influenced by many process parameters.

2. Literature review

2.1. Categories of Co-deposition of particles

2.1.1. Co-deposition of wear-resistant particles

Nano-diamond particles dispersed in Ni-Co matrix form good composite coating on AISI 1045 steel substrate [15]. This composite coating formed in a Watts-type bath using electro-

http://dx.doi.org/10.5772/62010

deposition showed enhanced hardness coupled with excellent anti-wear performance and lower frictional coefficient. This was due to well-dispersed diamond particles in the Ni-Co matrix and better wetting and bonding ability between the nano-diamond particles and Ni-Co matrix.

Zn-ZrO_2-SiC composite coating has been fabricated to improve the mechanical and thermal resilient properties of mild steel [16]. The surface properties imparted by this ternary- phase composite layer showed enhanced micro- hardness above 60% of the control sample. There was also minimal wear response ad abrasive deformation under the examined conditions.

Nano-particles of alumina (Al_2O_3) in nickel matrix have been found out to agglomerate [17, 18]. Agglomeration affects the amount and uniform distribution of co-deposited particles in the metal matrix. Hexadecylpridinium bromide (HPB) added as cation surfactant in the electro-deposition bath improved the quantity of Al_2O_3 particles co-deposited and also reduced particle agglomeration to achieve uniform distribution of Al_2O_3 particles in the nickel matrix. It was also found out that the wear resistance of the composite coatings increases as the concentration of the surfactant increases to a peak of 150 ml^{-1} after which a decreasing trend of wear resistance set in under -sliding and oil-lubricated conditions. This happened as a result of increased brittleness of metal matrix at peak of the surfactant concentration.

Composite coating of Ni-P Al_2O_3 was formed on material of AISI 1045 steel disks by electroless deposition technique [19]. The second phase particles of Al_2O_3 in the Ni-P –based matrix evidenced well the output of hardness and wear resistance of the deposits. Heat treatment was carried out at intervals of 1 h across three consecutive temperature ranges of 200, 400 and 600^0C. The result showed that composite coating heattreated at 400^0C has maximum hardness and wear resistance.

With the aid of cetyltrimethylammonium bromide (CTAB) in a modified Watts bath, co-deposit of Fe_2O_3 has been successfully dispersed in Ni-Co matrix [20] to form composite coatings of Ni-Co- Fe_2O_3. The results showed that co-deposition of Fe_2O_3 particles with Ni-Co matrix is favored at higher concentration and there is refinement of the crystallite of the composite deposit. The deposition of Co is favored at high concentration of CTAB.

The mechanical parts of machine under constant motion are subject to continuous friction, wear and tear. Nano- particles of Al_2O_3, TiO_2, Si_3N_4 and diamond were consecutively dispersed onto nickel matrix to form composite coatings to study their tribological behaviors and wear mechanisms [21]. The SEM results of the composite samples revealed refine microstructures and enhanced micro-hardness compared with pure nickel coating. Only the Ni- Al_2O_3 and Ni-diamond composite coatings showed improved tribological properties.

Nickel-based composite coating is the most popular wear-resistant composite coating used in abrasive tools, gear systems, chains assembly, measuring tools and gauges. Nickel matrix composites with various dispersed phases (Al_2O_3, SiO_2, SiC, WC and diamond) are fabricated by electrolytic co-deposition from Nickel sulphamate and Watts electrolytes.

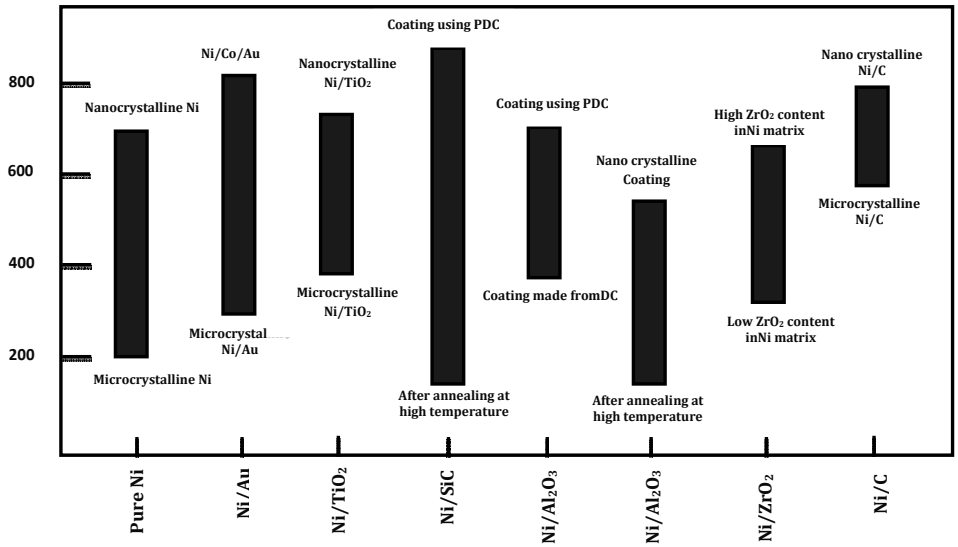

Figure 3. Vickers micro-hardness values for different ranges of particle size in a nickel deposit.

2.1.2. Co-deposition of corrosion -resistant particles

Apart from using the conventional electroplating technique (CEP), sediment co-deposition technique (SCD) has gained acceptance for higher level of co-depositing particles in the metal matrix with better dispersion and uniformity. Feng et al. [22] investigated the corrosion resistance and high-temperature oxidation resistance of Ni- Al_2O_3 nano- composite coatings using SCD technique. The incorporation of the nano-alumina particles in the Ni matrix refined the Ni crystallite and changed the preferential orientation of composite coating. Ni- Al_2O_3 composite coating produced compared with the one fabricated using CEP technique proved that the former had improved corrosion and oxidation resistance.

Fayomi et al. [23] carried out a research on mild steel protection in chloride medium to develop ceramic composite coating that will reduce its susceptibility to corrosion attack. Zn-TiC/TiB composite coating was produced via electro-deposition method. The coatings showed better adhesion strength, improved hardness and enhanced corrosion resistance compared to the TiC/TiB -coated mild steel.

Three different nano- oxides of Al_2O_3, Cr_2O_3 and SiO_2 have been reinforced in Zn matrix using electro-deposition process to produce composite coating on mild steel [24]. The incorporation of Al_2O_3, Cr_2O_3 and SiO_2 nanoparticles in the ternary composite showed grain refinement, modified orientation of Zn matrix and good synergetic effect on the corrosion resistance of Zn-based coatings. Zn-Cr_2O_3 nano- composite had the highest micro-hardness while Zn-Al_2O_3 nano-composite was found to exhibit the highest corrosion resistance coupled with lowest wear loss.

http://dx.doi.org/10.5772/62010

In the research work carried out by Yong et al [25], ultrasonic technique was used as a direct replacement of conventional mechanical agitation to foster effective stirring, dispersion and suspension of the second phase particles in the electrolytic bath. The XRD analysis of the developed nickel-based composite coatings containing TiN nano-particles shows that application of ultrasonic agitation and use of nano-particles of TiN refined the Ni grains, resulting in good corrosion resistance.

A comparative study of the properties of EN, EN-SiC, EN-PTFE and EN-SiC-PTFE composite coatings was conducted on the coating properties using electroless plating [26]. The results showed that electroless nickel (EN) composite coatings incorporated with PTFE and/or SiC particles demonstrated significantly improved mechanical and tribological properties as well as low surface energy, which are desired for anti-sticking and wear-resistant applications. It is evident that the Ni matrix substantially enhanced corrosion resistance by improving the autocatalytic properties and homogeneity.

Electro-deposition mechanism of Ni-Al composite coating was studied from a modified Watts solution by means of zeta potential analysis, voltammetry and electrochemical impedance spectroscopy (EIS) [27]. The findings showed that addition of Al particles shifts the reduction potential of Ni to more negative values, which is attributed to a decrease in the active surface area. Also the loop size of EIS curves increases with addition of Al particles to Ni electrolyte because of an increase in charge transfer resistance. It was also demonstrated that the co-deposition behavior of Ni−Al composite coatings obeys the Guglielmi's model.

Shi et al. [28] studied effects of current density, stirring rate, nanoparticle concentration and temperature of plating bath on the composition of Ni–Co/SiC nano- composite coatings with various contents of SiC nano-particulates by electro-deposition technique. The result showed that Ni–Co/SiC nano- composite coatings have higher micro-hardness and better wear resistance than the Ni–Co alloy coating, which is attributed to the grain-fining and dispersive strengthening effects of the co-deposited hard SiC nano-particulates. The better corrosion resistance of the Ni-Co/SiC nano -composite coatings may be ascribed to the favorable chemical stability of the SiC nano-particulates, which help to reduce the whole size in the nano composite coatings and prevent the corrosive pits from growing up.

To improve the resistance of the hydro-transport pipe steel to corrosion and erosion in oil sand slurry, a Ni–Co–Al_2O_3 composite coating was fabricated by [29] using electrolytic deposition on X-65 pipe steel substrate. Electrolytic deposition of Ni–Co/Al_2O_3 composite coating showed significant improvement in the resistance of hydro-transport pipe steel to corrosion and erosion in oil sand slurry. The micro-hardness and wear resistance of the composite coating are much higher than the steel substrate and increase with the increasing Al_2O_3 particle amount in the coating.

2.1.3. Co-deposition of solid lubricant particles

Cardinal et., al. investigated characterization and frictional behavior of nano-structured Ni-W-MoS_2 composite coatings by pulse plating from an Ni-W electrolyte containing suspended MoS_2 particle [30]. MoS_2 concentration was varied with the coating composition, morphology,

crystalline structure, micro-hardness and frictional behavior. The result obtained indicated that co-deposited lubricant particles strongly influenced the composite Ni-W coating properties. As the MoS_2 concentration in the coating increases, both the tungsten content and the coating micro-hardness decrease while the average grain size increases. With low MoS_2 content, result showed lesser friction coefficients and similar micro-hardness. Therefore, there is a solid lubricant concentration regime where co-deposition of MoS_2 particles into Ni-W nanostructure alloys improves the frictional characteristics of the coating with a consistently lower friction coefficient.

Sangeetha used direct current and pulse current methods to incorporate polytetrafluoroethylene (PTFE) polymer to an optimized Ni-W-BN nano -composite coating deposited on a mild steel substrate [14]. It was observed that the co-deposition of PTFE solid lubricant particles on the Ni-W-BN nano-composite coating resulted in a moderately smooth surface, greater micro-hardness, a lower friction coefficient, excellent water repellency and enhanced corrosion resistance. The pulse current technique showed enhanced performance over the direct current coating due to uniform and smaller grain deposits.

2.2. Applications of composite coatings

Composite coatings have been successfully used to overcome high temperature corrosion, oxidation and wear in many ground breaking applications. Nickel coatings with 8-10 volume % of silicon carbide are used to increase the life of internal combustion engine cylinder bores and in portable chain saws. Composite coatings based on chromium carbide in a cobalt matrix are used as wear-resistant coatings in gas turbines, where they are required to perform for extended periods at temperatures of up to 800^0C. Chromium deposits with alumina inclusions are used in piston rings for diesel engines. Single crystal diamonds locked into a nickel matrix form the cutting-edge in tools such as chainsaws, grinding disks or dental drills [31].

3. Mechanisms of co-deposition process

3.1. Definition of Co-deposition process

Co-deposition is a process of incorporating fine particles of metallic, non-metallic compounds, or polymers from an electrolytic or an electroless bath in the electroplated layer to improve material properties such as: hardness, wear-resistance, corrosion-resistance, tribological control, lubrication, tensile, and fracture strength [32].

Co-deposition of particles into metal deposit is governed by physical dispersion of particles in the electrolyte and electrophoretic migration of particles [33]. Among different models presented for co-deposition mechanism of solid particles into a metal matrix, Guglielmi's model is the most adopted one. It has also been examined with different co-deposition systems such as: Ni–SiC, Ni–TiO_2, Ni- Al_2O_3, Cu- Al_2O_3, Cr-C, Zn-Ni particles, Co-SiC, and Ni-MoS_2 [33, 34]

http://dx.doi.org/10.5772/62010

3.2. Co-deposition of particles on metal surface

One of the common mechanisms of co-deposition process consists of five consecutive steps:

- Formation of ionic clouds around the particles (bulk electrolyte, typical length in cm)
- Convective movement toward the cathode (convection layer, typical length < 1 mm)
- Diffusion through a hydrodynamic boundary layer
- Diffusion through a concentration boundary layer (diffusion layer, typical dimension of μm)
- Adsorption at the cathode where particles are entrapped within the metal deposit.

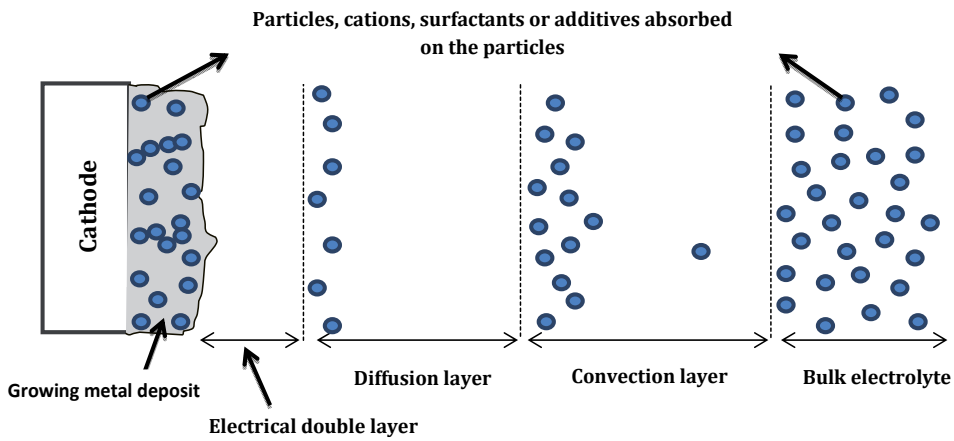

Figure 4. The processes involved in co-electro-deposition of insoluble particles into a growing metal matrix to form a composite metal coating

3.3. Description of Guglielmi's model

Guglielmi established in his findings that concentration of bath particles affects the rate at which an electro-deposit gets incorporated on metal. He therefore quantified the rate of particle incorporation as a function of current density. Guglielmi based his model on the similarity between the experimental co-deposition and Langmuir isotherm curves. Assumptions of Langmuir are as follows:

- The surface of the adsorbant (cathode) is in contact with a solution (electrolytic bath) containing adsorbate (second phase nanoparticles) which is strongly attracted to the surface.
- The surface has a specific number of sites (growing metal surface area) where the solute molecules can be adsorbed.
- The adsorption involves the attachment of only one layer of molecules to the surface, i.e. monolayer adsorption.

Using co-deposition of Ni-Al system as a case study [27], the mathematical equations deduced by Guglielmi's model are governed by the following parameters and equations:

α - Volume fraction of particles in the deposit; C - concentration of particles in the plating bath;

W- Relative atomic mass of metal; n- Valence of deposited metal; F- Faraday's constant; d - Density of deposited metal; v_0 - Constant for particle deposition; A and B are constant for metal deposition and particle deposition; k– Adsorption coefficient; J_o - Exchange current density of deposited metal; η - over-potential; θ- Surface coverage of embedded particles.

$$\frac{\alpha}{1-\alpha} = \frac{nFdv_0}{WJ_0}\exp\left[\left(A-B\right)\eta\right]\cdot\frac{kC}{1+kC} \tag{1}$$

Divide through by C: $\frac{\alpha}{C(1-\alpha)} = \frac{nFdv_0}{WJ_0}\exp[(A-B)\eta]\cdot\frac{k}{1+kC}$

Multiply through by $(1-\alpha)^{\left(\frac{B}{A}-1\right)}$:

$$\frac{\alpha}{C\left(1-\alpha\right)^{\left(2-\frac{B}{A}\right)}} = \frac{nFdv_0}{WJ_0}\exp\left[\left(A-B\right)\eta\right]\cdot\frac{k}{1+kC}\left(1-\alpha\right)^{\left(\frac{B}{A}-1\right)}$$

Take the reciprocal of each term:

$$\frac{C(1-\alpha)^{\left(2-\frac{B}{A}\right)}}{\alpha} = \frac{WJ_0}{nFdv_0}\exp\left[\left(B-A\right)\eta\right]\cdot\left(\frac{1+kC}{k}\right)\left(1-\alpha\right)^{\left(1-\frac{B}{A}\right)}$$

Rearrange the terms on the right:

$$\frac{C\left(1-\alpha\right)^{\left(2-\frac{B}{A}\right)}}{\alpha} = \frac{WJ_0^{\frac{B}{A}}}{nFdv_0}J_0^{\left(1-\frac{B}{A}\right)}\cdot\left(\frac{1}{k}+C\right)\cdot\left\{\exp\left[\left(B-A\right)\eta\right]\cdot\left(1-\alpha\right)^{\left(1-\frac{B}{A}\right)}\right\} \tag{2}$$

Assuming:

$$\exp\left[\left(B-A\right)\eta\right]\cdot\left(1-\alpha\right)^{\left(1-\frac{B}{A}\right)} = 1 \quad or \quad \exp\left[\left(A-B\right)\eta\right] = \left(1-\alpha\right)^{\left(1-\frac{B}{A}\right)}$$

Then

http://dx.doi.org/10.5772/62010

$$\frac{C\left(1-\alpha\right)^{\left(2-\frac{B}{A}\right)}}{\alpha}=\frac{WJ_0^{\frac{B}{A}}}{nFdv_0}J_0^{\left(1-\frac{B}{A}\right)}\cdot\left(\frac{1}{k}+C\right) \tag{3}$$

Expand the bracket on the right to get

$$\frac{C\left(1-\alpha\right)^{\left(2-\frac{B}{A}\right)}}{\alpha}=\frac{WJ_0^{\frac{B}{A}}}{nFdv_0}J_0^{\left(1-\frac{B}{A}\right)}\left(\frac{1}{k}\right)+\frac{WJ_0^{\frac{B}{A}}}{nFdv_0}J_0^{\left(1-\frac{B}{A}\right)}C$$

Compare with $y=mx+d$, the equation of a straight line. Where m is the slope (also written as $tan\varphi$), and d the intercept:

$$\underbrace{\frac{C\left(1-\alpha\right)^{\left(2-\frac{B}{A}\right)}}{\alpha}}_{y}=\underbrace{\frac{WJ_0^{\frac{B}{A}}}{nFdv_0}J_0^{\left(1-\frac{B}{A}\right)}\left(\frac{1}{k}\right)}_{d}+\underbrace{\frac{WJ_0^{\frac{B}{A}}}{nFdv_0}J_0^{\left(1-\frac{B}{A}\right)}}_{m}\underbrace{C}_{x}$$

Thus the slope is simply the coefficient of C. ie

$$slope=m=\tan\varphi=\frac{WJ_0^{\frac{B}{A}}}{nFdv_0}J_0^{\left(1-\frac{B}{A}\right)} \tag{4}$$

Equation (5) follows quickly from the logarithm law $\lg(PQ^R)=\lg P+R\lg Q$.

$$\lg\left(\tan\varphi\right)=\log\frac{WJ_0^{\frac{B}{A}}}{nFdv_0}+\left(1-\frac{B}{A}\right)\lg J_0 \tag{5}$$

where the slope is giving as $\left(1-\frac{B}{A}\right)$. The ratio $\frac{B}{A}$ of the slope can be pre-determined for fitting the experimental data. This ratio is obtained in the following way:

For coatings produced with different current densities, the plot of $C(1-\alpha)^{2-B/A}$ against C presents a series of straight lines. The selected $\frac{B}{A}$ ratio must converge these lines towards the same point on the C –axis i.e., $\left(C=-1/K\right)$

The logarithm of slopes of lines $\lg(\tan\varphi)$ obtained from the graph of $C(1-\alpha)^{2-B/A}$ versus C plotted against $\log J$, i.e., $\lg(\tan\varphi)$ versus $\log J$ lies on a straight line. According to Equation (5), the slope of this line is equal to $\left(1-\frac{B}{A}\right)$. The obtained $\frac{B}{A}$ ratio should be equal to the selected one.

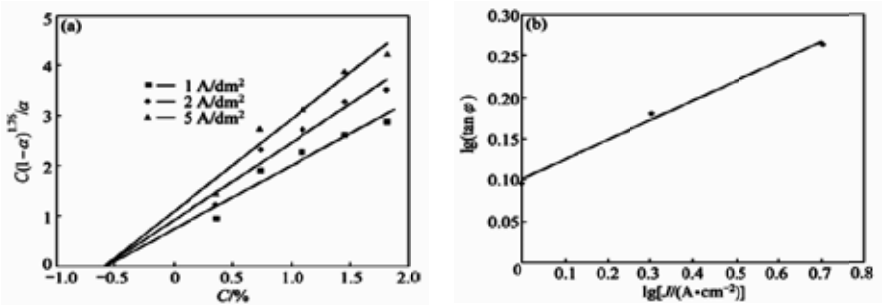

Figure 5. Graphical representation of experimental deductions of Ni-Al co-deposition system

In Fig. 5(a), the experimental results considering the $\frac{B}{A}$ ratio equal to 0.24, have been presented. It is clear that experimental data can be well-fitted on a series of straight lines, which converge toward the same point on the C -axis. From extrapolation of these lines, the $^{-1}/_{K}$ point of intersection with C-axis is equal to −0.62. This makes it possible to obtain the adsorption coefficient value of K.

In Fig. 5(b), the logarithm of the slopes of the straight lines lg(tanφ) is plotted against $\lg J$. The slope of this line is 0.76 and so the $\frac{B}{A}$ ratio is 0.24. This value is exactly equal to the $\frac{B}{A}$ value considered previously for initial curve fitting. Hence, the co-deposition behavior of Ni −Al system is in good agreement with the Guglielmi's model.

Composite electroplating is a two-step process according to Guglielmi's model. At first, solid particles during electro-deposition are surrounded with cloud of adsorbed ions, which are weakly adsorbed at cathode surface by van der waals forces. In the second step, the loosely adsorbed particles become strongly adsorbed onto cathode surface by Coulomb force and consequently entrapped within metal matrix. The main drawback of this model is absence of mass transfer effect during electro-deposition process such as the adsorption of ionic species on the particle surface, the nature of particle, the ions to be reduced, the bath components, and the hydrodynamic conditions.

Bonino et., al. in their model uses statistical approach that Gugliemi neglected [35]. The model describes the amount of particles that are likely to be incorporated at a given current density. Mass transport of particles is proportional to the mass transport of ions on the working electrode. Volume ratio of particles in the metal deposit will increase under charge transfer control and decrease under mass transport control.

A widely accepted model is developed by Kurozaki, which includes the transport of solid particles from the solution to the cathode surface by agitation. This model is developed in the following steps:

- Uniform dispersed particles are transported to the electric double layer via mechanical agitation.
- Charged particles are transported to the cathode surface by electrophoresis.

http://dx.doi.org/10.5772/62010

- Solid particles are adsorbed at the cathode surface due to Coulomb force between particles and adsorbed anions.
- Finally, the particles are incorporated into the growing metal.

Particles dispersed in the electrolyte bath are in constant Brownian motion. Whether the particles approach one another, their separation or agglomeration mainly depends on the existing energies between those particles. When attraction energy is larger than repulsion energy, particle agglomeration occurs and when repulsion energy is higher than attraction energy, particle separation occurs. The condition and nature of the system mainly determines the magnitude of net force for the production of agglomerated structures. Therefore, knowledge of interfacial region attraction is very important in understanding dispersion stability of solid particles with electrolyte.

4. Conclusions

The rate of embedding nanoparticles in matrix solution onto metal deposit depends on the applied current density, hydrodynamics and characteristics of the particles. High incorporation rates have been confirmed by using:

- High concentration of nanoparticles in the electrolytic bath.
- Particles at nano scale compared to micron scale.
- A lower concentration of the electro-active species.
- Ultrasonic agitation compared to mechanical agitation.
- Pulse reverse current technique compared to direct current technique.

Various electro-deposition techniques (direct current, pulsed direct current, and pulsed reverse current) have been employed to incorporate nano-sized particles into metal deposits. These techniques have enabled the fabrication of composite coatings with diverse properties not available with pure metal or alloy coatings. It has been established that pulse current deposition technique compared to direct current deposition for the production of nano-composite showed more refined surface microstructure and increased incorporation rate into the metal deposit.

Inorganic (inert) nanoparticles are used as second phase in composite coating. They possess good chemical stability, high micro-hardness and good wear resistance and enhance corrosion resistance in the composite coating. They modify crystal growth to form a nano-crystalline metal deposit and also cause a shift in the reduction potential of a metal ion.

Agglomeration of nanoparticles occurs under condition of greater attraction energy. The adverse effect can be reduced or eliminated by controlled application of ultrasonic agitation, surfactants, and pulse reverse direct current.

Author details

Peter Odetola[1], Patricia Popoola[1*], Olawale Popoola[2] and David Delport[1]

*Address all correspondence to: popoolaapi@tut.ac.za

1 Department of Chemical, Metallurgical and Materials Engineering, Tshwane University of Technology, Pretoria, South Africa

2 Centre for Energy and Electrical Power, Department of Electrical Engineering, Tshwane University of Technology, Pretoria, South Africa

References

[1] C.T.J. Low, R.G.A. Wills, F.C. Walsh. 2006. Electro-deposition of composite coatings containing nanoparticles in a metal deposit. *Surf. Coat. Technol., 201, 371-383.*

[2] Vaezi, M. R., Sadrnezhaad, S. K. & Nikzad, L. 2008. Electrodeposition of Ni-SiC nano-composite coatings and evaluation of wear and corrosion resistance and electroplating characteristics. *Coll. Surf., A-Physicochem and Engin Aspe,* 315, 176-182.

[3] Kim, S. K. & Yoo, H. J. 1998. Formation of bilayer Ni-SiC composite coatings by electrodeposition. *Surf. Coat. Technol.,* 108, 564-569.

[4] Bhat, A. & Bourell, D. 2015. Tribological properties of metal matrix composite coatings produced by electrodeposition of copper. *Mater. Sci. Technol.,* 31, 969-974.

[5] Raja, M., Bapu, G. N. K. R., Maharaja, J. & Sekar, R. 2014. Electrodeposition and characterisation of Ni-TiC nanocomposite using Watt's bath. *Surf. Engin.,* 30, 697-701.

[6] Sancakoglu, O., Ungan, G., Celik, E. & Aksoy, T. 2015. Fabrication of Cr-$Cr_{23}C_6$/Cr_2N composite coatings: Change in the phase structure and effect on the corrosion properties. *Int. J. Appl. Cera. Technol.,* 12, 830-836.

[7] Walsh, F. C., Low, C. T. J. & Bello, J. O. 2015. Influence of surfactants on electrodeposition of a Ni-nanoparticulate SiC composite coating. *Trans. Instit. Metal Finish.,* 93, 147-156.

[8] Sangeetha, S. & Kalaignan, G. P. 2015b. Tribological and electrochemical corrosion behavior of Ni-W/BN (hexagonal) nano-composite coatings. *Cera. Int.,* 41, 10415-10424.

[9] Subramania, S. R. V. S. M. A. 2009. Electrodeposition and characterization of Cu-TiO_2 nanocomposite coatings. *J Solid State Electrochem,* 13, 1777-1783.

[10] Kim, M. J., Kim, J. S., Kim, D. J., Kim, H. P. & Hwang, S. S. 2015. Effects of current density and agitation on co-deposition behaviour of electrodeposited Ni-TiO_2 composite coating. *Surf. Engin.,* 31, 673-678.

[11] Li, S., Yao, W., Liu, J., Yu, M., Wu, L. & Ma, K. 2015. Study on anodic oxidation process and property of composite film formed on Ti-10V-2Fe-3Al alloy in SiC nanoparticle suspension. *Surf. Coat. Technol.,* 277, 234-241.

[12] Liu, C., Su, F. & Liang, J. 2015. Producing cobalt-graphene composite coating by pulse electrodeposition with excellent wear and corrosion resistance. *Appl. Surf. Sci.,* 351, 889-896.

[13] Mohammadi, M., Ghorbani, M. & Azizi, A. 2010. Effect of specimen orientation and heat treatment on electroless Ni-PTFE-MoS2 composite coatings. *J. Coat. Technol. Res.,* 7, 697-702.

[14] Sangeetha, S. & Kalaignan, G. P. 2015a. Studies on the electrodeposition and characterization of PTFE polymer inclusion in Ni-W-BN nanocomposite coatings for industrial applications. *Rsc Adv.,* 5, 74115-74125.

[15] Wang, L. P., Gao, Y., Liu, H. W., Xue, Q. J. & XU, T. 2005. Effects of bivalent Co ion on the co-deposition of nickel and nano-diamond particles. *Surf. Coat. Technol.,* 191, 1-6.

[16] Fayomi, O. S. I., Popoola, A. P. I., Oheiza, A. & Adekeye, T. 2015b. Microstructure, tribological and mechanical strengthening effect of multiphase Zn/ZrO2 -SiC electrodeposited composite coatings. *Int. J. Adv. Manuf. Technol.,* 80, 1489-1495.

[17] Goral, A., Beltowska-Lehman, E. & Indyka, P. 2010. Structure characterization of Ni/Al(2)O(3) composite coatings prepared by electrodeposition. *In:* Stroz, D. & Karolus, M. (eds.) *Applied Crystallography Xxi.*

[18] Chen, L., Wang, L., Zeng, Z., & Zhang, J. 2006. Effect of surfactant on the electrodeposition and wear resistance of Ni–Al_2O_3 composite coatings. Mater. Sci. Eng., 434, 319-325.

[19] Alirezaei, S., Monirvaghef, S. M., Salehi, M. & Saatch, A. 2007. Wear behavior of Ni–P and Ni–P–Al2O3 electroless coatings. *Wear,* 262, 978-985.

[20] Ma, L., Zhou, K.-C. & Li, Z.-Y. 2009. *Synthesis of high Texture Orientated Ni-Co-*Fe_2O_3 *Composite Coatings by Electrodeposition*.

[21] Du, L. Z., Xu, B. S., Dong, S. Y., Hua, Y. & Tu, W. Y. 2004. Study of tribological characteristics and wear mechanism of nano-particle strengthened nickel-based composite coatings under abrasive contaminant lubrication. *Wear,* 257, 1058-1063.

[22] Feng, Q., Li, T., Teng, H., Zhang, X., Zhang, Y., Liu, C. & Jin, J. 2008. Investigation on the corrosion and oxidation resistance of Ni-Al_2O_3 nano-composite coatings prepared by sediment co-deposition. *Surf. Coat. Technol.,* 202, 4137-4144.

[23] Fayomi, O. S. I., Aigbodion, V. S. & Popoola, A. P. I. 2015a. Properties of Tic/Tib Modified Zn–Tic/Tib Ceramic Composite Coating on Mild Steel. *J. Fail. Anal. and Preven.*, 15, 54-64.

[24] Malatji, N., Popoola, A.P.I., Fayomi, O. S. I. & Loto, C. A. 2015. Multifaceted incorporation of Zn-Al_2O_3/Cr_2O_3/SiO_2 nanocomposite coatings: anti-corrosion, tribological,and thermal stability. *Int. J. Adv. Manuf. Technol*., DOI 10.1007/s00170-015-7463-x

[25] Yong, W., Fafeng, X., Chao, L. & Hongyan, Y. 2013. Nickel based coatings containing TiN nanoparticles prepared by ultrasonic-electrodeposition technology. *Res. J. Appl. Sci. Engin. Technol.*, 6, 1857-1861.

[26] Huang, Y. S., Zeng, X. T., Annergren, I. & Liu, F. M. 2003. development of electroless NiP-PTFE-Si composite coating. *Surf. Coat. Technol.,* 167, 207-211.

[27] Adabi, M. & Amadeh, A. A. 2014. Electrodeposition mechanism of Ni-Al composite coating. *Trans. Nonferrous Metals Soc. China,* 24, 3189-3195.

[28] Shi, L., Sun, C. F., Gao, P., Zhou, F. & Liu, W. M. 2006. Mechanical properties and wear and corrosion resistance of electrodeposited Ni-Co/SiC nanocomposite coating. *Appl. Surf. Sci.,* 252, 3591-3599.

[29] Tian, B. R. & Cheng, Y. F. 2007. Electrolytic deposition of Ni-Co-Al_2O_3 composite coating on pipe steel for corrosion/erosion resistance in oil sand slurry. *Electrochimica Acta,* 53, 511-517.

[30] Cardinal, M. F., Castro, P. A., Baxi, J., Liang, H. & Williams, F. J. 2009a. Characterization and frictional behavior of nanostructured Ni-W-MoS_2 composite coatings. *Surf. Coat. Technol.,* 204, 85-90.

[31] Kanani, N. 2004. Metal finishing- A key Technology? *Basic Principles, Processes and Practice*, 1-19.

[32] Borkar, T. 2010. Electrodeposition nickel composite coatings.

[33] Bercot, P., PENA-Munoz, E. & Pagetti, J. 2002. Electrolytic composite Ni-PTFE coatings: an adaptation of Guglielmi's model for the phenomena of incorporation. *Surf. Coat. Technol.*, 157, 282-289.

[34] Cardinal, M. F., Castro, P. A., Baxi, J., Liang, H. & Williams, F. J. 2009b. Characterization and frictional behavior of nanostructured Ni–W–MoS2 composite coatings. *Surf. Coat. Technol.,* 204, 85-90.

[35] Bonino, J. P., Loubiere, S. & Rousset, A. 1998. Reactivity and codeposition of Co3O4 powders with nickel in a Watts bath. *J. App. Electrochem*., 28, 1227-1233.

Chapter 4

A New Approach — In-Situ Codeposition of Composite Coatings

Orkut Sancakoğlu

Additional information is available at the end of the chapter

http://dx.doi.org/10.5772/61935

Abstract

Present chapter is organised to give general information about electrolytic coating and electro codeposition, factors affect the coating structure and the main layers'-property relation in details. This relation is expressed by a simple schematic and electrolytic co-deposition parameters affect the process such as pH, zeta potential, agitation and etc. are explained. Additionally, in-situ codeposition, the new approach is given with examples, and some experimental results belonging to our research group and with comparison to approaches belonging to some others.

Main aim of this chapter mentioned is to define electro codeposition technique and to introduce the relatively new technique, in-situ codeposition method. According to the specific research example on this process, fabrication of composite coatings by electro codeposition system and obtaining metal-ceramic composite structures with additional heat-treatments are discussed. The obtained results showed that the composite coatings can be fabricated successfully by in-situ codeposition technique with an additional heat-treatment. The effect of heat-treatment conditions on the in-situ phase formation and their corrosion and mechanical behaviors are given. The results mentioned, both corrosion and mechanical, implies that the metal matrix-carbide and/or nitride reinforced composite coatings have potential application to industrial fields in many respects.

Keywords: Coatings, Electro codeposition, In-situ method, Heat-treatment, Oxidation, Phase transformation, Structure

1. Introduction

In most cases, materials have a limited lifetime, which strongly depends on the actions of external factors and the operating environment. Occasionally, chemical or electrochemical

reactions with the environment take place, which will sooner or later damage functionality by attacking the surface. Because of the atomic structure, the surface of a material or a component is the most vulnerable site for various forms of attacks and, therefore; it might be deemed. These attacks could be present individually or in combination of mechanical, chemical, electrochemical or thermal in nature [1]. The coating processes which maximize the lifetime of the materials can be classified as evaporation, hot metal processes, painting, thermal spraying, and **metallising**. Metallising appears to have particular importance in these main coating processes compared to others. Metallising is devided in two sub-groups, such as **electroless metal coating**, and **electrolytic metal coating**.

Among the processes concerning the production of nanostructured composites, the electro-deposition technique has further demonstrated the following benefits: a smoother surface, a better bonding between particles and a metal, an easier control of the thickness of the coating, appropriacy to automation, availability for obtaining metallic alloys and composite coatings, and, finally, a possibility to achieve higher microhardness [2].

It is known that combining the best properties of different materials to obtain one material with excellent properties is the main idea of fabricating composites. **Electrolytic co-deposition technique** seems to be feasible based on the idea determined.

In the present chapter, entitled **A New Approach: In-situ Codeposition of Composite Coatings,** general information about electrolytic coating and electrolytic codeposition is given and the factors affecting the coating structure, the main layer-property relations are explained in details. The electrolytic codeposition section explains the parameters, such as pH, zeta potential, agitation and etc., affecting this process. Under the section 3, property-performance relations of these coatings are examined. Finally, **in-situ codeposition** is detailed with examples and the experimental findings of our and other research groups are presented.

2. Electrolytic coating

In this method, a metallic protective layer is applied to a surface as a coating for the component typically carried out in aqueous solution. This process is supported by using an external voltage source generally called rectifier. On the other hand, for electroless deposition, a reduction medium is present in the electrolyte. The latter process is widely used for non-conducting materials' coating such as ceramics and plastics. The electrochemical method (electrocoating, electroplating) is used for deposition onto electrically conducting substrates.

Electrochemical deposition onto an object is achieved by putting a negative charge on it to be deposited and immersing into a solution which contains a salt of the metal. The metallic ions of the salt carry a positive charge are thus attracted to the object providing electrons to reduce the positively charged ions to metallic form when they reach the negatively charged object [1].

http://dx.doi.org/10.5772/61935

2.1. Factors affecting the coating structure

In this complex phenomenon, there are many factors that affect the process, consequently the properties and the performance of the material. These factors can be classified in four groups basicly.

- Substrate: material of the substrate and the preparation before plating.
- Electrolyte: composition, pH value, temperature, filtration and agitation.
- Coating metal: main coating metal or alloy.
- System parameters: current type and density.

The factors are described in Section 3.1 in details for both electrodeposition and electro co-deposition techniques.

2.2. Layers and the Properties Related to

In a coating system four different zones are described by Holleck [3] when protecting materials with coatings. These are:

- Substrate;
- Substrate-coating interface;
- Coating and;
- Coating-environment interface (see Figure 1).

The first layer is substrate where potential hydrogen embrittlement effects are of concern. Commonly, metals are preferable for this layer, steel for engineering application in particular. The second zone is the basis metal interface. In this region adhesion of the coating and diffusion between the coating and substrate takes place. The coating itself is described as the third zone where composition and microstructure determine the properties and factors. The interactions between environment and the coating has to be taken into account in terms of corrosion and/or wear in the final zone environmental interface.

Obviously, numerous layers are influenced in more than one zone. This phenomenon could be illustrated by the following examples. Firstly, porosity and/or stress in the substrate, rather than just in the coating, can noticeably change coating properties. Secondly, porosity can affect corrosion resistance and mechanical behaviour, such as tensile properties. Another one is hydrogen embrittlement as a factor not only for the substrates (concentrates heavily on steels) but also for some coatings. This is a generic term used to describe a wide variety of fracture phenomena having a common relationship to the presence of hydrogen as a solute element in the alloy or as a gas in the atmosphere [4]. Nickel, aluminium, titanium [5] and even electroless copper coatings [6] exhibit the phenomenon. It explains that any material can weaken by this effect [7].

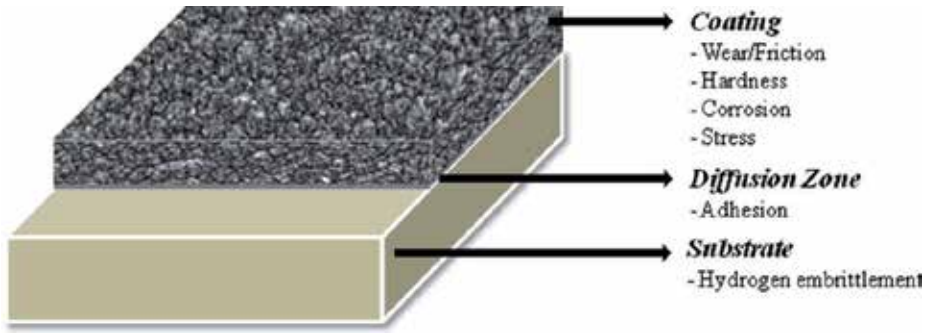

Figure 1. Zones in a coated material

The rest of the zones and the properties affected are clarified in Section 3.2 because these zones are related to the coating itself and the interfaces between coating.

3. Electrolytic codepositon

Codeposition of metals with ceramic particles is a new technique for obtaining hard, wear resistant coatings; therefore, its application to our daily life has not been studied in the engineering field enough. The deposition of two or more materials on a substrate simultaneously is defined as "electrolytic codeposition" or "electrolytic composite coating". In this process, both materials (the matrix and the reinforcement) are subjected to the surface and the desired properties can be obtained in one step process easily. When considering the codeposition of Cr and SiC, the metal matrix (Cr) increases the hardness and the wear resistance of the material. Additionally, the reinforcement (SiC) improves corrosion behaviour and boosts both, the hardness and the wear resistance of the structure.

First examples of electro codeposited composite coatings are known to have been used for antislip stairs of marines which are Ni matrix sand (SiO_2) particles. Fink and Prince investigated the self lubricant properties of Cu-Graphite electrolytic composites for car engine applications in 1928. At the beginning of the sixties, the interest in this specific topic was increased and researchers were focussed on the engineering applications of these specific coatings. Especially, the interest in the application of Ni-SiC and Ni-PTFE in the automobile industry has grown significantly in the last decades.

From this perspective, codeposited composite coatings have excellent wear resistance and permit emergency dry-running of machinery. The following examples of practical utilisation illustrate the benefits of the mentioned coatings: Ni matrix coatings with 8-10% vol. of SiC are used to increase the life of internal combustion engine cylinder bores; composite coatings based on Cr_xC_y (chromium carbide) in a Co matrix are used as wear resistant coatings in gas turbines. Cr deposits with Al_2O_3 inclusions are used in piston rings for diesel engines. Diamond embedded into a Ni matrix form the cutting edge in tools such as chainsaws, grinding discs or dental drills [1].

http://dx.doi.org/10.5772/61935

A number of scientists have investigated the mechanism of the electrodeposition of composites. The mechanisms proposed by most of them include these steps [1]:

- Electrophoretic movement of positively charged particles to the cathode;
- Adsorption of the particles on the cathode surface by Van der Waals forces;
- Embedding of the particles into the layer.

There are a variety of models with a quantitative approach to the incorporation rate of the particles into the matrix; however the current and most widely-known one has been suggested by Roos et al. in 1990 [8].

Similarly, Wan-chang Sun et al. [9] described codeposition process for Ni-Al_2O_3 system in three steps. This is illustrated in Figure 2.

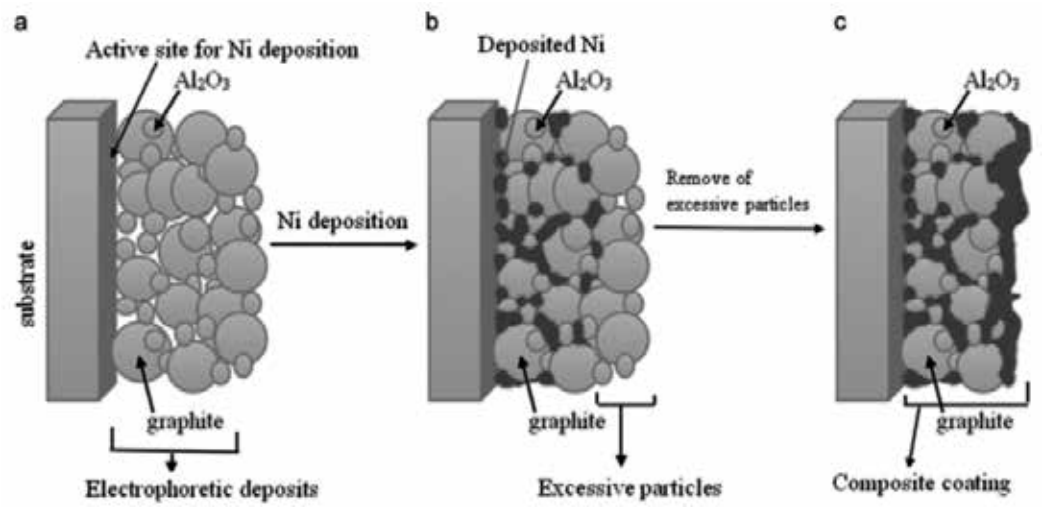

Figure 2. Schematic description of the three-step method of composite coating

These steps can be summerized for Ni-Al_2O_3/graphite system as follows:

a. nickel pre-plating and electrophoretic deposits of Al_2O_3 and graphite particles,

b. composite after nickel deposition in the three step, and

c. composite after removing the excess particles loosely adsorbed to the surface [9].

3.1. Effective parameters

The factors affecting the coating structure, subsequently, the properties and the performance of the material were given in previous sections (see Section 2.1 and 2.2). This section focuses on the specification of these factors; besides, the additional ones, which belong to the codeposition process, are described, namely zeta potential, particle size, circulation of the suspension (particle additional electrolyte) which belong to the codeposition process.

3.1.1. Substrate and substrate preparation

The main idea of coating processes is to protect the main material, to be specific, substrate, from environmental conditions, and to improve its mechanical properties. Undoubtedly, the perfect choice for such engineering applications is steel due to its unique properties. Even though this material group has a lot of advantages, the surface of the steel substrate has to be protected by several coating techniques. Electrical conductivity of steel substrates allows them to be coated by electrolytic deposition techniques, including electro codeposition. The quality of the substrate should be chosen according to the application and is the important detail; it should be coherent with the coating material properties-side (such as hardness and modulus of elasticity).

The preparation of the substrate before plating is another point to be taken into consideration. The coatings with perfect properties have no meaning without a good adhesion. Adhesion between the coating and the substrate identifies the coating quality and determines the life time of this structure. The preparation generally includes chemical and/or mechanical cleaning steps to remove contaminants from its surface [8].

3.1.2. pH

Electrolytes are prepared either acidic (nickel, copper, zinc and tin coating baths) or basic (zinc, cadmium, brass, gold and silver baths). It is important to know the pH in order to control and maintain the electrolyte composition stable for long term use. The electrolytes above or below specified pH values which show the acidic-basic characteristics affect and, generally decrease the coating quality [10].

In their research, Jia Man et al. [11] studied the zeta potential to describe the surface electrical behavior of nano-particles. Changes in the pH value of electrolyte can influence zeta potential. That means, zeta potential and pH are closely related to each other to determine the dispersive condition of particles in electrolytes.

3.1.3. Temperature

Temperature has two opposite effects on this process. On the one hand it increases the diffusion, and on the other hand, it also increases the crystal growth rate. It allows the grain size reduction, but decreases the cathode polarisation and because of hydrogen release this effect transforms the coating morphology into the spongy structure. Due to this reason, temperature should be adjusted and kept stable throughout the process [10].

3.1.4. Zeta potential

Zeta potential (ζ) of the particles is an essential parameter for the codeposition of composite coatings and provides details about the dispersion mechanisms of the particles. Simply, zeta potential can be defined as the value of attractive and repulsive forces between the particles. The behaviour of the particles in aqueous media is not determined by the surface charge but by zeta potential [10].

Zeta potential is directly related to pH due to the fact that in many aqueous systems, H^+ ions are the main ion content which determine potential. The value of zeta potential is measured

http://dx.doi.org/10.5772/61935

by zetameter in millivolts, which is important for the explanation of the colloidal suspension stability. The higher the zeta potential, the better the stability of colloidal suspensions [10]. This prevents the suspended particles from bein agglomerated. Stability can be achieved mainly by two ways. These are:

- providing the particles electrically charged; and
- coating the suspended particles by a protective chemical (surfactant) [12].

J. Man et al. revealed pH and zeta potential effect on the α-Al_2O_3 particle codeposition. Results showed that H+ absorbsion of particles at low pH can prevent the agglomeration of metallic ions, lower the size of grains and directly affect the particle content in the matrix [11]. Zeta potential and particle content versus pH value are given in Figure 3. It is obvious that zeta potential decreases with the increase of pH.

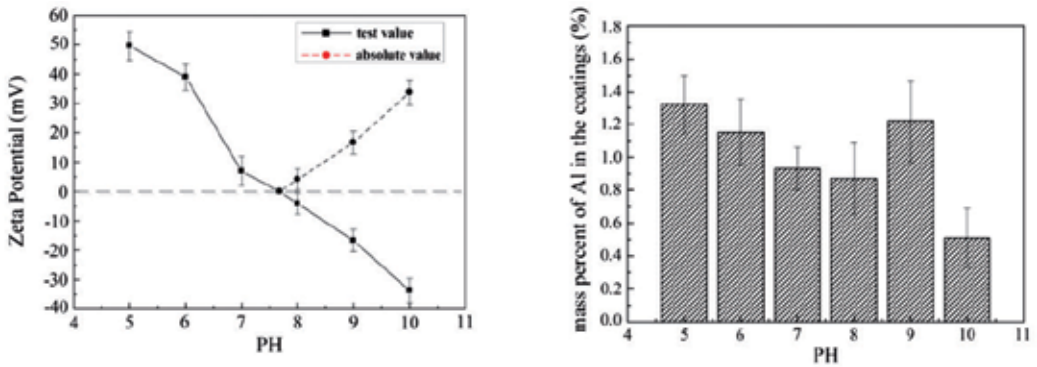

Figure 3. Zeta potential (left) and particle content (right) versus pH value [11]

In the case of ultrafine particles, a suitable surfactant, which, after ionising in solution, adsorbs on the surface of the particles allowing them to orient themselves according to their electric charge, is frequently added. Hence, the repulsive electrostatic forces minimise coagulation of the particles.

Meguno et al. accepted zeta potential as an effective quantitative parameter. According to their research, zeta potential values of both α-SiC and γ-SiC are negative but as a function of decreasing pH, the potential increases and reaches positive values for lower pH. In another study Lee and Wan mentioned that increasing the copper sulphate bath concentration and decreasing pH, zeta potential of α-Al_2O_3 approaches positive values. On the other hand, it is the oppsite for γ-Al_2O_3 under the same conditions. This situation explains why α-Al_2O_3 particles are codeposited much more than γ-Al_2O_3 particles [13].

3.1.5. Agitation and filtration

A further factor affecting the coating structure is defined as the electrolyte composition. In other words structure and the stability of electrolyte affect crystal formation rate direcly. With

the higher crytal formation rate, fine grained and better coatings coherent to the substrate can be obtained. In order to countervail the local ion concentration decrease near cathode surface, a motion can be given to the substrate. This is supported by the cathode motiont generally but in some coating processes it is satisfied by the circulation of the electrolyte by several methods. In this case, there is a possibility of sticking the precipitated contaminants on the cathode surface. It is better filtering the electrolytes periodically to prevent the coatings from unwanted contaminations [10].

The coating baths are usually agitated by several methods.

These are:

- Cathode motion (vertical, horizontal or rotating) [8];
- Low pressure gas blowing into the electrolyte or unbalanced air circulation [13];
- Magnetic or mechanical stirring [13];
- Circulating by pumps [14];
- Sound or ultrasound vibrations [15-16].

Agitation in an electrolyte which can sometimes be invarious combinations. To give an example, Tudela et al. used both the mechanical stirrer and ultrasonic agitation simultaneously. Figure 4 shows the sketch of the setup belong to their experimental set-up [16].

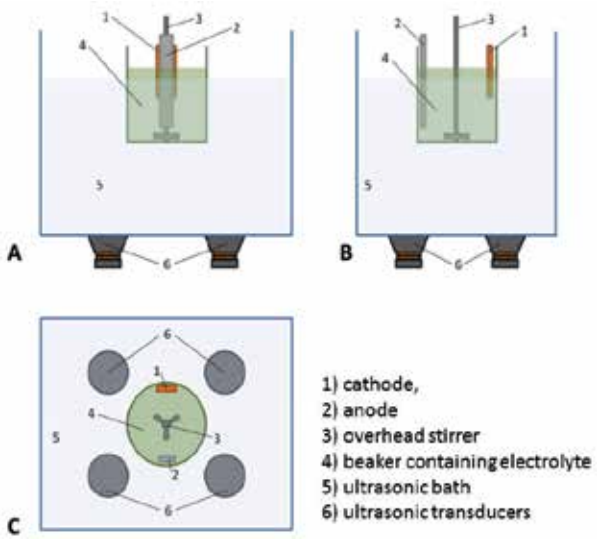

Figure 4. Schematic showing (a) front, (b) lateral, and (c) top views of the set-up [16]

Three main objectives for the agitation use are maintaining the temperature homogenous in the coating bath and carring both the metal ions and the suspended particles to the cathode surface.

http://dx.doi.org/10.5772/61935

3.1.6. Particle size

The properties of composite coatings also depend on the particle size and distribution of the second phase. The second phase particles have to be suspended in the electrolyte uniformly. For this purpose, the tendency to settle under gravity must be constantly overturned using stirring, pumping electrolyte flow, ultrasonic agitation or air injection where it is desired to achieve a uniform distribution of the second phase through the matrix.

While the fine particles are suspended in the electrolyte easily, the coarser ones tend to agglomerate and/or settle by the gravitational force. Consequently, because of the aggressive circulation of the electrolyte effect the codeposition conversely, stabilizing the suspension has much more importance in this specific process. In this situation there are two alternatives. One of them is using submicron or nano particles in the electrolyte and the other one is adding surface active chemicals (surfactant) into the electrolyte to solve the stabilization problem totally or partially. This phenomenon is explained in Section 3.1.4.

The properties of electrodeposited metals or alloys can be substantially modified by arranging the codeposition of fine particles with the metal or alloy. Such particles may be inorganic (oxides, carbides, diamond), metallic (chromium) or organic (PTFE). The amount of second-phase incorporated particles will be a function of the deposition which has to be taken into account [11-12].

3.1.7. Current type and density

Until quite recently electrodeposition was carried out using direct current (DC) [1]. DC electrolysis can be represented with the connection of two electrodes immersed in solution to the output of a DC power supply (rectifier). The cathode may itself be a metal or might be a semiconductor or a non-metallic conductor such as graphite. The primary purpose of this is to complete the electrical circuit.

Another type of current used in electrodeposition is pulse current (PC, pulse plating or pulse electrodeposition). In pulse electrodeposition the potential or current is alternated swiftly between two different values. It is possible to control the film properties in an atomic order by regulating the pulse width and amplitude [8].

Huang et al. compared DC and PC on chromium coatings and found that the coatings fabricated using PC are showing less surface cracks than that of the coatings fabricated using DC. Additionally, corrosion resistance of these coatings is higher than that of the coatings obtained under DC conditions [8].

Another research group studied three different electrodeposition methods (direct, pulse, and pulse reverse current). According to their results, nanocomposite coatings' microhardness values significantly improved. When compared to the methods, hardness values were shown higher in the PRC coated materials due to increased reinforcement content (see Figure 5a). Additionally, Ni-Co alloy matrix nanocomposites exhibited better wear resistance as compared to pure Ni–Co alloy coatings [17].

Similarly, Nemes et al. [18] focused on both current type and frequency which are effective parameters of codeposition process. For all the same conditions oxide (CeO_2) addition increase the overall hardness (see Figure 5b). These results are affected by not only the codeposited ceramic content but also by the decrease of the grain size and the increase of deposit compactness affect [18].

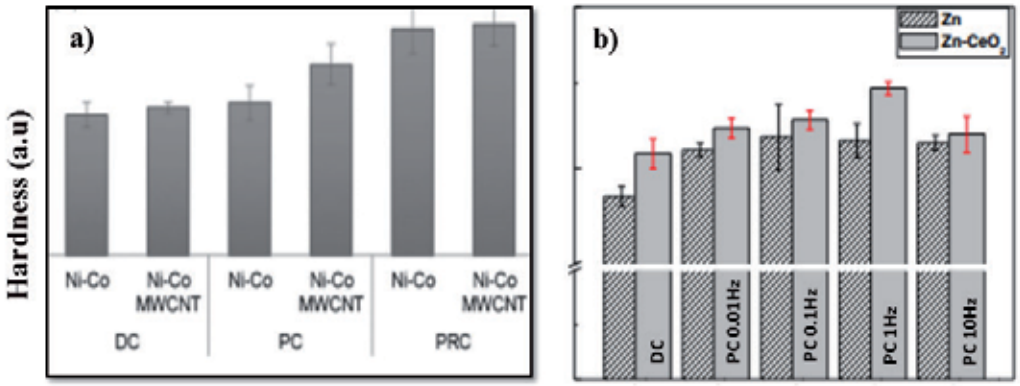

Figure 5. Hardness results of two different research due to process conditions

3.2. Property-performance relation

The properties of electrodeposits are important for several engineering applications. A fundamental concern of materials science is the connections between structure and properties, which is true for both bulk and coated materials. Properties of the electrodeposited composites are defined by the properties of the reinforcements used. Metal matrix is the phase for particles to be embedded. The particles used in applications such as diamond, SiC,and Al_2O_3 can be applied by vacuum coating techniques [1, 13-14] on metallic substrates. However, for the substrates that have girift geometry it is hard to obtain homogenous coatings with high adhesion. Metals and ceramics show different physical properties, such as thermal expansion coefficient; thus, multilayered structures could be necessary to acqiure better adhesion for codeposition process.

Electrochemically codeposited composite coating applications are devided into three groups. These are: dispersion hardening, wear, and electrochemical activity [13]. Dispersion hardening effect can be seen easily for oxide, nitride, carbide, and boride codeposited composite coatings when compared to pure metallic coatings. Dispersion hardening is defined as the increase against deformation. The main mechanism of deformation is motion of dislocations. The reinforcement in the composite coating structure blocks the dislocation motion and, as a result, strengthens the increase. Although there is no particular study of this phenomenon, grain size reduction can be seen in the matrix for codeposited composite coatings, which is thought to be the reason of increase in hardness. In scientific research, synergistic effect of grain size reduction and particles are given together [13]. Hardness is related to particle size, agglomer-

http://dx.doi.org/10.5772/61935

ation reduction and volume fraction of the particles in the metal matrix. Similarly, dislocation motion is defined with the distance of particles distributed in the coating layer. Increase in hardness is strongly affected by both the distance between particles and the volume fraction. However, it should be known that there is no limitless hardness increase in dispersion hardening, affected by reinforcement particles [13].

Composite coatings are commonly used in wear applications. Particle reinforcement to high and low frictional materials increases the wear resistance. Applications in equipments and contact surfaces of the motional parts of motors' can significantly extend their lifetime [13]. Composite coatings containing ceramic particles such as BN, diamond, SiC, WC, and Al_2O_3 show better abrasive wear resistance than the pure metallic coatings. Ramesh [19] found that Ni-TiC composite coatings with the volume ratio of 3% TiC showing four times less wear loss than the metallic Ni coatings.

In another research, open circuit potentials (the OCP curves) clarified that the values for in-situ co-deposited samples were shifted toward nobler potentials when compared. In addition, polarization curves of the coated samples were shifted toward the lower current densities. Upon the reversal of scanning, the increase in the zero-current potential also indicated the increased corrosion protection due to the in-situ phase transformations of electro codeposited composite coatings in inert atmospheres [15].

3.2.1. Porosity and grain structure

Porosity is the main sources of discontinuities in electrodeposites. It can noticeably affect corrosion behaviour, mechanical, and electrical properties, and also diffusion characteristics. It is influenced by the substrate, the plating solution and its operating conditions, and post-treatments [15]. An efficient method to minimize porosity is to use an under plate.

Moreover, the grain size of the coating metal affects several properties of the coating structure. The following properties change in size, hardness, surface roughness, brightness, resistance to deformation, stress, corrosion, and several mechanical properties. For a decorative coating, brightness is the major property, whereas the other properties are most important for industrial and engineering applications. If the grains consisting of the coating metal are coarser, coating will be both less hard and mat. On the contrary, metallic coating will be harder, smoother and brighter. Besides, coatings with finer grain size are expected to be less porous when compared to the coatings with coarser grains [10].

It is known that the reinforcement of ceramic particles dispersed in the metal matrix can increase the overall composite coating hardness by two possible hardening mechanisms. One of them is the dispersion of sub-micron sized hard particles in the matrix and another one is the grain size refinement of the metal matrix assisted by dispersed ceramic second phase particles. Therefore, according to the Hall-Petch effect, an increase in the hardness of matrix can be expected [20].

Bahkit & Akbari [21] revealed the synergistic effect of grain size reduction and particle reinforcement on the composite coatings fabricated by sediment codeposition technique

(SCD). In Figure 6, both metallic and composite coatings' hardness and grain size measurements are given, respectively.

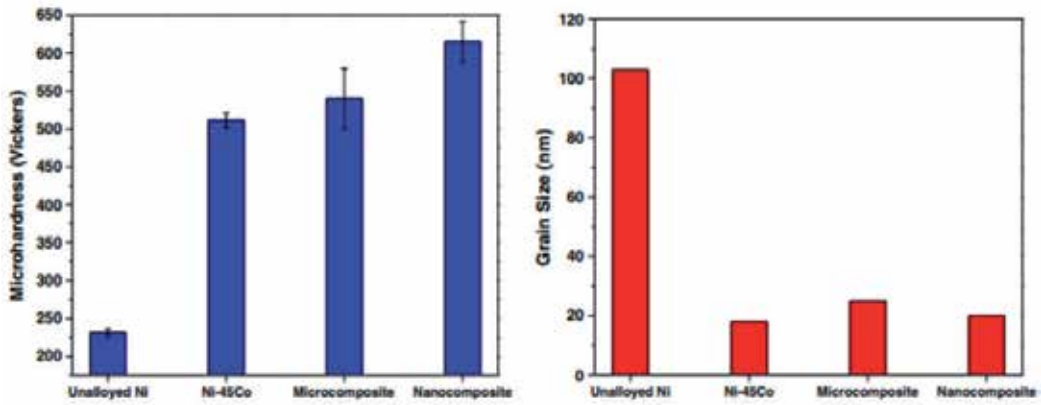

Figure 6. Hardness (left) and grain size (right) of unalloyed, Ni-45Co, microcomposite and nanocomposite coatings produced by SCD [21]

It is clearly seen that average particle size used in the process also affect the properties under same deposition conditions especially the grain size refinement of the metal matrix.

3.2.2. Size of the particles and second phase

The particles can create a dispersion-hardening effect so that they hinder the formation of dislocation in the grain, and act as pinning agents. Analogically, they can also hinder grain growth caused by annealing [8].

Reduction in the size of the particles in the composite coating increase the abrasion resistance. The reason for this case is less delimitation of the particles in the metal matrix. In a study on Cr-Al_2O_3 composite coatings, researchers indicated the reduction in the wear strength and brittleness when the amount of the particles was too big [10].

Another way to reduce the wear loss of surfaces moving relatively is to decrease the friction coefficient or lubrication. SiC particles create a lubricant film on the surface of Ni-SiC coatings. Because of the lubrication the wear resistance of the composite structure increases up to 2-3 times of a pure Ni coating. This has been proved by similar studies [10].

3.2.3. Particle distribution

The distribution of the particles and the second phase are important to obtain homogenous coatings. Otherwise, properties can chance locally, regions to regions and can cause the decrease of coatings' lifetime. This would be because of local corrosion attacs and/or wear loss. However, it is hard to obtain a homogenous structure since it can be controlled by agitation of the electrolyte during the co-deposition process. For more details on several agitaton types, revise Section 3.1.5.

http://dx.doi.org/10.5772/61935

3.2.4. Hardness/elastic module

The indentation hardness of materials can be measured in several ways by forcing an indenter having specific geometry [22]. The hardness and Young's modulus, two of the most commonly measured mechanical properties of materials, can be determined in an easy and reliable way due to the development of depth-sensing indentation equipment [23].

Furthermore, dynamic indentation method is more beneficial than the conventional Vickers microhardness testing in two aspects. Apart from microhardness the dynamic indentation method can also provide well-defined mechanical parameters such as elastic modulus of the material. Secondly, difficult and inaccurate optical observation and measurement of diagonal length of the indent/impression is no longer required because of the continuous monitoring of the load and depth of an indentation [24].

With the development of the nanoindentation technique, the mechanical properties within a sub-micron or nano scale have been widely discussed. The techniques are expected to be convenient for measurement of the mechanical properties of thin films [14].

The greater hardness values for composite coatings can be attributed to the greater hardness values of the reinforcements. The explaination of this phenomenon is based on the rule of mixture for composite materials. The rule states that the hardness of a composite can be formulated based on the volume fraction and the hardness of each individual component [20].

It is also known that the amount of wear volume (Q) during the wear tests is directly proportional to the compressive load (W), sliding distance (x) and inversely proportional to the hardness (H). It can be expressed by the Archard Equation (Eq.1) given below, where k_o is a non-dimensional wear coefficient that is specific to each material [20].

$$Q = k_o \frac{W.x}{H} \tag{1}$$

On the contrary, H/E ratio of materials gives an extremely close agreement to their raking in terms of wear behaviour. This is detailed by a similar research [25].

Some of the experimental results are given in Section 4.3 in comparison for in-situ codeposition process. According to these results, one can easily understand the relation between hardness and elastic modulus and also how the second phase particles change these properties.

3.2.5. Adhesion and diffusion

Adhesion of the coatings can be identified both qualitatively and quantitatively by a specific testing method called scratch test. This test is applied according to the procedure of mechanical failure modes and adhesion strength of ceramic materials. It is appropriate for adhesion measurement and possible failure modes prediction of metallic and ceramic substrates coated by thin ceramic films. This method does not give a characteristic value of the material. Instead, it reveals a practical engineering approach for substrate-coating system because the results are

obtained depending on the several test parameters. Details of the test method can be reached from ASTM-C1624 standard [26].

3.2.6. Corrosion

Corrosion is known to be influenced by a variety of factors. It is not possible to separate corrosion from many of the other property issues related to coatings. For the proper selection of a coating, it is necessary to take its position, with respect to its substrate in the galvanic series for the intended application, into consideration [27]. Decorative nickel-chromium coatings developed for automotive industry applications are a suitable example of the application of materials science and electrochemistry for the corrosion protection of materials.

There are several examples of electro codepositited composite coatings for corrosion protection [28-30]. According to these results, it is supported that corrosion resistance of composite coatings increase significantly with respect to the pure metallic or alloy coatings [15, 21]. This phenomenon is suggested to be the effect of the inert properties of the reinforcements.

For the Ni-Co alloy matrix SiC reinforced composite coatings, Bahkit & Akbari [21] expressed the corrosion behaviour of these coatings through potentiodynamic polarization curves (Figure 7). Calculated corrosion current densities and measured corrosion potentials are summerized in Table 1.

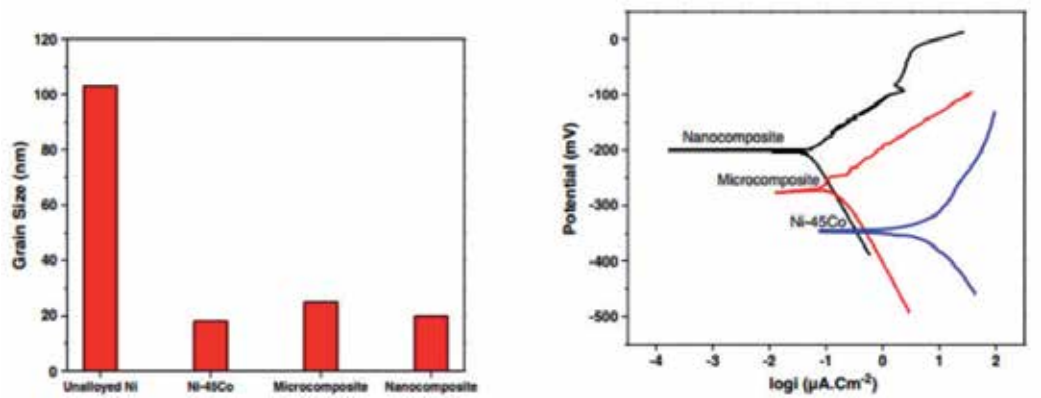

Figure 7. The potentiodynamic polarization curves of alloy coating and composite coatings

Coating	Eocp (mV)	βa (mV/dec)	βc (mV/dec)	Ecorr (mV)	icorr (μA.cm−2)	Rp (kΩ.cm2)
Ni-Co	-346	177.26	120.9	-354	6.570	4.75
Microcomposite	-277	71.94	162.1	-257	0.137	158.48
Nanocomposite	-201	71.18	176.5	-199	0.050	439.46

Table 1. Calculated and measured corrosion data for alloy and composite coatings

http://dx.doi.org/10.5772/61935

Based on the data, Ni-Co/SiC nanocomposite coating has the highest corrosion potential whereas the pure alloy coating (Ni-Co) has the lowest. Additionally, the corrosion current density of nanocomposite coating is lower than the micro scale SiC reinforced composite coating and shows the higher corrosion resistance (R_p) [21].

Additional examples belong to the main topic of the present chapter, in-situ codeposition, and the relation between metal matrix and inert reinforcements are given in Section 4.3.

3.2.7. Wear/friction

To give some examples for the practical wear applications of coatings, one can count chromium, electroless nickel, precious metals, anodized aluminium and so on [31]. But for engineering applications pure metallic coatings, or the conventional coatings mentioned are not enough to satisfy. Based on this idea, researchers have been focussed on recent advancements include codeposition of dispersed particles with metals. There are two alternatives to improve the wear resistance of a composite coating. The first method is to use hard particles in the metal matrix so as to increase the strenght of the surface against to the other frictive part. The second way includes creating the composite structure by using self lubricant reinforcements such as graphite, MoS_2, h-BN and WS_2 [16, 32-34].

Due to their specific study [9], as a function of graphite particle content in the electrolyte, reduction in the hardness is appeared but decrease in the wear loss (Figure 8a). It can be expressed by the self lubricant property of graphite. Furthermore, the phenomenon of composite friction/wear for Ni-Al_2O_3/graphite composite structure are described in Figure 8b as shown.

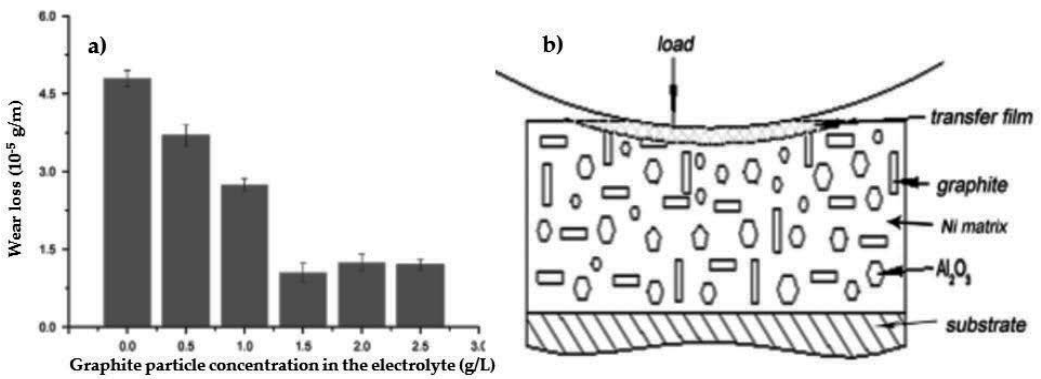

Figure 8. Wear loss versus graphite content in the electrolyte (a) and the schematic illustration of composite friction/wear phenomenon [9]

Friction coefficient and wear loss of composites initially decrease and then increase slowly back with the graphite particle concentration in the electrolyte. The results show an optimum graphite concentration in the electrolyte as 1.5g/L. Under this condition, the lowest friction coefficient, relatively high microhardness, and less wear loss was obtained.

3.2.8. Residual stress

Stress in coatings also adversely affects properties. Nowadays, a variety of options are available for stress reduction of coatings. These include: choice of substrate plating solution, use of additives, and higher plating temperatures. A number of theories have been assumed regarding the origins of stress, however, none of them covers every single situation. Several methods for stress measurement vary from the simple rigid strip technique to complicated methods. Both phase transformations in the composite and additional post-treatment of the coatings can decrease residual stress value in a composite coating [12].

4. In-situ codeposition

Until this section some of the details, advantages and additional performance criterias, related to the properties, were given about electo codeposition technique. When considering this technique, which is applied to metal-ceramic couples for some decades, researchers are tend to deposit the reinforcement and the metal directly. This technique is called *ex-situ codeposition* method. In this method, ceramic particles are suspended in the electrolyte and codeposited together with matrix metal directly. Of course, it brings some disadvantageous situations together because of the surface properties of the particles.

Some of the research groups improved ex-situ codeposition technique in last few years to eliminate the disadvantages. The new technique modified by researchers is called *in-situ codeposition* method and identifies the phase transformation of the reinforcement in the composite structure by various additional treatments such as heat-treatments between elements and/or compounds. Using this approach it is possible to obtain composite structures with wide range matrix metal (aluminium, titanium, iron, nickel, chromium and copper) and second phase particles (borides, nitrides, carbides, oxides and mixture of them) [12].

4.1. Comparison of ex-situ and in-situ methods

There are some advantages of in-situ codeposition technique when compared to the conventional codeposition (ex-situ method) route. These are:

- Reinforcement should be fabricated separately before electro deposition process in ex-situ production method. In this situation, the size of the reinforcement particles limited by the initial particle size and for practical applications size of the particles are rarely in sub-micron scale because of the economic reasons of nano particle production routes.
- Another advantage of in-situ method is particle-matrix interface. Surface structure of second phase particles and contaminants can cause a weak wettability between the particles and the matrix phase and this would be effective for the final properties of the composite structure. Especially the mechanical properties. On the other hand, coherently developed interface between the reinforcement and the matrix can be obtained strongly in in-situ production method.

http://dx.doi.org/10.5772/61935

- Additionally, thermally stable ceramic particles transformed in the composite structure can be distributed homogenously by this method. It is well known that homogeneity in the composite materials bring enhanced mechanical properties with itself.

All the advantageous and disadvantageous are summerized in Table 2.

Ex-situ (conventional method)	In-situ (new approach)
X Seperately reinforcement fabrication	√ Phase transformation during process
X Particle size is limitted	√ Controllable second phase size
X Weak particle-matrix interface	√ Coherently developed interface
X Possible but hard to achieve homogeneity	√ Homogenous particle distribution
√ Applicable with any oxide, boride, nitride, carbide, and also polymers	X Limited by the matrix metal and chemical affinity between additionals
√ No need for additional process	X Generally need additional heat-treatment

Table 2. Comparison summary of two methods

4.2. Post-treatment and transformations

In-situ codeposition method includes phase transformations and these come from additional post-treatments (heat-treatment) generally. There is a major point to be known about heat-treatment processes. It is called the stability of oxidation products such as carbides, nitrides, and oxides under different temperature and atmosphere conditions. Scientific reality that lies down this phenomenon is the change (decrease and increase) in the free energy of these components as a function of temperature (and aslo partial gas pressure). The tendency is important to predict the way of phase transformations according to the heat-treatment processes and defined by using special diagrams called Ellingham Diagrams which show the free energy change versus temperature [35].

4.3. Properties and performance

Traditionally, in electro codeposition technique for fabrication of metal-ceramic composites, ex-situ method is used [36-39]. In this method, ceramic particles are codeposited on cathode directly from the electrolyte (ceramic particle containing suspension). During the last decade, much attention has been paid to the preparation of metal matrix composites by a method that combines several techniques with an in-situ reaction method providing some advantages [40]. Differently, phase transformation of codeposited particles, such as carbon black with an additional heat treatment step has its special attention in this specific production route. It is because carbon is the unique element to compose carbide phase by in-situ transformation. From this perspective, the production route for this kind research includes both the codeposition of less studied carbon structures and in-situ phase transformation of metal matrix, such as chromium and various size of carbon black particles. Additionally, many different carbon sources in in-situ method codeposition can be used. To give some examples, they can be

directly carbon based particles, such as carbon black and graphite, or steel substrate itself, and etc.

Based on some former studies [14] the following section discusses fabrication of Cr-C composite coatings on steel substrates by electro codeposition technique and transformation of the layers into chromium matrix, carbide, and/or nitride reinforced composite phase structures with an additional heat treatment process for enhanced corrosive and mechanical applications. The discussion is based on the comparison of the similar research in the sphere.

The present section includes the production of functionally modified hard chromium coatings with a new approach. In addition to this, the observations of the property-performance relation for a specific Cr-C composite coating fabrication are provided. According to the experimental studies researchers fabricated three different coating groups. The identification of these groups are given in Table 3.

Sample-R	Traditional hard Cr coating (reference coating)
Sample-N	Electrodeposited Cr/C_{micro} composite (heat-treated under N_2 atmosphere)
Sample-A	Electrodeposited Cr/C_{micro} composite (heat-treated under Ar atmosphere)

Table 3. Identification of the samples [15]

XRD patterns are shown by annealing as-deposited Cr–C coatings, crystallization into a crystalline structure would occur. In the same results, it is clearly identified that for the Cr-C composite coatings give peaks that belong to carbide ($Cr_{23}C_6$), nitride (Cr_2N), oxide (Cr_2O_3) and pure metallic Cr phases after annealing (800°C/3h N_2 or Ar). The results showed that a small amount of Cr_2O_3 and $Cr_{23}C_6$ phases transformed under inert gas atmosphere (Ar) in some regions. On the other hand, change in heat treatment atmosphere (N_2) formed a new phase structure with the form of Cr_2N.

When compared the surface morphologies micro-cracked structure is visible along the surface for metallic chromium (fabricated by conventional methods). The similar surface structure with cracks is seen for the sample heat treated under Ar atmosphere with an increased crack width and density against the reference sample. Nevertheless, nitride phase formation modifies the surface denser and makes it crack-free with respect to the reference coating (see Figure 9 for details) [15].

Researchers have revealed that nitride formation takes place near the cracks and enlargens nitride-gas interface by the oxidation mechanism as expected [35]. Similarly, an interlayer is formed between the interfaces of coating and substrate. The cross-section of Sample-A gives the same interlayer lying between the coating-substrate interfaces (dark grey contrast). Since atomic carbon in the Cr-C layer can diffuse faster than chromium, the excess carbon atom in the Cr-C layer tends to form carbide phases [41]. The reason for this phenomena is the diffusion of C atoms from the steel substrate to the coating. Carbon atoms diffused from then transform to carbide phase due to the high chemical affinity of C atoms to the Cr atoms [42].

http://dx.doi.org/10.5772/61935

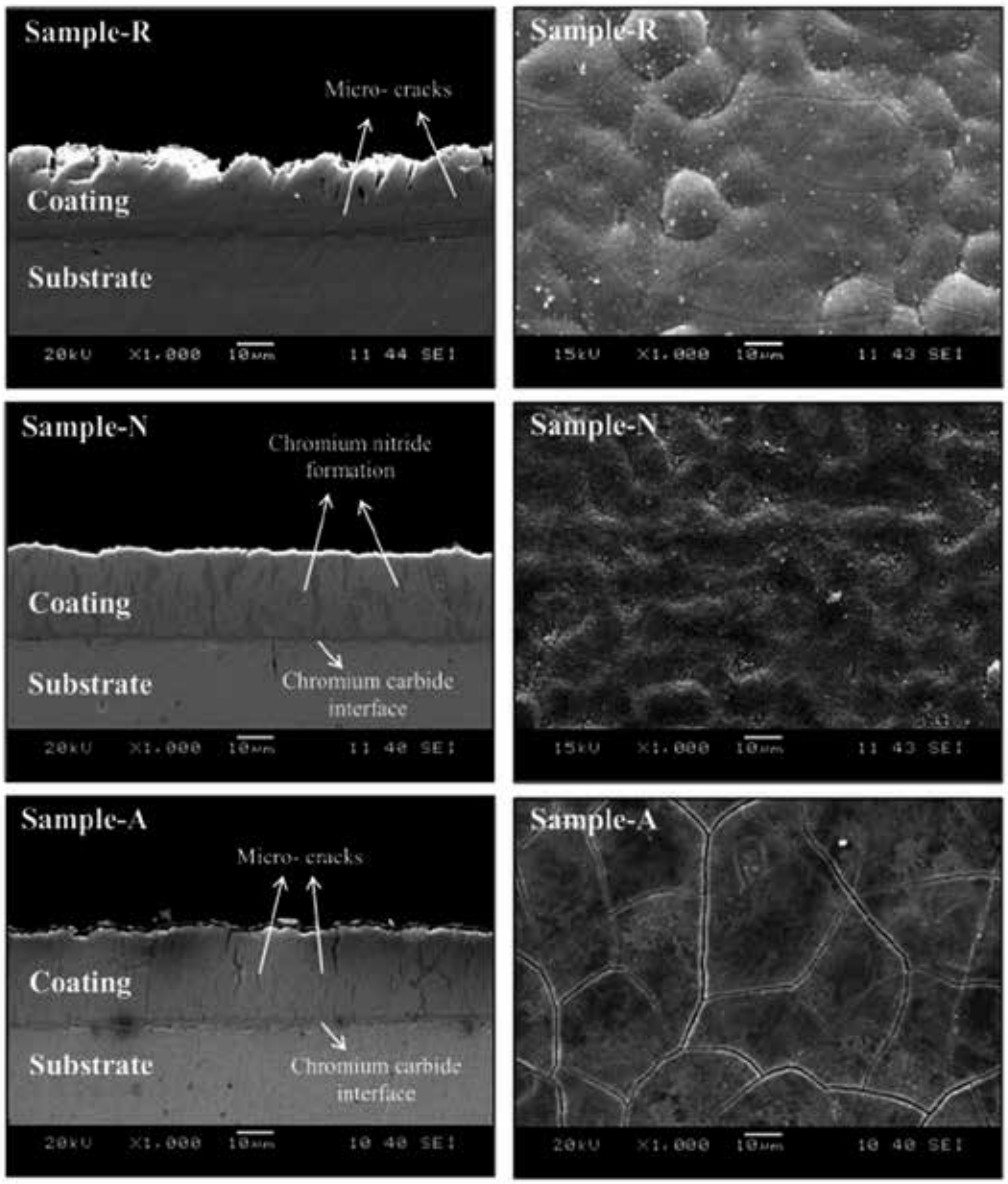

Figure 9. SEM micrographs of Sample-R, -N, and -A from the cross section and the surface

According to the EDS analysis taken, it was assumed that the dark regions are nitride phase for Sample-N and carbide formation occurred in the matrix and also along the interface for the both samples (Sample-N and Sample-A) [42]. Additionally, some of the zones are identified as nitride containing field and some not only nitride phase but also carbide. This is explained

by the N atoms diffusion from atmosphere into the and finally nitride phase formation in the micro-cracks [35].

Until this point, the details which render the study specificly are given about phase structure, transformations, and morphological structure of the composite coatings fabricated by this new method. The technique repeatedly shows its importance when considering the experimental results on both corrosion and mechanical behaviour.

Here are the results summarizing this specific study of the corrosion behaviour of coatings mentioned. Open-circuit potentials and cyclic polarization curves of steel substrate (1040) and, Sample-R, -N, and -A in aerated 3.5wt% NaCl solution are demonstrated in Figure 10 and some quantitative corrosion results are given in Table 4 in details.

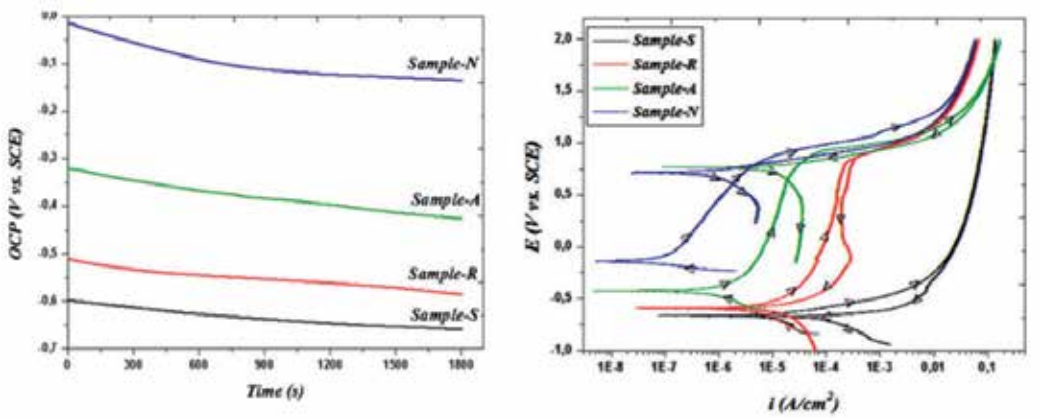

Figure 10. Open-circuit potentials (left) and cyclic polarization curves (right) of steel substrate (1040), and Sample-R, -N, and -A in aerated 3.5wt% NaCl solution [15]

Corrosion test results reveale that the passive current density of the heat-treated samples are lower than those of the untreated samples. That means it is possible to change the corrosion behaviors of the coatings by atmosphere controlled heat-treatments. In addition, Sample-N exhibits the higher polarization resistance and the lower corrosion current density as compared to the others.

	E_{corr} (mV)	I_{corr} (A)	Rp (Ω)
Sample-S	-635	$5.65x10^{-6}$	1.99
Sample-R	-587	$1.53x10^{-6}$	21.40
Sample-A	-394	$4.85x10^{-7}$	42.28
Sample-N	-124	$2.90x10^{-8}$	538.77

Table 4. Quantitative corrosion data of steel substrate and, Sample-R, -N, and -A [15]

http://dx.doi.org/10.5772/61935

It is clearly seen from the SEM micrographs of the coatings that countless number of superficial cracks exist all over the surface. Some of them lying from the coating surface through the cross-section. According to the microstructures it becomes clear that the presence of micro-cracks in Cr coating is the main reason on the corrosion resistance decrease. When it comes to the heat-treated samples, it is improved by the crack-filling effect of Cr_2N phase formation as seen in the cross-sectional images.

After the corrosion property, hardness and elastic modulus values are investigated for this study due to the heat-treatment effect on the in-situ phase transformations. It is shown that these phase formations are in a competition with stress relaxation on the hardness of composite coatings. While the relaxation decreases the hardness value, phase formations support the increase in the total hardness. The mentioned hardness values were decreased up to $480H_v$ level for only carbide formed composite coatings (see Table 5).

	E (GPa)	*H (GPa)*	*H (Vickers)*
Sample-R	147	14.1	1381
Sample-A	115	4.9	481
Sample-N	155	6.2	604

Table 5. Hardness and elastic modulus data of Sample-R, -N, and -A [12]

Nevertheless, this value is about $600H_v$ for the composite coatings which have both carbide and nitride phase. This result can be explained solely by the in-situ nitride formation with a crack filling effect. Similar results are explained on the elastic modulus increase for this specific research.

Two ways to improve the wear resistance of a composite coating were explained previously. One of them is to decrease the friction coefficient. The results of this study showed that the friction coefficient decrease was found to be about 50% for the samples in which nitride formation occurred. As a result of this effect, it is possible to suggest that the need of lubrication, vibrations and over heating can be decreased for engineering machinery applications by using these type functionally modified surfaces [12].

To take into account the adhesion behaviour of these composite coatings, there are no adhesive damage observed up to 30N maximum load for these samples (Sample-N, and -A). Only a little amount of cohesive damage occurred. In contrast, for the nitride formed samples this effect was seen much less. The coherence between the coating and the substrate is explained and supported by the diffusion of C atoms from the substrate to the coating and the formation of carbide interface for the samples.

Finally, as another mechanical result, residual stress values of the coatings were measured for these electro codeposited composites in this research. It is stated that the reference sample, which has only the pure metallic chromium phase, showing tensile stress in a high level as it was expected. Against, residual stresses are compressive and found to be about -380MPa and

-664MPa for the Sample-A and -N, respectively, while it is about +225MPa for Sample-R (reference coating). The reason for the decrease of residual stress is given as the increase in the volume of the in-situ transformed ceramic phase structures (see Figure 11 for details) [12].

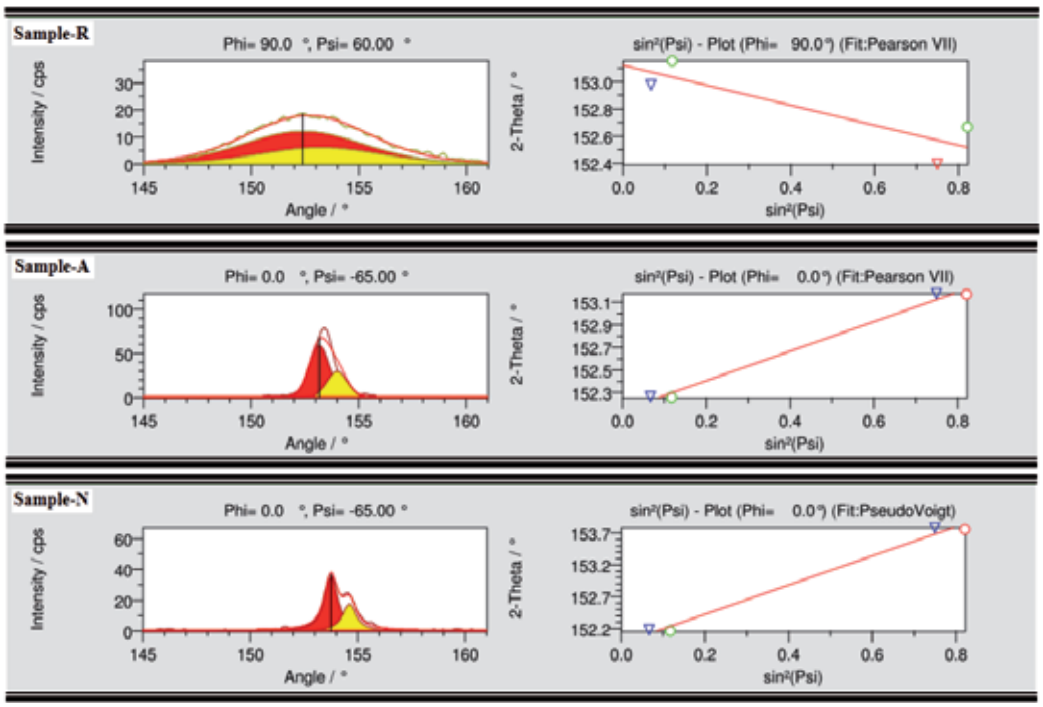

Figure 11. Intensity-angle, intensity-sin^2(Psi) fit curves residual stress values calculated from

The coatings are compared with respect to the conventional hard chromium coatings. In regard to the electrochemical behavior, the chromium-carbon black composite coatings heat-treated under nitrogen atmosphere showing a rehabilitated crack-free microstructure, exhibited better corrosion resistance than the conventional hard chromium structures. Therefore, the increase in corrosion potential suggests improvement of corrosion resistance due to the formation of carbide/nitride. Characteristic properties, such as hardness, and modulus of elasticity are determined for carbide and nitride formed composite coatings. It is observed that the following phase transformations support the recovery of friction-wear characteristics and accordance of substrate-coating interface belonging to the material. According to the detailed inspections, it is assigned that the definite results directly correlate with both the magnitude and the direction of the residual stresses. As a result, the corrosion behaviour and the mechanical properties of the in-situ electro codeposited coatings are believed to be controlled by microstructure and surface properties of the metallic chromium layer, which is modified by the formation of carbide and/or nitride phase, and can be used for many engineering applications instead of traditional metallic coatings.

Author details

Orkut Sancakoğlu*

Address all correspondence to: orkut.sancakoglu@deu.edu.tr

Orkut Sancakoğlu, Dokuz Eylül University, Metallurgical and Materials Engineering Department, Izmir, Turkey

References

[1] Kanani N. Electroplating-Basic Principles, Processes and Practice. Berlin: Atotech Deutschland GmbH; 2004. 347 p.

[2] Ciubotariu A.C, Benea L, Lakatos M, Dragan V. Electrochimica Acta. 2008;53:4557-4563. DOI: 10.1016/S0257-8972(03)00107-5

[3] Holleck H. Journal of Vacuum Science and Technology A. 1986;4(6):2661-2669. DOI: 10.1116/1.573700

[4] Birnbaum H.K. Hydrogen Embrittlement. Encyclopedia of Materials Science and Engineering, Pergamon Press; 1986. 2240p.

[5] Nguyen D, Thompson A.W, Bernstein I.M. Acta. Metall. 1987;35:2417-2425. DOI: 10.1016/0001-6160(87)90139-8

[6] Nakahara S, Okinaka Y. Acta Metall.1983; 31:713-724. DOI: 10.1016/0001-6160(83)90086-X

[7] Durney L.J. Hydrogen Embrittlement. Baking Prevents Breaking Products Finishing. 1985;49:90.

[8] Sancakoglu O. Co-deposition of Metal Films with Ceramic Nanoparticles on Metallic Substrates by Electrodeposition System [thesis] Izmir: Dokuz Eylul Univesity; 2009.

[9] Sun W, Zhang P, Zhao K, Tian M, Wang Y. Wear 2015;342-343:172-180. DOI: 10.1016/j.wear.2015.08.020

[10] Ertan C. Electrolytic Co-deposition of SiC and Al_2O_3 Nanoparticles with Chromium, Coating Characterization and Investigation of Mechanical Properties [thesis] Izmir: Dokuz Eylul Univesity; 2010.

[11] Man J, Zhang S, Li J, Zhao B, Chen Y. Surf. Coat. Technol. 2014;249:118-124. DOI: 10.1016/j.surfcoat.2014.03.054

[12] Sancakoglu O. Electrolytic Co-deposition of Carbon Nanoparticles with Metals, Improvement of Corrosive and Mechanical Properties [thesis] Izmir: Dokuz Eylul Univesity; 2013.

[13] Sancakoglu O, Erol M, Agaday B, Celik E. Mater. Technol. 2013;47(2):601-604.

[14] Sancakoglu O, Culha O, Toparli M, Agaday B, Celik E. Mater. Des. 2011;32(7): 4054-4061. DOI: 10.1016/j.matdes.2011.03.027

[15] Sancakoglu O, Ungan G, Celik E, Aksoy T. Int. J. Appl. Ceram. Technol. 2015;12(4)830-836. DOI: 10.1111/ijac.12257

[16] Tudela I, Zhang Y, Pal M, Kerr I, Cobley A. Surf. Coat. Technol. 2015;276:89-105. DOI: 10.1016/j.surfcoat.2015.06.030

[17] Karslioglu R, Akbulut H. Appl. Surf. Sci. 2015;353:615-627. DOI: 10.1016/j.apsusc. 2015.06.161

[18] Nemes P, Lekka M, Fedrizzi L, Muresan L. Surf. Coat. Technol. 2014;252:102-107. DOI: 10.1016/j.surfcoat.2014.04.051

[19] Bapu G.N.K. Surface and Coatings Technology. 1994;67(1-2):105-110. DOI: 10.1016/ S0257-8972(05)80033-7

[20] Farrokhzad M.A, Saha G.C, Khan T.I. Surf. Coat. Technol. 2013;235(1-2):75-85. DOI: 10.1016/j.surfcoat.2013.07.015

[21] Bakhit B, Akbari A. Surf. Coat. Technol. 2012;206:4964-4975. DOI: 10.1016/j.surfcoat. 2012.05.122

[22] Gogotski Y, Miletich T, Gardner M, Rosenborg M. Rev. Sci. Instrum. 1999;70:4612-4617. DOI: 10.1063/1.1150122

[23] Zhu W, Bartos P.J.M. Cem. Concr. Res. 2000;30:1299-1304. DOI: 10.1016/ S0008-8846(00)00322-7

[24] Uzun O, Kolemen U, Celebi S, Guclu N. J. Eur. Ceram. Soc. 2005;25;969-977. DOI: 10.1016/j.jeurceramsoc.2004.03.031

[25] Silva F.J.G, Martinho R.P, Baptista A.P.M. Thin Solid Films 2014;550: 278-284. DOI: 10.1016/j.tsf.2013.11.042

[26] ASTM C1624-05. (2010). Standard test method for adhesion strength and mechanical failure modes of ceramic coatings by quantitative single point scratch testing. West Conshohocken: American Society for Testing and Materials International.

[27] Sard R, Leidheiser H, Ogburn F, editors. Corrosion in Electronic Applications: Properties of Electrodeposits, Their Measurement and Significance. The Electrochemical Soc. 1975.

[28] Edigaryan A.A, Safonov V.A, Lubnin E.N, Vykhodtseva L.N, Chusova G.E, Polukarov Y.M. Electrochim. Acta. 2002;47:2775-2786. DOI: 10.1016/S0013-4686(02)00163-9

[29] Chen Z.Y, Li Z.Q, Meng X.H. Appl. Surf. Sci. 2009;255:7408-7413. DOI: 10.1016/ j.apsusc.2009.04.009

[30] Zeng Z, Wang L, Liang A, Zhang J. Electrochim. Acta. 2006;52:1366-1373. DOI: 10.1016/j.electacta.2006.07.038

[31] Ozkan E. Wear and Corrosion Behaviour of Electrochemically Deposited Bioactive Hydroxyapatite Coatings on Implant Materials [thesis] Izmir: Dokuz Eylul Univesity; 2006.

[32] Yang J, Zhang Y, Zhao X, An Y, Zhou H, Chen J, Houa G. Tribology International. 2015;90:96-103. DOI: 10.1016/j.triboint.2015.04.022

[33] Lingsen W, Bing Y, Yi F. J. Cent. S. Univ. Technol. 1996;27:194–201.

[34] Chen B, Bi Q, Yang J, Xia Y, Hao J. Tribology International. 2008;41:1145-1152. DOI: 10.1016/j.triboint.2008.02.014

[35] Roberge P.R. Handbook of Corrosion Engineering. New York: McGrawHill. 2000.1141p.

[36] Vinokurov E.G, Arsenkin A.M, Grigorovich K.V, Bondar V.V. Prot. Met. 2006;42:204-207. DOI: 10.1134/S0033173206020160

[37] Lubnin E.N, Polyakov N.A, Polukarov Y.M. Prot. Met. 2007;43:186-193. DOI: 10.1134/S0033173207020117

[38] Surviliene S, Jasulatiene V, Lisowska-Oleksiak A, Safonov V.A. J. Appl. Electrochem. 2005;35:9-15. DOI: 10.1007/s10800-004-1760-7

[39] Rudnik E. Appl. Surf. Sci. 2008;255:2613-2618. DOI: 10.1016/j.apsusc.2008.07.143

[40] Zhong L, Xu Y, Hojamberdiev M, Wang J, Wang J. Mater. Des. 2011;32:3790-3795. DOI: 10.1016/j.matdes.2011.03.031

[41] Kwon S.C, Kima M, Parka S.U, Kima D.Y, Kima D, Nama K.S, Choi Y. Surf. Coat. Technol. 2004;183:151-156. DOI: 10.1016/j.surfcoat.2003.09.069

[42] Kim D, Kim M, Nam K.S, Chang D, Kwon S.C. Surf. Coat. Technol. 2003;169-170:650-654. DOI: 10.1016/S0257-8972(03)00107-5

Chapter 5

Electrodeposition of Cu–Ni Composite Coatings

Casey R. Thurber, Adel M.A. Mohamed and Teresa D. Golden

Additional information is available at the end of the chapter

http://dx.doi.org/10.5772/62111

Abstract

The electrodeposition of Cu–Ni incorporated with nano- to microparticles to produce metal matrix composites has been reviewed in this chapter. The inclusion of particles into the metal matrix produced enhanced properties in the areas of electronics, mechanics, electrochemistry, and corrosion. In electronics, an increase in the magnetic properties and durability for microactuators was observed. Measurements of the mechanical properties showed an increase in hardness, wear resistance, shear adhesion, and tensile strength for the material. The corrosion resistance of the metal matrix coatings was improved over that of pure Cu–Ni. As the accessibility of nanoparticles continues to increase, the interest in reduced cost and low-temperature electrodeposited metal matrix composites continues to rise. However, only a small number of articles have investigated Cu–Ni composite coatings; these composite coatings need further examination due to their advantageous properties.

Keywords: Electrodeposition, Metal Matrix Composites, Cu-Ni alloys, Coatings, Nanoparticles

1. Introduction

Metal matrix composite (MMC) coatings engineered using an electrodeposition method are examined in this chapter. The electrodeposition of a composite involves the electrolysis of plating baths where nano- to micro- sized particles are dispersed and various quantities of the particles become imbedded within the plated metal matrix, providing special properties to the coating (Figure 1) [1]. The process of particle incorporation into metal coatings can be simplified into four steps: (1) particles dispersed in solution form a surface charge; (2) from the bulk solution, there is mass transport of the particles to the surface of the electrode typically through convection; (3) there is interaction between the particle and the electrode; (4) the particles become trapped within the growing metallic film [2]. The earliest example of electrodeposited

composites dates back to the 1920s where Cu–graphite coatings were developed for automotive bearings [3, 4]. Enhanced corrosion, tribological, and mechanical properties were the main research focus of the automotive and aerospace industries in the 1970s–1990s, leading to significant technological advancements. In the early 2000s, some of the focus started to shift to electrical components and electronic devices [5–10]. As the accessibility of nanoparticles continues to rise, the interest in reduced cost and low-temperature electrodeposited MMCs continues to escalate [2].

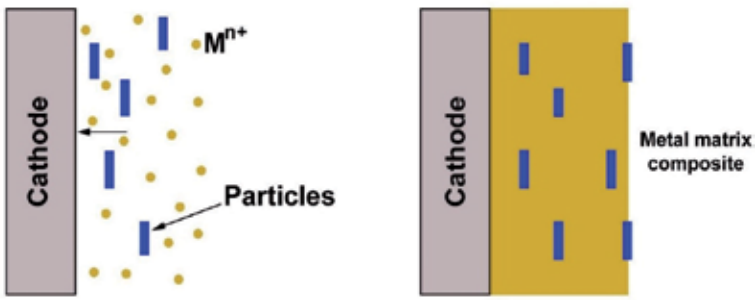

Figure 1. Schematic displaying the growth of MMCs by electrodeposition.

Coatings can be produced by using several different approaches, and electrodeposition remains a prominent technique to produce novel materials for science and engineering applications. Electrodeposition also offers low cost, convenience, ability to work at low temperatures, and the ease of application to complex geometries [11, 12]. Other advantages for using electrodeposition include the ability to quickly scale to an industrial setting, uniform coating of large samples, and accurate control of the coating thickness [2]. Other methods for producing MMCs include commercial pressing [13], laser cladding [14], hot pressing [15], plasma transferred-arc surfacing [16], stir casting [17], diffusion bonding [18], powder metallurgy [19], and chemical vapor deposition [20]. Each of these methods has different advantages and disadvantages. However, some of the drawbacks include production at high temperatures or under vacuum, difficulty in controlling the thickness, and cost.

MMCs coatings combine the advantageous properties of each individual material together which is not possible with the non-composite metal films [21, 22]. An extensive amount of work has gone into examining copper-based MMCs [23–27] and nickel-based MMCs [28–32] since individual metals can exhibit a limited range of properties. An important route to improving the properties of individual metals is the deposition of alloys such as Zn–Ni, Ni–Mo, and Cu–Ni [33–35]. Successful incorporation of particles into the metal matrix by electrocodeposition relies on many different parameters, including the composition of the electrolyte, pH, current density, and properties of the particles [36]. Incorporating particles such as TiO_2, SiC, Al_2O_3, carbon fibers, Ni, Al, and Cr into the Cu–Ni matrix of different coatings enhances the electrical, mechanical, and corrosion properties of the coatings [5–9, 21, 37–40].

Copper alloys, such as Cu–Ni, have been studied because of their good electrical and thermal properties, machinability, and resistance to corrosion [41–44]. Copper is relatively soft and

http://dx.doi.org/10.5772/62111

needs to be alloyed with another metal, such as nickel, to increase the hardness of the material [43, 45]. Also, with the addition of Ni into the Cu matrix during electrodeposition, it is possible to grow films with minimal strain due to both Cu and Ni having face-centered cubic crystal structures and similar lattice parameters [46]. The electroplating of copper alloy films has an instrumental role in many different industry-related applications. For instance, electroplating has found a niche in microelectromechanical systems (MEMS) because the process can deposit different alloys onto depressed and oddly shaped geometric substrates [5, 6, 10, 45]. Cu–Ni coatings have been evaluated for use as inert anodes in the fabrication of aluminum because of their enhanced electrical and thermal conductivity [8, 9]. In marine environments, copper alloys are used to defend against biofouling of materials by inhibiting microbial-induced corrosion (MIC) [47–50].

Understanding the incorporation of particles into these alloys requires mathematical modeling. Early models dating back to the 1960s from Williams and Martin [51] proposed that particles were transported to the cathode surface via a convection transport mechanism facilitated by stirring the plating bath. Brandes and Goldthorpe [52] hypothesized that entrapment by mechanical means was not the only factor at play and decided that an electrostatic force must be aiding the inclusion of the particles into the metal matrix. In 1972, Guglielmi [53] became the first to propose a mathematical model that explained the inclusion of particles into the metal matrix. The model followed a simple two part approach: (a) the particles slowly move toward the surface of the cathode and adsorb very loosely and (b) then the particles become securely adsorbed by shedding their ionic cloud. The derived model equations are [40, 53]:

$$\frac{C\left(1-\alpha\right)}{\alpha}=\frac{Wi_{o}}{nFd\upsilon_{o}}e^{(A-B)\eta}\left(\frac{1}{k}+C\right) \tag{1}$$

$$i=\left(1-\vartheta\right)i_{o}e^{A\eta} \tag{2}$$

where C is the vol.% of particles in the electrolyte solution and α is the vol.% of the particle incorporated in the composite film. W corresponds to the atomic weight of the metal in the coating, F is Faraday's constant, d is the density of the metallic coating, and n is the valence of the metallic coating. η relates to the overpotential, i is the current density, and i_o is the current density from the metallic coating. The υ term is a constant from the deposition of the particle, A is a constant from the deposition of the metal, and B is a constant from the particle inclusion. The ϑ relates to the coverage of the surface by the particle that is incorporated into the metal coating and k is the adsorption coefficient. Although the model has some holes, such as not taking into account the mass transport of the metal ions or the particles and the nature of the particle or the shape, it is still one of the most widely used models to date. In 1987, Celis et al. [54] hypothesized a nnew five part model, which is built on the idea of Guglielmi's two part model. The drawback of this model is that factors need to be created that are specific to each individual system. As late as 2002, Bercot's group [55] proposed an addition to Guglielmi's original model that included a polynomial for the purpose of correcting for different effects presented by adsorption and flow.

A survey of the literature for the incorporation of particles into Cu–Ni coatings is shown in Table 1. The composite coatings described in Table 1 are for electrodeposited processing only. Other Cu–Ni composites have been made using different techniques, but fall outside the scope of this chapter.

This chapter will cover the electrodeposition of Cu–Ni alloys onto steels and other substrates to improve corrosion resistance and mechanical properties. The influence of the deposition parameters will be covered as well as the electrodeposition mechanism. The resulting mechanical and corrosion properties will also be discussed in the chapter.

Reference	Possible Applications	Deposition Conditions	Composite
Panda et al. [5]	Recessed microelectrodes for MEMS devices	1.0 M $NiSO_4 \cdot 6H_2O$ 0.04 M $CuSO_4 \cdot 5H_2O$ 0.3M $Na_3C_6H_5O_7 \cdot 2H_2O$ 3.125–12.5 g/L Al_2O_3 j = 2–50 mA/cm^2 26°C	Cu–Ni alloy incorporated with γAl_2O_3 (~30 nm)
Huang et al. [10]	Magnetic microactuators for MEMS Devices	200–250 g/L $CuSO_4 \cdot 5H_2O$ 45–90 g/L H_2SO_4 Plating rate: ~0.2 μm/min 40°C	Cu incorporated with Ni nanopowder (~50 nm)
Chen et al. [6]	Electrical and electronics (speakers)	Alkaline noncyanide-based copper-plating solution 2–8.5 g/L Ni 40°C Stir rate: 250 rpm	Cu incorporated with Ni nanoparticles
Huang et al. [8, 9]	Electrical and electronics (MEMS devices)	120 g/L $Na_3C_6H_5O_7 \cdot 2H_2O$ 25 g/L H_3BO_3 12 g/L $NiCl \cdot 7H_2O$ 100 g/L $NiSO_4 \cdot 7H_2O$ 5–25 g/L $CuSO_4 \cdot 5H_2O$ j = 0.5–2 A/cm^2 35°C	Cu–Ni incorporated with Cr nanoparticles (~40 nm)
Chrobak et al. [21]	Mechanical and Young's modulus	150 g/L $CuSO_4 \cdot 5H_2O$ 10 g/L H_2SO_4 Ni 0.1–20 mg/mL j = 1–100 mA/cm^2	Cu incorporated with Ni nanoparticles (~100 nm)
Fawzy et al. [37]	Mechanical and hardness	50 g/dm^3 $Na_3C_6H_5O_7 \cdot 2H_2O$ 25 g/dm^3 H_3BO_3 50 g/dm^3 $Na_2SO_4 \cdot 10H_2O$ 40 g/dm^3 $NiSO_4 \cdot 7H_2O$ 5–25 g/dm^3 $CuSO_4 \cdot 5H_2O$ j = 0.33–1.33 A/dm^2 0–20 g/dm^3 Al_2O_3 and TiO_2	Cu–Ni incorporated with Al_2O_3 and TiO_2

Reference	Possible Applications	Deposition Conditions	Composite
Hashemi et al. [38]	Mechanical, hardness, and wear	90 g/L $H_3C_6H_5O_7$ 60 g/L NaOH 60 g/L $Na_2WO_4 \cdot 2H_2O$ 20 g/L $NiSO_4 \cdot 7H_2O$ 1 g/L $CuSO_4 \cdot 5H_2O$ 0–25 g/L SiC j = 10–50 mA/cm^2 Stir rate = 100–600 rpm	Cu–Ni–W incorporated with SiC (~50 nm)
Wan et al. [39]	Mechanical and tensile strength	*Bath Conditions Not Given	Cu–Ni reinforced carbon fibers (6–8 μm)
Cui et al. [40]	Electrochemical Study for Magnetic and mechanical properties	184 g/dm^3 $NiSO_4 \cdot 6H_2O$ 6.24 g/dm^3 $CuSO_4 \cdot 5H_2O$ 76.47 g/dm^3 $Na_3C_6H_5O_7 \cdot 2H_2O$ 0.2 g/dm^3 Sodium dodecyl sulfate 0.5 g/dm^{3}saccharin Stir rate = 200 rpm j = 10-20 mA/cm^2 30°C	Cu–Ni incorporated with Al nanoparticles (3 μm)
Thurber et al. [60]	Mechanical, hardness, shear and corrosion	0.24 M $Ni(NH_4)_2(SO_4)_2 \cdot 6H_2O$ 0.06 M $CuSO_4 \cdot 5H_2O$ 0.25 M $Na_3C_6H_5O_7 \cdot 2H_2O$ MMT 0–0.2% E_{app} = –1.0V 25°C	Cu–Ni incorporated with MMT platelets

Table 1. A summary of the work produced on electrodeposited Cu–Ni composite coatings.

2. Cu–Ni MMCs in MEMS and Electronics

Cu–Ni composites have shown to be beneficial in the area of MEMS devices, microactuators, and electronics. Al_2O_3, Ni nanoparticles, and Cr particles have been incorporated into the metal matrix to produce improved mechanical properties, magnetic properties, and chromia scale for oxidation resistance [5, 6, 8–10].

Panda et al. [5] evaluated the electrodeposition of graded Ni–Cu alloys and Ni–Cu–γAl_2O_3 composites into deeply depressed electrodes made using X-ray lithography for use in MEMS devices. The rotating cylinder experiment showed that the current efficiency was below 100% for the deposition over a diverse range of current densities. With the inclusion of 12.5 g/L of alumina at a rotation rate of 1,000 rpm, it was found that the current efficiency was drastically lowered by the incorporation of the nanoparticles below 20 mA/cm^2 but produced deposits with higher copper content which was preferred. At the greater current densities (30–50 mA/cm^2), the current efficiency was less effected but lead to coatings with higher nickel content.

The Cu weight ratio was studied at different heights on the micropost for pure Cu–Ni and Cu–Ni–Al_2O_3 at current densities of 10 and 15 mA/cm^2, seen in Figures 2 and 3, respectively. A rise in the concentration of Cu along the post was expected due to the reduction of boundary layer thickness because of the diffusion-controlled reaction mechanism of copper. The composite micropost showed a sharp increase in the Cu concentration starting at about a height of 300 μm with the incorporation of alumina, which suggests that the incorporated nanoparticles into the plating bath helped to improve the mass transport at the site of the recess.

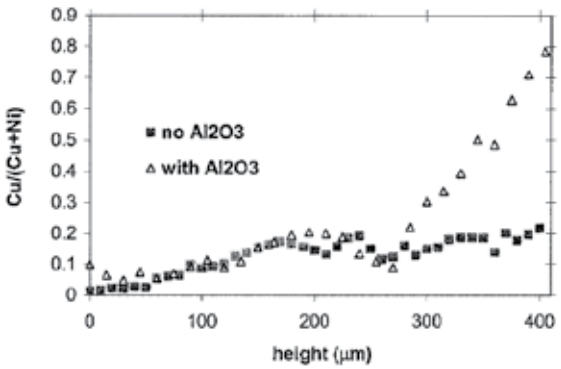

Figure 2. The copper weight ratio versus the height of the micropost with and without alumina for the current density of 10 mA/cm^2 and a duty cycle of 0.125. "Reproduced by permission of The Electrochemical Society." [5].

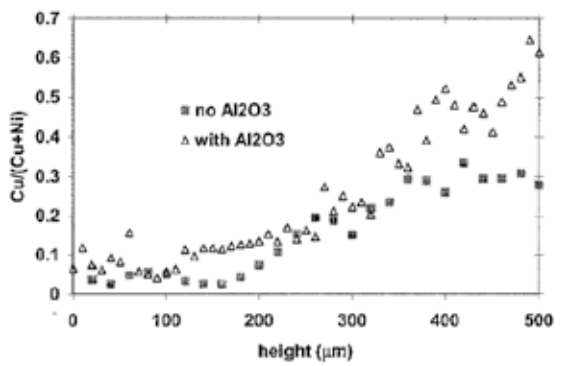

Figure 3. The copper weight ratio versus the height of the micropost with and without alumina for the current density of 15 mA/cm^2 and a duty cycle of 0.125. "Reproduced by permission of The Electrochemical Society." [5].

Huang et al. [10] experimented with a Cu–Ni composite from a plating bath consisting of an alkaline copper solution incorporated with 2–5 g/L of ~50 nm nickel nanoparticles to increase the performance in magnetic microactuators for MEMS. The superconducting quantum interference device (SQUID) measurements for magnetism seen in Figure 4 demonstrates that with the inclusion of ferromagnetic Ni particles into the copper matrix, the film shifts from

http://dx.doi.org/10.5772/62111

diamagnetic to ferromagnetic in nature as the curve becomes larger. The vertical displacement of the magnetic microactuator was measured for the actuator coils fabricated from copper and Cu–Ni composite materials. Figure 5 indicates that under the same experimental conditions, the Cu–Ni composite coil possessed a greater vertical displacement versus the pure Cu film, leading to about a 9% increase in the actuation enlargement performance.

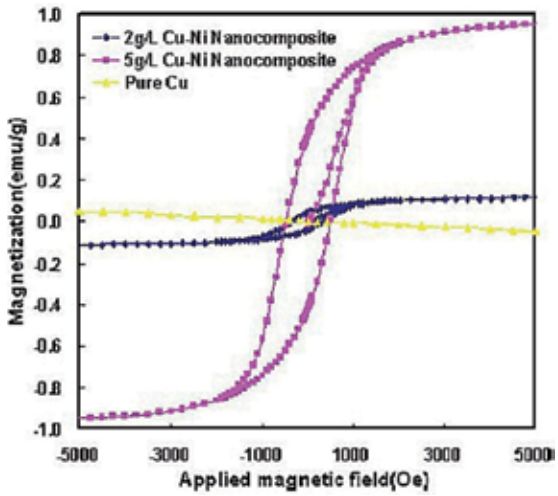

Figure 4. The SQUID measurements of copper versus the Cu–Ni composite electrodeposited from a bath that contained 2–5 g/L of nickel nanopowder. "Reprinted with permission from [10]. Copyright [2007], AIP Publishing LLC."

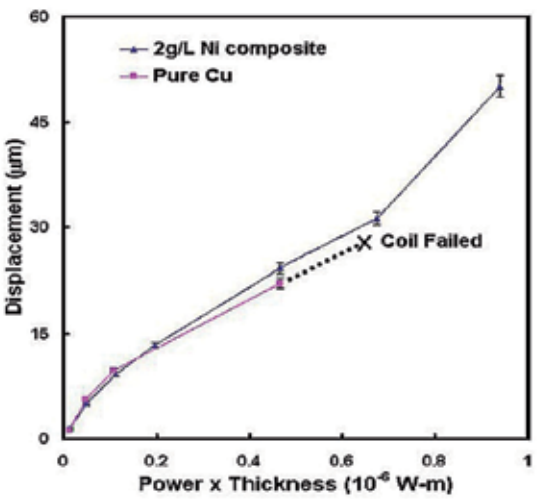

Figure 5. The vertical displacement results of the diaphragms compared to the normalized input experienced by the driving coils, which consists of the copper and Cu–Ni composite."Reprinted with permission from [10]. Copyright [2007], AIP Publishing LLC."

Chen et al. [6] proposed a new coil material for a reduced power electromagnetic microactuation device using Cu–Ni nanocomposites from an alkaline Cu-plating bath integrated with 2–8.5 g/L 100 nm nickel nanoparticles. Different coil widths ranging from 10–500 μm were examined with SQUID and resistivity measurements to determine the optimal power-saving microspeaker device. The SQUID and resistivity analysis found that the 200 μm wide inductive coil from the bath containing 2 g/L of Ni nanoparticles had optimal ferromagnetic characteristics with low resistivity. The sound pressure level was then evaluated for the pure copper and optimal Cu–Ni nanocomposite wire for a frequency ranging from 1–6 kHz, which resulted in a 40% power savings for the Cu–Ni nanocomposite versus the pure copper coil [6].

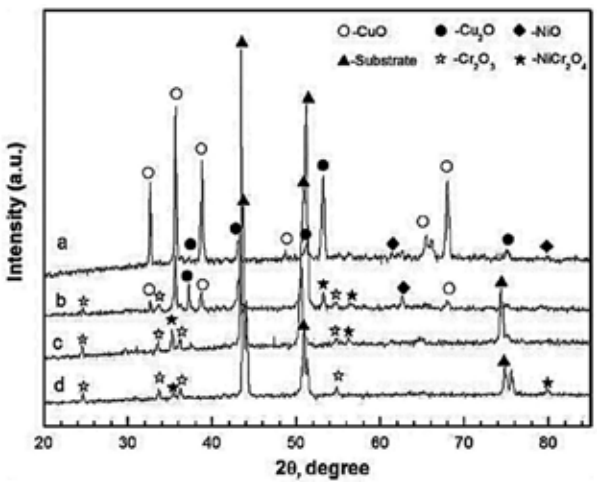

Figure 6. The stacked X-ray diffraction patterns of the Cr_2O_3 scale generated on four different samples after oxidation in atmosphere at 800 °C for 20 h: [a] commercial grade Cu–30Ni–20Cr, [b] commercial grade Cu–50Ni–20Cr, [c] electrodeposited Cu–30Ni–20Cr composite, and [d] electrodeposited Cu–50Ni–20Cr composite [9]."Reprinted with the permission of Cambridge University Press."

A crucial problem for extending the applications of Cu–Cr MMCs is poor resistance to oxidation, specifically in high-temperature environments for the electrical and electronic industries [8, 9]. This is due to the fact that at high temperatures chromium has a low solubility into copper, which greatly decreases the chromium amount diffusing to the surface of the copper matrix, preventing growth of the protective Cr_2O_3 scale. Nickel can be added into the matrix to increase the solubility of Cr into the composite to help increase the resistance to oxidation [9]. Huang et al. [8] discussed the electrodeposition of Cu–Ni–Cr, where copper and nickel were at a 1:1 ratio. They found that incorporating 15–20 wt.% Cr nanoparticles (~40 nm) into the Cu–Ni matrix allowed for a good chromia scale to form during the oxidation process in atmosphere at 800°C. It was found that incorporating less than 15 wt.% Cr lead to non-uniform growths of the chromia scale. Huang et al. [9] also examined the electrodeposition of Cu–30Ni–20Cr and Cu–50Ni–20Cr for the formationof the Cr_2O_3 protective scale. Figure 6 displays an X-ray diffraction pattern for the two electrodeposited coatings plus two commercially available alloys of the same composition after oxidation in atmosphere at 800°C. The

http://dx.doi.org/10.5772/62111

result shows that the commercial alloys mainly consist of more NiO, Cu_2O, and CuO after oxidation, whereas the electrochemically prepared coatings consist primarily of Cr_2O_3 and $NiCr_2O_4$. Figure 7 shows SEM pictures of the Cr_2O_3 scale created from the oxidation process at 800°C. It was discovered that for the electrodeposited samples the Cr_2O_3 scale quickly formed in the initial stage of growth and continued through the steady-state stage, where the coating acts as a reservoir for Cr to maintain the chromia scale growth. The commercially available sample Cu–50Ni–20Cr showed a similar result to the electrodeposited coatings but the Cu–30Ni–20Cr showed virtually no growth of the Cr_2O_3 scale, which showed that the commercial grade relied on an increase in Ni content to grow the chromia scale [9].

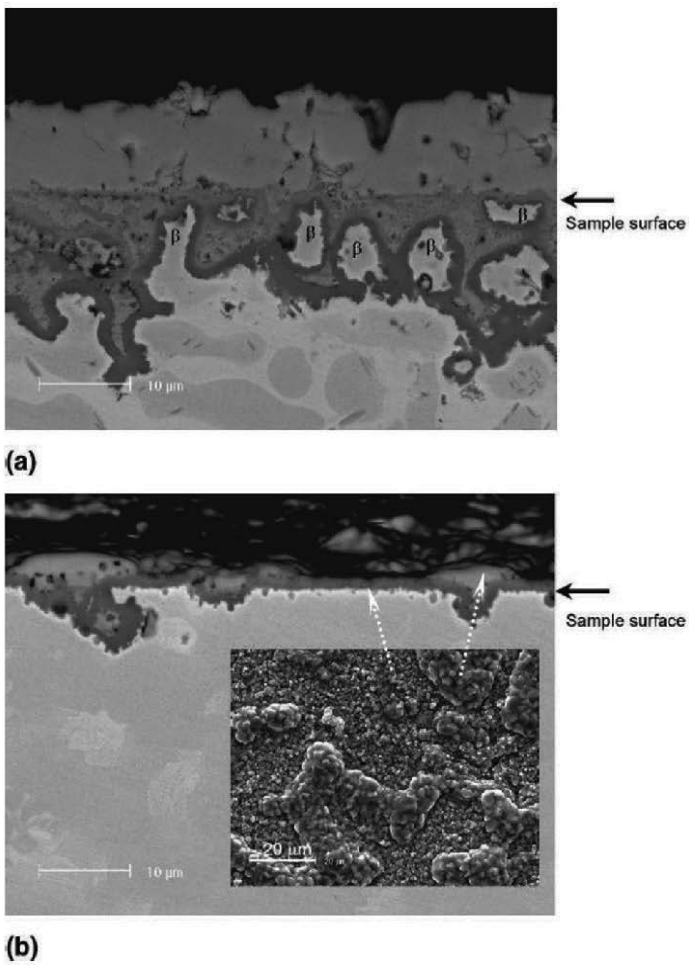

Figure 7. The cross-sectional SEM of the Cr_2O_3 scales formed on the surface of the Cu–Ni–Cr alloys of [a] Cu–30Ni–20Cr and [b] Cu–50Ni–20Cr, which was oxidized for 20 h in atmosphere at 800°C and the inset displays the structure of the different oxides at the surface, which are designated by arrows [9]."Reprinted with the permission of Cambridge University Press."

3. Cu–Ni MMCs for Enhanced Mechanical Properties

Particle incorporation can be used to improve mechanical properties for MMC coatings over that of the pure metal matrix. The Cu–Ni matrix has been incorporated with Ni particles, TiO_2, Al_2O_3, SiC, carbon fibers, and montmorillonite to increase the hardness, wear resistance, shear adhesion, and tensile strength [21, 37–39, 60].

Chrobak et al. [21] examined the electrodeposited copper incorporated with Ni powder (~100 nm) at varying current densities to examine the effects to Young's modulus. They experimented with current densities ranging from 1–100 $mAcm^{-2}$ and found that the concentration of Ni in the coating increases linearly with current density but the thickness of the coating decreases because the transport of Cu to the electrode surface is suppressed by the Ni particles. They also discovered that adding 25 vol.% of glycerol to the bath helped reduce agglomeration and decrease the grain size of the MMC coatings. The Young's modulus was found to decrease when the Ni concentration was increasing. This trend was even more drastic as the current density was increased because an increased current density leads to higher concentrations of Ni [21].

Fawzy et al. [37] examined how the current density, concentration of ceramic particles in the electroplating solution, and pH of the plating bath affected the hardness for Cu–Ni, Cu–Ni–αAl_2O_3, and Cu–Ni–TiO_2 composite coatings. By increasing the current density from 0.33 to 1.33 Adm^{-2} for the Cu–Ni–αAl_2O_3 and Cu–Ni–TiO_2 depositions, an increase in the Ni percentage in the coating and hardness was observed versus the pure Cu–Ni coating, but the percentage of the ceramic particles in the coating decreased. Increasing the pH of the plating solutions from 2.5 to 4.05 lead to an escalation in the Ni percentage in the film, loading percentage of the ceramic particles, and hardness. The hardness increased as the Al_2O_3 and TiO_2 increased in the plating solution from 170 to 248 kgf mm^{-2} for the addition of αAl_2O_3 particles with no effect to the Ni concentration in the coating, whereas the addition of TiO_2 particles produced an increase from 170 to 231 kgf mm^{-2} and helped to increase the Ni percentage in the coating. The optimal coating parameters were determined to be 1.33 A dm^{-2} for the current density, at pH 4.05, and incorporating 20 g dm^{-3} of the ceramic particles into the plating bath [37].

Hashemi et al. [38] studied the electrodeposition of Cu–Ni–W incorporated with SiC nanoparticles. They investigated the effects of different concentrations of SiC ranging from 0 to 25 g/L, stir rates ranging from 100 to 600 rpm, and the change in current density from 10 to 50 $mAcm^{-2}$. They optimized the plating conditions to obtain the best wear protection and hardness for the coatings. With the change in concentration from 0 to 25 g/L SiC in the plating solution, 15 g/L was found to have the highest incorporation of SiC into the coating. Also, the 15 g/L incorporation of SiC into the Cu–Ni matrix increased hardness and had the lowest weight loss factor and friction factor from the wear results. It was hypothesized that any amount over 15 g/L caused agglomeration of the SiC particles, which produced observable voids on the surface of the coating in the SEM pictures. A 400 rpm stir rate and the 20 $mAcm^{-2}$ current density proved to be the optimal conditions for the best wear resistance and hardness. The SEM of the coating incorporated with 15 g/L of SiC, stirred at 400 rpm, and electrodepos-

http://dx.doi.org/10.5772/62111

ited with a current density of 20 $mAcm^{-2}$ showed the least amount of visible wear on the surface after testing [38].

Wan et al. [39] developed a continuous three step deposition process to produce Cu, Cu–Fe, and Cu–Ni reinforced carbon fiber (6–8 μm in diameter) composites. Cu–C, Cu–Fe–C, and Cu–Ni–C composites display similar strength vs. temperature graphs to each other, but the decreasing trend seen in the tensile strength is controlled by a different mechanism. A decrease in the tensile strength for the Cu–C composite was due to interfacial bonding at the carbon fiber interface. Interfacial debonding was found to be absent for Cu–Ni–C and Cu–Fe–C composites because its larger interfacial bonding strength is due to a diffusion reaction and a chemical reaction at the interface of the fiber–metal matrix. The maximum tensile strength value was obtained with the addition of Cu–Ni onto the carbon fiber interface, but the optimal tensile strength value was not found to be proportional to the interfacial bonding strength, whereas the highest bonding strength was found for the Cu–Fe–C composite [39].

Our group studied electrodeposited 70–30 Cu–Ni coatings incorporated with a platelet-clay known as montmorillonite (MMT) from a citrate bath. Layered silicates have several advantageous properties to be utilized for composites, such as a high surface area, chemical inertness, resistance to extreme temperatures, and resistance to pH changes. The inclusion of layered silicates, such as MMT, has shown an increase in hardness, adhesion, and corrosion resistance in Ni and Ni–Mo coatings [56–59]. MMT has a 2:1 layered structure, with two layers of the silicon tetrahedral sandwiching one layer of an aluminum octahedral. Seen in Figure 8, MMT is a hydrous aluminum silicate with the formula $(Na,Ca)(Al, Mg)_6(Si_4O_{10})_3\text{-}(OH)_6 \cdot nH2O$ and measures 1 nm in height and 1–2 microns in width [12]. The Al^{3+} and Si^{4+} locations can be replaced by lower valent cations, causing the montmorillonite structure to have an excess of electrons. The negative charge is compensated through loosely held cations from the associated water. Within aqueous solutions, MMT can be completely delaminated and incorporated into other materials, forming continuous, crack-free films, which is a necessary requirement of corrosion resistant coatings [12]. For this work, a solution of MMT was stirred vigorously for 24–48 h to exfoliate the layered silicates. Seen in Table 2, the zeta potential of the plating solution with the dispersed MMT was also evaluated to check the stability of the particles in solution. When dealing with the electrocodeposition of a MMC, understanding the particle stability in the colloidal plating solution is vital because the properties of composites increase significantly with the preferential inclusion of individual particles [2].The exfoliated MMT is stable in solution and easily dispersed into aqueous solutions, while the non-exfoliated MMT precipitates. For stable nanoparticle suspensions, the ideal zeta potential would be a value greater than ±25 mV. The Cu–Ni–MMT plating solutions were around –19 to –20 mV. The adsorption of the Ni and Cu at the surface of the MMT platelet moves the zeta potential toward a more positive value and helps to increase the particle size, which slightly decreases the electrostatic stabilization of the dispersion compared to pure MMT solution. However, the plating solutions still had enough stability for deposition purposes to stay suspended in solution throughout the deposition cycle. Once exfoliated and freely dispersed throughout the electrolytic bath, the MMT platelets can slowly settle down onto the surface of the electrode and be incorporated into the forming alloy coating structure as shown in Figure 1.

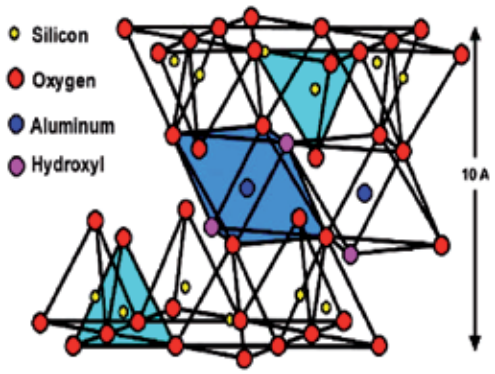

Figure 8. The structure and thickness of montmorillonite [12].

Solutions	Zeta Potential (mV)
0.05% MMT	–38.8
0.1% MMT	–39.2
0.2% MMT	–38.7
Cu–Ni–0.05% MMT	–20.2
Cu–Ni–0.1% MMT	–19.5
Cu–Ni–0.2% MMT	–19.2

Table 2. Zeta potentials for pure MMT and 70–30 Cu–Ni–MMT plating solutions [60].

A copper–nickel alloy (70–30 ratio) was electrochemically deposited from a citrate bath and compared to a composite coating incorporated with 0.05–0.2% MMT to study the effects of the mechanical properties.The adhesion shear strength (Figure 9) and the hardness (Figure 10) for the MMC coatings were investigated. The adhesion shear strength (measured by resistance to knife movement) (Figure 9) was evaluated with MMT amounts in solution ranging from 0 to 0.2% and all of the nanocomposite coatings surpass the strength of the pure Cu–Ni matrix. The shear adhesion tests were measured using the XYZTEC instrument paired with a 2-mm wide knife. The knife was placed at 5 μm above the substrate-coating interface and moved 2 mm horizontally at a velocity 150 (μm/s) through the coatings. With the addition of MMT into the Cu–Ni coating, a greater resistance to the knife movement was observed. The nearly 300% increase from pure Cu–Ni to Cu–Ni–0.05% MMT displays the value that the platelets can have at low loading values.As the MMT in solution increases to 0.1–0.2%, the mechanical resistance of the coating begins to decrease. This indicates that the increased amount of platelets incorporated into the coating leads to more substrate–platelet contact which would reduce the effective area of the matrix–substrate contact and leads to a reduction in the adhesion strength of the coatings. The microhardness test (Figure 10) revealed an increase of about 25% for the Cu–Ni coatings incorporated with MMT versus the pure Cu–Ni coating [60].

http://dx.doi.org/10.5772/62111

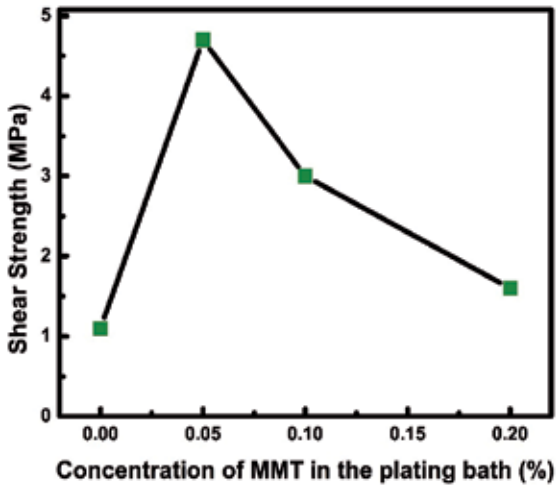

Figure 9. The adhesion shear strength of different coating layers with varying amounts of MMT in the electroplating solution [60].

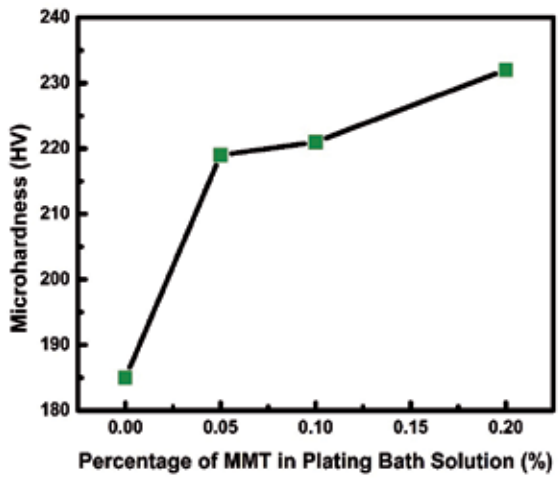

Figure 10. Vickers microhardness for the 70–30 Cu–Ni Coatings incorporated with MMT [60].

4. Cu–Ni MMCs in Electrochemistry and Improved Corrosion Protection

Understanding the relationship between the electrochemical deposition parameters and the resulting corrosion properties is of great importance for creating optimal coatings that will endure harsh environments. MMC coatings that reduce the rate of corrosion at a lower cost have been extensively studied. Exposing films to an unfavorable environment accelerates the

degradation of the coating, which can lead to many different types of corrosion phenomena [61, 62]. The rate of corrosion can be slowed using five universal approaches which include the choice of materials, chemical inhibitors, altercations in the environment, cathodic protection, or coatings [63]. Al particles and MMT were incorporated into the Cu–Ni matrix to understand how magnetic particles affect the metal matrix and MMT to observe how platelets affect the corrosion resistance of the Cu–Ni coating [40, 60].

Cui et al. [40] successfully codeposited Cu–Ni–Al MMCs and noted that high amounts of Al (~3 μm) particles, 29 vol. %, could be deposited into the Cu–Ni coating matrix. They investigated whether the conductive Al particles would behave similar to inert particle codeposition according to the Guglielmi's model. Adding the conductive aluminum particles into the Cu–Ni matrix caused the polarization curve to shift to more negative potentials, which was credited to the non-active surface of the aluminum metal particles during the deposition of Cu–Ni following a similar codeposition path for inert particles defined by Guglielmi. The parameters used in Guglielmi's model for the codeposition of non-conductive inert particles can also model the deposition of charged particles presented in this research [40].

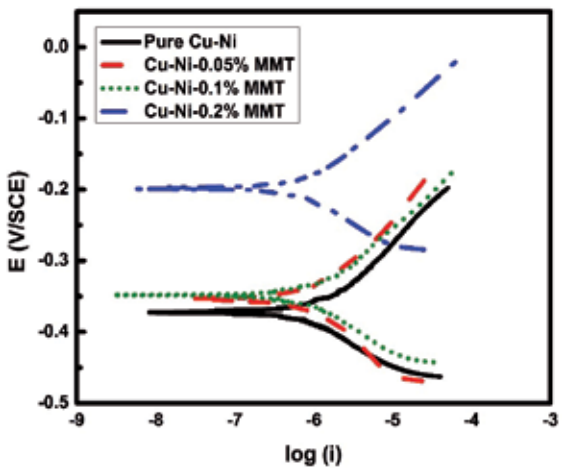

Figure 11. Tafel plots for the 70–30 Cu–Ni coatings with and without MMT after being submerged in a 3.5 % NaCl solution for two weeks [60].

In addition to the mechanical properties, our group studied the corrosion behaviors of the 70–30 Cu–Ni–MMT coatings by the use of Tafel polarization and electrochemical impedance spectroscopy (EIS). The corrosion of 70–30 Cu–Ni and 70–30 Cu–Ni–MMT composite coatings were evaluated using potentiodynamic polarization, as seen in Figure 11. The corrosion parameters were measured after immersing the 70–30 Cu–Ni coatings for two weeks in 3.5% NaCl solution at 25°C. The E_{corr} and I_{corr} correlation for the Cu–Ni–MMT coatings can be seen in Figure 12. Figure 12 shows E_{corr} shifting to more positive potentials and the I_{corr} shifting to lower current values leading to the Cu–Ni–0.2% MMT having the best corrosion properties. Nyquist plots (Figure 13) of pure Cu–Ni and Cu–Ni–0.2% MMT composite coatings after 14 days immersion in 3.5 % NaCl at 25°C showed the diameter of the depressed uncompleted

semicircles is larger in case of Cu–Ni–MMT compared to pure Cu–Ni, which displays increased stability of the passive film in the case of Cu–Ni–MMT compared to that of pure Cu–Ni coating. The equivalent circuit parameters of the fitting procedure showed an increase in R_p from 2.87 kΩcm^2 (pure Cu–Ni) to 13.77 kΩcm^2 (Cu–Ni–0.2% MMT), as seen in Table 3. The calculated parameters show higher resistance for the inner layer in case of Cu–Ni–MMT composite coating compared to that of pure Cu–Ni; this resistance increases as the MMT content in the metallic matrix increases, which is consistent with the data obtained from potentiodynamic polarization, and also confirms that embedding of layered silicate particles into the Cu–Ni metallic matrix increases its corrosion resistance [60].

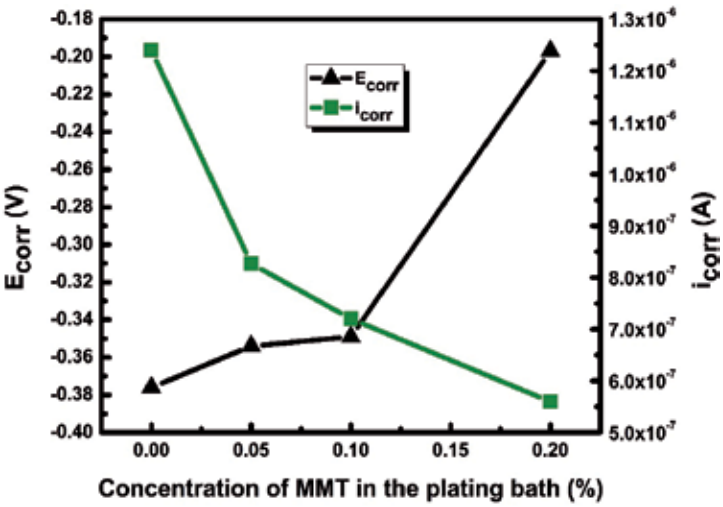

Figure 12. E_{corr} and i_{corr} of 70–30 Cu–Ni coatings incorporated with MMT [60].

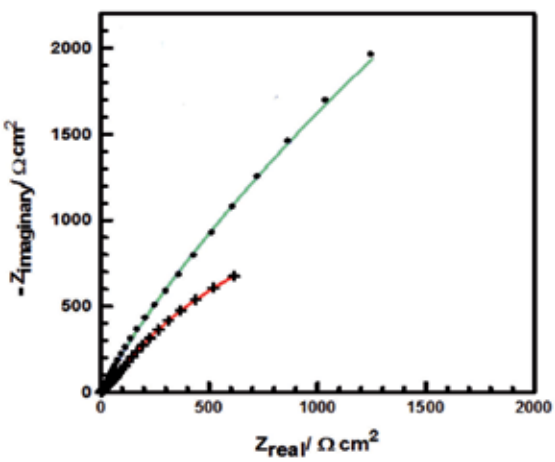

Figure 13. Nyquist impedance plots of pure Cu–Ni (A) and Cu–Ni–0.2% MMT (B) after being submerged in a 3.5% NaCl solution for two weeks [60].

Coatings	R_s (Ω cm^2)	R_1 (Ω cm^2)	Q_1 (Ω^{-1} s$^{\alpha}$ cm^{-2})	α_1	R_p (kΩ cm^2)	Q_2 (Ω^{-1} s$^{\alpha}$ cm^{-2})	α_2
Cu–Ni	2.25	49.78	2.95×10^{-3}	0.56	2.87	1336×10^{-6}	0.73
Cu–Ni–0.05% MMT	0.78	5.45	6.20×10^{-3}	0.75	3.02	954×10^{-6}	0.75
Cu–Ni–0.1% MMT	5.01	54.0	1.26×10^{-3}	0.68	4.92	709×10^{-6}	0.80
Cu–Ni–0.2% MMT	8.32	95.20	2.33×10^{-6}	0.99	13.77	583×10^{-6}	0.76

Table 3. The equivalent circuit parameters of Cu–Ni and Cu–Ni–MMT composite coatings after two weeks submersion in a 3.5% NaCl solution [60].

5. Conclusions

Electrodeposition provides a versatile and convenient route for controlled coating of composites (i.e. materials having more than one phase) containing nano- to microparticles dispersed in a metal matrix for material science and engineering applications. Enhancement of the electrical, mechanical, and corrosion properties of the coatings is observed with the inclusion of different particles into the Cu–Ni matrix. With the increase in availability of micro- and nanoparticles, more research needs to be performed in the area of Cu–Ni MMCs to further explore their beneficial properties.

Acknowledgements

This work was made possible by NPRP Grant 4-306-2-111 from the Qatar National Research Fund (a Member of the Qatar Foundation). The statements made herein are solely the responsibility of the authors. The authors would also like to thank Jonathan Bishop for help with the figures.

Author details

Casey R. Thurber[1], Adel M.A. Mohamed[2,3*] and Teresa D. Golden[1]

*Address all correspondence to: adel.mohamed25@yahoo.com

1 Department of Chemistry, University of North Texas, Denton, Texas, USA

2 Department of Metallurgical and Materials Engineering, Faculty of Petroleum and Mining Engineering, Suez University, Egypt

3 Center for Advanced Materials, Qatar University, Doha, Qatar

References

[1] Musiani M. Electrodeposition of composites: an expanding subject in electrochemical materials science. Electrochim. Acta. 2000;45:3397–3402. DOI: 10.1016/S0013-4686(00)00438-2.

[2] Gomes A, Pereira I, Fernández B, Pereiro R. Electrodeposition of metal matrix nanocomposites: Improvement of the chemical characterization techniques. Advances in Nanocomposites - Synthesis, Characterization and Industrial Applications. Intech. 2011;21:503-526. DOI: 10.5772/15557.

[3] Walsh FC, Ponce de Leon C. A review of the electrodeposition of metal matrix composite coatings by inclusion of particles in a metal layer: an established and diversifying technology. Trans. Inst. Met. Finish. 2014;92:83-98. DOI: 10.1179/0020296713Z.000000000161.

[4] Hovestad A, Jansen LJJ. Electrochemical codeposition of inert particles in a metallic matrix. J. Appl. Electrochem. 1995;25:519-527. DOI 10.1007/BF00573209.

[5] Panda A, Podlaha EJ, Nanoparticles to improve mass transport inside deep recesses. Electrochem. Solid St., 2003;6:C149-C152. DOI: 10.1149/1.1614452.

[6] Chen YC, Liu W, Chao T, Cheng YT. An optimized Cu-Ni nanocomposite coil for low-power electromagnetic microspeaker fabrication. Transducers. 2009:25-28. DOI: 10.1109/SENSOR.2009.5285572.

[7] Chiriac H, Moga AE, Constantin VA. Synthesis and magnetic properties of Fe-Ni and Cu-Ni composite coatings. J. Optoelectron Adv. M. 2007;9:1161-1164.

[8] Huang Z, Peng X, Wang F. Preparation and oxidation of novel electrodeposited Cu–Ni–Cr nanocomposites. Oxid. Met. 2006;65:223-235. DOI: 10.1007/s11085-006-9017-y.

[9] Huang Z, Peng X, Xu C, Wang F. On the exclusive growth of external chromia scale on the novel electrodeposited Cu–Ni–Cr nanocomposites. J. Mater. Res. 2007;22:3166-3177. DOI: 10.1557/JMR.2007.0411.

[10] Huang YW, Chao T, Chen CC, Cheng YT. Power consumption reduction scheme of magnetic microactuation using electroplated Cu–Ni nanocomposite. App. Phys. Letters. 2007;90:1-3. DOI: 10.1063/1.2748301.

[11] Bard AJ, Faulkner LR. Electrochemical Methods: Fundamentals and Applications. New York, 2000. ISBN: 0-471-04372-9.

[12] Horch RA, Golden TD, D' Souza NA, Riester L. Electrodeposition of nickel/montmorillonite layered silicate nanocomposite thin films. Chem. Mater. 2002;14:3531-3538. DOI: 10.1021/cm010812+.

[13] Harrigan WC. Commercial processing of metal matrix composites. Mater. Sci. Eng. 1998;A244:75–79. DOI: 10.1016/S0921-5093(97)00828-9.

[14] Zeng X, Tao Z, Zhu B, Zhou E, Cui K. Investigation of laser cladding ceramic-metal composite coatings: processing modes and mechanisms. Surf. Coat. Tech. 1996;79:209-217. DOI: 10.1016/0257-8972(95)02431-X.

[15] Lindroos VK, Talvitie MJ. Recent advances in metal matrix composites. J. Mater. Process. Tech. 1995;53:273-284. DOI: 10.1016/0924-0136(95)01985-N.

[16] Deuis RL, Yellup JM, Subramanian C. Metal-matrix composite coatings by PTA surfacing. Compos. Sci. Technol. 1998;58:299-309. DOI: 10.1016/S0266-3538(97)00131-0.

[17] Hashim J, Looney L, Hashmi MSJ. Metal matrix composites: production by the stir casting method. J. Mater. Process. Tech. 1999;92-93:1-7. DOI: 10.1016/S0924-0136(99)00118-1.

[18] Muratoglu M, Yilmaz O, Aksoy M. Investigation on diffusion bonding characteristics of aluminum metal matrix composites (Al/SiCp) with pure aluminum for different heat treatments. J. Mater. Process. Tech. 2006;178:211–217. DOI: 10.1016/j.jmatprotec.2006.03.168.

[19] Tan MJ, Zhang X. Powder metal matrix composites: selection and processing. Mater. Sci. Eng. 1998;A244:80–85. DOI: 10.1016/S0921-5093(97)00829-0.

[20] Popovskaa N, Gerhard H, Wurm D, Poscher S, Emig G, Singer RF. Chemical vapor deposition of titanium nitride on carbon fibers as a protective layer in metal matrix composites. Mater. Design. 1997;18:239-242. DOI: S0261–3069(97)00057–5.

[21] Chrobak A, Kubisztal M, Kubisztal J, Chrobak E, Haneczok G. Microstructure, magnetic and elastic properties of electrodeposited Cu+Ni nanocomposites coatings. J. Achieve. Mater. Manufac. Eng. 2011;49:17-26.

[22] Rosso M. Ceramic and metal matrix composites: Routes and properties. J. Mater. Process. Tech. 2006;175:364–375. DOI: 10.1016/j.jmatprotec.2005.04.038.

[23] Pradhan AK, Das S. Pulse-reverse electrodeposition of Cu–SiC nanocomposite coating: Effect of concentration of SiC in the electrolyte. J. Alloy Compd. 2014;590:294–302. DOI: 10.1016/j.jallcom.2013.12.139.

[24] Zamblau I, Varvara S, Muresan LM. Corrosion behavior of Cu–SiO_2 nanocomposite coatings obtained by electrodeposition in the presence of cetyl trimethyl ammonium bromide. J. Mater. Sci. 2011;46:6484–6490. DOI: 10.1007/s10853-011-5594-5.

[25] Ramalingam S, Muralidharan VS, Subramania A. Electrodeposition and characterization of Cu-TiO_2 nanocomposite coatings. J. Solid State Electrochem. 2009;13:1777–1783. DOI: 10.1007/s10008-009-0870-x.

[26] Gan Y, Lee D, Chen X, Kysar JW. Structure and properties of electrocodeposited Cu–Al_2O_3 nanocomposite thin films. J. Mater. Process. Tech. 2005;127:451-456. DOI: 10.1115/1.1925292.

[27] Mangam V, Bhattacharya S, Das K, Das S. Friction and wear behavior of Cu–CeO_2 nanocomposite coatings synthesized by pulsed electrodeposition. Surf. Coat. Tech. 2010;205:801–805. DOI: 10.1016/j.surfcoat.2010.07.119.

[28] Rusu DE, Cojocaru P, Magagnin L, Gheorghies C, Carac G. Study of Ni-TiO_2 nanocomposite coating prepared by electrochemical deposition. J. Optoelectron Adv. M. 2010;12:2419-2422.

[29] Sen R, Das S, Das K. Synthesis and properties of pulse electrodeposited Ni-CeO_2 nanocomposite. Metall. Mater. Trans. A. 2012;43A:3809-3823. DOI: 10.1007/s11661-012-1170-0.

[30] Vaezi MR, Sadrnezhaad SK, Nikzad L. Electrodeposition of Ni–SiC nano-composite coatings and evaluation of wear and corrosion resistance and electroplating characteristics. Colloids and Surf. A. 2008;315:176-182. DOI: 10.1016/j.colsurfa.2007.07.027.

[31] Chang LM, Liu JH, Zhang RJ. Corrosion behaviour of electrodeposited Ni/Al_2O_3 composite coating covered with a NaCl salt film at 800 °C. Mater. Corros. 2011;62:920-925. DOI: 10.1002/maco.200905617.

[32] Kasturibai S, Kalaignan GP. Physical and electrochemical characterizations of Ni-SiO_2 nanocomposite coatings. Ionics. 2012:1-8. DOI 10.1007/s11581-012-0810-0.

[33] Conrad HA, Corbett JR, Golden TD. Electrochemical deposition of γ-phase zinc-nickel alloys from alkaline solution. J. Electrochem. Soc. 2012;159:C29-C32. DOI: 10.1149/2.027201jes.

[34] Ahmad YH, Mohamed AMA, Golden TD, D'Souza N. Electrodeposition of nanocrystalline Ni-Mo alloys from alkaline glycinate solutions. Int. J. Electrochem. Sci. 2014;9:6438-6450.

[35] Yuan SJ, Pehkonen SO. Surface characterization and corrosion behavior of 70/30 Cu–Ni alloy in pristine and sulfide-containing simulated seawater. Corros. Sci. 2007;49:1276-1304. DOI: 10.1016/j.corsci.2006.07.003.

[36] Low CTJ, Wills RGA, Walsh FC. Electrodeposition of composite coatings containing nanoparticles in a metal deposit. Surf. Coat. Tech. 2006;201:371–383. DOI:10.1016/j.surfcoat.2005.11.123.

[37] Fawzy MH, Ashour MM, El-Halim ABD. Effect of some operating variables on the characteristics of electrodeposited Cu-Ni alloys with and without α-$A1_2O_3$ and TiO_2 inert particles. J. Chem. Tech. Biotechnol. 1996;66:121-130. DOI: 10.1002/(SICI)1097-4660(199606)66:2<121::AID-JCTB475>3.0.CO;2-A.

[38] Hashemi M, Mirdamadi SH, Rezaie HR. Effect of SiC nanoparticles on microstructure and wear behavior of Cu-Ni-W nanocrystalline coating. Electrochim. Acta. 2014;138:224–231. DOI: 10.1016/j.electacta.2014.06.084.

[39] Wan YZ, Wang YL, Luo HL, Dong XH, Cheng GX. Effects of fiber volume fraction, hot pressing parameters and alloying elements on tensile strength of carbon fiber reinforced copper matrix composite prepared by continuous three-step electrodeposition. Mater. Sci. Eng. 2000;A288:26–33. DOI: S0921-5093(00)00887-X.

[40] Cui X, Wei W, Liu H, Chen W. Electrochemical study of codeposition of Al particle—Nanocrystalline Ni/Cu composite coatings. Electrochim. Acta. 2008;54:415–420. DOI: 10.1016/j.electacta.2008.07.066.

[41] Mohan S, Rajasekaren N. Influence of electrolyte pH on composition, corrosion properties and surface morphology of electrodeposited Cu-Ni alloy. Surf. Eng. 2011;7:519-523. DOI: 10.1179/026708410X12786785573472.

[42] Green TA, Russell AE, Roy SJ. The development of a stable citrate electrolyte for the electrodeposition of copper-nickel alloys. J. Electrochem. Soc. 1998;145:875-881. DOI: 10.1149/1.1838360.

[43] Varea A, Pellicer E, Pané S, Nelson BJ, Suriñach S, Baró MD, Sort J. Mechanical properties and corrosion behavior of nanostructured Cu-rich CuNi electrodeposited films. Int. J. Electrochem. Sci. 2012;7:1288-1302.

[44] Rode S, Henninot C, Vallières C, Matlosz M. Complexation chemistry in copper plating from citrate baths. J. Electrochem. Soc. 2004;151:C405-C411. DOI: 10.1149/1.1869980.

[45] Orniakova R, Turonova A, Kladekova D, Galova M, Smith RM. Recent developments in the electrodeposition of nickel and some nickel-based alloys. J. Appl. Electrochem. 2006;36:957–972. DOI: 10.1007/s10800-006-9162-7.

[46] Alper M, Kockar H, Safak M, Baykul MC. Comparison of Ni-Cu alloy films electrodeposited at low and high pH levels. J. Alloys Compd. 2008;453:15-19. DOI: 10.1016/j.jallcom.2006.11.066.

[47] Metikos-Hukovic M, Skugor I, Grubac Z, Babic R. Complexities of corrosion behaviour of copper–nickel alloys under liquid impingement conditions in saline water. Electrochim. Acta. 2010;55:3123-3129. DOI: 10.1016/j.electacta.2010.01.066.

[48] Boyapati VAR, Kanukula CK. Corrosion inhibition of Cu-Ni (90/10) alloy in seawater and sulphide-polluted seawater environments by 1, 2, 3-Benzotriazole. ISRN Corros. 2013;2013:1-22. DOI: 10.1155/2013/703929.

[49] Bautista BET, Carvalho ML, Seyeux A, Zanna S, Cristiani P, Tribollet B, Marcus P, Frateur I. Effect of protein adsorption on the corrosion behavior of 70Cu-30Ni alloy in artificial seawater. Bioelectroch. 2014;97:34-42. DOI: 10.1016/j.bioelechem. 2013.10.004.

[50] Milosev I, Metikos-Hukovic M. The behaviour of Cu-xNi (x = 10 to 40 wt%) alloys in alkaline solutions containing chloride ions. Electrochim. Acta. 1997;42:1537-1548. DOI: S0013-4686(96)00315.

[51] Williams RV, Martin PW. Electrodeposited composite coatings. Trans. Inst. Met. Finish. 1964;42:182-187.

[52] Brandes EA, Goldthorpe D. Co-deposition of metals and ceramic particles. Metallurgia. 1967;76:195–198.

[53] Guglielm N. Kinetics of the deposition of inert particles from electrolytic baths. J. Electrochem. Soc. 1972;119:1009-1012. DOI: 10.1149/1.2404383.

[54] Celis JP, Roos JR, Buelens C. A mathematical model for the electrolytic codeposition of particles with a metallic matrix. J. Electrochem. Soc. 1987;134:1402–1408. DOI: 10.1149/1.2100680.

[55] Bercot P, Pena-Munoz E, Pagetti J. Electrolytic composite Ni PTFE coatings: An adaptation of Guglielmi's model of the phenomena of incorporation. Surf. Coat. Technol. 2002;157:282–289. DOI: S0257-8972Ž02.00180-9.

[56] Tientong J, Thurber CR, D'Souza N, Mohamed AMA, Golden TD. Influence of bath composition at acidic pH on electrodeposition of nickel-layered silicate nanocomposites for corrosion protection. Int. J. Electrochem. 2013;2013:1-8. DOI: 10.1155/2013/853869.

[57] Tientong J, Ahmad YH, Nar M, D'Souza N, Mohamed AMA, Golden TD. Improved mechanical and corrosion properties of nickel composite coatings by incorporation of layered silicates. Mater. Chem. Phys. 2014;145:44-50. DOI: 10.1016/j.matchemphys. 2014.01.025.

[58] Ahmad YH, Tientong J, D'Souza N, Golden TD, Mohamed AMA. Salt water corrosion resistance of electrodeposited Ni-layered silicate nanocomposite coatings from Watts' Type Solution. Surf. Coat. Tech. 2014;242:170-176. DOI: 10.1016/j.surfcoat. 2014.01.040.

[59] Thurber CR, Calhoun MC, Ahmad YH, D'Souza N, Mohamed AMA, Golden TD, Electrodeposition of Cu-Ni incorporated with layered silicates for corrosion protection. ECS Trans. 2014;61:49-60. DOI: 10.1149/06120.0049ecst.

[60] Thurber CR, Ahmad YH, Sanders SF, Al-Shenawa A, D'Souza N, Mohamed AMA, Golden TD. Electrodeposition of 70-30 Cu-Ni nanocomposite coatings for enhanced mechanical and corrosion properties. Curr. Appl. Phys. 2016;16:387-396. DOI: 10.1016/j.cap.2015.12.022.

[61] Chang YY, Wang DY. Corrosion behavior of electroless nickel-coated AISI 304 stainless steel enhanced by titanium ion implantation. Surf. Coat. Tech. 2005;200:2187-2191. DOI: 10.1016/j.surfcoat.2004.07.118.

[62] Tang PT, Pulse reversal plating of nickel alloys. Institute of Metal Finishings. 2007;85:51-56. DOI: 10.1179/174591907X162459.

[63] Painting: New Construction and Maintenance, U.S Army Corps of Engineers EM 1110-2-3400, 2-1 1995.

Chapter 6

Nanocomposite Coatings Deposited by Sol-Enhanced Electrochemical Methods

Yuxin Wang and Wei Gao

Additional information is available at the end of the chapter

http://dx.doi.org/10.5772/62042

Abstract

Nano-composite coatings have wide applications for their superior mechanical and corrosion properties. Many efforts have been devoted to the development of different types of nano-composite coatings in the last decade. Various techniques are used to modify the coating microstructure at the nano scale in order to further improve the properties of coatings. We recently developed a novel method which combines sol-gel process and electrochemical deposition process to produce nano-composite coatings. This simple method can lead to a highly dispersed distribution of oxide nano-particles in the metal coating matrix, resulting in significantly improved mechanical properties. This Chapter introduces the principle of this innovative method, the basic theory behind the deposition process, and an overview of current results. It also describes the dopant technology that is derived from this novel technique. The future development potentials and industrial applications of these coatings are also discussed.

Keywords: Nanocomposite coatings, Electrochemical deposition, Nanoparticle distribution, Dopant technology

1. Introduction

Coatings are widely used on the surface of different substrates in order to improve the durability of working parts by increasing their resistance against wear, erosion, and corrosion. Comparing with the general coatings and conventional composite coatings, the nanocomposite coatings possess much improved properties because of the "nanosize dispersion effect". It contains nanoparticles of a wide range of materials including oxides, carbides, metals, silicates and other ceramics with a size range of 1 to 100 nm. With the development of nanotechnology, the nanocomposite coatings are not only used as a surface protection material but also for developing special functional properties. Nowadays, the nanostructured coatings

with desired properties are widely used in military, aerospace, automotive, electronics and many other industries [1-2].

Much effort has been made to improve coating properties and design new nanocomposite coatings in the past decades. One of the focuses is how to achieve better "nano-dispersion". It was well known that the properties such as strength, hardness and wear resistance of coatings can be greatly improved by a good dispersion of the second-phase particles in the matrix. Generally, the nanocomposite coatings are synthesized by directly adding nano-size solid powders into the plating solution. The nanoparticles can be incorporated into the metal matrix during the deposition process. However, it is difficult for the second phase nanoparticles to achieve a good dispersion in the matrix because of their large surface area [3]. The nanoparticles tend to agglomerate because of their high surface energy. In order to achieve a good dispersion of the second-phase particles in the coating matrix, the powder suspension has to be maintained in the electrolyte solution by vigorous agitation, air injection, ultrasonic vibration, or adding surfactants and other types of stabilizers, etc.

However, it is always difficult for the nanoparticles to achieve a good suspension because they have very large surface area, especially when the particle size is in a nanometer level. The high surface energy leads to the agglomeration of the nano-particles even though combinations of the above methods are used to reduce the particle agglomeration. Therefore, it has been a challenge to explore new techniques to produce highly dispersive nanoparticles reinforced composite coatings, which can take the advantage of the unique properties of the nano-particles to develop nanocomposite coatings with superior mechanical and other properties [4-5].

We have developed a novel technique: sol-enhanced composite plating, to synthesize highly dispersive oxide nano-particle reinforced composite coatings. In this new method, transparent sol solution containing desirable oxide components is directly introduced into the electrolyte solution at a controlled concentration and/or speed. Nano-particles with a size of below 25 nm will be in-situ generated and then incorporated into the coating matrix. This method can lead to a highly dispersive distribution of desired nanoparticles in the coating, resulting in significantly improved mechanical properties [6-10]. In this paper, we will introduce the basic theory of this method, report the current results and discuss the strengthening mechanism. We will also describe the dopant technology that is derived from this novel technique. The potential industrial applications of these technologies are also discussed.

2. The basic theory of sol-enhanced method

2.1. Brief introduction of sol-gel process

Sol-gel processes are versatile solution processes which have been widely applied to synthesize nano-particles, nano-composites, thin films, fibers and ceramics. They have shown considerable advantages, including excellent chemical stoichiometry, compositional homogeneity and low crystallization temperature due to the mixing of liquid precursors on a molecular level [5].

http://dx.doi.org/10.5772/62042

The sol-gel process can be described as the creation of an oxide/chloride network by progressive condensation reactions of molecular precursors in a liquid medium.

The sols can be basically classified as inorganic sols and organic sols. The most widely used is the organic sols, which are generally fabricated by using solutions of metal or metalloid alkoxide precursors $M(OR)_n$ in organic solvents [11]. Typically, a sol-gel process comprises solution, gelation, drying and densification. The precursors are subjected to a series of hydrolysis and polycondensation reactions to form a colloidal suspension, namely sol. Further processing of the "sol" makes it possible to form materials in different shapes, such as spinning or dipping to produce coatings and films, drawing from a liquid to produce fibers, precipitating or spray pyrolysis to get ultrafine uniform powders and processing in a vessel to produce aerogels and monoliths.

2.2. The evolution of the sol solution in the electrolyte

The evolution of the sol solution in the electrolyte was analyzed from two parts: (1) the formation of nano-particles, and (2) the size evolution of nano-particles before and after adding into electrolyte [9-10]. Considering the comparability of different kinds of sol, we hereby illustrate the behavior of TiO_2 sol in electroplating bath to explain the general electrochemical process of the sol-enhanced composite plating.

The transparent liquid TiO_2 sol was made by using metal alkoxide tetrabutylorthotitanate ($Ti(OBu)_4$) as the precursor. This metal alkoxide is dissolved into a mixed solution of ethanol and diethanolamine (DEA). It then formed a colloidal suspension under a series of hydrolysis and polymerization reactions. The small particles in sol with the charge on the surface cannot grow up for the covered layer of solvent molecules. Different small particles can be well suspended in the solvent, subjecting to the combined effect of charge, van der Walls force and gravity [9-10, 12-13].

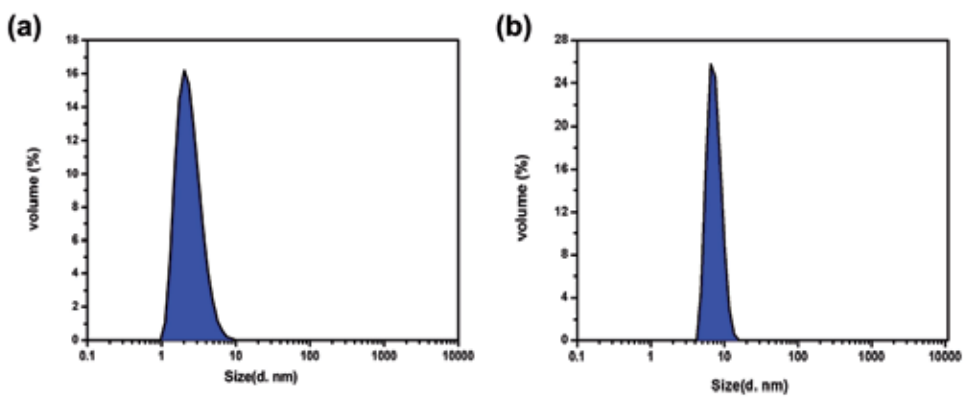

Figure 1. Size distribution of nano-particles in: (a) TiO_2 sol and (b) Ni electrolyte after adding TiO_2 sol.

The hydrolysis reaction and condensation process of TiO_2 sol has been widely investigated. Generally the stereo-hindrance and solvation effects are the main factors to make the sol

solution stable. Before TiO_2 sol is added into the electrolyte, the sol can be regarded as a stable system without solid liquid interface. Under neutral and basic conditions, the condensation process of Ti macromolecule ions started before the completion of hydrolysis; and the formation of an ordered structure was hindered.

After TiO_2 sol is added into the electrolyte, water in electrolyte aggravates the hydrolysis reaction and breaks up the dynamic balance. The sol system becomes unstable and the interface between solid and liquid emerges. Thus the amorphous TiO_2 nano-particles formed in situ [5, 9-10]. Fig. 1 presents the size distribution of nano-particles in the sol and the Ni electrolyte after adding the sol. The particle size was characterized by a laser diffraction particle analyzer (Malvern Mastersizer Hydro 2000S). The particle size of TiO_2 sol was distributed in the range of 1-10 nm, with a mean value of 2.5 nm as shown in Fig. 1a. The size distribution of sol added electrolyte keeps in a same level with the TiO_2 sol. The mean value of the particle size was increased to 7.4 nm and the particle size distribution was in the range of 3-20 nm which means no significant agglomeration occurs (Fig. 1b). The size measurement results are consistent with the HRTEM observation as shown in Fig. 2. The TiO_2 nano-particle got from electrolyte has an amorphous structure with a size of ~10 nm.

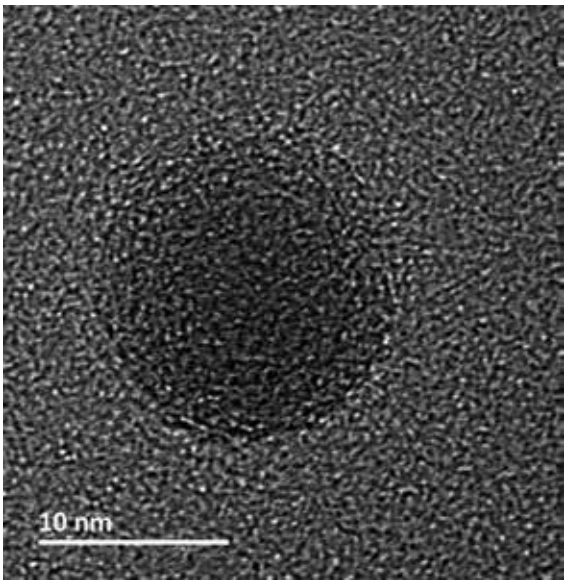

Figure 2. TEM bright field image of TiO_2 nano-particles separated from the Ni electrolyte with TiO_2 sol addition

2.3. Deposition process of sol-enhanced plating

The overall sol-enhanced deposition process can be typically divided into several steps. These steps describe the process of particles from the solution to their incorporation in the metal matrix. The first step is the in-situ generation of nano-particles after adding the sol into the electrolyte. Once the nano-particles formed in the electrolyte, some of them are immediately

http://dx.doi.org/10.5772/62042

physically adsorbed onto the freshly deposited surface based on the Martin-Williams model. Some of them were immediately adsorbed by hydrate metal ions due to their large surface areas based on the Whithers model [10]. Correspondingly, they were highly dispersed in the electrolyte as shown in Fig. 1b. The organic solvents probably also contribute to the dispersion of the ions-adsorbed nano-particles. Under the combination effect of migration, diffusion and convection, the coating matrix grows up with fine particles, and finally forms a highly dispersive nano-particle reinforced metal-based composite coating as shown in Fig. 3 [5, 9-10].

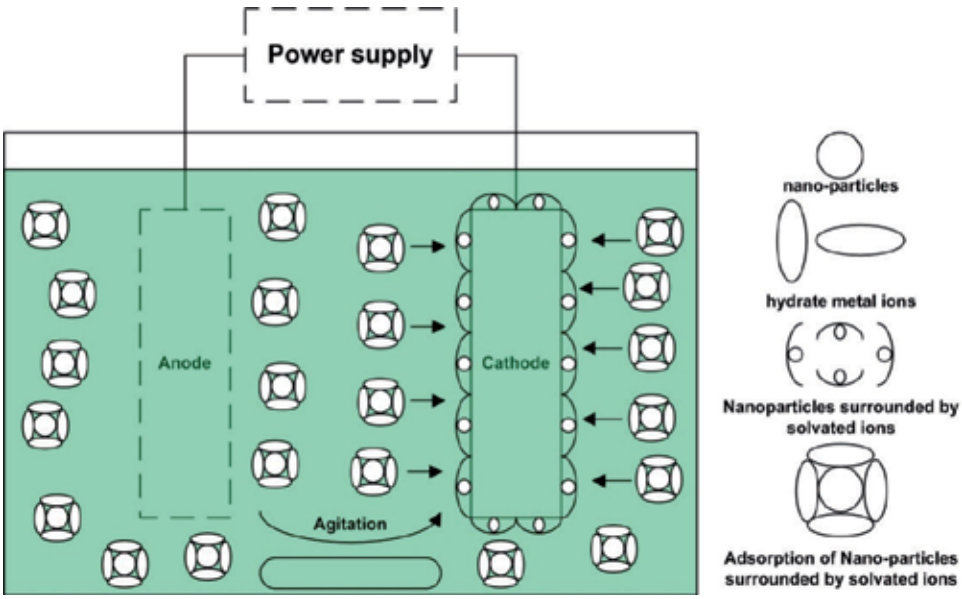

Figure 3. Sketch map of the sol-enhanced plating deposition process

3. Microstructure and property of sol-enhanced coatings

3.1. Microstructure of sol-enhanced coatings

The microstructure of sol-enhanced coatings was studied by various characterization methods. We hereby elaborate the related characterization results of cross-section, surface morphology and intrinsic microstructure of sol-enhanced coatings.

3.1.1. Cross-section images of sol-enhanced coatings

Fig. 4 shows the cross-section morphologies of Ni-P and sol-enhanced Ni-P-TiO_2 coatings. Sol-enhanced Ni-P-12.5 mL/L TiO_2 nano-composite coating has a similar cross-section image with traditional Ni-P coating. No obvious TiO_2 particles could be seen in the SEM cross-section, indicating their small size and relatively low content. However, with increasing TiO_2 addition,

the agglomerated TiO_2 particles can be clearly seen in Ni-P-50 mL/L TiO_2 composite coating. In addition, many voids were observed in the coatings [14]. When the sol concentration is relatively low (e.g., for sol-enhanced Ni-P-TiO_2 coating, the TiO_2 sol concentration is below 20 mL/L), the cross-section image of sol-enhanced coatings is similar with the traditional coating. However, when the sol concentration is relatively high (e.g., for sol-enhanced Ni-P-TiO_2 coating, the TiO_2 sol concentration is above 20 mL/L), a porous structure may form and large cluster area could be seen in the cross-section of sol-enhanced coatings due to the nano-particle agglomeration.

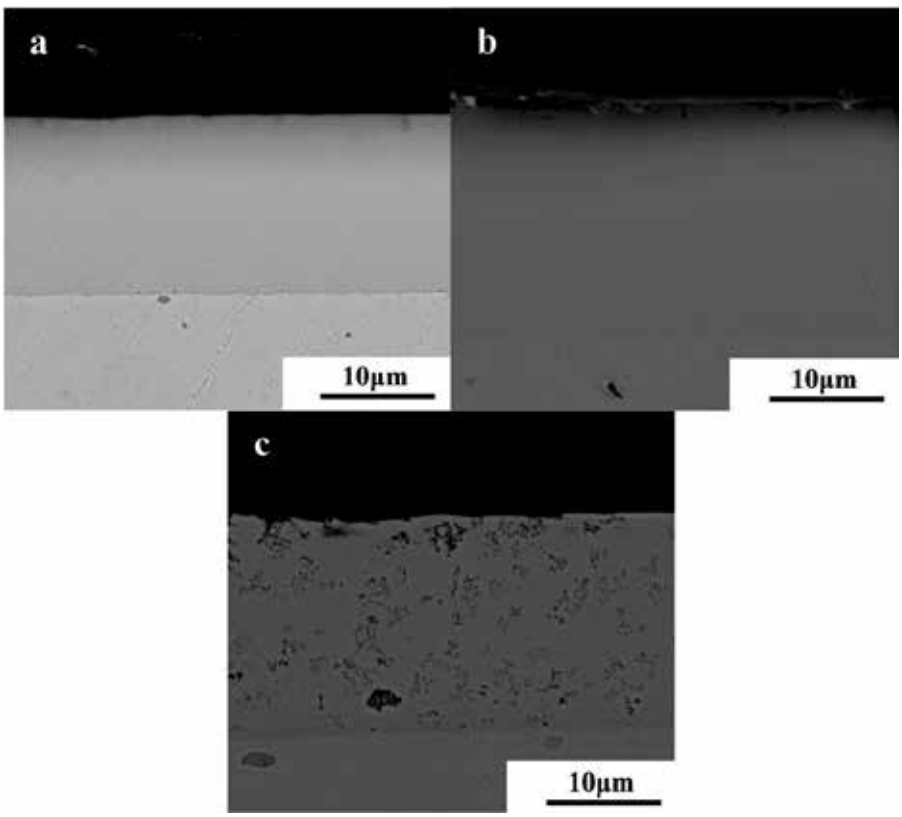

Figure 4. Cross-sectional morphologies: (a) traditional Ni-P coating, (b) sol-enhanced Ni-P-12.5 mL/L TiO_2 coating, and (c) Ni-P-TiO_2 coating with high concentration of sol (50 mL/L).

3.1.2. Surface morphology of sol-enhanced coatings

Fig. 5 shows the surface morphology of Au-Ni coating and TiO_2 sol enhanced Au-Ni-TiO_2 coatings with different TiO_2 sol concentrations. The Au-Ni coating shows typical granular morphology with the large protrusion size of ~400 nm. Some pores can be found on the Au-Ni coating surface, as shown by the white arrows in Fig. 4a, probably due to the formation of H_2 during the electro-deposition process. The morphology of 12.5 mL/L TiO_2 sol enhanced

http://dx.doi.org/10.5772/62042

composite coating shows a uniform spherically nodular structure with a size of ~300 nm (Fig. 5b). A great number of black dots were seen on the surface of 50 mL/L TiO_2 sol added composite coating, as shown by the white arrows in Fig. 5(c). The size of black dots ranges from ~50 nm to ~150 nm. Some of the black dots were attributed to the clusters formed by TiO_2 nano-particles, which confirmed by the EDS results. The Ti concentration in those locations was higher than other areas. As abundant TiO_2 nano-particles agglomerate into clusters, porous structure formed in the nearby area. The other black dots are the voids that may come from the H_2 release during the electro-deposition process [12-13].

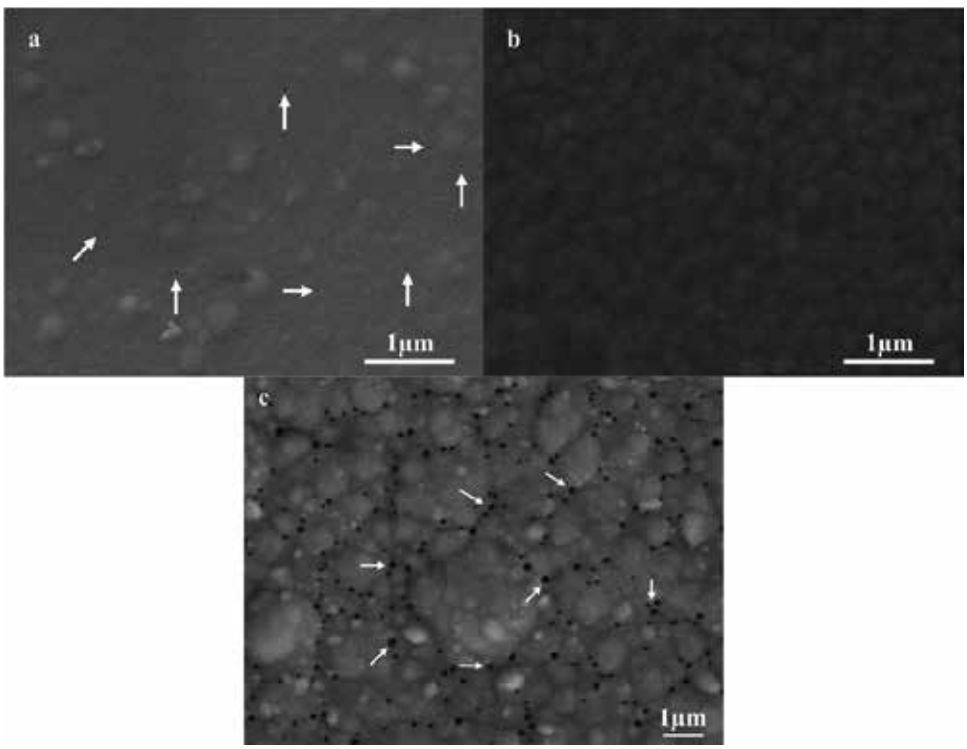

Figure 5. Surface morphology of sol-enhanced Au-Ni-TiO_2 nano-composite coatings: (a) Au-Ni as a comparison, (b) Au-Ni-12.5 mL/L TiO_2, and (c) Au-Ni-50mL/L TiO_2

3.1.3. TEM microstructure of sol-enhanced nano-composite coatings

Fig. 6 presents the bright field image TEM and HRTEM image of sol-enhanced Ag-TiO_2 nano-composite coating. It can be seen that many white small nano-particles with a size of 10-25 nm were distributed quite uniformly in the grain boundary areas and inside the coating matrix as shown in Fig. 6a. The nanoscale probe EDX analysis indicates the white nano-particles contain Ti. HRTEM indicates that the small nano-particles have an amorphous microstructure, as shown in Fig. 6b. The grain size of the coatings can be calculated from the measured XRD patterns by using Scherrer's formula. The average grain size of sol-en-

hanced Ag-12.5 mL/LTiO_2 composite coatings shows a clear decrease from 38.5 nm of pure Ag coating to 25.7 nm [15].

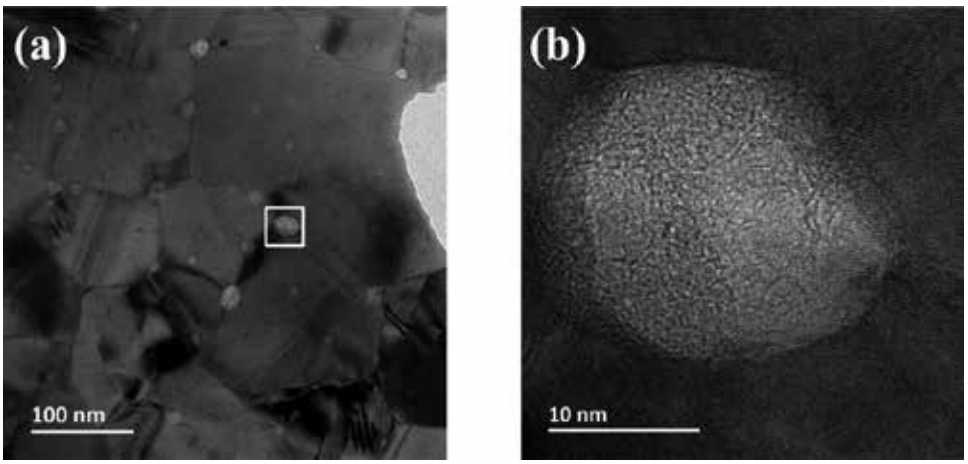

Figure 6. Bright field image and HRTEM image of sol-enhanced Ag-TiO_2 coating

Based on the results described above, we can concluded that when proper sol was added into the electrolyte, small nano-particles will be formed in-situ and co-deposited with the metal ions onto the substrate. These small amorphous nano-particles were distributed uniformly in the grain boundaries and inside the coating grains. Due to their small size, it is hard to detect them by using conventional microscopic tools such as optical microscope and scanning electron microscope.

These nano-particles incorporated into the coating matrix can increase the number of nucleation sites, while the other nano-particles distributed in the grain boundary can act as the obstacles that restrict the grain growth. The increasing nucleation center and obstacles for grain growth finally lead to an obvious grain refinement. However, when excessive sol was added into electrolyte, the nanoparticles start to agglomerate and tend to form voids in the coating matrix, finally causing a porous structure and deteriorating the property of coatings.

3.2. Mechanical property of sol-enhanced coatings

Several different kind of sol-enhanced coatings including Ni [8-10, 16-17], Ni-P [7, 14, 18], Ni-B [19-21], Ag [15] and Au-Ni [12-13, 22-24] nano-composite coatings were developed. Their mechanical property and microstructure were systematically studied. The mechanical properties of these sol-enhanced coatings are summarized in Table 1.

Based on the experimental results of mechanical properties and related microstructure of coatings, the corresponding strengthening mechanisms were suggested. A clear model of particle nano-dispersion, grain size and mechanical properties was established. We select sol-enhanced Au-Ni-TiO_2 nano-composite coating as an example to demonstrate the strengthening mechanism as below.

http://dx.doi.org/10.5772/62042

Type of coatings	Microhardness or Nano-hardness (optimum value)
Ni electroplating (on mild steel)	~320 $HV_{0.1}$
Sol-enhanced Ni-TiO_2 electroplating (on mild steel)	~430 $HV_{0.1}$
Sol-enhanced Ni-TiO_2 pulseelectroplating (on mild steel)	~503 $HV_{0.1}$
Ni-P electroplating (on copper)	~520 $HV_{0.1}$
Sol-enhanced Ni-P-TiO_2 electroplating (on copper)	~710 $HV_{0.1}$
Ni-B electroplating (on mild steel)	~677 $HV_{0.2}$
Sol-enhanced Ni-B electroplating (on mild steel)	~1061 $HV_{0.2}$
Ni-P electroless plating (on AZ31 Mg alloy)	~590 $HV_{0.2}$
Sol-enhanced Ni-P-TiO_2 electroless plating (on AZ31 Mg alloy)	~1025 $HV_{0.2}$
Sol-enhanced Ni-P-ZrO_2 electroless plating (on AZ31 Mg alloy)	~1045 $HV_{0.2}$
Au-Ni electroplating (on Ni coated brass)	2.55±0.13 GPa
Sol-enhanced Au-Ni-TiO_2 electroplating (on Ni coated brass)	3.20±0.15 GPa
Sol-enhanced Au-Ni-TiO_2 pulse electroplating (on Ni coated brass)	3.48±0.07 GPa
Sol-enhanced Au-Ni-ZrO_2 electroplating (on Ni coated brass)	2.89±0.07 GPa
Sol-enhanced Au-Ni-ZrO_2 pulse electroplating (on Ni coated brass)	3.31±0.11 GPa
Ag electroplating (on Ni coated brass)	1.33±0.05 GPa
Sol-enhanced Ag-TiO_2 electroplating (on Ni coated brass)	1.64±0.05 GPa

Table 1. The mechanical properties of sol-enhanced coatings

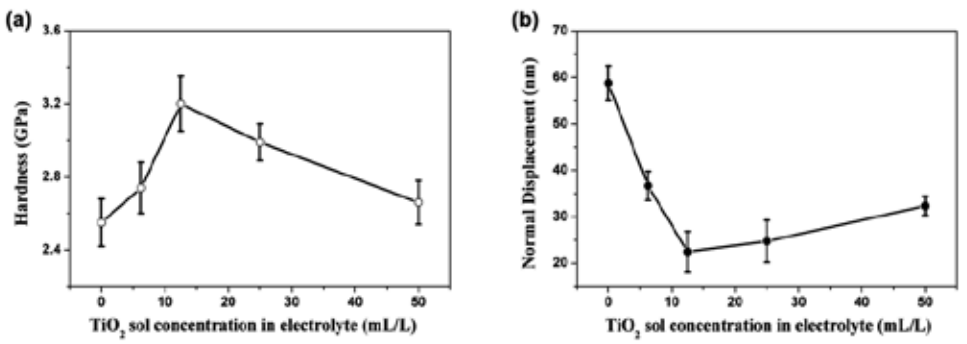

Figure 7. Nano-hardness and nano-scratch displacement results of sol-enhanced Au-Ni-TiO_2 nano-composite coatings

Fig. 7 shows the nano-hardness and scratch displacement of Au-Ni-TiO_2 coatings with different sol additions. The nano-indentation hardness and scratch tests were conducted on a Nanoindentor (Hystron, USA). Nano-scratch resistance tests were performed by using a conical tip with a 1000 μN constant load to 10 μm distance. The deeper of the scratch dis-

placement, the better wear resistance of coating. The nano-hardness and scratch displacement of Au-Ni coating was 2.55 ± 0.13 GPa and 58.8 ± 3.7 nm, respectively. At a low sol concentration, nano-hardness increases and scratch displacement decreases gradually with increasing TiO_2 content. 12.5 mL/L TiO_2 sol enhanced composite coating to the highest nano-hardness of 3.20 ± 0.15 GPa (26% increase) and the lowest scratch displacement of 22.5 ± 4.3 nm (reduced to 38%). However, further increasing the concentration of TiO_2 to 50 mL/L led to a decrease of nano-hardness to 2.66 ± 0.12 GPa, although it was still higher than that of the un-doped Au-Ni coatings. Meanwhile, the scratch displacement increases to 32.3±2.1 nm.

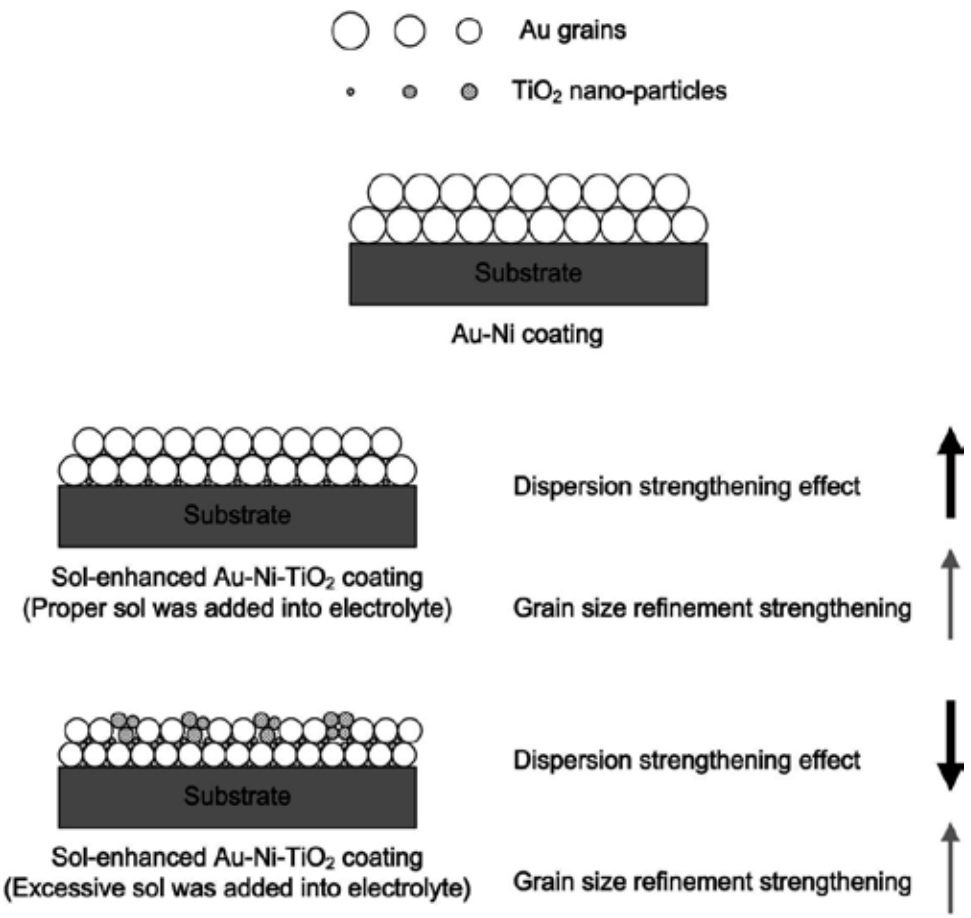

Figure 8. Schematic drawings of the enhancement mechanism of TiO_2 sol in the composite coating

The enhancement mechanism of TiO_2 sol on the composite coating can be elaborated in Fig. 8. The improved nano-hardness of sol-enhanced Au-Ni-TiO_2 coating could be attributed to the combined effects of grain refinement and dispersion strengthening. The highly dispersed reinforced phase should play a more important role as the grain size change is rather small. When proper TiO_2 sol was added into electrolyte, a good dispersion strengthening and grain

http://dx.doi.org/10.5772/62042

refinement can be achieved, resulting in a significant improvement of mechanical property for the coating. However, when excessive TiO_2 sol was added into electrolyte, TiO_2 nanoparticles start to agglomerate and tend to cause porous structure in the grain boundaries, which reduced the effect of dispersion strengthening; finally lead to a deterioration of the mechanical property although the grain size was continuously decreased [12-13].

3.3. Corrosion property of sol-enhanced coatings

Corrosion resistance is another important property for many coating applications. It was generally understood that materials with two phase microstructure may promote galvanic corrosion in corrosive environments therefore reducing their corrosion resistance. However, the nano-dispersion of a second phase can largely avoid galvanic corrosion and does not reduce the corrosion resistance of the composite coatings.

Fig. 9 shows the surface morphologies of Ni-B and sol-enhanced Ni-B-TiO_2 composite coatings after salt spray test for 120 h. The traditional Ni-B coating presented a corroded surface and the rust area can be clearly seen in Fig. 9a. The sol-enhanced Ni-B-12.5 mL/L TiO_2 coating displays an improved corrosion resistance as only two small corrosion pits can be seen by the white arrows in Fig. 9b. However, the sol-enhanced Ni-B-50 mL/L TiO_2 coating surface exhibited a corroded surface, similar to the un-doped Ni-B coating. A large area of coating surface was covered by rusts as shown in Fig. 9c.

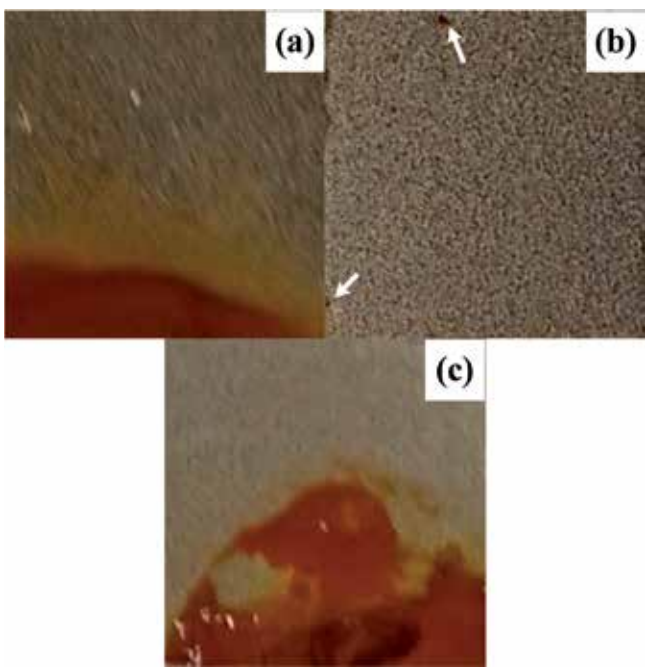

Figure 9. Surface morphologies of coatings after salt spray test in 5 wt. % NaCl solution for 120 h without removing the corrosion products: (a) Ni-B, (b) Ni-B-12.5 mL/L TiO_2 coating, and (c) Ni-B-50 mL/L TiO_2 coating.

The corrosion behaviors of coatings have a close relationship with the sol content due to its influence on the coatings microstructure. As it is well known that the corrosion resistance of a coating largely affected by its compactness, porosity is often the cause that a coating failure from corrosion. During the sol-enhanced electroplating process, the in-situ formed nanoparticles well distributed in the grain boundary areas can decrease the quantity of defects in the coating layer, making the coating more compact and less penetrable. Additionally, the nanoparticle itself is an inert compound, in the form of uniformly distributed nanoparticles in the coating, does not form micro galvanic cells. Instead, it may play a role of reducing the reactivity of matrix metal, therefore improving the corrosion resistance of the nano-composite coatings. However, when excessive sol was added into the electrolyte, the nanoparticles tend to agglomerate which increases the quantity of defects (voids) and lead to a porous structure in the coating, resulting in significant deterioration of corrosion resistance [19].

3.4. The other properties of sol-enhanced coatings

Metallic coatings and thin films have very wide applications which require not only mechanical and corrosion properties but also some functional properties. Here we use sol-enhanced Au-Ni coatings as an example to present the effect of sol addition on the surface gloss and conductivity property.

3.4.1. Surface gloss of sol-enhanced coatings

Surface gloss and color is important properties for gold and many other coatings as it dictates the quality and value of many products. Delta E (ΔE) is widely used to present the colour difference between samples being compared. It is generally accepted that if the difference of ΔE value between two samples is less than 1.0, they can be considered as the same colour, while 3.0 is the smallest colour difference that can be recognized by human naked eyes.

Fig. 10 presents the ΔE-values of Au-Ni coatings with different dopants. It can be seen that the sol addition impose a weak influence on the surface gloss and colors of coatings, which even cannot be detected by human naked eyes. The sol-enhanced coatings present almost identical surface gloss with the traditional coating due to the highly dispersed nano-structure [25].

3.4.2. Conductivity of sol-enhanced coatings

Both electrical conductivity and wear resistance are important properties for Au and Ag based coatings as these are required by applications of electric contacts. Traditional solid state alloying hardening techniques improve the wear resistance of Au and Ag coatings but severely reduce the conductivity due to the lattice distortion. The sol-enhanced strengthening technique improves the hardness of the coatings significantly but does not cause severe lattice distortion, therefore keeping the good conductivity for electrical applications.

Conductivity is frequently expressed in terms of IACS percent for convenience. An IACS value of 100% refers to a conductivity of 5.80×10^7 siemens per meter (58.0 MS/m) at 20°C. Fig. 11 shows the electrical resistivity and conductivity of sol-enhanced Au-Ni-TiO_2 coatings as a function of TiO_2 sol concentration. Comparing with the Au-Ni coating, the electrical conduc-

http://dx.doi.org/10.5772/62042

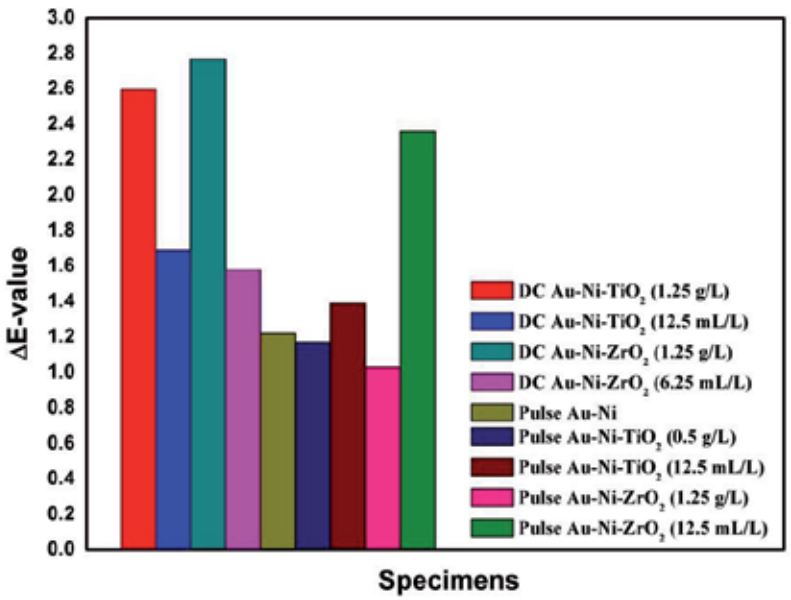

Figure 10. ΔE-values of Au-Ni coatings with different dopants

tivity of sol-enhanced coatings show a slight decrease (~4%) but keep at the same level with increasing sol content. After adding 50 mL/L TiO_2 sol, the electrical conductivity of coating is still higher than 50% IACS.

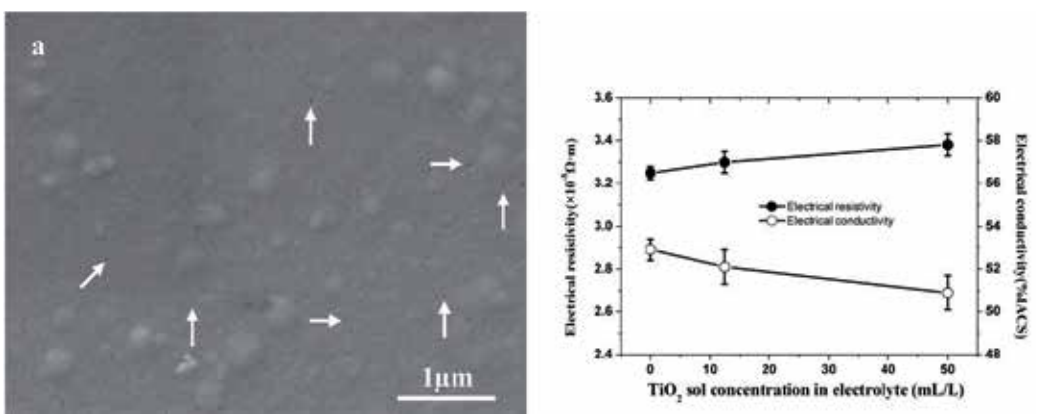

Figure 11. Electrical resistivity and electrical conductivity of sol-enhanced Au-Ni-TiO_2 nano-composite coatings

The same level conductivity of sol-enhanced coatings can be mainly attributed to the highly distribution of small nano-particles in the coating. The electron wave can bypass these small nano-particles and form a conductive network during the transportation process. Furthermore, the sol addition does not change the alloy solubility and cause lattice distortion. The

slight decrease of electrical conductivity can be attributed to the increment of scattering effect. The increase of grain boundaries and the scattering effect of electron wave strengthened by the second phase lead to the decrease of electrical conductivity [13].

4. Dopant technology derived from sol-enhanced plating and future industrial application of sol-enhanced coatings

In order to utilize this novel sol-enhanced technology and promote this technology into real production, the dopant technology has been developed based on the sol-enhanced method. Different types of sol were added into various commercial electrolytes to study their effects on the plating bath and property of coatings. Comprehensive investigations on the technical datasheet for different types of sol are being conducted. Table 2 briefly summarized the different types of sol which can take significant effect on commercial baths according to our studies. It can be seen that this sol dopant technology can be used in almost all types of commonly used commercial baths, which gives a broad application prospect.

Types of sol	Name of sol	Types of commercial bath
Inorganic	Al_2O_3	Zn-Ni [26]
Organic	TiO_2	Ni, Ni-P, Ni-B, Ni-Co [27-28], Cu [29], Au, Au-Ni, Ag, Co, Co-W, Sn, Ni-P(EP), Ni-B(EP)[*]
	ZrO_2	Ni, Ni-P, Ni-B, Ni-Co, Au, Au-Ni, Au-Co, Ni-P(EP), Ni-B(EP)
	Al_2O_3	Cu
Note: [*] EP means electroless plating, (eg. Ni-B(EP) means electroless Ni-B)		

Table 2. The sols have significant effect on the commercial baths

The sol-enhanced coatings have a highly dispersed nano-structure with superior performance. This sol-enhanced technology based on a simple and feasible process which is also compatible with the commercial solution. Therefore, it has great economic potential and market value in the future industrialization. For example, the micro-hardness of sol-enhanced Ni-P and Ni-B coating can reach up to above ~1000 HV, the same level of the widely used hard chrome coatings which require an environmentally harmful fabrication process. Hence, this sol-enhanced coating technology provides a potential replacement to the hard chrome coatings process [4]. On the other hand, the mechanical property of sol-enhanced Au and Ag coating can be increased up to more than 20% while keep the same level of conductivity and surface gloss. These research outcomes will find wide applications such as jewelry, craftwork and electronics.

A combination of different coatings can maximize the performance and functionality of coating by utilizing the different properties of each layer. Recently, we apply multi-layer technology to new sol-enhanced coatings systems in order to optimize the surface properties of coatings [20, 30-31]. Electroless double-layered Ni-P/Ni-P-XZrO_2 coatings with different phosphorus

http://dx.doi.org/10.5772/62042

(P) contents have been prepared. The high P inner layer provides high corrosion resistance while the sol-enhanced composite outer layer provides excellent mechanical properties. This controllable duplex electroless coating system possesses excellent anticorrosion and mechanical properties. Pilot scale production and tests are being conducted in order to realize the future industry applications.

5. Conclusion

A novel sol-enhanced method was developed to prepare nano-composite coatings. A small amount of oxide contained sol was added into the traditional electrolyte to in-situ form nanostructured composite coatings with highly dispersed nano-particles. The effect of sol addition on the microstructure and properties of composite coatings has been elaborated. The sol-enhanced nano-composite coatings have much improved mechanical property than that of the traditional coatings without sacrificing corrosion resistance, surface gloss and electrical conductivity. Dopant technology was developed to promote the real application of sol-enhanced coating method. Multiple sol-enhanced coatings were also developed in order to further improve the property of coatings. Scaling up tests is being conducted in an effort to realize industrial applications.

Acknowledgements

The project is supported by a New Zealand Marsden Grant, the National Natural Science Foundation of China (Grant NO 51401024) and Auckland UniServices project. The authors would like to thank the group members especially Weiwei Chen, Ying Ju, Shanghai Wei, Bo Hu and See Leng Tay, technical stuff in the Department of Chemical and Materials Engineering and the Research Centre of Surface and Materials Science for various assistances. We also want to express our gratitude to Mr Glen Slater, Chris Goode and technical stuff in Rigg Electroplating Ltd.

Author details

Yuxin Wang and Wei Gao*

*Address all correspondence to: w.gao@auckland.ac.nz

Department of Chemical and Materials Engineering, The University of Auckland, Auckland, New Zealand

References

[1] C. Corti, R. Holliday, editors. Gold: Science and Applications. CRC Press, Boca Raton; 2010.

[2] Arthur A. Tracton, editor. Coatings Technology Handbook. CRC Press, Boca Raton; 2006.

[3] Nasser Kanani, editor. Electroplating. Oxford: Elsevier Advanced Technology; 2004.

[4] Weiwei Chen, Wei Gao: Microstructures and properties of sol-enhanced nanostructured metal-oxide composite coatings. Progress in Natural Science: Materials International. 2011; 21: 355-362. DOI:10.1016/S1002-0071(12)60069-0

[5] Weiwei Chen. Sol-enhanced Nanostructured Metal-oxide Composite Coatings: Structures, Properties and Mechanisms (Thesis). The University of Auckland; 2010.

[6] Weiwei Chen, Wei Gao. Plating or coating method for producing metal-ceramic oating on a substrate, Patent NZ578038, New Zealand, 2009.

[7] Weiwei Chen, Wei Gao, Yedong He: A novel electroless plating of Ni-P-TiO_2 nanocomposite coatings. Surface & Coatings Technology. 2010; 204: 2493-2498. DOI: 10.1016/j.surfcoat.2010.01.032

[8] Weiwei Chen, Yedong He, Wei Gao: Electrodeposition of sol-enhanced nanostructured Ni-TiO_2 composite coatings. Surface & Coatings Technology. 2010; 204: 2487-2492. DOI:10.1016/j.surfcoat.2010.01.036

[9] Weiwei Chen, Wei Gao: Sol-enhanced electroplating of nanostructured Ni-TiO_2 composite coatings-the effects of sol concentration on the mechanical and corrosion properties. Electrochimica Acta. 2010; 55: 6865-6871. DOI:10.1016/j.electacta.2010.05.079

[10] Weiwei Chen, Yedong He, Wei Gao: Synthesis of nanostructured Ni-TiO_2 composite coatings by sol-enhanced electroplating. Journal of The Electrochemical Society. 2010; 157: E122-E128. DOI: 10.1149/1.3442366

[11] Duhua Wang, Gordon. P. Bierwagen: Sol-gel coatings on metals for corrosion protection. Progress in Organic Coatings. 2009; 64: 327-338. DOI:10.1016/j.porgcoat. 2008.08.010

[12] Yuxin Wang, Shanghai Wei, Ying Ju, Wei Lu, Biao Yan, Wei Gao: Mechanical properties and microstructure of Au-Ni-TiO_2 nano-composite coatings. Materials characterization. 2015; 102: 189-194. DOI:10.1016/j.matchar.2015.03.008

[13] Yuxin Wang, Ying Ju, Shanghai Wei, Wei Lu, Biao Yan, Wei Gao: Au-Ni-TiO_2 nanocomposite coatings prepared by sol-enhanced method. Journal of The Electrochemical Society. 2014; 161: D775-D781. DOI:10.1149/2.0331414jes

[14] Yuxin Wang, Weiwei Chen, R. A. Shakoor, R. Kahraman, Wei Lu, Biao Yan, Wei Gao: Ni-P-TiO_2 composite coatings on copper produced by sol-enhanced electroplating. International journal of electrochemical science. 2014; 9: 4384-4393.

[15] Bo Hu. Sol (TiO_2) Enhanced Nanocomposite Silver Coatings by Electroplating (Thesis). The University of Auckland; 2015.

[16] Yuxin Wang, Ying Ju, R. A. Shakoor, Ramazan Kahraman, Wei Gao: Nanocomposite Ni-TiO_2 coatings produced by pulsed electroplating. Materials Research Innovations. 2014; 18: 1102-1106. DOI:10.1179/1432891714Z.000000000883

[17] Yuxin Wang, Ying Ju, Biao Yan, Wei Gao: Sol-enhanced Ni-TiO_2 composite coating on hypereutectic Al-Si alloy. Materials Research Innovations. 2014; 18: 1107-1111. DOI: 10.1179/1432891714Z.000000000884

[18] Yongjian Yang, Weiwei Chen, Chungen Zhou, Huibin Xu, Wei Gao: Fabrication and characterization of electroless Ni-P-ZrO_2 nano-composite coatings. Applied Nanoscience, 2011; 1:19-26. DOI:10.1007/s13204-011-0003-6

[19] Yuxin Wang, Shu-jen Wang, Xin Shu, Wei Gao, Wei Lu, Biao Yan: Preparation and property of sol-enhanced Ni-B-TiO_2 nano-composite coatings. Journal of alloys and compounds. 2014; 617: 472-478. DOI:10.1016/j.jallcom.2014.08.060

[20] Shu-Jen Wang, Yuxin Wang, Wei Gao, R. A. Shakoor, Ramazan Kahraman: Preparation and property of Duplex Ni-B-TiO_2/Ni nano-composite coatings. International Journal of Modern Physics B. 2015; 29: 1540022. DOI: 10.1142/S0217979215400226

[21] Xin Shu, Yuxin Wang, Chuming Liu, Wei Gao: Microstructure and properties of Ni-B-TiO_2 nano-composite coatings fabricated by electroless plating. Materials Technology. 2015; 30: A41-A45. DOI: 10.1179/1753555714Y.0000000190

[22] Ying Ju, Yuxin Wang, A. Aljaafari, Wei Gao: Mechanical property of solid ZrO_2 powder enhanced Au-Ni coating. Materials Research Innovations. 2014; 18: 1132-1136. DOI: 10.1179/1432891714Z.000000000862

[23] Ying Ju, Yuxin Wang, Wei Gao: Sol-enhanced Au-Ni-TiO_2 electroplated coatings. Modern Physics Letters B. 2013; 27: 1341010. DOI: 10.1142/S0217984913410108

[24] Ying Ju, Yuxin Wang, Yi Wen, Wei Gao: Pulse plating enhanced Au-Co nanocomposite coatings. Modern Physics Letters B. 2013; 27: 1341011. DOI: 10.1142/S021798491341011X

[25] Ying Ju. Powder/Sol-enhanced Au-Ni Electroplated Composite Coatings: Structures, Properties and Mechanisms (Thesis). The University of Auckland; 2013.

[26] S. Ghaziof, P.A. Kilmartin, W. Gao: Electrochemical studies of so-enhanced Zn-Ni-Al_2O_3 composite and Zn-Ni alloy coatings. Journal of Electroanalytical Chemistry. 2015; 755: 63-70. DOI:10.1016/j.jelechem.2015.07.041

[27] Yuxin Wang, Xin Shu, Wei Gao, R. A. Shakoor, Ramazan Kahraman, Pengfei Yan, Wei Lu, Biao Yan: Microstructure and properties of nano-composite Ni-Co-TiO_2 coat-

ings fabricated by electroplating. International Journal of Modern Physics B. 2015; 29: 1540008. DOI: 10.1142/S0217979215400081

[28] Yuxin Wang, See Leng Tay, Shanghai Wei, Chao Xiong, Wei Gao, R.A. Shakoor, Ramazan Kahraman: Microstructure and properties of sol-enhanced Ni-Co-TiO_2 nano-composite coatings on mild steel. Journal of alloys and compounds. 2015; 649: 222-228. DOI: 10.1016/j.jallcom.2015.07.147

[29] Xiaojin Wei, Zhendi Yang, Ying Tang, Wei Gao: Influence of Al_2O_3 sol concentration on the microstructure and mechanical properties of Cu-Al_2O_3 composite coatings. International Journal of Modern Physics B. 2015; 29:1540021. DOI: 10.1142/S0217979215400214

[30] Yuxin Wang, Xin Shu, Shanghai Wei, Chuming Liu, Wei Gao, R A Shakoor, Ramazan Kahraman: Duplex Ni-P-TiO_2/Ni-P electroless coating on stainless steel. Journal of alloys and compounds. 2015; 630: 189-194. DOI: 10.1016/j.jallcom.2015.01.064

[31] Xin Shu, Yuxin Wang, Chuming Liu, Abdullah Aljaafari, Wei Gao: Double Layered Ni-P/Ni-P-ZrO_2 Electroless Coatings on AZ31 Magnesium Alloy with Improved Corrosion Resistance. Surface Coating & Technology. 2015; 261: 161-166. DOI:10.1016/j.surfcoat.2014.11.040

Chapter 7

Electrodeposition of Ni-P/SiC Composite Films with High Hardness

Alma Martínez-Hernández, Federico Manríquez-Guerrero, Julieta Torres, Raúl Ortega, José de Jesús Pérez-Bueno, Yunny Meas, Gabriel Trejo and Alia Méndez-Albores

Additional information is available at the end of the chapter

http://dx.doi.org/10.5772/61858

Abstract

This chapter describes the effect of SiC particle concentrations on the metallic continuous phase of the coating and the effect of heat treatment on the crystalline structure, hardness, and wear resistance of electrodeposited Ni-P-SiC coatings. The deposits were obtained via electrodeposition onto an AISI 1018 steel electrode and then heat treated at various temperatures ranging from 300 °C to 600 °C for 60 min in air. The tribological characteristics studied included hardness, friction coefficient, and wear resistance. The results indicated that the dispersion of SiC particles in the metallic matrix improves coating tribological properties such as hardness and wear resistance while diminishing the friction coefficient. The Ni-P-SiC alloy was originally amorphous and was transformed into a mixture of amorphous and crystalline phases when was thermally treated in the range from 400 °C to 500 °C. This phase transformation was associated with the precipitation of a mixture of Ni_3P intermetallic compound and pure Ni crystals. In addition, the results showed that the wear resistance of the Ni-P-SiC coating increased with hardness. The maximum hardness (1453.4 HV) was obtained when the Ni-P-SiC coatings were thermally treated at 500 °C.

Keywords: Ni-P-SiC, electrodeposition, heat treatment, microhardness, wear resistance

1. Introduction

Electrodeposition as an industrial activity has been practiced for over 150 years. Currently, the electrodeposition industry is undergoing fundamental changes as a result of environmental concerns, which increasingly necessitate that certain established plating processes be replaced

with more environmentally friendly technologies. The development of "clean" technologies in the electroplating industry is an essential task required and initiated by environmental protection laws worldwide [1]. From an environmental point of view, chromium (Cr) electrodeposition, which occurs in a wide range of industrial applications in the automotive, aerospace, mining, and petrochemical fields [2], is undoubtedly one of the most damaging electrodeposition processes. In environmental regulations, chromic acid (CrO_3), which is mainly used in hard Cr plating, has been recognized as both highly toxic and carcinogenic and was identified by the U.S. Environmental Protection Agency (EPA) as one of 17 high-priority toxic chemicals [3]. Consequently, the use of hexavalent chromates requires special waste disposal methods and expensive breathing apparatus, and exhaust systems must be employed to address emissions during processing. For these reasons, substitute materials and new designs have been under study for many years. Alloy electrodeposition alternative systems including Ni-W, Ni-P, and Co-W have been considered to replace conventional hard Cr deposition [4,5]. Unfortunately, it is challenging to replace Cr because of its comprehensively favorable material properties, including high hardness, low friction coefficient, and excellent wear and corrosion resistance. A possible approach for the preparation of Ni-based alloy coatings as an alternative to hard Cr is to introduce the new concept of functionally graded deposits (FGDs), which originally evolved from the application of functionally graded materials (FGMs) in which a property gradient arises from position-dependent chemical composition, microstructure, or atomic order [6,7]. Wang et al. [8] found that Ni-P deposits that were heat treated at 400 °C exhibited more than two orders of magnitude higher corrosion resistance than hard Cr deposits. It was found in our previous research that the hardness of Ni-P alloys after heat treatment at 500 °C is close to that of conventional hard Cr [9] and that they exhibited better wear resistance than hard Cr.

Alternatives such as composite coatings have been investigated in recent years. A study on Ni-P-Si_3N_4 composite deposition revealed that increasing the Si_3N_4 content in the deposit greatly increases the hardness and that the wear resistance of the Ni-P-Si_3N_4 composite deposit is four times higher than that of the Ni-P deposit [10]. Other reports [11,12] have concluded that the addition of hard microceramic particles (SiC, Si_3N_4, Al_2O_3, WC, B_4C, BN, CNTs) to the metal matrix can improve its hardness and wear resistance.

An important condition to enhance the hardness of the obtained coatings is by using particles with an average size of less than 1 μm evenly distributed on the surface. In these sense, Guo et al. [13] showed that the presence of carbon nanotubes (CNTs) in the composite coatings improves toughness, strength, and corrosion resistance of the coatings. Likewise, the addition of boron nitride (BN) particles (0.5 μm) to Ni coatings was studied by Pompei et al. [14], and the results showed that Ni-BN coatings present more hardener and wear resistance than those with neat Ni. Similarly, Malfatti et al. [15] found that the incorporation of SiC particles in Ni-P coatings results in higher polarization resistance (lower electrochemical activity) compared to coatings containing only the metallic matrix (Ni-P) for heat-treated specimens. This behavior was associated with a lower superficial active area produced by the nonconductive SiC particles.

http://dx.doi.org/10.5772/61858

Additionally, Zhang et al. [16] and Farzaneh et al. [17] found that Ni-P-SiC composite coatings with high SiC content exhibit better oxidation resistance than Ni-P coatings. Furthermore, Hansal et al. [18] demonstrated that the application of pulse current leads to a more compact composite coating that significantly improves the hardness and tribological behavior of the Ni-P-SiC deposits.

The aim of this work was to study the effect of SiC particle concentrations on the metallic continuous phase of the coating and the effect of heat treatment on the crystalline structure, hardness, and wear resistance of electrodeposited Ni-P-SiC coatings.

2. Materials and methods

2.1. Turbiscan lab expert stability analyses

The obtention of the Ni-P-SiC coatings require the stable dispersion of the SiC particles in the electrolytic bath. An efficient and widely employed method to achieve the effective dispersion of the particles is through the modification of the particle surfaces via the adsorption of a water-soluble polymer [19,20]. The high stability of the suspensions using this methodology is mainly related to electrostatic and steric mechanisms.

The adsorption of cationic surfactant molecules around the SiC particles causes a net positive charge on its surface as a result of increased electrostatic repulsion and steric hindrance between SiCPs. This phenomenon facilitates the migration of the particles toward the surface of the cathode, where they are dispersed during the formation of the Ni-P/SiC coating.

The effect of the surfactant concentration on the stability of SiCPs in an electrolytic bath was studied throughout the next procedure: 0.0625 g of SiC particles (99.9%, 100 nm, SkySpring Nanomaterials, Inc.) was added to 25 mL of a base solution containing 0.2 M NaCl + 0.65 M $NiSO_4 \cdot 6H_2O$ + 0.75 M $NiCl_2$ $6H_2O$ + 0.1 M H_3BO_3 + 0.1 M H_3PO_3 + x mM decyltrimethylammonium bromide (DTAB) (98%, Spectrum Labs, USA) (x = 0.02, 0.04, 0.06, 0.08, 1.00).

The stability of the SiCPs suspended in solution was measured using the methodology describes by Trejo et al. [21]. The typical transmission and backscattering profiles of SiCPs in the electrolytic bath without surfactant CTAB are shown in Figure 1.

2.2. Electrodeposition of Ni-P/SiC composites

Ni-P-SiC electrodeposits were obtained from a modified Watts Ni bath (solution S: 0.15 M H_3BO_3, 2 M NaCl, 0.65 M $NiSO_4 \bullet 6H_2O$, 0.75 M $NiCl_2 \bullet 6H_2O$, and 0.10 M H_3PO_3 with a pH of 1.5 adjusted with 1 M HCl) + 0.084 mM DTAB + x g mL^{-1} SiC (x = 0.00125, 0.0025, 0.005, 0.01, 0.015, or 0.02) using a parallel plate cell with an inter-electrode distance of 5 cm. The solutions were prepared immediately prior to each experiment using deionized water (18 MΩ cm) and analytical-grade reagents of the highest purity available (Sigma-Aldrich). The temperature of the electrolytic bath was controlled at 25 °C. Ni plates (99%, Atotech) were used as the anodes, and a plate of AISI 1018 steel of exposed area 10 × 15 cm^2 was used as the cathode. All reagents were analytical grade.

The electrodeposition current density was selected on the basis of additional tests using a Hull cell. The coatings obtained were of commercial quality, which is suitable for industrial application.

2.3. Morphological and tribological characterization

Crystalline phases were identified by powder X-ray diffraction (XRD) using a Bruker diffractometer model D8 Advance (Bragg-Brentano arrangement, Cu rotating anode). The samples were evaluated over the 2θ range from 30° to 95° at a rate of 0.2° s^{-1}.

Glow discharge spectrometer (GDS) (Leco, Mod. 850A) was employed to obtain elemental composition of the coatings as a function of depth into the coatings.

The coatings hardness value was the average of ten measurements obtained on a Matsuzawa MXT-α7 on the Vickers scale with a load kept at 10 g for 15 s.

A reciprocating ball-on-disk tribometer (CSM tribometer instruments) was used to wear tests. All tests were nonlubricated and carried out under dry at 25 °C temperature and relative humidity of 39%. A 3-mm AISI 8620 ball bearing was used as the counter body under a 2-N load at a sliding speed of 1 cm s^{-1}. The friction coefficient of the three wear tests was recorded, and the wear volume was measured according to the ASTM G99 standard method.

3. Results and discussion

3.1. SiC Particle (SiCP) suspension stability measurements

The transmission profile (Figure 1a) shows a rapid increase in the transmittance signal from the first scans and remains stable in the 1- to 50-mm range. Additionally, the transmittance signal increased with time, a behavior that is indicative of the formation of a clarifying zone in this region (Figure 1b). Additionally, the backscattering profile (Figure 1c) shows an increase in the backscattering signals as a function of time, which is the characteristic of an increase in particle size. This behavior is related to a phenomenon called differential sedimentation [22]. These results revealed that unstable suspensions of SiCPs were obtained when a surfactant was not used.

Figure 2 shows the typical transmission and backscattering profiles of SiCPs in the electrolytic bath with the surfactant DTAB. The transmission profile (Figure 2a) shows increases with time throughout the length of the vial. This increase is more pronounced in the region from 18 to 50 mm, which indicates the formation of a clarifying zone in this region. Furthermore, in the region from 0 to 48 mm, the transmission signals are less than 10% during the first 13 h of the experiment, indicating that the solution is opaque in this range.

The backscattering profile (Figure 2c) shows a decrease in the signals as a function of time, another indication of differential sedimentation [22,23].

The above results revealed that stable suspensions (less than 10% transmission during the first 13 h) of SiCPs were obtained when DTAB was used as a surfactant.

http://dx.doi.org/10.5772/61858

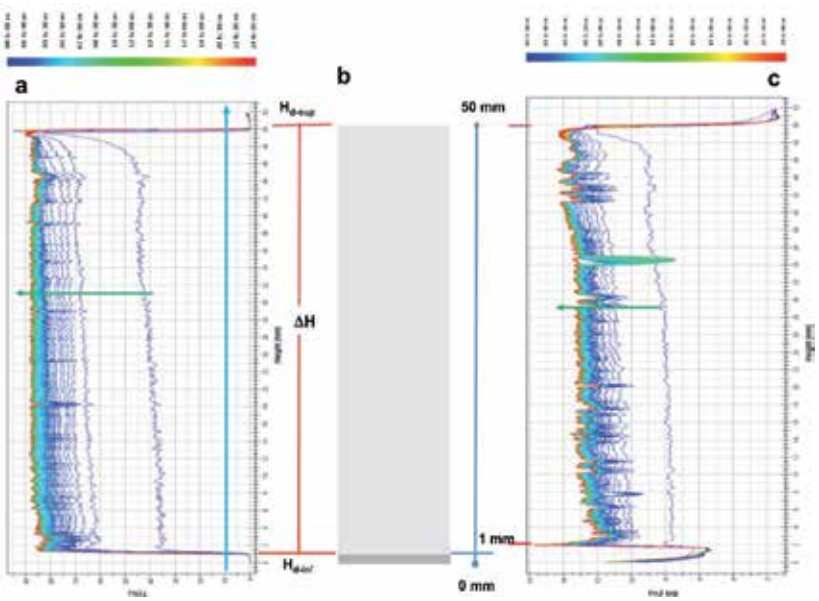

Figure 1. (a) Transmission and (b) backscattering profiles typical of an electrolytic bath of Ni-P-SiC with SiC particles (SiCPs) and without the surfactant DTAB. The data are reported as a function of time (0 to 24 h) and sample height (0 to 50 mm).

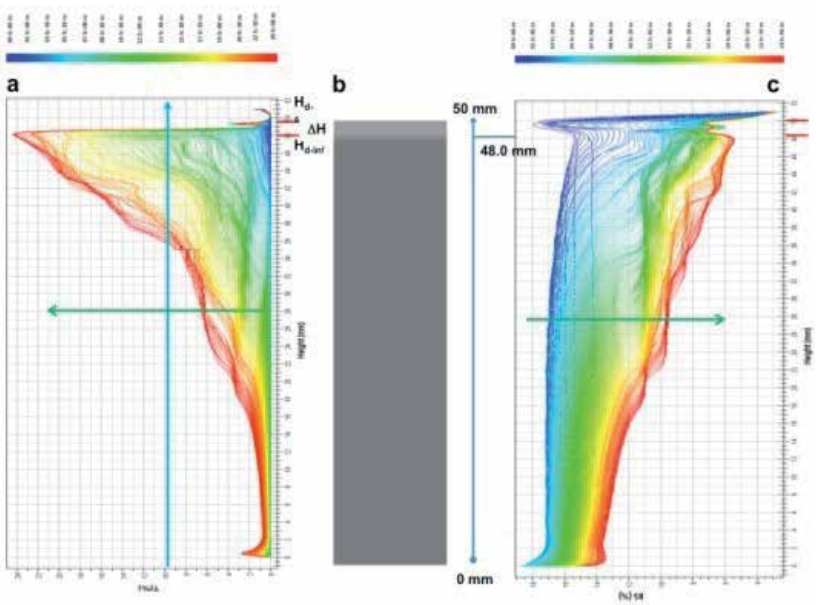

Figure 2. (a) Transmission and (c) backscattering profiles typical of an electrolytic bath of Ni with SiCPs and 0.08 mM CTAB. The data are reported as a function of time (0 to 24 h) and sample height (0 to 50 mm).

Figure 3 shows that the values of the thickness of the clarifying layer (ΔH) in the upper portion of the aqueous SiCP suspension decreased significantly in the presence of the dispersant and increased over time. The best results were obtained for the highest concentrations of CTAB. During the time period from 0 to 13 h, the ΔH value of the aqueous SiCP suspensions with both 0.08 and 0.10 mM CTAB was only 0.85 mm, whereas for the suspension without surfactant, ΔH was 48 mm beginning in the first minutes of the experiment. After 20 h, the ΔH value of the aqueous SiCP suspension with 0.08 mM CTAB was only 6.92 mm.

The greater stability of the SiCPs in the suspension with the dispersant is attributed to the modification of the solid surfaces of the SiC particles via the adsorption of CTAB. Because of its spatial structure and hydrophilic functional groups, CTAB can enhance the electrostatic repulsion and steric hindrance between SiC particles.

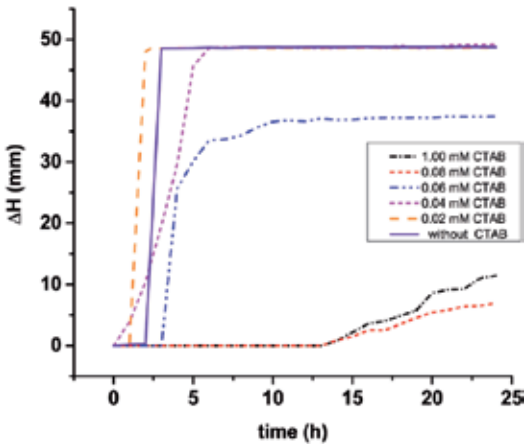

Figure 3. Effect of DTAB dosage on the clarifying-layer thickness (ΔH) as a function of time (0 to 24 h).

3.2. Electrodeposition of composite Ni-P-SiC: Influence of the concentration of SiC particles in solution, on the composition of SiC particles in the matrix Ni-P-SiC composites

3.2.1. Hull cell studies and electrodeposition of Ni-P-SiC composites

A Hull electrochemical cell was used as a first step to find the suitable values of current density that promote uniform coatings of Ni-P-SiC. Prior to the test, an AISI 1018 steel plate was pickled and activated. For pickling, the steel plate was immersed in a 30% HCl solution for 10 s, immediately washed, and then subsequently activated by its immersion in a 10% HCl solution. Immediately after activation, the AISI 1018 steel plate was submerged in a Hull cell containing solution S (= 0.2 M NaCl + 0.65 M $NiSO_4 \cdot 6H_2O$ + 0.75 M $NiCl_2 \cdot 6H_2O$ + 0.1 M H_3BO_3 + 0.1 M H_3PO_3) + 0.084 mM DTAB + x g mL^{-1} SiC (x = 0.00125, 0.0025, 0.005, 0.01, 0.015, or 0.02) (see Figure 4a). Each test was repeated three times for each given SiC concentration. Tests were performed by applying a current of 1 A for 12 min. Ni plates (99%, Atotech) were used as the anodes.

http://dx.doi.org/10.5772/61858

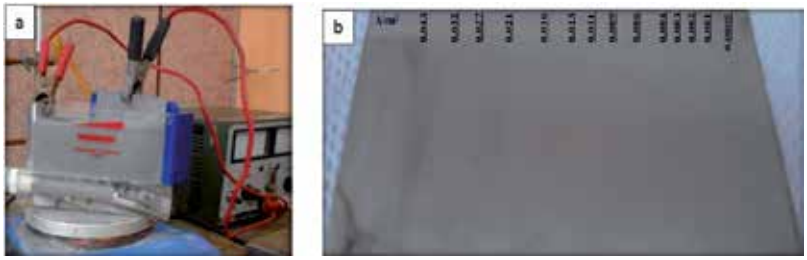

Figure 4. (a) Hull cell containing solution S + 0.084 mM DTAB + 0.02 g mL^{-1} SiC and the AISI 1018 steel plate electrically wired to a power source. (b) Plates with a Ni-P-SiC composite coating obtained after applying 1 A for 12 min.

Figure 4b shows an AISI 1018 steel plate coated with Ni-P-SiC obtained using a solution S + 0.084 mM DTAB + 0.02 g mL^{-1} SiC solution. It was found that current density (j) values between 0.043 and 0.0005 A/cm^2 are adequate to obtain coatings with an appearance and adhesion of acceptable quality.

From this result, Ni-P-SiC coatings were obtained from a solution of composition S + 0.084 mM DTAB + x g mL^{-1} SiC (x = 0.00125, 0.0025, 0.005, 0.01, 0.015, or 0.02) using 1 cm^2 AISI 1018 steel disks as cathodes by applying 0.042 A/cm^2 for 10 min. The obtained coatings are shown in Figure 5. Coatings exhibiting metallic luster were obtained when the solution with the highest concentration of SiC (0.02 g mL^{-1}) was used as an electrolyte.

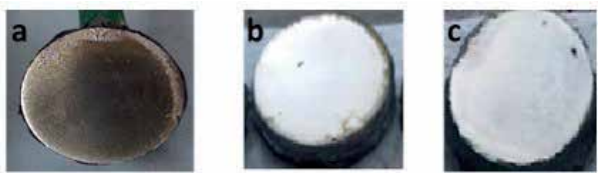

Figure 5. Ni-P-SiC coatings obtained by applying a current density of 0.042 A/cm^2 for 10 min from an electrolytic bath of S (= 0.2 M NaCl + 0.65 M $NiSO_4 \cdot 6H_2$ + 0.75 M $NiCl_2 \cdot 6H_2O$ + 0.1 M H_3BO_3 + 0.1 M H_3PO_3) + 0.084 mM DTAB + x g mL^{-1} SiC, (a) x = 0.02, (b) x = 0.015, (c) x = 0.01.

3.2.2. Characterization of Ni-P-SiC composites

Glow discharge spectroscopy (GDS) was used to obtain the elemental composition profiles of Ni-P-SiC coatings obtained from S solutions having different SiC concentrations. The analysis of the sample was performed at successive depths until the substrate (Fe) was reached.

Figure 6 shows a typical composition profile obtained by GDS. The thickness of the coating was approximately 15 μm. At the surface of the coating, a higher concentration of oxygen was present, presumably indicating surface oxidation. After the oxide layer was removed from the surface, Ni, P, Si, and C were observed; in the range of 2.5 to 25 μm, the composition of Ni and P changed slightly as a function of depth, whereas the Si concentration remained constant but increased inside the AISI 1018 steel matrix. Additionally, the oxygen concentration decreased. A similar behavior was observed for all the SiC concentration values tested.

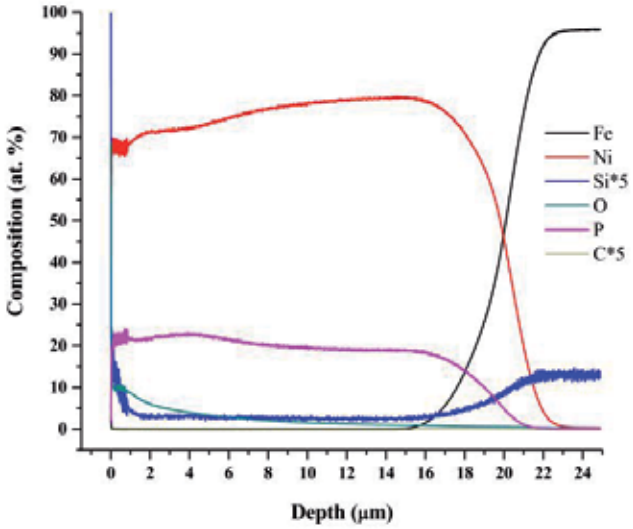

Figure 6. Typical GDS elemental composition profiles of Ni-P-SiC coatings electrodeposited at 0.042 mA/cm^2, t = 10 min from solutions S (0.2 M NaCl + 0.65 M $NiSO_4 \cdot 6H_2O$ + 0.75 M $NiCl_2 \cdot 6H_2O$ + 0.1 M H_3BO_3 + 0.1 M H_3PO_3) + 0.084 mM DTAB + 0.02 g mL^{-1} SiC.

Figure. 7 shows the variation of the SiC content in the coating matrix as a function of SiC concentration in the electrolytic bath. With an increase in SiC concentration in the solution, the concentration of SiC dispersed in the obtained coating increases until a maximum value of 0.6 at.% is reached when a solution with a SiC concentration of 0.015 g/mL is used. With higher concentration values, the percentage of SiC in the coating matrix decreases.

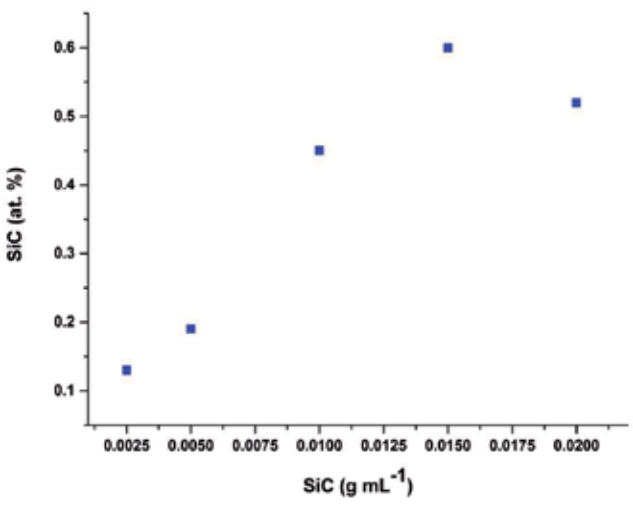

Figure 7. Change in the SiC concentration in the Ni-P-SiC coating matrix as a function of the SiC concentration in the solution. Coatings were obtained at 0.042 mA/cm^2, t = 10 min.

http://dx.doi.org/10.5772/61858

Figure 8 shows the XRD patterns obtained for Ni-P-SiC coatings having different SiC concentrations in the metallic matrix. The peaks that correspond to different crystallographic orientations of Ni are most prominent. No significant changes were found in the Ni XRD patterns recorded for coatings with different SiC concentrations in the metallic matrix.

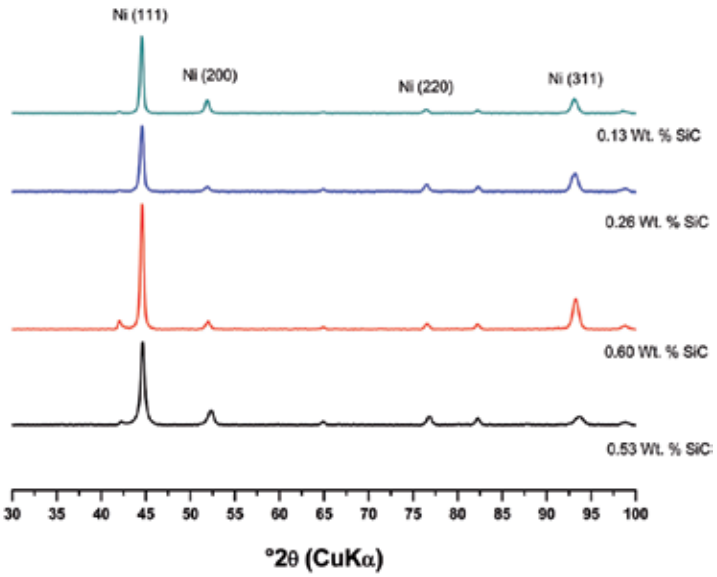

Figure 8. XRD patterns for Ni-P-SiC coatings with different SiC contents in the metallic matrix that were electrodeposited onto AISI 1018 steel.

3.2.3. Microhardness of Ni-P-SiC electrodeposits

The microhardness of the Ni-P-SiC coatings with different SiC concentrations was measured. Figure 9 illustrates the surface microhardness of the electrodeposited Ni-P-SiC coatings as a function of the SiC concentration in the metallic matrix. As observed from the curve, the hardness of the coating increases to values in the range of 580 to 620 HV when SiC particles are dispersed in the metallic matrix. This behavior is associated with increased hard sites. Despite such increases, the obtained hardness was less than that of a hard Cr coating, which has a microhardness of 1020 HV [24].

3.2.4. Wear resistance

To understand the wear mechanism of the electrodeposited Ni-P-SiC composite coatings, the wear track patterns were studied by SEM. As shown in Figure 10, there were many adhesive tearing and plough lines in the sliding direction. Compared to the other Ni-P-SiC coatings, the coating with 0.52 at.% SiC (Figure 10e) exhibited the narrowest and shallowest plough lines. These findings indicated that the coating with 0.52 at.% SiC had the best wear resistance.

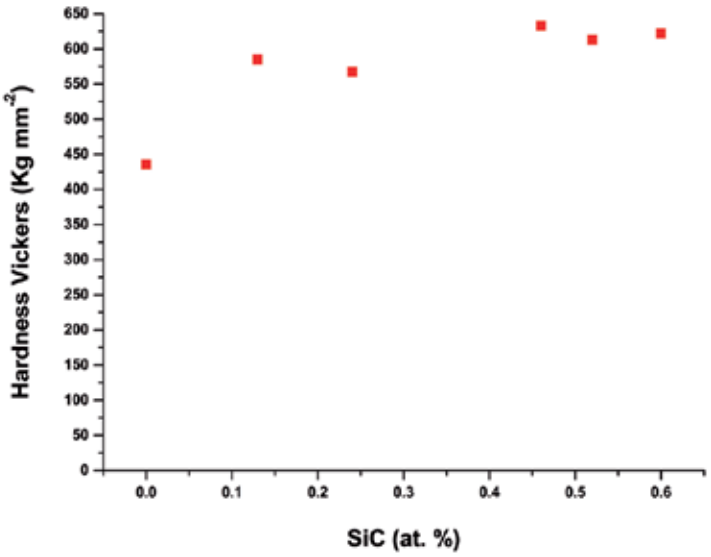

Figure 9. Hardness of the electrodeposited Ni-P-SiC coatings depending on the concentration of SiC in the metallic matrix.

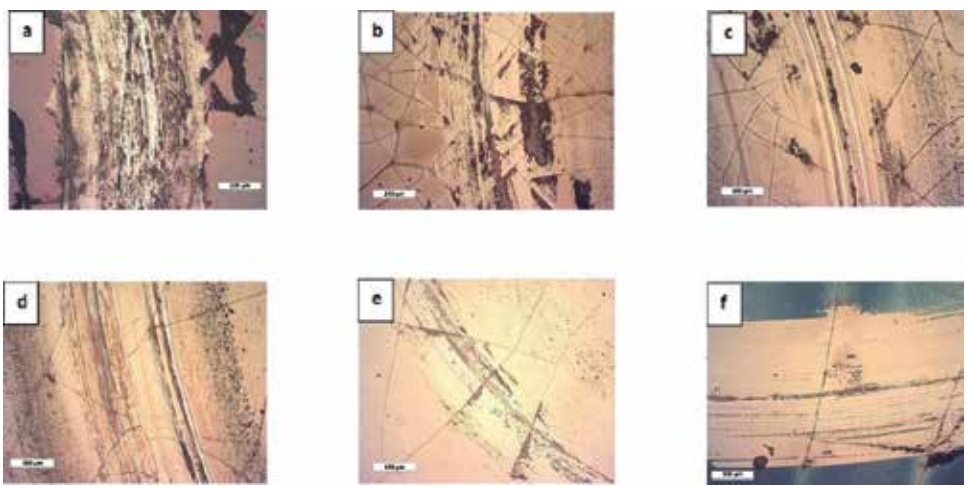

Figure 10. SEM images of wear track of Ni-P-SiC coatings, with different SiC at.% after sliding against AISI 8620 ball in air: (a) 0.0, (b) 0.13, (c) 0.24, (d) 0.46, (e) 0.52, (f) 0.60 at.% SiC.

Figure 11 shows the curves of the wear volume of the electrodeposited Ni-P-SiC coatings as a function of the content of SiC in the metal matrix. The presence of SiC in the metallic matrix of the coating decreases volume wear. The lowest wear volume value was obtained when the SiC concentration in the metallic matrix of the Ni-P-SiC coating was 0.52 at.%. Wear volume values for the other tested concentrations were in the range of 150 to 200 $\mu m^3 N^{-1}m^{-1}$.

http://dx.doi.org/10.5772/61858

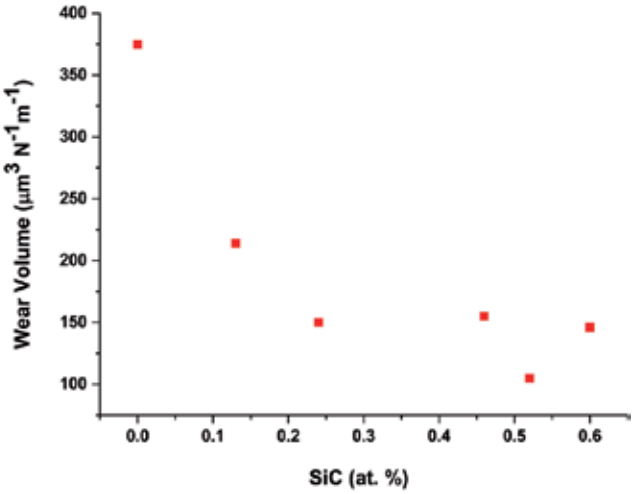

Figure 11. The wear volume of the Ni-P-SiC coatings as a function of the content of SiC in the metal matrix.

3.2.5. Friction coefficients

Figure 12 shows the behavior of the values of the friction coefficients of the Ni-P-SiC coatings obtained. After 5000 cycles, the coating Ni-P-SiC with 0.6 at.% had the lowest value of friction coefficient (0.12 μ), which is similar to the value measured for a hard Cr coating (0.11 μ).

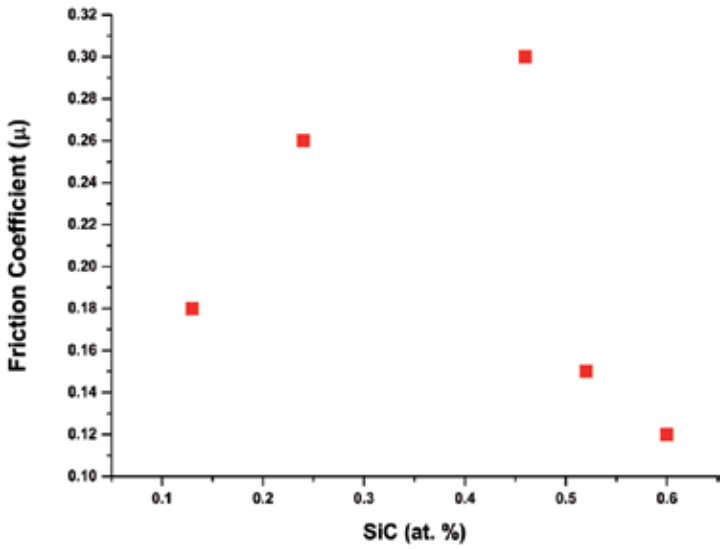

Figure 12. Variation of friction coefficient values as a function of the SiC (at.%) concentration in Ni-P-SiC composite coatings.

3.3. Effects of heat treatment on the tribological properties of electrodeposited Ni-P-SiC composites

Over the last two decades, a variety of surface engineering processes have been developed to enhance the wear resistance, hardness, and corrosion performance of materials. Today, Ni-P alloys are widely used in the aerospace, automotive, and electronic industries because they possess a high degree of hardness, wear resistance, and corrosion resistance, as well as a low friction coefficient [25–28]. In this regard, Malfatti et al. [29] found that the transition from crystalline to amorphous structures occurs progressively over the range of several atomic percent of P and that as-deposited Ni-P coatings are amorphous when the P content exceeds 15 at.%. In contrast, the amorphous alloys can be crystallized via heat treatment, followed by decomposition to nickel phosphide (Ni_3P) and face-centered cubic (fcc) Ni crystals at temperatures above 350 °C [30]. The tribological characteristics of the Ni-P coatings can generally be improved via an appropriate heat treatment [31–33], which can be attributed to precipitation of fine Ni crystallites and hard intermetallic Ni_3P particles during the crystallization of the amorphous phase [34]. In this respect, the wear resistance of the Ni-P alloys increases after heat treatment [35]. Moreover, Wang et al. [8] recently showed that Ni-P electroless coatings heat treated at 400 °C exhibited corrosion resistances of over two orders of magnitude better than hard Cr deposits.

The aim of this section was to study the effects of heat treatment on the physical properties of electrodeposited Ni-P-SiC coatings, including their crystalline structure, hardness, and resistance to wear.

3.3.1. Materials and methods

Ni-P-SiC electrodeposits were obtained from a modified Watts Ni bath (containing 0.2 M NaCl, 0.65 M $NiSO_4 \cdot 6H_2O$, 0.75 M $NiCl_2 \cdot 6H_2O$, 0.1 M H_3BO_3, 0.1 M H_3PO_3 [36]) + 0.084 mM DTAB + 0.02 g mL^{-1} SiC, with a pH of 1.5 adjusted with 1 M HCl) (solution S_1). These solutions were prepared immediately prior to each experiment using deionized water (18 MΩ cm) and analytical-grade reagents of the highest purity available (Sigma-Aldrich).

The Ni-P-SiC coatings were obtained via electrodeposition of solution S_1 under galvanostatic conditions. The coatings were then annealed in air for 60 min at one of four temperatures: 300 °C, 400 °C, 500 °C, or 600 °C.

An atomic force microscope (AFM) (Digital Instruments, Mod. Nanoscope E) was used in contact mode to image the deposited Ni-P-SiC on the steel substrate. These measurements were performed in air (ex situ) using silicon nitride AFM tips (Digital Instruments). All images were obtained at 2 Hz and are represented in the so-called height mode, in which the highest portions appear brighter.

The deposited phases were identified via X-ray diffraction (XRD) using a Bruker diffractometer (Mod. D8 Advance) (Bragg-Brentano arrangement) with CuKα radiation (λ = 1.54 Å). The range of 2θ from 40° to 95° was recorded at a rate of 0.2° s^{-1}.

The elemental composition of the coatings as a function of the thickness was obtained using a glow discharge spectrometer (GDS) (Leco, Mod. 850A).

Hardness was measured with a Matsuzawa MXT-ALFA Vickers microhardness tester with a 10-g load applied for 15 s. The final value quoted for the coating hardness was the average of ten measurements.

Wear tests were performed on a reciprocating ball-on-disk tribometer (CSM tribometer) in air at a temperature of approximately 25 °C and a relative humidity of approximately 39% under dry, nonlubricated conditions. Balls (3 mm diameter) made of AISI 8620 with a hardness of 25 HRC were used as the counter body in the wear tests. All wear tests were performed under a 2-N load at a sliding speed of 1 cm s^{-1}. The friction coefficient and the sliding time were automatically recorded during the test. The wear volume was measured according to the ASTM G99 standard method. Three wear tests were conducted for each sample.

3.3.2. Results

3.3.2.1. Electrodeposition of Ni-P-SiC composites

Hull cell tests were performed using an S solution + 0.084 mM DTAB + 0.02 g/mL SiC, an applied current of 1 A, and a test time of 12 min. Each test was repeated three times. The typical behavior obtained for this system is shown in Figure 13.

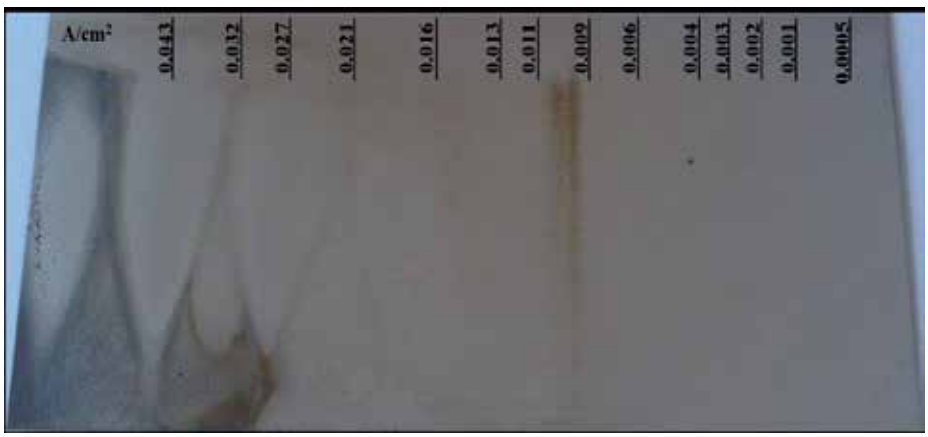

Figure 13. Surface morphology of Ni-P-SiC composite deposited by a Hull cell, i = 1 A, t = 12 min, obtained from solution S + 0.084 mM DTAB + 0.02 g mL^{-1} SiC.

Figure 13 indicates that homogeneous coatings can be obtained when current densities (j) between 0.021 and 0.003 A cm^{-2} are applied. These results demonstrate that 20 μm thick Ni-P-SiC coatings can be obtained by applying 0.021 A cm^{-2} for 20 min. The obtained coating is shown in Figure 14. Ni-P-SiC coatings obtained through the parallel plate technique are of metallic appearance, are well attached, and exhibit metallic luster.

Figure 14. Surface morphology of Ni-P-SiC composite obtained from an S solution (= 0.2 M NaCl, 0.65 M $NiSO_4 \cdot 6H_2O$, 0.75 M $NiSO_4$ $6H_2O$, 0.1 M H_3BO_3, 0.1 M H_3PO_3) + 0.084 mM DTAB + 0.02 g mL^{-1} SiC and j = 0.021 A/cm^2 for 20 min.

3.3.2.2. Thermal treatment

The Ni-P-SiC composite coatings obtained in the previous section were thermally annealed at different temperatures: 300 °C, 400 °C, 500 °C, and 600 °C for 60 min. Each test was repeated three times for each temperature set point.

Figure 15 shows the Ni-P-SiC plates after annealing. Annealed Ni-P-SiC coatings exhibit evident changes in surface morphology with respect to their nonannealed counterparts (see Figure 14).

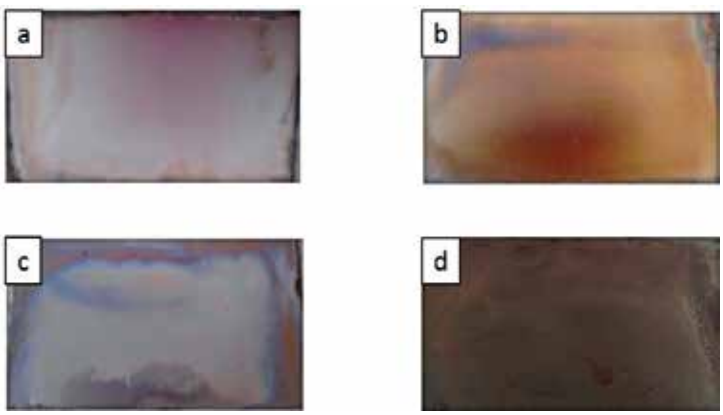

Figure 15. Surface morphology of Ni-P-SiC composite coatings after thermal annealing at (a) 300 °C, (b) 400 °C, (c) 500 °C, and (d) 600 °C.

3.3.2.3. Glow discharge spectroscopy characterization

Figure 16 shows the typical concentration profile of a Ni-P-SiC coating after thermal annealing. The oxygen found on the coating surface is associated with superficial oxidation. After removing the oxide layer, a constant composition of Ni and P is observed through the entire

http://dx.doi.org/10.5772/61858

coating thickness (24 μm). The Si concentration, however, is lower in the upper layers of the coating (5 to 22 μm) and increases in the deeper layers (22.5 to 25 μm). A similar behavior was observed for all the analyzed coatings.

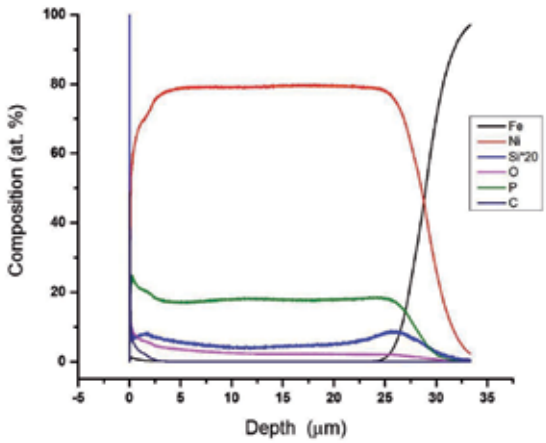

Figure 16. GDS elemental distribution profiles of a Ni-P-SiC coating after thermal annealing and electrodeposited under galvanostatic conditions (j = 0.021 A/cm^2, t = 20 min) in solution S + 0.084 mM DTAB + 0.02 g mL^{-1} SiC.

Table 1 shows the variation of SiC content in the Ni-P-SiC coating matrix after thermal annealing at different temperatures. A decrease in Si content is observed on thermally treated coatings. An approximate 57% loss of Si was observed in the range of 300 °C to 500 °C and increased to 70% when the coating was annealed at 600 °C. This observed behavior could be related to the detachment of SiC particles from the coating matrix during thermal annealing, which is corroborated by composition profile analysis. GDS composition profiles show that the SiC composition remains constant inside a certain range of the coating thickness but increases at the deepest point. This indicates that SiC particle detachment occurs in the upper and middle coating layers.

Annealing Temperature / °C	0.0	300	400	500	600
at. % Si	0.77	0.33	0.32	0.39	0.23

Table 1. Atomic percentages of Si in the Ni-P-SiC composite coatings after 60 min thermal annealing at different temperatures.

3.3.2.4. XRD characterization

Figure 17 shows the XRD patterns for the Ni-P-SiC coatings without heat treatment and with heat treatment (60 min) at different temperatures. Without heat treatment and at annealing temperatures below 400 °C, only a small broad peak appears in the XRD patterns, suggesting

an amorphous structure without phase transition. However, when the heat treatment temperature was close to 500 °C, the structure became crystalline and the XRD pattern shows new sharp peaks corresponding to crystalline fcc Ni (JCP2 04-0850) and Ni_3P (JCP2 89-2743). The transition can be related to the crystallization of neat Ni and the consecutive precipitation of Ni_3P from the supersaturated Ni-P solid solution [30,13,37-38]. Studies of similar systems [39–41] have established that amorphous Ni-P alloys are less dense than crystalline Ni-P alloys, and as consequence, the transition from amorphous to crystalline structure is accompanied by a volume contraction [13]. In agreement with this statement, after the thermal treatment at 500 °C of the Ni-P-SiC composites, a signal corresponding to SiC particles appears.

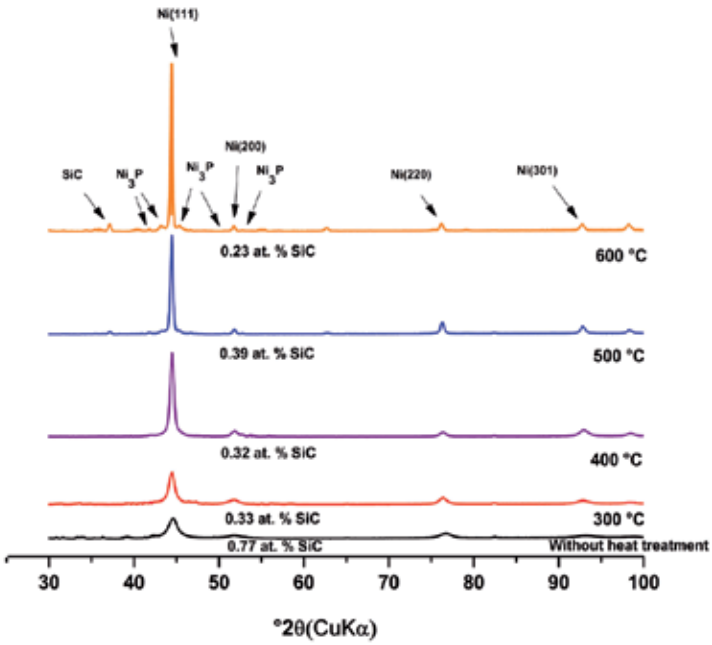

Figure 17. XRD patterns for Ni-P-SiC coatings electrodeposited onto AISI 1018 steel and heat treated at different temperatures. Ni (JCP2 04-0850) and Ni_3P (JCP2 89-2743).

3.3.2.5. AFM characterization

AFM in contact mode was used to obtain images of the Ni-P-SiC coatings both with and without heat treatment for 60 min at different temperatures. Figure 18 shows the AFM images obtained from Ni-P-SiC coatings thermally treated at different temperatures: without thermal annealing, 300 °C, 400 °C, 500 °C, and 600 °C. When the coating was treated at 300 °C (Figure 18b), an amorphous structure containing some crystals was observed; these crystals are associated with the initial formation of the Ni_3P species. At 500 °C (Figure 18d), a larger quantity of crystals associated with the formation of the Ni_3P species was observed in addition to smaller crystals corresponding to fcc Ni. Finally, at 600 °C (Figure 18e), the entire surface was covered with Ni_3P and Ni crystals. These results confirm the phase transition and formation of the Ni_3P and fcc Ni species observed by XRD.

http://dx.doi.org/10.5772/61858

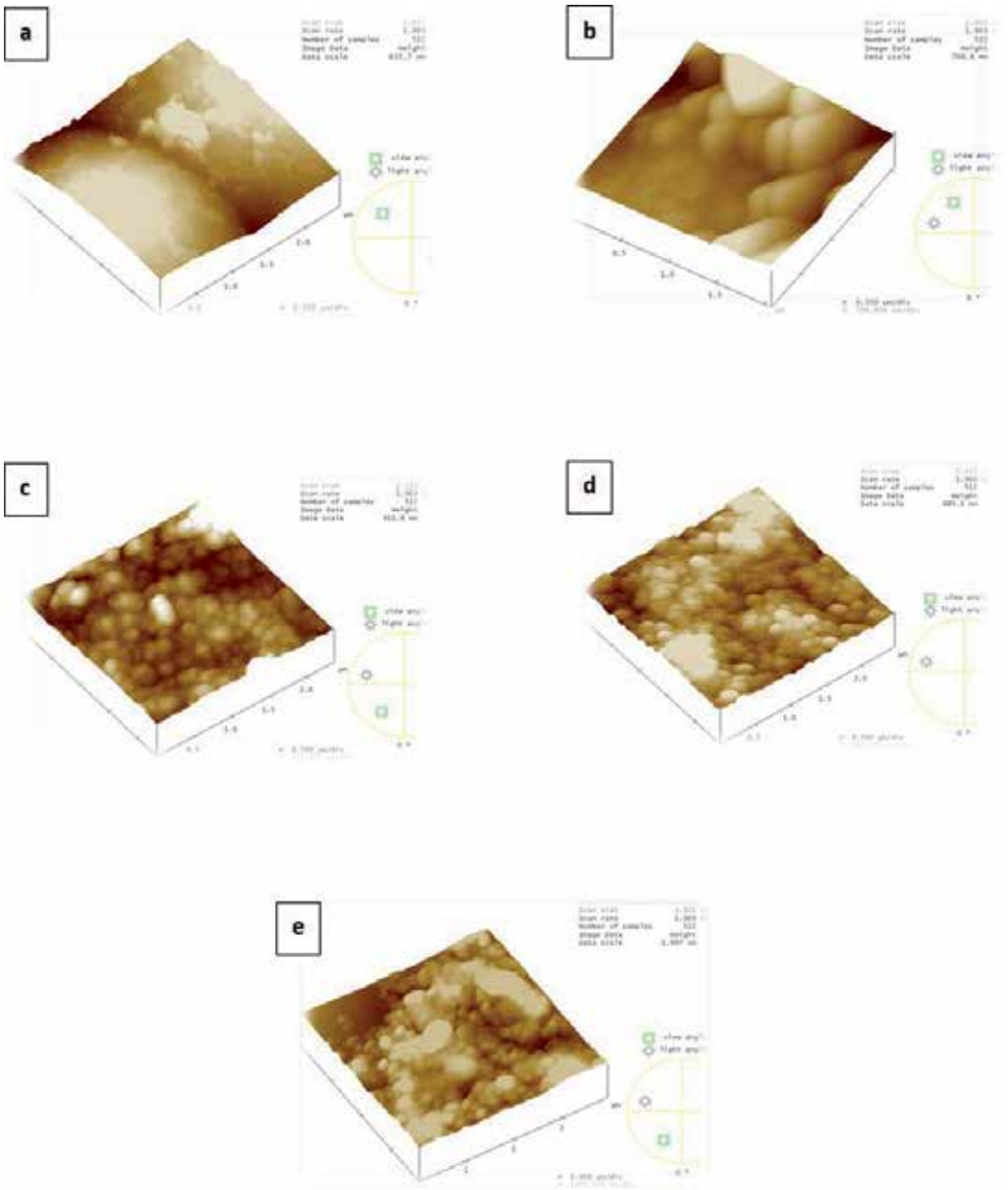

Figure 18. AFM images of Ni-P-SiC electrodeposited onto AISI 1018 steel under galvanostatic conditions (j = 0.021 A/cm^2, t = 20 min) from solution S + 0.084 mM DTAB + 0.02 g mL^{-1} SiC and heat treated at different temperatures: (a) without thermal annealing, (b) 300 °C, (c) 400 °C, (d) 500 °C, and (e) 600 °C.

3.3.3. Tribological properties

3.3.3.1. Microhardness of Ni-P-SiC coatings

Figure 19 shows the surface microhardness of the Ni-P-SiC composites as a function of the annealing temperature. When the annealing temperature was less than 400 °C, a slight increase in the hardness values is observed; however, when the heat treatment was in the range of 400 °C to 500 °C, the hardness value change significantly (from 1057.2 HV to 1453.4 HV). This increase in hardness was associated with a structural change due to the formation of hard intermetallic Ni_3P particles within the Ni-P-SiC coating. The obtained hardness value of the Ni-P-SiC composites at 500 °C (1453.4 HV) is greater than that of a hard Cr coating, which a microhardness value of 1020 HV [24]. Finally, at annealing temperatures above 500 °C, the hardness of the Ni-P-SiC coating decreased sharply. At higher temperatures, the coating began to soften because the Ni_3P particles conglomerated, reducing the number of hardening sites. This process also removes P and SiC from the alloy, producing a separate phase of soft Ni within the matrix and further reducing the bulk hardness.

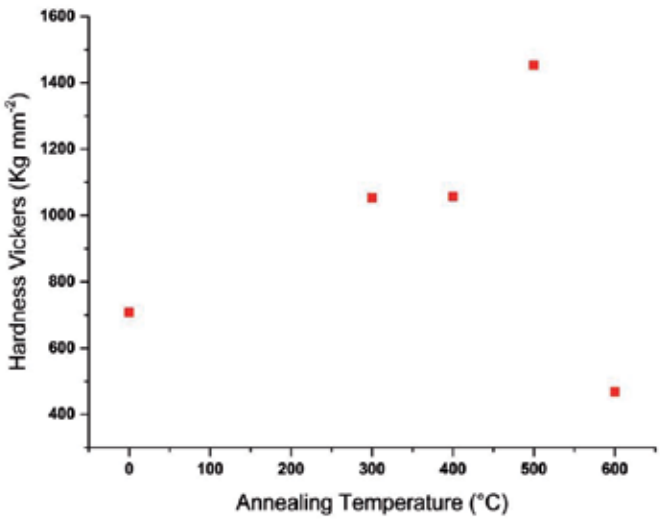

Figure 19. Hardness of the electrodeposited Ni-P-SiC coatings after a 60-min heat treatment.

3.3.3.2. Wear resistance

Figure 20 shows the wear volume of the electrodeposited Ni-P-SiC coatings as a function of the annealing temperature. Once the coating began to harden to approximately 400 °C, the decrease in the wear volume was small. When the coating was heat treated at 500 °C, the wear volume decreased sharply (i.e., the wear resistance increased). The coating that was heat treated at 600 °C contained cracks in its surface that could negatively affect its abrasion resistance.

http://dx.doi.org/10.5772/61858

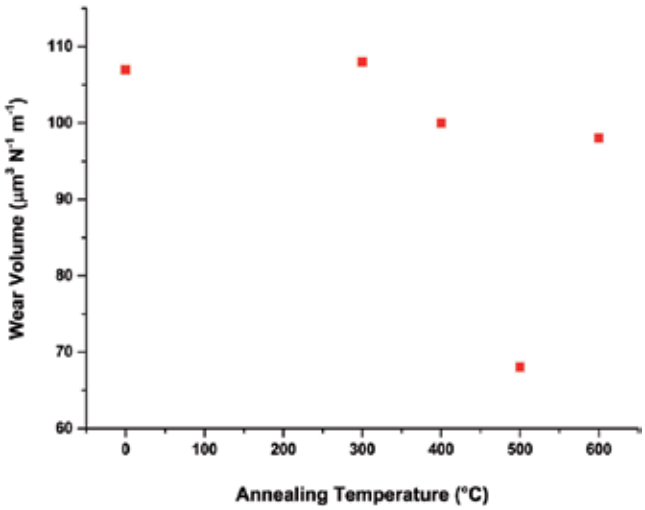

Figure 20. The wear volume of the Ni-P-SiC coatings after a 60-min heat treatment at different temperatures.

3.3.3.3. Friction coefficients

Figure 21 shows the characteristic profile of the coefficient of friction of the Ni-P-SiC coatings without and with heat treatment at different temperatures. When the Ni-P-SiC coatings were treated at temperatures above 200 °C, the coefficient of friction rapidly reached equilibrium. After 1000 cycles, coatings treated at 500 °C had the lowest friction coefficient.

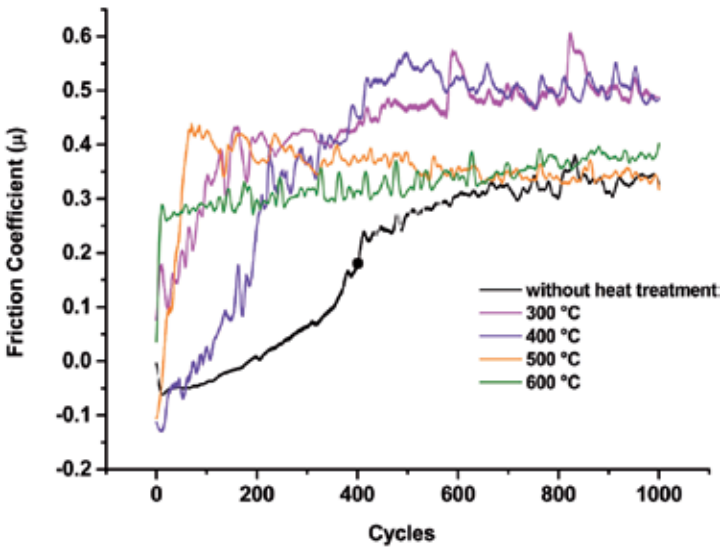

Figure 21. Frictional coefficient for the Ni-P-SiC coatings after a 60-min heat treatment at different temperatures.

4. Conclusions

This work presents the results obtained from a study of the effects of both: SiC dispersion in the metallic matrix and thermal treatment on the tribological characteristics (hardness, wear resistance, and coefficient of friction) of electrodeposited Ni-P-SiC coatings.

Our results show that the dispersion of SiC particles in the metallic matrix improves coating tribological properties such as hardness and wear resistance while diminishing the friction coefficient.

The best results were obtained when a current density of 0.042 A/cm^2 was used in an electrolytic bath containing 0.02 g mL^{-1} of SiC. Such conditions produce a metallic matrix with a concentration of 0.52 at.% SiC particles that in turn increase the Ni-P hardness from 430 HV (for the case when SiC particles are absent) to 600 HV. Despite the observed enhancement in hardness, such values are still below those exhibited by hard Cr coatings (1020 HV).

The XRD results indicated that the Ni-P-SiC composites were amorphous in nature. Thermal treatment between 400 °C and 500 °C changed the microstructure of the Ni-P-SiC matrix from amorphous to crystalline. Thermally treating the Ni-P-SiC coatings at temperatures ≥500 °C transformed the amorphous alloy into a continuous Ni_3P layer containing isolated Ni crystals.

An increased hardness and a decreased wear coefficient were observed after heat treatment for 60 min at 500 °C because of the formation of a Ni_3P phase.

We also observed that the wear volume was inversely proportional to the microhardness of the deposits. As a result, the Ni-P-SiC coatings that were thermally treated at 500 °C possessed the greatest wear resistance; this resistance was superior even to that of hard Cr coatings.

Author details

Alma Martínez-Hernández[1], Federico Manríquez-Guerrero[1], Julieta Torres[1], Raúl Ortega[1], José de Jesús Pérez-Bueno[1], Yunny Meas[1], Gabriel Trejo[1*] and Alia Méndez-Albores[2]

*Address all correspondence to: gtrejo@cideteq.mx

1 Laboratory of Composite Materials and Functional Coatings, Center of Research and Technological Development in Electrochemistry (CIDETEQ), Querétaro, México

2 Center of Chemistry-ICUAP Benemérita Universidad Autónoma de Puebla, Puebla, México

References

[1] Navisek B, Panjan P, Milosev I. PVD coatings as an environmentally clean alternative to electroplating and electroless processes. Surf. Coat. Technol. 1999;116–119:476–487. DOI: 10.1016/S0257-8972(99)000145-0

[2] Heydrzadeh Sohi M, Kashi AA. Comparative tribological study of hard and crack-free electrodeposited chromium coatings. J. Mater. Process. Technol. 2003;138:219–222. DOI: 10.1016/S0924-0136(03)00075-X

[3] Eskin S, Berkh O, Rogalsky G, Zahavi J. Co-W alloys for replacement of conventional hard chromium.. Plat. Surf. Finish. 1998;85:79–83.

[4] Donten M, Casiulis H, Stojek Z. Electrodeposition and properties of Ni-W, Fe-W and Fe-Ni-W amorphous alloys. A comparative study.. Electrochim. Acta. 2000;45:3389–3396. DOI: 10.1016/S0013-4686(00)00437-0

[5] Capel H, Shipway PH, Harris SJ. Sliding wear behaviour of electrodeposited cobalt-tungsten and cobalt-tungsten-iron alloys.. Wear. 2003;255:917–923. DOI: 10.1016/S0043-1648(03)00241-2

[6] Kieback B, Neubrand A, Riedel H. Processing techniques for functionally graded materials. Mater. Sci. Eng. A. 2003;362:81–106. DOI: 10.1016/S0921-5093(03)00578-1

[7] Wang L, Gao Y, Xu T, Xue Q. Graded composition and structure in nanocrystalline Ni–Co alloys for decreasing internal stress and improving tribological properties.. J. Phys. D. Appl. Phys. 2005;38:1318–1324. DOI: 10.1088/0022-3727/38/8/033

[8] Wang L, Gao Y, Xu T, Xue Q. Corrosion resistance and lubricated sliding wear behaviour of novel Ni–P graded alloys as an alternative to hard Cr deposits. Appl. Surf. Sci. 2006;252:7361–7372. DOI: 10.1016/j.apsusc.2005.08.040

[9] D. Nava D, Dávalos CE, Martínez-Hernández A, Manríquez F, Meas Y, Ortega-Borges R., Pérez-Bueno JJ, Trejo G. Effects of heat treatment on the tribological and corrosion properties of electrodeposited Ni-P alloys. Int. J. Electrochem. Sci. 2013;8:2670–2681.

[10] Balaraju JN, Seshadri SK. Synthesis and corrosion behavior of electroless Ni-P-Si_3N_4 composite coatings. J. Materials. Sci. Lett. 1998;17:1297–1299.

[11] Lee Hong-Kee, Lee Ho-Young, Jeon Jun-Mi. Electrolytic deposition behaviors of Ni-SiC composite coatings containing submicron-sized SiC particles. Met. Mater. Int. 2008;14:599–605. DOI: 10.3365/met.mat.2008.10.599

[12] Chou Min-Chieh, Ger Ming-Der, Ke Shih-Tsung, Huang Ya-Ru, Wu Shinn-Tyan. The Ni–P–SiC composite produced by electro-codeposition. Mater. Chem. Phys. 2005;92:146–151. DOI: 10.1016/j.matchemphys.2005.01.021

[13] Guo Ch, Zuo Y, Zao X, Zhao J, Xiong J. The effects of electrodeposition current density on properties of Ni-CNTs composites coatings. Surf. Coat. Technol. 2008;202:3246–3250. DOI: 101016/j.surfcoat.2007.11.032

[14] Pompei E, Magagnin L, Lecis N, Cavallotti PL, Electrodeposition of Nickel-BN composite coatings. Electrochim. Acta. 2009; 54:2571–2574. DOI:10.1016/j.electacta. 2008.06.034

[15] Malfatti CF, Ferreira JZ, Oliveira CT, Rieder ES, Bonino JP. Electrochemical behavior of Ni-P-SiC composite coatings: effect of heat treatment and SiC particle incorporation.. Mater. Corros. 2012;63:36–43. DOI: 10.1002/maco.200905611

[16] Zhang S, Han K, Cheng L. The effect of SiC particles added in electroless Ni–P plating solution on the properties of composite coatings.. Surf. Coat. Technol. 2008;202:2807–2812. DOI: 10.1016/j.surfcoat.2007.10.015

[17] Farzaneh A, Mohammadi M, Ehteshamzadeh M, Mohammadi F. Electrochemical and structural properties of electroless Ni-P-SiC nanocomposite coatings.. Appl. Surf. Sci. 2013;276:679–704. DOI: 10.1016/j.apsusc.2013.03.156.

[18] Hansal WEG, Sandaluche G, Mann R, Leisner P. Pulse-electrodeposited NiP–SiC composite coatings. Electrochim. Acta. 2013;114:851–858. DOI: 10.1016/j.electacta. 2013.08.182

[19] Chen H, Ravishankar S, Farinato R. Rational polymer design for solid–liquid separations in mineral processing applications. Rational polymer design for solid–liquid separations in mineral processing applications. Int. J. Miner. Process. 2003;72:75–86. DOI: 10.1016/S0301-7516(03)00088-7

[20] Nguyen AV, Schulze HJ. Colloidal Science of Flotation. 1st ed. NewYork: Marcel Dekker; 2004. 843 p.

[21] Reyes Y, Suarez R, Ruiz C, Torres J, Mendez A, Trejo G. Electrodeposition, characterization and antibacterial activity of zinc/silver particle composite coatings. Appl. Surf. Sci. 2015; 342: 34–41. DOI: i.org/10.1016/j.apsusc.2015.03.037

[22] Celia C, Trapasso E, Cosco D, Paolino D, Fresta M. Turbiscan Lab® expert analysis of the stability of ethosomes® and ultradeformable liposomes containing a bilayer fluidizing agent. Colloids Surf. B. 2009;72:155–160. DOI: 10.1016/j.colsurfb.2009.03.007

[23] Bordes C, Snabre P, Frances C, Biscans B. Optical investigation of shear- and time-dependent microstructural changes to stabilized and depletion-flocculated concentrated latex sphere suspensions. Power Technol. 2003;130:331–337. DOI: 10.1016/S0032-5910(02)00212-7

[24] Apachitei I Tichelaar FD, Duszczyk J, Katgerman L. The effect of heat treatment on the structure and abrasive wear resistance of autocatalytic NiP and NiP–SiC coatings. Surf. Coat. Technol.. 2002;149:263–278. DOI: 10.1016/S0257-8972(01)014

[25] Zeller RL, Salvati L. Effects of phosphorus on corrosion resistance of electroless nickel in 50% sodium hydroxide. Corrosion. 1994;50:457–467.

[26] Garcia-Alonso MC, Escudero ML, Lopez V, Macias A. The corrosion behaviour of laser treated Ni/P alloy coatings on mild steel. Corros. Sci. 1996;38:515–530. DOI: 10.1016/0010-938X(96)00151-5

[27] Huang YS, Cui FZ. Effect of complexing agent on the morphology and microstructure of electroless deposited Ni–P alloy. Surf. Coat. Technol. 2007;201:5416–5418. DOI: 10.1016/j.surfcoat.2006.07.189

[28] Alirezaei S, Monirvaghefi SM, Salehi M, Saatchi A. Wear behavior of Ni–P and Ni–P–Al_2O_3 electroless coatings. Wear. 2007;262:978–985. DOI: 10.1016/j.wear.2006.10.013

[29] Malfatti CF, Zoppas Ferreira J, Santos CB, Souza BV, Fallavena EP, Vaillant S, Bonino JP. NiP/SiC composite coatings: the effects of particles on the electrochemical behavior. Corros. Sci. 2005;47:567–580. DOI: 10.1016/j.corsci.2004.07.011

[30] Bonino JP, Bruet-Hotellaz S, Bories C, Pouderoux P, Rousset A. Thermal stability of electrodeposited Ni–P alloys. J. Appl. Electrochem. 1997;27:1193–1197. DOI: 10.1023/A:1018423701791

[31] Tachev D, Georgieva J, Armyanov J, C. Magnetothermal study of nanocrystalline particle formation in amorphous electroless Ni-P and No-Me-P alloys. Electrochim. Acta. 2001;47:359–369. DOI: 10.1016/S0013-4686(01)00587-4

[32] Hu Chi-Chang, Bai A. Influences of the phosphorus content on physicochemical properties of nickel–phosphorus deposits. Mater. Chem. Phys. 2002;77:215–225. DOI: 10.1016/S0254-0584(01)00592-2

[33] Bai A, Hu Chi-Chang. Effects of annealing temperatures on the physicochemical properties of nickel–phosphorus deposits. Mater. Chem. Phys. 2003;79:49–57. DOI: 10.1016/S0254-0584(02)00455-8

[34] Keong KG, Sha W, Malinov S. Hardness evolution of electroless nickel–phosphorus deposits with thermal processing. Surf. Coat. Technol.. 2003;168:263–274. DOI: 10.1016/S0257-8972(03)00209-3

[35] Bozzini B, Martini C, Cavallotti PL, Lanzoni E. Relationships among crystallographic structure, mechanical properties and tribological behaviour of electroless Ni–P(9%)/B4C films. Wear. 1999;225–229:806–813. DOI: 10.1016/S0043-1648(98)00389-5

[36] Magdy AM. Black nickel electrodeposition from a modified Watts bath.. J. Appl. Electrochem. 2006;36:295–301. DOI: 10.1007/s10800-005-9077-8

[37] Lewis DB, Marshall GW. Investigation into the structure of electrodeposited nickel-phosphorus alloy deposits. Surf. Coat. Technol. 1996;78:150–156. DOI: 10.1016/0257-8972(94)02402-2

[38] Rabizadeh T, Reza Allahkaram S, Zarebidaki A. An investigation on effects of heat treatment on corrosion properties of Ni–P electroless nano-coatings. Mater. Des. 2010;31:3174–3179. DOI: 10.1016/j.matdes.2010.02.027

[39] Lu K, Sui ML, Lück R. Supersaturation of phosphorus in nanophase nickel crystallized from an amorphous Ni-P alloy. Nanostr. Mater. 1994;4:465–473. DOI: 10.1016/0965-9773(94)90118-X

[40] Serebryakov A, Stelmukh V, Voropaeva L, Novokhatskaya N, Levin Yu. Nanocrystallization of Co/Si/B/Zr amorphous alloy. Nanostr. Mater. 1994;4:645–650. DOI: 10.1016/0965-9773(94)90016-7

[41] Lu K. The thermal instability of nanocrystalline Ni/P materials with different grain sizes. Nanostr. Mater. 1993;2:643–652. DOI: 10.1016/0965-9773(93)90039-E.

Chapter 8

A review of Corrosion Resistance Nanocomposite Coatings

Thais G.L. Rezende, Deborah V. Cesar, Dalva C.B. do Lago and Lilian F. Senna

Additional information is available at the end of the chapter

http://dx.doi.org/10.5772/62048

Abstract

The deterioration of materials, particularly metals, under the influence of electrochemical corrosion is a high cost problem faced by nearly all industries. The reduction of corrosion processes and the prevention of future problems require a detailed knowledge of these processes and of the strategies to avoid them. In this context, it is essential to use methodologies that may prevent the electrochemical deterioration of materials as well as monitor their performance in aggressive environments. Among them, it is possible to cite the use of functional coatings, particularly nanocomposite coatings. Therefore, this chapter proposes a review concerning the production of nanocomposite coatings with anticorrosive application obtained by electrodeposition technique (electrochemical codeposition). The production of such coatings is in agreement with the current needs of innovation, which drives a requirement for scientific advancement and the need for fundamental research. In this context, nanocomposite coatings with anticorrosive properties promote changes in metal surfaces, creating new materials with improved characteristics compared to those originally observed and maintaining the integrity of these surfaces.

Keywords: Corrosion resistance, mechanical characteristics, nanocomposite coatings, electrochemical codeposition, metallic matrix composite

1. Introduction

It is known that corrosive processes handle many failures and accidents, involving among other drawbacks, environmental damage, and stops in the production with high economic losses. The monitoring and prevention of corrosion processes of materials in industrial plants is a worldwide need, improving the development of new (or advanced) materials, modified surfaces, and engineering processes. The conception of advanced materials is directly linked

to investigations involving the production, degradation, and, consequently, ways to protect materials. In addition, environmental requirements considering technologies and processes must also be considered.

Functional coatings are so called because they present an additional functionality (such as corrosion protection, improved mechanical resistance or abrasion resistance, and thermal or electrical conductivity/isolation) besides their usual decorative or protection properties. These coatings are generally used to modify the surface of a substrate producing materials with enhanced or even new properties compared to those presented by the substrate itself [1–3]. Thus, depending on the application, several different ceramic, metallic, polymeric, or composite functional coating/substrate systems with own characteristics can be produced by different techniques [1,2].

The coatings constituted by a metallic matrix containing a second phase of a polymeric, metallic, or ceramic material are called metallic matrix composite coatings (MMC coatings) [4]. The second-phase materials are most commonly added to the metallic matrix as particles or nanowires, whose nature depends on the properties required for the development and application of the MMC coatings, based on the association properties of the particle and the matrix [5]. The materials most used as a second phase in MMC coatings are Al_2O_3, TiO_2, SiO_2, Cr_2O_3, ZrO_2, WC, SiC, polystyrene, talc, and MoS_2, in sizes ranging from micrometers to nanometers [6–8]. The use of these coatings for corrosion application will be the subject more deeply discussed in this chapter.

MMC coatings containing ceramic nanoparticles are very useful for advanced surface finishing applications, presenting wide application in engineering processes. The dispersion of hard nanoparticles, such as silicon carbide, silica, and alumina, or of nonmetallic nanowires on a metal matrix can yield materials with improved properties, such as hardness, wear and corrosion resistances, self-lubrication, and higher temperature stability, compared to single metal or even alloy metallic coatings [9]. High-pressure valves, drilling and car accessories, engineering and aerospace precision devices, medical, marine, and agriculture devices, mining and nuclear apparatus, microelectronics, corrosion protection for lubrication in sliding electrical contacts, and aircraft systems are some examples of fields in which these coatings are used [10,11].

The literature describes various techniques to produce functional MMC coatings, such as physical vapor deposition (PVD), chemical vapor deposition (CVD), chemical reduction (CR) or electroless process, dip coating, thermal spraying (TS), brush plating (painting) (BP), electrophoretic deposition, and electroplating (electrochemical codeposition). All of these processes aim to achieve coatings with improved uniformity, good reproducibility, high adhesion, high deposition rate, low roughness, and low cost [12–15]. It is important to mention that these features, as well as the coating morphology and microstructure, the incorporated particle size (particle clusters), and the amount of particle in the coating, depend on both the substrate and the deposition process used to produce the MMC coatings, influencing the properties of the coating/substrate system [16–22]. Table 1 presents some examples of MMC coatings produced with different deposition processes and the main results achieved by the researchers. As the present revision concerns about the corrosion resistance of nanocomposite coatings, only the coatings produced on metallic substrates will be considered.

http://dx.doi.org/10.5772/62048

Deposition process	Substrate	Metallic matrix	Second phase	Main features	Ref.
CVD	AISI 316L steel	Ni powders	B_4C, with 35 and 140 μm	- Particle agglomeration; - The formed single layer of nickel had lamellar structure; - The coatings produced from the smaller particles show higher hardness and higher B_4C content than the coatings produced with the coarse particle size	[16]
CR	Steel	Cu	SiC and graphite (C_g), ranging from 4 to 10 μm	- Coating thickness of approximately 5 μm were obtained; - Different phases, depending on which particle was used; - The Cu-P-SiC coatings had higher hardness (280±1 HV) than the Cu-P coating (190±1 HV); - The coefficient of friction and surface energy of Cu-P-C_g coatings (0.225±0.012) was smaller than that of Cu-P coatings (0.302±0.023); - Cu-P-SiC-C_g coatings showed the combinations of Cu-P-SiC (high hardness, 183±1 HV) and Cu-P-C_g (low friction coefficient, 0.014±0272) coating properties	[18]
TS	AZ91D Mg alloy	Al	α-Al_2O_3, ranging from 1 to 30 μm	- Coatings containing either 25 or 50 wt% α-Al_2O_3 particles had lower porosity and better adhesion compared to pure aluminum coating; - The corrosion current densities (j_{corr}) of these composite coatings (j_{corr} = 1.6×10^{-7} and 3.0×10^{-7} A m^{-2} for 25 and 50 wt% α-Al_2O_3) were not different from the value obtained for the pure aluminum coating (j_{corr} = 4.6×10^{-7} A m^{-2})	[20]
BP	Steel	Ni	Nano-Al_2O_3	- Coating thickness of 50 μm was obtained; - Coatings with smooth, dense, and uniform morphology were obtained	[21]

Deposition process	Substrate	Metallic matrix	Second phase	Main features	Ref.
				with the automatic process compared to the manual one; - Coatings with high hardness were obtained for both automatic and manual processes, independent of the indentation direction, as soon as the deposition parameters can be well adjusted	

Table 1. Examples of MMC coatings produced by different deposition processes.

Although all of the aforementioned processes may be used to produce functional MMC coatings, the most widely used production method is electrochemical codeposition, also known as electrocodeposition, which consists of incorporating nanoparticles or nanowires (generally nonmetallic ones) intentionally added to the electrolyte to the metallic matrix during the electrodeposition process. This technique has been under investigation for several decades, and some authors have proposed models to explain the codeposition phenomenon of the particles during the formation of a cathodic deposit by electrodeposition [6,8,11,23–25]. This topic is still up to date because the process is more complex than the traditional electrodeposition and no commercial electrochemical baths have been developed so far for industrial production of these types of composite coatings. The main parameters that affect the process (e.g., solution pH, stirring speed, and current density) were related; however, there is no consensus in the literature concerning their effects in the nanoparticle content in the coating and in the anticorrosive performance of the coating/substrate system [5,6,8,11,12,17,23,26–28]. It is also necessary that the nanoparticles be maintained suspended and dispersed (nonagglomerated) in the electrolyte during the deposition process; otherwise, the precipitation of the nanoparticles occurs and causes the loss of control of the electrochemical codeposition process. Therefore, it is important to present a more fundamental review of the parameters that involve the electrodeposition process of these coatings to obtain a better understanding of the electrochemistry codeposition phenomenon and its consequence on the anticorrosive properties of the composite coatings. Consequently, it will lead to an improvement of the processes for the development of new functional nanocomposite coatings and increase their reliability to prevent corrosion.

2. Electrochemical codeposition of MMC coatings

Electroplating or electrodeposition is an electrochemical process that occurs at the interface between a conductive material (electrode) and a conductive solution (electrolyte). As a whole, the process can be explained as the result of applying an electrical potential to the electrochemical system by an external source, and the consequent flow of electric current through the

http://dx.doi.org/10.5772/62048

electrode-electrolyte interface can be measured (chronoamperometry) [29–31]. On the contrary, an electric current can also be applied, and the generated potential difference is then the measured variable (chronopotentiometry) [32]. In the electrolytic cell of an electrodeposition process, the cathode is generally the working electrode, which will be coated during the procedure, whereas the anode is the counter-electrode. The third electrode is the reference electrode used to monitor the working electrode potential [30,33–35].

The main advantage of this technique is the production of coatings with thickness varying from a few layers up to 40 μm, relatively free of pores. Compared to the plasma processes (PVD or CVD), it is a less expensive technique and can be conducted at room temperature, normal pressure, and high deposition rate [34,36,37]. In addition, it is economically important because even thin-layer coatings produced by electrodeposition can offer adequate protection to the substrate, avoiding excess of electrodeposited metal [29,34]. The most common coatings produced by this process are the metallic ones: nickel, chromium, copper, zinc, tin, brass, silver, and cadmium [31].

The electrodeposition technique also allows the production of coatings composed by a second phase dispersed in a metallic matrix, producing MMC coatings. This second phase can be an organic or inorganic compound or even a metal particle suspended in the solution [8,34]. This is the main difference between the usual electrodeposition of metallic ions and the electrodeposition of MMC coatings (electrochemical codeposition): instead of using a pure ionic soluble solution as the electrolyte, particles of nonconductive, semiconductive, and/or conductive nature are suspended in electrolyte solution [11,26,38–40]. Thus, during the codeposition process, both the metal matrix and the particles are deposited on the substrate, producing the MMC coatings [26,38,39].

The greatest challenge faced by those who study the codeposition of nanoparticles in MMC coatings by electrochemical codeposition seems to be the development of a methodology to deposit a sufficient amount of particles to promote the desired improvements in the properties (anticorrosive characteristics, mechanical resistance, etc.) of coatings compared to those obtained with the pure metallic coating. Additionally, it is also necessary to prevent the agglomeration of the particles in the electrolyte solution [23].

A better understanding of the electrocodeposition process is obtained by the knowledge of the process and mechanisms that involve the metal/particle codeposition. Several parameters influence the deposition process, such as applied current density (or potential), concentration of particles in the bath, size of the particles, stirring speed of the suspension, time of previous stirring, solution pH, bath temperature, and electrical nature of the particles. The stability of the suspension of particles to be added to metallic matrix also affects the codeposition process. Although these parameters will be presented in this revision separately, it is important to point out that several of them usually present mutual interactions and these effects can also influence the final results (the amount of codeposited particles, for example) as well as the final properties of the coating.

2.1. Parameters affecting the codeposition of particles in metallic matrix

2.1.1. Particle concentration in solution

The particle concentration in the electrolyte may affect the deposition process, changing the ratio metal/particle in the coating and its grain size and causing variations on the coating properties. The incorporation rate per volume of the particles in the deposit is an increasing function of the concentration of particles in the electrolyte suspension [23,41] and is a parameter often used to control the amount of particles in the coating [27,28]. However, as shown in several studies, it is evident that the amount of particles in the deposit does not grow infinitely but reaches a limit value [5,27,42], which depends on the deposition conditions. The concentration of particles in the electrolyte can also result in problems relating to the homogeneity of their suspension, agglomeration, and precipitation [27,28].

Composite coatings of Zn-SiO_2 were produced in the presence of N,N-dimethyldodecylamine and there was a direct trend in the increase of the amount of incorporated particles up to 100 g L^{-1} of silica particles in the solution [6]. Beyond this concentration, however, the increasing incorporation response is oscillating. This behavior was related to the fact that any concentration beyond 100 g L^{-1} of particles might be sufficiently high to induce localized agglomeration, which could lead to uneven distribution of particles in the coatings.

The TiO_2 particle concentration (5.0, 10.0, and 15.0 g L^{-1}) in the electrolytic bath also influenced the content of these particles in a zinc matrix composite coating [43]. Although the increase of particle concentration in the bath elevated the content of particles in the coatings, concentrations higher than 10.0 g L^{-1} caused a decrease in the codeposited particle content in the metallic matrix. This effect was explained by the agglomeration of particles in the coating due to their poor wettability [43].

The dependence of TiO_2 nanoparticles (1.0, 1.6, 10.0, and 16.0 g L^{-1}) added to different concentrations of Zn(II) electrolyte (0.5, 0.3, and 0.1 mol L^{-1}) on the grain size of the Zn matrix was also investigated [44]. It was observed that the grain size of the metal matrix decreases with the increase of the nanoparticles added to the bath, which was related to changes in the nucleation and growth processes of zinc crystals due to the presence of these particles. Similar results were obtained for nickel deposition in the presence of SiC nanoparticles [44] and for copper codeposition with SiO_2 nanoparticles [45]. These results are in agreement with the literature, which relates this grain refining effect to the nanoparticle abilities of providing more nucleation sites and, consequently, decreasing the velocity of the crystal growth process [45].

2.1.2. Particle size in the suspension

Several works report the influence of the particle size in suspension on the homogeneity of the coating, its microstructure and morphology, and on the particle incorporation in the metal matrix [37,46,47]. The number of particles incorporated per area is associated with the selectivity related to the particle size in suspension, as observed for the NiP–SiC coatings, where the amount of SiC particles in the coating increased due to the decreased size of the SiC particles in the electrolyte [27,28]. However, it is not a consensus in the literature, as there are

http://dx.doi.org/10.5772/62048

reports showing a reduction in the amount of codeposited particles as their size decreases [5, 6]. In aqueous ionic solution, the particles are easily bonded to each other due to the compression of the diffusion double layer around them, originated by the high ionic strength. Although the stirring of the electrolytic bath may decrease the particle aggregation and favors their codeposition, this effect is more pronounced for particles of micrometric size, as the shear forces on the agglomerates generated by the stirring process decrease with the particle size [5].

The influence of SiC particle size (1 μm and 45–55 nm) in the microstructure and morphology of the nickel MMC coatings was evaluated [46]. The results showed that, whereas the pure nickel coating presented a pyramidal morphology, the addition of SiC nano- or microparticles produced a coating with a rough nodular surface. This new morphology was related to the presence of nickel grains surrounding the SiC particles, forming globular aggregates. It has been argued that the introduction of the ceramic particles disturbed the formation of the metallic matrix and decreased the grain size of the coating [46]. However, no differences were observed concerning the size of the particles.

The effect of microparticle concentration of SiC (5 and 0.3 μm) in the volumetric percentage of metal deposited on the nickel matrix was evaluated [26], and it was observed that there was an increase in the volumetric percentage of deposited SiC particles as their concentration in the bath increased, independent of the particle size. However, the greatest volumetric percentage of codeposited SiC particles was obtained using 5 μm particles, whereas the lowest percentage was deposited using 0.3 μm particles. It was pointed out that a direct comparison of the volumetric percentage of codeposited particles with different sizes may lead to a misunderstanding because of the differences in the particle density on the composite coating [26].

The effect of SiC particle size (1.2, 8.0, 14.0, and 20.0 μm) on nickel composite coatings was investigated by Kim and Yoo [48], and it was verified that an increase in the size of the particle (until 14 μm) added to the electrolytic bath induced an increase in the content of the particles in coatings. This fact was explained by the adsorption of Ni^{2+} ions on the particles, resulting in a strong Coulomb force and an increase of the SiC particles codeposited. Above 14 μm, however, the particles presented a sedimentation tendency due to their weight, which decreased the suspension stability and the content of SiC particles codeposited in the metallic matrix [48].

2.1.3. Current density

Besides the particle concentration of the suspension, the applied current density is certainly the parameter most studied by several authors [37,38,47,49] and there are evidences concerning its effect on the particle incorporation. The literature [5] reports that the particle incorporation in the coating is a function of the current density and that this effect can be divided in four current density regions. Initially, there is a region where the particle incorporation increases rapidly reaching a maximum followed by the second region where a marked decrease in the process occurs. Then, a third region takes place, where the process is fairly constant, followed by another fall in the particle content in the current density region where the metal reduction is limited by mass transfer. It seems that an optimum range of current density is necessary to

favor the codeposition of the particles. This range, however, depends on the studied particle and on other deposition parameters, such as bath composition or stirring.

For example, the greatest amount of α-Al_2O_3 nanoparticles was incorporated to a copper matrix at low current density values (between 1 and 2 A dm^{-2}), whereas, outside this range, the content of particles in the coating significantly decreased [11]. This dependence between the content of nanoparticles in the coating and the current density is explained by the mechanism by which the particles are captured. The increase in the particle content in the coatings occurs in the region where the reduction of the metallic ions is under charge transfer control and where the reduction of adsorbed cations on alumina is the determining step of the deposition rate. As the reduction of metal ions occurs under diffusion control at current densities higher than 2 A dm^{-2} (the hydrodynamic conditions are not mentioned), the codeposition of alumina particles gradually decreases with increasing current density [11].

It was also observed that increasing current density caused a decrease in the initial rate of incorporation of SiO_2 particles in the zinc matrix; however, at current densities approximately 30 A dm^{-2}, an increase in SiO_2 deposition rate was noted, mainly for the particles with the highest size (2 μm) [6]. Moreover, the regions in which the particle incorporation increased or decreased markedly with current density were sensitive to particle size. The authors suggested that the deposition process was controlled by mass transfer until the maximum value of current density, where the codeposition process was favored. Otherwise, the process was controlled by the particle adsorption on the substrate, and a further increase in current density resulted in the rapid deposition of the metallic matrix and less particles were included in the coating [6]. Similar results were obtained for composite coatings of Ni-Co alloy matrix containing SiC particles with 50 nm of diameter [37].

The literature reports that this relationship between the current density and the amount of incorporated particles also influences the microstructure of the produced MMC coatings [47,49]. For example, the Ni/Al_2O_3 coatings produced at current density values of 10 A dm^{-2} from an acid sulfamate-based bath (pH 4.3) presented a more refined microstructure than the coatings produced at lower current density values [50]. It is an important feature, as the microstructure of the coatings can be consequently related to their corrosion resistance.

In addition, the mode of applied current [continuous (DC) or pulsed current (PC)] may also influence the microstructure and corrosion properties of the MMC coatings. Composite coatings of copper matrix and β-SiC particles were produced under DC and PC conditions [51]. The coatings containing β-SiC particles deposited under DC conditions showed grains more refined than those observed from the copper coating. However, this coating presented voids between the incorporated particles and the metal matrix, which influenced the anticorrosive properties of the composite coating, as evidenced by the corrosion tests performed in 0.5 mol L^{-1} Na_2SO_4 solution (pH 2). These coatings showed less resistance to both uniform and localized corrosion compared to the pure metal coating. On the contrary, the coatings produced using PC presented a more compact microstructure and, as a consequence, showed elevated resistance to uniform corrosion, similar to pure copper coating and greater than the coatings produced under DC [51].

Another example is the study that evaluated the influence of DC, PC, and pulsed reverse current (PRC) on the content of particles incorporated to a nickel metallic matrix [36]. The particles used were Al_2O_3 (150 nm), SiC (30–60 nm), and ZrO_2 (200 nm), and for all systems studied, the particle content in the composite coatings increased when the coatings were produced by PC and PRC; the amount of particles obtained using DC was always lower. The periodic switching of current (between positive values and zero for PC and between positive and negative values for PRC) permitted the discharging of the double layer, allowing a higher access of the particles (with adsorbed ions on their surfaces) toward the cathode. The ions adsorbed on the particles were subsequently reduced on the cathode surface causing a capture of the reinforcement material during coating growth.

2.1.4. Stirring speed

The electrolyte stirring speed plays an important role in any electrodeposition process, as it favors the transport of metallic ions to the electrode, increasing the deposition rate [52]. In the electrochemical codeposition process of MMC coatings, however, the influence of this parameter is even greater because it affects the homogeneous dispersion of the particle in the suspension and controls the frequency of collision between the particles and the cathode. Furthermore, the stirring speed of the electrolyte influences the mechanism of particle deposition onto the cathode surface as well as the time they will remain adsorbed [27,41].

In general, if the stirring speed of the bath is too slow, it prevents the complete dispersion of the particles, and their sedimentation during the deposition process cannot be avoided. On the contrary, if the stirring speed is too high, the particles do not have enough time to be adsorbed to the substrate surface, resulting in a low amount of particle incorporation [5]. Moreover, under excessive high stirring speed values, the amount of particles transported to the cathode is too large to be trapped by the matrix growth, which causes the collision of the free particles (those particles that have not been adsorbed or incorporated yet) with other particles that are reaching to the cathode. These collisions result in a decrease in the incorporation rate [5].

Therefore, this parameter should be optimized to avoid both particle sedimentation and the removal of the particles, which are already in the adsorption phase on the cathode. Nonetheless, the stirring speed range that must be used to achieve the MMC coatings is not a consensus in the literature and it seems to depend on the kind of particle, the metallic ions and bath composition used, as well as the cell configuration and volume [30,47,53,54].

The incorporation of particle α-Al_2O_3 in a Co-Ni matrix from a Ni(II)/Co(II) sulfamate acid bath containing the suspended particle was studied, under magnetic stirring varying between 40 and 160 rpm [12]. The volume fraction of Al_2O_3 particles in the composite coating (V_p) increased with stirring speed and reached a maximum value (approximately 8 vol%) at 100 rpm, decreasing with further increased stirring. The authors suggested that the codeposition of Al_2O_3 particles in the Co-Ni alloy was apparently controlled by the particle transfer up to 100 rpm. A further increase the stirring speed could have displaced the particles spontaneously adsorbed onto the surface of the cathode, causing a reduction in the V_p values of the codeposited particles.

Another study [47] showed that there is a maximum value of particles of CeO_2 (between 15 and 20 nm) incorporated to nickel matrix when the stirring speed was varied (100, 250, 350, 450, and 550 rpm). The highest quantity of particles in the matrix was obtained at 450 rpm; above this value of stirring speed, the content of CeO_2 decreases. This phenomenon was explained by the collision of particles on the cathode under high values of stirring speed. Moreover, the increase of stirring speed also enhanced the turbulence in the flux suspension, which could have removed the weakly adsorbed particles from the cathode surface [47]. Similar results were obtained by other research groups [15,49,54] for different nickel composite coatings.

2.1.5. Solution temperature

The solution temperature affects several physical properties of the suspension (such as the viscosity and the sedimentation rate) and influences the reduction kinetics of the free and adsorbed cations as well as the possible adsorption of particles on the cathode [27]. Although there are few works in the literature studying the effects of this parameter in the electrochemical codeposition process, these works show the relationship between the solution temperature and the increase of codeposited particles in metallic matrix or the morphology of the coating. Thus, this parameter is still scarcely explored and understood.

The temperature of 50°C was considered the most beneficial one for the incorporation of alumina particles in Co-Ni matrix from an acidic Ni(II)/Co(II) sulfamate bath instead of 60°C [12]. For the codeposition of alumina particles in Cr matrix from a sulfate bath containing a rare earth element (not mentioned), the best temperature range for particle incorporation was from 30°C to 40°C. When the temperature was below 30°C, the composite coating was rough, whereas, when it was above 40°C, the composite coating decreased; beyond 55°C, there was no Al_2O_3 codeposited with Cr [55].

Research works carried out for Zn-SiC composite coatings [56] showed that the increase of solution temperature (33–45ºC) caused a significant reduction of particle content in the coating. The authors considered that the increase in the solution temperature favored the electroactive species reduction, while it did not increase the codeposition of the SiC particles. Kim and Yoo [48] verified the same behavior for Ni-SiC composite coatings.

It is important to mention that the overall result concerning the temperature variation on the codeposition process for producing MMC coatings is difficult to predict, as the parameter most affected by the solution temperature is not generally identified in the usual used deposition mechanisms [12,27].

2.1.6. Composition of the electrolyte bath

The production of MMC coatings by electrodeposition is highly influenced by the composition of the electrolytic bath, as the presence of complexants, surfactants, or dispersant agents may affect the metallic ion deposition process, the suspension stability, and the particle incorporation in the coating. Moreover, the acidity of the bath (pH) as well as the concentration of the baths components may also influence the particle dispersion and the codeposition of the

species. Therefore, bath composition is one of the most studied topics in the production of MMC coatings by this technique, and the properties of the produced coatings obtained from different baths may certainly vary.

The electrolyte composition and the solution pH directly influence the ζ potential measurements, which is the main variable related to the stability of solid particle dispersions in aqueous solution [57]. Charged surface particles form more stable suspensions because the mutual repulsion between the particles increases, decreasing their agglomeration [27,45,58]. Therefore, the increase in the particle charge (in modulus) will result in a higher (also in modulus) ζ potential and in a more stable suspension.

Surfactants agents are generally used to promote a better dispersion of suspensions because they reduce the surface energy of the particles, deeply influencing the codeposition process. The surfactants or surface-active agents are characterized by having two distinct regions on the same molecule: a hydrophilic polar region and a hydrophobic nonpolar region. These compounds have activity at the surface interfaces between two phases, such as water–air and oil–water, and the solid–liquid interface [46]. For experimental evaluation, these additives apparently act in two ways: by modifying the properties of the particle surface and stabilizing the suspension and/or by affecting the reduction of metal ions during electrodeposition [4].

Nanoparticles of Al_2O_3 suspended in a 0.001 mol L^{-1} KCl solution presented ζ potential values almost constant and positive for a pH range between 2 and 6. However, at higher pH values, the ζ potential shifted to less positive values until it reached the isoelectric point (IEP), where the particles had no charge and then precipitated (pH 9.2) [59]. On the contrary, in the presence of nickel sulfamate bath, the ζ potential of these particles was positive in the entire pH range between 2 and 12 probably due to the adsorption of nickel cations on the alumina particles; in the case of pyrophosphate electrolytes, the ζ potential remained negative, which was related to the adsorbed pyrophosphate anion. Both in the presence of sulfamate and the pyrophosphate baths, it was not possible to determine the IEP in the pH range studied. Thus, the authors concluded that alumina particles take on negative charges in alkaline baths, whereas, in acidic electrolytes, they assume positive charges.

The sign of the charges on the particle surface will also influence the deposition process, although both positive and negative charges are considered to improve the incorporation of the particles. For example, the codeposition of α-Al_2O_3 particles in a Co-Ni matrix from a Ni(II)/Co(II) acid sulfamate bath was found to be enhanced by the presence of Co(II) ions adsorbed on the particle surface, which charged them positively [12]. In opposition, the presence of negatively charged alumina particles (due to the presence of citrate or pyrophosphate anions adsorbed on them) also increased the codeposition of Al_2O_3 particles on Cu matrix [10]. In this last case, the negatively charged particles were codeposited in the metallic matrix in higher amounts than the positively charged ones. A possible explanation is that the negatively charged particles would be attracted by the double layer of the substrate that was charged with excessive positive charge [probably Cu(II) ions] under the conditions of the electrodeposition experiment [10]. Although these arguments do not imply that the electrodeposition is completely governed by electrostatic forces, the proposed mechanism helps streamline the experimental results for the present system [10,59].

However, each system can produce unique responses to the addition of surfactants or changes in the bath composition. The addition of N,N-dimethyldodecylamine in Zn(II) baths containing SiO_2 particles (20 nm) has not caused a significant increase in the incorporation rate of these particles, as similar amounts (approximately 5 wt%) were obtained in both the presence and absence of the amine. Nonetheless, for particles with size of 2 μm, there was an increase in the incorporation rate with the addition of the surfactant and the SiO_2 content on the coating was 14 wt%. Therefore, there was a joint effect of the particle size and the dispersion effect caused by the presence of the surfactant in the bath [6].

The effects of adding cetyltrimethylammonium bromide (CTAB), a cationic surfactant, at concentrations of 10^{-5} to 10^{-3} mol L^{-1} on the codeposition process of SiO_2 particles in a copper matrix was also investigated [45]. It was found that the ζ potential of the suspension in the absence of the additive was negative in the whole pH range studied (3–9). It was assumed that, at high pH values, there were hydroxyl groups (negative ions) on the surface of silica particles.

The introduction of small concentrations of CTAB in the $CuSO_4$ solution induced changes in the ζ potential of the nanoparticles, which assumed positive values for all CTAB concentration ranges. A reasonable explanation for this behavior would be the easy adsorption of the cationic surfactant on the surface of silica nanoparticles because of the positive charge in the polar part of CTAB molecules. These molecules reacted with the hydroxyl groups on the silica surface, decreasing the surface energy of the nanoparticles, improving the state of dispersion of SiO_2 particles [45]. In addition, the steric effect between the SiO_2 nanoparticles became higher as the CTAB chain was grafted on their surfaces.

However, it is very difficult to correlate the results obtained in the ζ potential measurement, which is generally carried out at low electrolyte ion concentrations (low ionic strength), with the behavior of a particle in an electrolyte used for electrodeposition (i.e., high ionic strength). Therefore, it is not easy to verify the dispersion influence of the surfactants in the electrochemical codeposition process [10,48]. Moreover, the addition of surfactants should be carefully used, because an excessive increase in their concentration may create a large repulsion force between the surfactant layer next to the cathode and the surface of the particle. At high concentrations, the surfactants form micelles in solution and the uniform dispersion of previously formed nanoparticles is interrupted, promoting their agglomeration and reducing their incorporation in coatings [7].

The concentration of the metallic ion in the electrolyte also affects the properties of the MMC coatings produced by electrodeposition. The grain size of Zn metallic matrix was substantially independent of the concentration of TiO_2 particles for concentrated ionic solutions. However, for more dilute solutions (0.1 mol L^{-1}), it was observed that the grain size decreased with the increase of the nanoparticle amount. This was explained mainly by changes in the growth and nucleation of zinc crystals due to the concentration of the metallic ions and the presence of semiconductor particles. For dilute solutions, the evolution of hydrogen and the presence of particles should promote a detrimental effect on the crystal growth, leading to smaller grains in the zinc matrix [44].

http://dx.doi.org/10.5772/62048

2.1.7. Electrical nature of the particles

The electrical nature of the particles used to produce the MMC coatings has drawn the attention of very few researchers. However, it is important to have information about how the codeposition of inert, semiconductor, or conductive particles influence the overall process [11]. Apparently, conductive particles are readily incorporated into the metallic coatings, although dendritic, uneven, and very rough deposits are obtained. On the contrary, the codeposition of insulating particles is very slow, producing relatively homogeneous and smooth deposits [17]. This fact can be used for the production of composite coatings with different applications: the smooth ones could be applied for mechanical and/or anticorrosion uses, whereas those with very high specific surface area and using conductive particles with some catalytic properties entrapped in the coatings could act as catalysts in some chemical or electrochemical processes [60].

The codeposition of inert (α-Al_2O_3), semiconductive (SiC, MoS_2), and conductive (graphite) particles in a copper metallic matrix was studied and it was found that the distribution of inert particles in the coating was uniform and an acceptable surface quality (no roughness) was obtained even at high current density values [11]. When semiconductive and, especially, conductive particles were incorporated to the copper matrix, however, spongy and irregular coatings were produced, showing high surface roughness mainly at high values of current density. Therefore, the increase in the conductivity of the particles changed the specific surface area and increased the roughness of the coating.

These results confirm that the codeposition process as well as the morphology and microstructure of the coatings are affected by the electrical nature of the particles. The presence of more conductive particles in suspension, such as graphite for example, may act as a suspension electrode in the process, as shown by Iwakura [60]. Graphite particles in contact with the cathode were polarized and the deposition of copper could have occurred onto the particles as well as onto the cathode. Such codeposition mechanism could explain the unsuitable deposit structures and the coppering of graphite particles, as observed by Stankovic and Gojo [11]. However, to the best of our knowledge, this mechanism has not been validated yet.

2.1.8. Previous stirring time of the particles in the solution

The effects of the period of time the particles are maintained suspended in the solution before the electrochemical codeposition process occurs (the previous stirring time) on the characteristics of the codeposited coatings are not usually investigated in the literature. However, it is possible to verify that composite coatings are produced after previous stirring time values ranging from 30 min to 24 h, without any explanation about this choice even if the same kind of particle was used [18,26,38,51]. The suspension is generally stirred to enhance the dispersion of the particles and promote their codeposition [11,18,26,34,38,51,61,66]. Therefore, the time used to keep the nanoparticles suspended must be directly related to the codeposition process.

An introductory study concerning the effect of the previous stirring time was performed to produce copper MMC coatings reinforced with micrometric γ-Al_2O_3 onto steel substrate (AISI 1020) [61]. The coatings were produced by chronoamperometry, using a pyrophosphate-based

bath, under constant stirring speed (800 rpm) and using different values of previous stirring time (ranging from 1 to 5 h). Figures 1 to 3 present the surface morphology of the coatings obtained under these conditions.

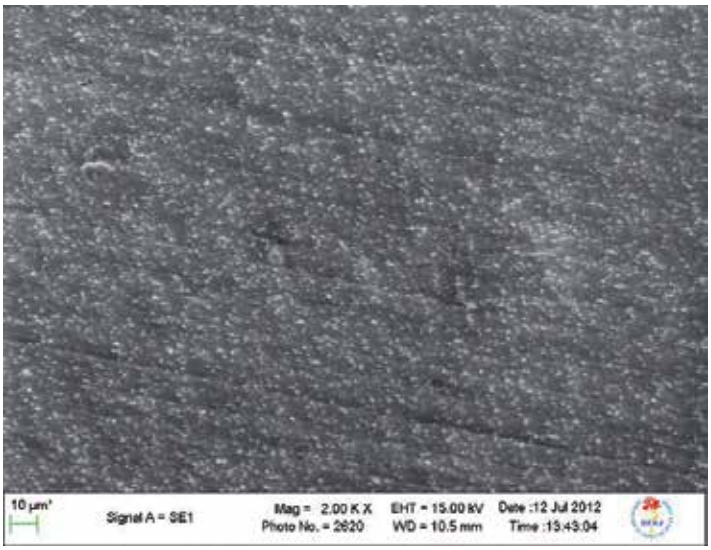

Figure 1. Surface morphology of Cu/γ-Al_2O_3 coatings produced at -1.20 V_{SSE} from pyrophosphate bath previously stirred for 1 h at 800 rpm [61].

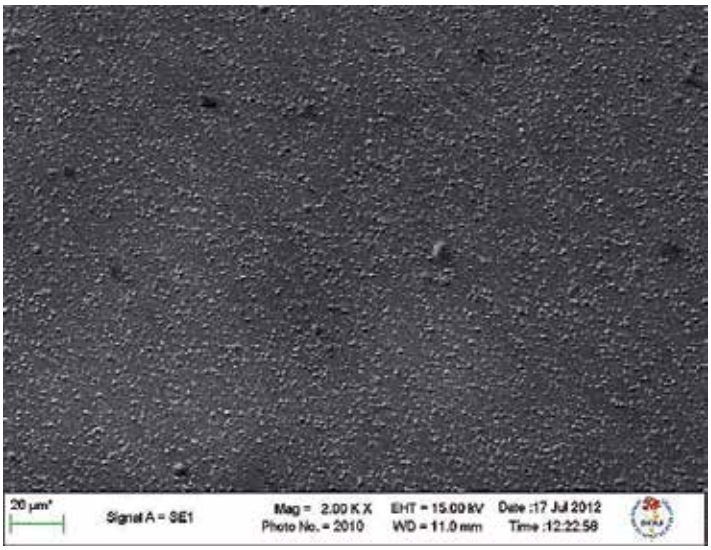

Figure 2. Surface morphology of Cu/γ-Al_2O_3 coatings produced at -1.20 V_{SSE} from pyrophosphate bath previously stirred for 3 h at 800 rpm [61].

http://dx.doi.org/10.5772/62048

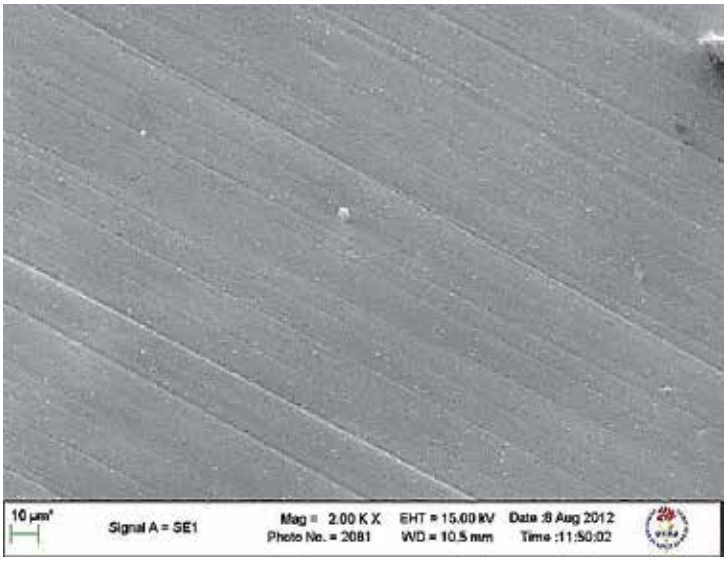

Figure 3. Surface morphology of Cu/γ-Al_2O_3 coatings produced at -1.20 V_{SSE} from pyrophosphate bath previously stirred for 5 h at 800 rpm [61].

It is possible to observe that the previous stirring time influenced the dispersion of the γ-Al_2O_3 particles in the copper matrix. The particle agglomerates in the coating produced after 1 h of previous stirring (Figure 1) seem to decrease when the previous stirring time increased to 3 h (Figure 2). After 5 h of previous stirring, the particles seem to be homogeneously dispersed in the copper matrix (Figure 3). These results indicated that this parameter may have a fundamental role to produce coatings presenting dispersed second-phase particles and consequently enhanced mechanical and anticorrosive resistances.

Additionally, the coatings produced after 1, 3, and 5 h of stirring (Figures 1–3) were chemically analyzed, producing 9.74 wt% Al_2O_3, 16.7 wt% Al_2O_3, and 9.98 wt% Al_2O_3, respectively [61]. There is an increase in the Al_2O_3 content from the experiment conducted after 1 to 3 h of stirring and a small decrease when the previous stirring time increases to 5 h. This result indicates that it must be an optimum time to stir the suspension before electrodeposition be performed to produce coatings with completely dispersed particles and presenting high amount of particulate material incorporated into the metallic matrix. These initial results suggest that the previous stirring time must be carefully studied to produce high-quality composite coatings.

2.2. Electrochemical codeposition mechanisms

The electrochemical codeposition process has been under investigation for several years. Many works have demonstrated the influence of the cations and anions present in the electrolyte and the effects of organic and inorganic additives in the incorporation of the particulate material on the composite coatings. Moreover, as the particulate material should be kept suspended in solution throughout the deposition process, the stirring process is also important for obtaining the MMC coatings [62–67]. Thus, some studies concerning the codeposition mechanism have

been carried out trying to propose models that could explain the influence of the deposition parameters on the codeposition phenomenon of inert particles in metallic matrix during the electroplating of a cathodic composite coating [6,8,11,23,24,62–64].

The main problem faced by the authors who proposed such mechanisms was the physical explanation concerning the direct influence of deposition parameters, such as current density, particle concentration in the bath, stirring speed of the suspension, solution pH, and temperature, for example, on the codeposition phenomenon [38,47,48]. It is a very hard task, and only two models, regarding the codeposition of inert particles, are well accepted [63,64].

2.2.1. Two-step adsorption codeposition model

Earlier codeposition mechanisms [68–70] suggested that two different phenomena should be taken into account to explain the deposition of inert particles: electrophoresis and adsorption. Although both possibilities can be supported by good arguments, there are also effective contradictions.

An electrophoretic effect could explain the observed effect of the current density on the coating. However, there are some difficulties to explain the effects of other parameters, such as, for example, the nonlinear dependence on the particle concentration. Two main objections can be made against the possibility of an electrophoresis effect controlling the codeposition of these particles. First, it should consider the fact that electroplating baths are high ionic strength media, thus presenting no electrophoretic effect. Second, as the mechanism considers only the inert particles (uncharged), they should not respond to a negatively charged electrode. On the contrary, it would be a mistake to consider only a mechanism based on particulate adsorption, because a simple adsorption mechanism could not give a satisfactory explanation for the effect of the current density on the coating [63,71].

Guglielmi [63] developed a hypothesis that used some concepts of the two previously described mechanisms, although the author tried to eliminate the earlier mentioned contradictions. The proposed model was based on two consecutive adsorption steps. The first step is substantially of physical nature and leads to the production of a layer of weakly adsorbed particles on the cathode, with a very high coverage; the second step was dependent on an auxiliary electric field, and thus substantially of electrochemical character, producing a strong adsorption of the particles on the electrode. The strongly adsorbed particles are then progressively covered by the metal growth and become incorporated to the coating.

This model presents a good physical meaning. It is possible to infer that, in the first step, the inert particles are surrounded by a thin layer of adsorbed ions and solvent molecules; these charged particles can then interact with the electrode. In the second step, the existing electric field at the interface between the substrate and the inert particles (charged by the electrolyte components) contributes to produce a strong adsorption field. There is a clear analogy between the two-step adsorption postulated for particles and the adsorption of ions on the external and internal Helmholtz plans, respectively [63].

Figure 1 shows a generic representation of the model proposed by Guglielmi [63]. It can be shown that the postulated mechanism is not affected by the above-mentioned contradictions

http://dx.doi.org/10.5772/62048

and makes it possible to justify the influence of both the current density and the nonlinear particle concentration on the deposition process.

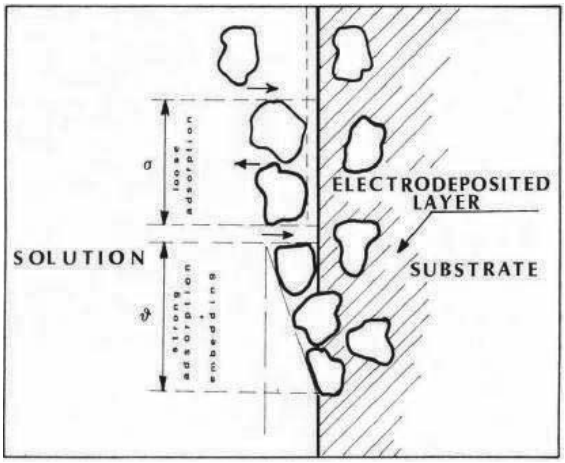

Figure 4. Schematic representation of the different stages of the electrochemical codeposition, as suggested by Guglielmi [63].

The proposed model was then validated by a mathematic treatment and submitted to an experimental evaluation [63]. It used a nickel sulfamate bath containing TiO_2 particles (1 μm) and SiC (2 μm). It is important to mention, however, that none of these particles present inert electrical nature. The deposits were obtained at current densities of 2, 5, and 10 A dm^{-2}, and the analysis of particle concentration in the coating was performed by gravimetric methods. The experimental data agreed with the codeposition proposed mechanism based on a two-step adsorption process. It was found that the concentration of the weakly adsorbed particles was twice the concentration of the particulate material in the suspension, thus justifying the premature saturation of the surface that was indicated by the first step model. However, in highly diluted suspensions, a fraction of the particles weakly adsorbed on the electrode was removed. The lowest concentration of the strongly adsorbed particles, as suggested by the second step model, was related to the reduction of the ions, which was relatively slow, compared to the rate of adsorption of the first step. The deposition of inert particles depended on the studied deposition parameters (current density and particle concentration in the bath). This model also explains the strong dependence on the particle concentration in the solution observed during codeposition, because the behavior of the particles strictly depended on the structure of molecules and ion layers adsorbed on the particle surface and indirectly on the electrolyte composition [62].

2.2.2. Five-step codeposition model for inert particles [63]

The groundings of Guglielmi's model [63] proved the importance of the mathematical treatment of the electrolytic bath in the codeposition process. However, some derivations and

unexplained questions have arisen, and the generality of the model was questioned. Considering only current density and particle concentration in the solution as the single parameters that control the process, this model ignored other important process parameters, such as hydrodynamics and the effect of bath constituents and its electrolytic conditions, such as pH and bath temperature. Therefore, the Guglielmi's model [62] was not considered able to predict how these other parameters affect the electrolytic codeposition of the particles [64].

The electrolytic codeposition mechanism of inert metal particles, proposed by Celis et al. [64], was based on two fundamental assumptions:

1. A layer of adsorbed ionic species is created around the inert particles when the particles are added to the solution or during pretreatment of the particles in ionic solutions, and
2. The reduction of some of these adsorbed ionic species is required for embedding particles in the metal matrix.

Thus, the incorporation of inert particles in the metal matrix proposed by Celis et al. [64] follows the next five stages and is schematically shown in Figure 5.

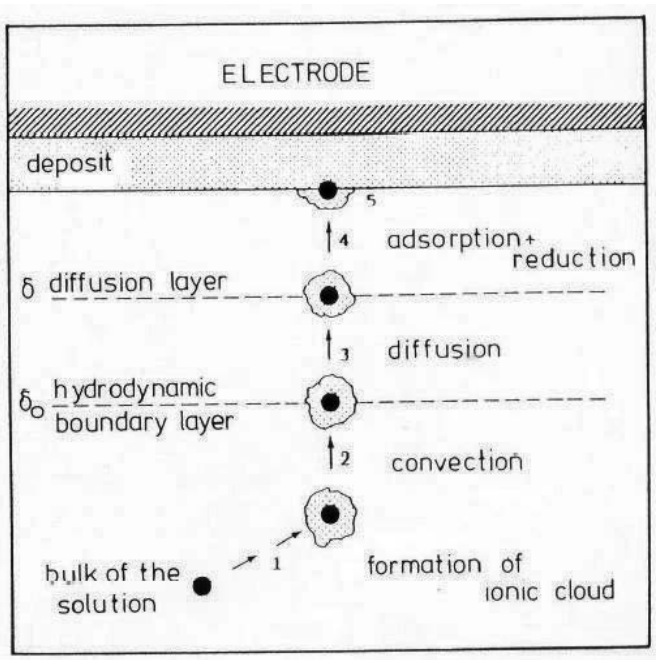

Figure 5. Model proposed by Celis et al. [64] to describe the incorporation of a particular material in composite coatings.

1. Adsorption of ions and molecules occurs on the surface of the particles suspended in the electrolyte.
2. The particles are transferred to the hydrodynamic boundary by convection.

3. The particles diffuse through the cathode diffusion layer.
4. The particles adsorb on the surface of the deposit.
5. The particles are trapped into the coating by the reduction of the ions adsorbed on their surface and the growth of the metallic matrix begins.

The model was constructed assuming the steady-state conditions, so that there are no variations in concentration, pressure, temperature, or overpotentials during the process. It was also assumed that the cathode surface could be uniformly accessible by both the ionic solution and the inert particles. Finally, it was considered that a homogeneous suspension of particles in the coating solution was maintained [63]. In the diffusion layer, the ions move toward the cathode and carry the inert particles with them; simultaneously, a certain amount of ions is adsorbed. Once on the electrode surface, the ions are reduced to meet the demands of the reduction process [64].

This model showed that the codeposition process depends on many variables, although the most important are the current density and the overpotential. These two parameters influenced all the others, except those related to the particle (the nature of the particle, its weight, and its quantity in the suspension), the hydrodynamic conditions that influence the content of incorporated particles, and the probability that the codeposition occurs [64].

However, it is necessary to consider that particles of different nature can be used and differentiate the codeposition process of inert and conductive particles. Conductive particles are generally deposited in a greater amount than the inert particles and tend to cause dendrite growth of the metal matrix [5,11,44,45]. Neither the model proposed by Celis et al. [64] nor that suggested by Guglielmi [62] included the electrical nature of the particles as an important and influent parameter to be considered in their models. However, if all parameters are considered constant, there is a high probability of codeposition of conductive particles using the same mechanism proposed by Celis et al. [64].

Similar to what has been described for the first model, the present model was also validated by a mathematic treatment and submitted to an experimental evaluation [51]. In this case, it used $CuSO_4$ or $KAu(CN)_2$ solutions (pH 0.3 and 4.0, respectively), in which particles of γ-Al_2O_3 (0.05 μm; 20.0 g L^{-1}) were added. The conditions of the experiments are shown in Table 2. The model proved to be valid for the codeposition of composite Cu/γ-Al_2O_3 coatings from sulfate acid baths and for Au/γ-Al_2O_3 coatings from cyanide acid baths.

Studied parameters	Cu matrix	Au matrix
pH	0.3	4.00
Temperature (ºC)	20.0	40.00
Stirring speed (rpm)	400	600
Current density (A dm^{-2})	2.0; 10.0	0.35; 4.25

Table 2. Conditions used to produce copper and gold matrix composite coatings containing γ-Al_2O_3 particles [64].

3. Functional composite coatings with improved mechanical properties

It is well known that the mechanical characteristics of coating materials produced by electrodeposition are related to their microstructure, concerning the effects of grains and grain boundaries and also the preferred orientation of the deposits, which are dependent on the electroplating parameters [72–74]. The presence of particles in the electrolytic bath that are incorporated to the final electrodeposited coating will also contribute to changes in the coating microstructure and can create new mechanical features for these coatings.

There are several works in the literature in which MMC functional coatings are produced to improve the mechanical properties of the substrate. Some of them are presented here [37,38,40,47,75] as an example, because this item alone could be the topic of another review chapter. The generally studied electrodeposition parameters, such as stirring speed or current density, are still mentioned [47,75]. For example, the electrolytic bath stirring speed affected the hardness of nickel matrix composite coatings produced with the addition of particles of CeO_2 (size between 15 and 20 nm) in the electrolytic bath [47]. The hardness of the MMC coatings increased with the stirring speed, reaching its maximum value (760±80 HV) at 450 rpm. Above this stirring speed value, however, there was a reduction in the coating hardness, which would be associated with the agglomeration of the particles of CeO_2 in metallic matrix.

Most of the works found in the literature, however, are related to the mechanical effects concerning the presence of the particle in the coating, the amount of these particles, and their size [38,75–78]. As the MMC coatings reinforced by particles with larger sizes (μm or higher) are susceptible to the formation of defects during mechanical loading, resulting in a premature failure of the composite coatings, it is expected that coatings containing nanorange particles present superior mechanical properties. Therefore, nanocomposite coatings could overcome some limitations, such as poor ductility and elongation, poor wear resistance, and reduced fracture toughness presented by some MMC coatings [77,78].

Nanohardness evaluations were performed by applying normal and lateral force (friction) on nickel metallic matrix reinforced (or not) with SiC particles measuring 10 nm, 50 nm, or 5 μm [38]. It was observed that the addition of the particles in the composite coating decreased the penetration of the Berkovich's indentation in the normal direction, compared to the nickel coating, independent of the particle size. Moreover, the smallest the particle size used, the highest was the nanohardness of the composite coatings. However, there were no significant differences among the composite coatings concerning the applied lateral force, although all of them could support homogeneously frictional force compared to the pure nickel coating [38]. Similar results, concerning the hardness measurements, were found for zinc composite coating matrix reinforced with TiO_2 particles (size between 100 and 200 nm) [76]. The higher hardness of the coating was related to the fine-grained structure of the deposit. During hardness measurements, the dispersed particles in the fine-grained matrix might have obstructed the easy movement of dislocations, which was shown by the higher hardness values of composite-coated samples [76].

Nickel MMC coatings containing 7.9 and 11.5 wt% SiC (particle size of 10 nm), obtained by PC electrodeposition, also presented nanohardness values (3.98±0.032 and 4.10±0.065 GPa,

http://dx.doi.org/10.5772/62048

respectively) higher than the value found for pure nickel coatings (3.00±0.090 GPa) [75]. Considering the effect of the particle amount on hardness values, it is apparent that the higher hardness values were found for the electrodeposited nanocomposite with more SiC content in the coatings. The hardness values depended strongly on the embedded SiC particles in electrodeposited coatings [75]. Similar behavior was observed to composite coatings of Ni-Co reinforced with SiC particles, with size of 50 nm [37]. The authors observed that the composite coating obtained with 4.68 wt% SiC in metallic matrix had maximum hardness (approximately 700 Hv) and minimum wear rate (approximately 2.0×10^{-6} mm^3 N m^{-1}). The increase in the microhardness and the decrease in the wear rate of the Ni-Co/SiC nanocomposite coatings were explained by the grain fining and dispersive strengthening effects of the SiC nanoparticulates codeposited in the Ni-Co alloy matrix, which could have restrain the growth of the Ni-Co alloy grains and the plastic deformation of the matrix under loading. These effects became stronger as the nano-SiC content in the matrix increased, affecting the microhardness and the wear resistance of the Ni-Co/SiC composite coatings [37].

4. Functional composite coatings with improved anticorrosive properties

The amount of works in the literature concerning the production of functional MMC coatings with anticorrosive properties is relatively smaller than those works dealing with mechanical properties. As the anticorrosive performance of these MMC coating/substrate systems depend directly on the deposition parameters, the coatings must also be chemically, morphologically, and structurally characterized to make a relationship between the responses obtained with these analyses and the anticorrosive protection generated by the coating.

4.1. Electrochemical techniques used to evaluate the anticorrosive properties of MMC coatings

The anticorrosive properties of MMC coatings are investigated mainly using three electrochemical techniques: polarization curves, linear polarization resistance (LPR), and electrochemical impedance spectroscopy (EIS). A brief resume concerning the use of these techniques to evaluate electrodeposited coatings are now presented. More details about the techniques, however, can be found elsewhere [32,79–81].

4.1.1. Polarization curves

The polarization curves are used to evaluate the behavior of the coating/substrate system in a certain medium when the potential is varied from the corrosion potential of the system to both anodic and cathodic directions [56]. When the metal is far apart of its corrosion potential (more than ±50 mV), it is said that the metal is polarized [32]. These curves are not related to one particular electrochemical reaction; instead, they show the overall effects of all reactions that occur simultaneously on the electrode [32].

The Tafel extrapolation of the straight part of the polarization curves permits the quantitative measurement of various electrochemical parameters very useful for corrosion evaluation. The

most used are the corrosion potential (E_{corr}), which shows the nobility of the coating compared to the substrate, and the corrosion current density (j_{corr}), which is related to the intensity of the corrosion process. Based on the j_{corr} values, it is possible to calculate the corrosion rate and the coating efficiency (Ef_{Coat}) [32,52] as well as to estimate the coating porosity [82]. It is also possible to determine the Tafel anodic and cathodic slopes (β_a and β_c, respectively), which are related to the kinetic aspects of the anodic and cathodic electrochemical reactions [32,79].

The anodic branch of the polarization curve can also be used to study the passivity of the coatings and evaluate parameters such as the passivation potential ($E_{passivation}$), the critical current density for passivation (j_{crit}), and the pitting potential ($E_{pitting}$) [32].

4.1.2. Linear polarization resistance

LPR is a real-time technique regulated by the ASTM G59 standard method and is based on the potential variation around the open circuit potential (OCP; typical variations approximately ±10 mV [76] to ±20 mV are used) [83,84]. The current required to maintain a specific displacement of the resting potential is directly related to the corrosion process on the electrode surface. This technique is particularly useful in aqueous systems and is applicable to obtain the polarization resistance (R_p) [75]. It is also possible to calculate the current and the corrosion rate if the values of R_p and the Tafel slopes are known [32,83]. In addition, it is possible to evaluate the porosity of the coating by comparing the R_p values of the coating and of the substrate [82].

4.1.3. Electrochemical impedance spectroscopy

EIS is a technique that provides detailed information on the electrical characteristics of the electrode/solution interface. EIS is based on the application of a small sinusoidal signal of potential (or current) to the working electrode according to a particular desired frequency range. As a response, it obtained the impedance (Z), which can be related to the opposition to the current flux in the system [32]. Important information about the charge transfer kinetics, structure, and properties of the interface electrode/electrolyte can also be achieved. The frequency range usually used for disturbing the system varies from 100 kHz to 10 MHz, using the amplitude signal in the range of 5 to 50 mV rms, depending on the studied system [32,85].

The results obtained from the EIS measurements can be used to construct diagrams representing the behavior of the electrode in a particular electrochemical process. One of these diagrams is the Nyquist diagram, in which the real (Z) and imaginary (Z) impedance data are represented in a complex plane. The real impedance (Z) incorporates the ohmic resistance (i.e., the pure resistance that is independent of the frequency). The imaginary impedance (Z) incorporates the capacity and/or inductive reactance (i.e., the resistance that is dependent on the frequency applied to the system) [32].

The Bode and phase diagrams are also used to represent the EIS results. These diagrams show the variations of the impedance modulus ($|Z|$) or the phase angle with the frequency, respectively. An advantage of the Bode diagram is the possibility of observing the impedance

variation at high frequencies, which is generally omitted in the Nyquist diagram representation [32].

EIS can be considered as a nondestructive technique [32,85,86]. The application of this technique in electrochemical systems considers the combination of physical and chemical interfacial processes with the components of an equivalent electrical circuit as an analogy of the electrochemical phenomena. Therefore, it is possible to obtain the electrolyte resistance (R_e), the charge transfer resistance (R_{ct}), the polarization resistance (R_p), and the double layer capacitance (C_{dl}) as variables that allow the assessment of coating/substrate characteristics [32,86]. In addition, it is also possible to evaluate the corrosion rate and the porosity of the coating by comparing the R_p values of the coating and of the substrate in the same electrolytic medium [32,82].

4.2. Main results concerning the corrosion resistance of MMC coatings

The comparison between the anticorrosive performance of metallic and MMC coatings was studied for several metallic matrix/ceramic particles (or nanoparticles) systems using different corrosive media [26,37,40,45,47]. Most of the results affirm that the presence of the particles increases the corrosion resistance of the MMC coating/substrate system, although it is important to mention that the optimum values of particle content in the metallic matrix to produce a coating with good anticorrosive performance directly depend on the metal/particle system produced and on the deposition parameters used. Moreover, the corrosion mechanism of the metallic coatings containing these particles is not completely elucidated; the process is generally related to blocking effects or to the creation of a more difficult path to the electrolyte attack in the coating [47,58,75,87]. In addition, there are also inconclusive results, as the conditions used to produce the coatings were not always adequate or the used parameters were not always completely mentioned (for example, the kind of substrate or the stirring time). Finally, the results presented here also show that the deposition parameters earlier described may have synergistic and/or antagonistic effects on the coating deposition process and on the anticorrosive properties of the coatings.

4.2.1. Ni and Ni-alloy matrix composite coatings

Nickel is the most studied metallic matrix to produce composite coatings with improved corrosion properties, and different ceramic particles and nanoparticles were used to this purpose. The corrosion resistance of nickel matrix composite coatings using α-Al_2O_3 particles (smaller than 1 μm; 98% purity) as the second phase on steel substrate, compared to a standard nickel coating produced onto the same substrate, was studied [87]. The corrosion evaluation data of the coating/substrate systems (from polarization curves and electrochemical impedance experiments) were performed in 0.5 mol L^{-1} Na_2SO_4 solution with different exposure times. Despite the physical (defects and dislocations) and chemical heterogeneities (the presence of nickel oxides or impurities), Al_2O_3 particles in the nickel coatings disturbed the electrochemical electrode reactions. As a result, the corrosion process was enhanced in some parts of the coating, whereas the phenomenon was inhibited in other parts. Therefore, no significant differences were observed concerning the anticorrosive behavior of the standard

nickel coating and of the composite coating for the data obtained in the first days of exposure. Although the corrosion rates of both coatings increased with the exposure time, the corrosion resistance of Ni/Al_2O_3 composite coatings was always higher than the standard nickel coating in Na_2SO_4. Because of the adsorption of water, OH^- ions, and oxygen, the surfaces of both coatings were covered with a thin layer of nickel oxides and hydroxides causing an increase in R_{ct} during the first 3 days of the experiment [87].

The EIS measurements showed that this result was related to the fact that the resistance of the electrolyte in the pores of the composite coating was much lower than in the pores of the standard nickel coating. It means that the presence of Al_2O_3 particles in the voids of the coating increases its porosity and the discontinuity of the passive layer formed on its surface. In the cracks and pores of the passive layer, the electrolytic solution is in contact with either nickel or dielectric Al_2O_3 particles. However, the passive layer on the surface of the Ni/Al_2O_3 coating was tighter possibly due to the more finely crystalline structure of the composite coating in comparison with that of the nickel standard coating. As a result, the pores and cracks in the passive layer on the composite coating were sufficiently small to reduce the diffusion of metal corrosion products from their inside effectively, and they built up in the pores, blocking them and decreasing the corrosion process [87]. After 14 days of exposure in the corrosive medium, the corrosion rate of the Ni/Al_2O_3 composite coating was three times lower than that of the nickel coating.

Ni/CeO_2 composite coatings were produced on steel from an acid electrolyte containing CeO_2 nanoparticles using square-wave pulse current mode under different stirring speed conditions and at 45°C. The corrosion behavior of these coatings was evaluated in a 3.5 g L^{-1} NaCl solution and compared to that observed from a nickel coating in the same medium [47]. More positive corrosion potentials and higher R_p values were obtained for the composite coatings (ranging from 3.54×10^3 to 9.772×10^3 Ω) compared to those verified for the nickel coating (2.05×10^3 Ω). Once more, the presence of the inert particles in the coating was considered important in the improvement of the corrosion resistance of composite coating because they may have acted as a physical barrier to the propagation of defects. The dispersion of the nanoparticles in the metallic matrix formed corrosion microcells, which facilitated the anodic polarization, resulting in the inhibition of pitting corrosion and in the promotion of uniform corrosion of the coating. If the crystallites in the coating remained on their nanometer size, the corrosion process could be explained considering that the electrolyte must travel a tortuous path to reach the substrate and this path is longer in the Ni/CeO_2 composite coatings than in the nickel coating [47].

The increase in the stirring speed until 450 rpm increased the CeO_2 particles in the nickel matrix coating, as well as the R_p values measured for these coatings, indicating a relationship between the content of particles in coating and its anticorrosive performance. Further increase in stirring speed, however, decreased both the particle incorporation and the R_p value, showing that it must be an optimum stirring speed condition to produce coatings with high corrosion resistance [47]. However, the effects of the pulse plating and the deposition temperature on the corrosion performance of the coating/substrate system were not evaluated.

http://dx.doi.org/10.5772/62048

EIS analysis was performed in aqueous NaOH (1 mol L^{-1}) and HNO_3 (1 mol L^{-1}) solutions to evaluate the anticorrosive properties of Ni/TiO_2 nanocomposite coatings. The coatings containing different TiO_2 contents, (A: Ni-3.9 wt% TiO_2, B: Ni-6.5 wt% TiO_2, and C: Ni-8.3 wt % TiO_2) were produced onto steel from an acid Ni(II) bath. The charge transfer resistances of pure nickel and Ni-TiO_2 coatings [49] are shown in Table 3.

R_{ct} (Ω cm^2)×10^3		
Coatings	NaOH	HNO_3
Pure Ni	203	2.0
A	383	3.3
B	491	3.9
C	634	4.3

Table 3. Charge transfer resistance for pure nickel coating and Ni-TiO_2 nanocomposite coatings (A–C) obtained from EIS data [49] after fitting by the equivalent circuit model

The Nyquist diagrams obtained from the experiments carried out in NaOH showed a capacitive loop at high frequencies followed by an almost straight line at low frequencies, suggesting that the corrosion mechanism was controlled by both charge transfer and diffusion processes. The corrosion rate was affected by the interdiffusion of Ni^{2+} and OH^- ions, confirming that there should be an effect related to the diffusion of these ions in the coating. The R_{ct} values for the composite coatings exposed in this medium were improved with the increase of the TiO_2 nanoparticle content in the coating, because they probably decreased the diffusion process [49].

In the experiments performed in HNO_3, there was an observed discrete capacitive loop at high frequencies of the Nyquist diagram. An inductive loop was also observed at low frequencies, which was attributed to the relaxation process of H^+ and NO^{3-} species adsorbed on the electrode surface [49]. As observed in the experiments carried out in NaOH medium, the increase in the TiO_2 content in the coating caused an increase in the charge transfer resistance of the composite coating. However, the R_{ct} values obtained in acidic medium were significantly smaller than those verified in alkaline medium [49]. These results suggested that the acidic medium may have damaged the coating or that the corrosion mechanism has changed in this medium.

The presence of different concentrations of sodium dodecyl sulfate (SDS) in the electrodeposition bath to produce nickel/α-Al_2O_3 and its influence on the anticorrosive performance of the coating produced onto steel in NaCl (3.5% m/v) was also studied [8]. Although the use of a surfactant may enhance the incorporation of inert particle in the metallic matrix, it also has some disadvantages, as they can be incorporated in the metallic matrix and change the mechanical properties of the deposit (e.g., internal stress and fragility). This is why the concentration of surfactants in the deposition bath should be very well controlled [88]. The nanocomposite coatings produced using the optimum SDS concentration (125 g L^{-1}) contained higher levels of alumina nanoparticles in the metallic matrix. This coating presented a more positive corrosion potential (E_{corr} = -0.209 $V_{Ag/AgCl}$) and a lower corrosion current density (j_{corr} =

1.141×10^{-7} A cm^{-2}) than the bare substrate (E_{corr} = -0.488 and j_{corr} = 4.832×10^{-6} A cm^{-2}). It was considered that the incorporation of such low reactive nanometer alumina particles played an important role in improving the corrosion resistance of the coating/substrate system, as they apparently filled the pores and micropores of the coating and thereby reduced the corrosion process [8].

The corrosion performance of Ni-Co alloy matrix composite coatings containing different contents of SiC nanoparticles was evaluated [37]. The coatings were produced onto copper substrate from acid Ni(II) and Co(II) sulfamate solutions using DC and different stirring speeds. The polarization curves of both the composite coatings and the Ni-Co alloy coatings were performed in a 0.5 mol L^{-1} NaCl solution. It was found that the composite coating produced at 0.03 A cm^{-2} contained 3.2 wt% SiC and that this coating showed a lower corrosion current density and a more positive corrosion potential (E_{corr} = -0.33 V_{SCE}, j_{corr} = 7.9×10^{-3} A cm^{-2}) compared to the results of a Ni-Co alloy coating (E_{corr} = -0.39 V_{SCE}, j_{corr} = 3.98×10^{-2} A cm^{-2}). The better result obtained by this nanocomposite coating was attributed to a decrease in the size of the defects related to the incorporation of SiC nanoparticles, which is useful for creating a tortuous path to the corrosive medium attack the substrate, preventing pitting corrosion and enhancing the corrosion resistance of these nanocomposite coatings [37]. However, the results concerning Ni-Co/SiC coatings containing other SiC contents were not mentioned in the work.

Composite coatings of Ni-Zn matrix containing TiO_2 nanoparticles (Degussa P-25 anatase, 25 nm) as the strengthening phase were produced onto a mild steel (DIN C25-AISI 1025) substrate using ultrasonic-assisted electrodeposition process [89]. These coatings were electrochemically evaluated in a natural 3.5 wt% NaCl solution using EIS measurements at the OCP. The results showed that higher R_{ct} values were obtained for samples produced using 108 and 216 W cm^{-2} of ultrasonic powder densities, indicating a better anticorrosion performance of these coatings. On the contrary, the R_{ct} values of coatings produced without using the ultrasonic-assisted process were smaller than that obtained for the alloy Ni-Zn coating. The authors claim that the use of ultrasonic vibration together with electrodeposition might have improved the coating nanoparticles uniform dispersion and hence improved the anticorrosive ability of the composite coatings [89].

4.2.2. Copper matrix composite coatings

The corrosion behavior of electrodeposited Cu/SiO_2 nanocomposite coatings, produced onto steel (OL 37) in a bath containing (or not) a surfactant agent $C_{16}H_{33}N(CH_3)_3Br$ (CTAB) in different concentrations, was evaluated in 0.2 g L^{-1} Na_2SO_4 solution at room temperature and pH 3 [45]. A decrease of the corrosion current density for the composite deposit Cu/SiO_2 was also observed in comparison with the pure copper coating, suggesting that the presence of nanoparticles had a beneficial effect in decreasing the corrosion rate as shown in Table 4. These results were confirmed by the R_p values obtained from a linear polarization experiment in the same corrosion medium. This behavior was explained by the lowering of the electrode surface area in contact with the electrolyte due to the presence of the nanoparticles and by a more fine-grained compact structure of the coating.

http://dx.doi.org/10.5772/62048

Coating*	E_{corr} ($V_{Ag/AgCl}$)	Average of j_{corr} (A cm^{-2})	R_p (Ω cm^2)
Cu	-0.588	75×10^{-6}	500
Cu-SiO_2 (A)	-0.563	40×10^{-6}	1000
Cu-SiO_2 (B)	-0.597	30×10^{-6}	1341
Cu-SiO_2 (C)	-0.592	40×10^{-6}	628
Cu-SiO_2 (D)	-0.578	20×10^{-6}	1769

*The composite coatings were produced from Cu(II) solutions containing SiO_2 10 g L^{-1} + CTAB (A) 0.00 mol L^{-1}, (B) 10^{-5} mol L^{-1}, (C) 10^{-4} mol L^{-1}, and (D) 10^{-3} mol L^{-1}.

Table 4. Corrosion data for Cu and Cu-SiO_2 deposits obtained by Zamblau et al. [45] in the absence and presence of different concentrations of CTAB.

The increase of CTAB concentration in the electrolyte hindered the corrosion process even more when CTAB concentration was increased from 1.0×10^{-5} to 1.0×10^{-2} mol L^{-1} and then to 1.0×10^{-3} mol L^{-1}. As the surfactant increased the incorporation of SiO_2 in the coating by modifying the surface charge of the nanoparticles (the negative initial charge turns into a positive one) and their hydrophilicity, the anticorrosive performance of the coating was enhanced [89]. The highest R_p value was obtained for a bath containing 10 g L^{-1} SiO_2 and 1.0×10^{-3} mol L^{-1} CTAB, confirming the good effect of this additive in the electrolytic deposition of metal-nanoparticle composites [45].

The protective and anticorrosive properties of copper coatings, Cu+μSiC composite coatings (particle size of 1–2 μm), and Cu+*n*SiC composite coatings (particle size of 20 nm), produced on standardized steel Q-pane, were evaluated by potentiodynamic curves in two different environments. An acidic solution (0.5 mol L^{-1} Na_2SO_4 at pH 2) was used to evaluate the uniform corrosion rate, whereas an alkaline solution (0.5 mol L^{-1} Na_2SO_4 at pH 12) was employed to evaluate if the presence of the particles influenced the passive potential range and current [91]. Table 5 shows that, in acidic environment, the specimens coated by the Cu+μSiC composite deposit presented the most negative corrosion potential and the highest corrosion rate, expressed by the corrosion current density (j_{corr} = 5.0 μA cm^{-2}). This behavior was attributed to the voids between the ceramic particles and the metallic matrix that allow the access of the electrolyte to the substrate. These voids were larger in the Cu+μSiC composite coatings than in the Cu+*n*SiC composite ones. In fact, the value of the corrosion potential of the Cu+μSiC composite coatings was comparable to the value obtained by this research group for the bare steel substrate in the same acidic corrosion medium. On the contrary, the Cu+*n*SiC composite coating samples presented no differences in the corrosion potential compared to the pure copper coatings. However, the nanocomposite samples showed a lower corrosion current density and, consequently, a lower corrosion rate than the copper coating, which might be attributed to their more compact microstructure [91].

Nevertheless, the potentiodynamic curves obtained in the alkaline environment showed no differences for the three types of coatings before their passivation. The two composite coatings

Coating	E_{corr} ($V_{Ag/AgCl}$)	j_{corr} (μA cm^{-2})
Cu	-0.053	0.7
Cu-μSiO_2	-0.456	5.0
Cu-*n*SiO_2	-0.013	0.3

Table 5. Results for corrosion evaluation of Cu, Cu-μSiO_2, and Cu-*n*SiO_2 deposits produced by Lekka et al. [91] in acidic (pH 2) 0.5 mol L^{-1} Na_2SO_4 solution.

showed an improved passive domain in comparison to the pure copper coating, with only one, continuous, and stable passive zone. On the contrary, the pure metallic coating presented two passive regions corresponding to the formation of two different types of oxides. The voids between the SiO_2 microparticles and the metallic matrix earlier mentioned seemed to cause no influence on the behavior of the Cu-μSiO_2 composite coating in an alkaline environment because the compact oxide film could have covered them. The samples covered by the Cu+*n*SiC composite coatings also presented the lowest passive current density. Thus, the compact microstructure of the Cu+*n*SiC composite coatings also led to the formation of a compact and protective oxide in alkaline solutions [91].

The cathodic efficiency and consequently the thickness of the Cu-μ(γ-Al_2O_3) coatings produced from pyrophosphate bath decreased with the increase (in modulus) of the cathodic potential (*E*) independent of the previous stirring time (*t*) used [61]. Thinner coatings can directly influence the anticorrosive performance of the coatings. On the contrary, Figure 6 indicates that there may be a joint influence of both parameters, *E* and *t*, in the coating composition, although none of them alone presented a significant influence.

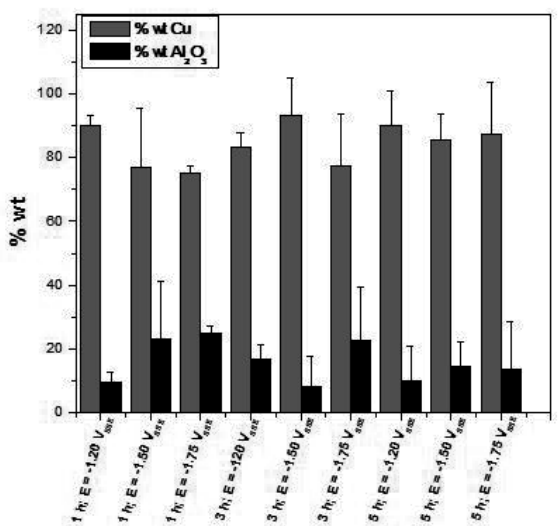

Figure 6. Cu and Al_2O_3 contents (wt%) in the composite coatings produced from baths containing $CuSO_4$ 0.02 mol L^{-1}, $K_4P_2O_7$ 0.90 mol L^{-1}, and γ-Al_2O_3.

http://dx.doi.org/10.5772/62048

Although there was no direct relationship between the applied cathodic potential and the γ-Al_2O_3 content in the coating, the increase in this parameter also seemed to increase the dispersion of the particles in the coating, as shown in Figures 7 and 8, for the coatings produced after 5 h of stirring at (800 rpm).

Figure 7. Surface morphology of Cu/γ-Al_2O_3 coatings produced at -1.20 V_{SSE} from pyrophosphate bath previously stirred for 5 h at 800 rpm [61].

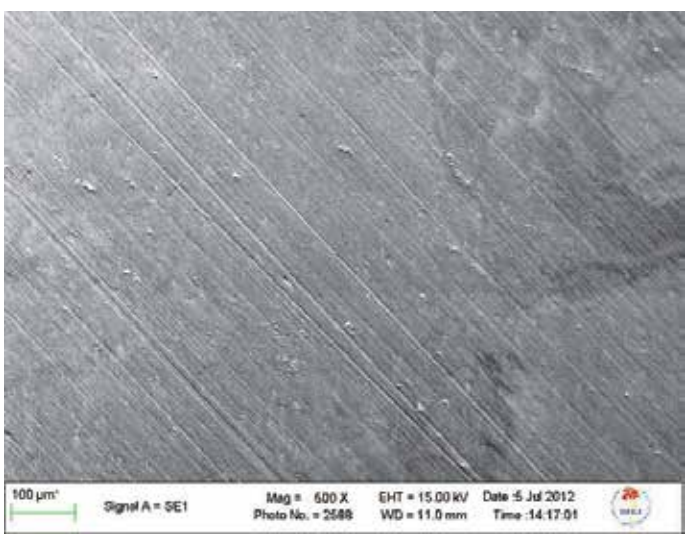

Figure 8. Surface morphology of Cu/γ-Al_2O_3 coatings produced at -1.50 V_{SSE} from pyrophosphate bath previously stirred for 5 h at 800 rpm [61].

It was expected that a coating presenting a well-dispersed second phase and a high amount of micrometric γ-Al_2O_3 particles presented the best anticorrosive performance. However, these effects had no direct influence on the corrosion performance of these coatings in 0.5 mol L^{-1} NaCl, and no significant differences could be noted among their E_{corr}, as shown in Table 5 and Figure 9, whereas the j_{corr} values increased when the applied potential became more negative. Moreover, the anticorrosive performance of these coatings, in terms of j_{corr}, was worse than the values obtained for the pure copper coating (5.27 $\mu A\ cm^{-2}$). The thin layers produced under the deposition conditions could have probably masked the effects of the deposition parameters on the anticorrosive performance of these coatings. In addition, the micrometric size of the γ-Al_2O_3 particles could have contributed to create defects and voids in the coatings, enhancing the corrosion process, confirming the results earlier shown for Cu-μSiO_2 coatings [91], and showing that the size of the particle is an important parameter to produce composite coatings with high anticorrosive characteristics.

Experiments	Applied cathodic potencial (V_{SSE})	j_{corr} ($\mu A\ cm^{-2}$)	E_{corr} (V_{SCE})
1	-1.20	10.3	-0.411
2	-1.50	62.2	-0.423

Table 6. and E_{corr} values of composite coatings Cu/γ-Al_2O_3 in 0.5 mol L^{-1} NaCl. The coatings were produced at -1.20 and -1.50 V_{SSE} after previous stirring for 5 h of at 800 rpm [61].

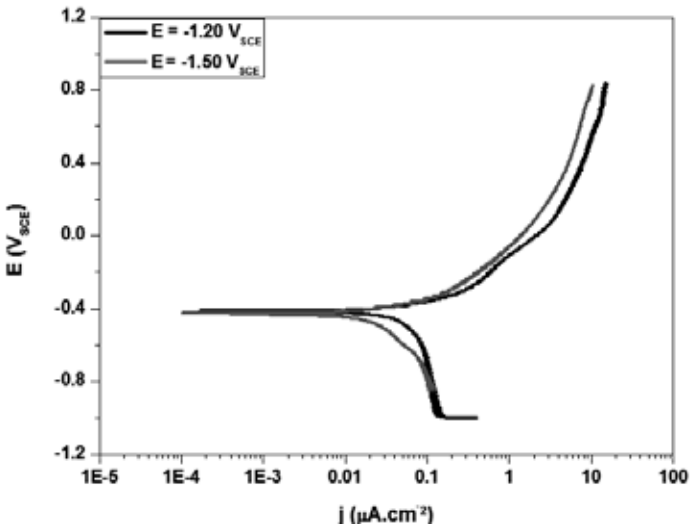

Figure 9. Polarization curves of Cu/γ-Al_2O_3 coatings/steel substrate systems in 0.5 mol L^{-1} NaCl.

Cu/boehmite nanocomposite coatings [AlO(OH) Disperal P2, 25 nm size; Sasol®] was produced onto steel substrate (AISI 1020) by DC electrodeposition using j = 7.0 and 21.0 A

m^{-2} from a pyrophosphate bath, containing (or not) allyl alcohol as an additive agent, under 1000 and 1300 rpm of stirring speed [61]. The allyl alcohol has been reported in the literature as a brightening agent and relieving stress in the production on Cu coatings and Cu-Zn alloy [92]. The corrosion resistances from these coatings were obtained using the linear polarization experiments (R_p). The results showed that the presence of allyl alcohol improved the corrosion resistance of the composite coatings in 0.1 mol L^{-1} Na_2SO_4 compared to those produced from baths without this additive under the same deposition conditions [61]. For example, the composite coating produced at 1000 rpm and 7 A m^{-2} presented R_p = 2956 Ω, when a bath without allyl alcohol was used, and Rp = 2.0×10^7 Ω, when a bath containing this additive was employed. This behavior can be related to the effect of this type of compound, usually used to refine the coatings in an electrodeposition process and favor the formation of layers without cracks or defect, improving the corrosion resistance [92].

5. Conclusions

It is possible to conclude that, although composite coatings have been under investigation for many years, their application as anticorrosive coatings still needs more research. The effects of the electrical nature of the particle and the bath composition (e.g., complexant, additives, and surfactants) on the anticorrosive characteristics of the MMC coatings must be studied. Other parameters, such as stirring speed, previous stirring time, and solution temperature, must also be optimized to enhance the incorporation of the nanoparticles to the coatings and relate this effect to their anticorrosive properties. In addition, the corrosion processes in different electrolytic media must be evaluated and be related with the deposition parameters. Therefore, there is a great research opportunity involving the production of MMC coatings by electrodeposition and their characterization as anticorrosive coatings.

Author details

Thais G.L. Rezende, Deborah V. Cesar, Dalva C.B. do Lago and Lilian F. Senna*

*Address all correspondence to: lsenna@uerj.br

Laboratório de Eletroquímica e Corrosão, Departamento de Química Analítica, Universidade do Estado do Rio de Janeiro, Rio de Janeiro, RJ, Brazil

References

[1] Oniciu L., Muresan L. Some fundamental aspects of levelling and brightening in metal electrodeposition. Journal of Applied Electrochemistry. 1991; 21(7): 565–574. DOI: 10.1007/BF01024843.

[2] Adamian R. Novos Materiais Tecnologias e Aspectos Econômicos. Rio de Janeiro: Setor de Publicações e Programação Visual/COPPE/UFRJ; 2009. 400 p.

[3] Callister W.D. Materials Science and Engineering: An Introduction. 7th ed. USA: John Wiley & Sons, Inc.; 2006. 832 p.

[4] Malfatti C.F. Estudo das propriedades de revestimentos compósitos de níquel com Al_2O_3 e SiC [dissertation]. Porto Alegre, RS: Universidade Federal do Rio Grande do Sul; 2000. 118 p. Available from: http://hdl.handle.net/10183/3428.

[5] Musiani M. Electrodeposition of composites: An expanding subject in electrochemical materials science. Electrochimica Acta. 2000; 45(20): 3397–3402. DOI: 10.1016/S0013-4686(00)00438-2.

[6] Tuaweri T.J., Wilcox G.D. Behaviour of Zn-SiO_2 electrodeposition in the presence of N,N-dimethyldodecylamine. Surface and Coatings Technology. 2006; 200(20–21): 5921–5930. DOI: 10.1016/j.surfcoat.2005.09.023.

[7] Wang Y.L., Wan Y.Z., Zhao Sh.M., Tao H.M., Dong X.H. Electrodeposition and characterization of Al_2O_3-Cu(Sn), CaF_2-Cu(Sn) and talc-Cu(Sn) electrocomposite coatings. Surface and Coatings Technology. 1998; 106(2–3): 162–166. DOI: 10.1016/S0257-8972(98)00522-2.

[8] Sabri M., Sarabi A.A., Kondelo S.M.N. The effect of sodium dodecyl sulfate surfactant on the electrodeposition of Ni-alumina composite coatings. Materials Chemistry and Physics. 2012; 136(2–3): 566–569. DOI: 10.1016/j.matchemphys.2012.07.027.

[9] Bund A., Thiemig D. Influence of bath composition and pH on the electroco-deposition of alumina nanoparticles and copper. Journal of Applied Electrochemistry. 2007; 37(3): 345–351. DOI: 10.1007/s10800-006-9264-2.

[10] Gül H., Kiliç F., Aslan S., Alp A., Akbulut H. Characteristics of electro-co-deposited Ni-Al_2O_3 nano-particle reinforced metal matrix composite (MMC) coatings. Wear. 2009; 256: 976–990. DOI: 10.1016/j.wear.2008.12.022.

[11] Stankovic V.D., Gojo M. Electrodeposited composite coatings of copper with inert, semiconductive and conductive particles. Surface and Coatings Technology. 1996; 81(2–3): 225–232. Available from: http://dx.doi.org/10.1016/0257-8972(95)02486-7.

[12] Wu G., Li N., Zhou D.R., Mitsuo K. Electrodeposited Co-Ni-Al_2O_3 composite coatings. Surface and Coatings Technology. 2004; 176(2): 157–164. DOI: 10.1016/s0257-8972(03)00739-4.

[13] Fundo A.M.B. do. Modificação de superfícies para aplicações em electrocatálise: deposição autocatalítica de ligas metálicas e incorporação de partículas de metais em matriz polimérica [thesis]. Lisboa, Portugal: Universidade de Lisboa; 2007. 174 p. Available from: http://hdl.handle.net/10451/1667.

[14] Lencina D.C., Ahrens C.H., Salmoria G.V., Lafratta F.H. Moldagem por injeção da PA 6.6 em moldes de estereolitografia metalizados com Ni-P pelo processo electroless.

Polímeros: Ciência e Tecnologia 2007; 17(2): 88–92. DOI: 10.1590/S0104-14282007000200006.

[15] Lee E.C., Choi J.W. A study on the mechanism of formation of electrocodeposited Ni-diamond coatings. Surface and Coatings Technology. 2001; 148 (2–3): 234–240. DOI: 10.1016/S0257-8972(01)01352-4.

[16] Feng Q., Li T., Zhang Z., Zhang J., Liu M., Jin J. Preparation of nanostructured Ni/Al_2O_3 composite coatings in high magnetic field. Surface and Coatings Technology. 2007; 201(14): 6247–6252. DOI: 10.1016/j.surfcoat.2006.11.019.

[17] Guo D., Zhang M., Jin Z., Kang R. Effect of direct current and pulse plating on the EDM performance of copper-zirconium diboride composites. Journal of University of Science and Technology Beijing, Mineral, Metallurgy, Material. 2007; 14(5): 464–468. DOI: 10.1016/S1005-8850(07)60091-7.

[18] Faraji S., Abdul Rahim A., Mohamed N., Sipaut C.S. A study of electroless copper-phosphorus coatings with the addition of silicon carbide (SiC) and graphite (Cg) particles. Surface and Coatings Technology. 2011; 206(6): 1259–1268. DOI: 10.1016/j.surfcoat.2011.08.032.

[19] Sánchez F.A.L., Reifler F.A., Clemens F., Amico S.C., Bergmann C.P. Obtenção de um revestimento compósito de poliéster-uretana reforçado com alumina pela técnica de deposição por imersão sobre fibras de poliamida 6. Cerâmica. 2009; 55: 379–384. DOI: 10.1590/S0366-69132009000400007.

[20] Tao Y., Xiong T., Sun C., Jin H., Du H., Li T. Effect of α-Al_2O_3 on the properties of cold sprayed Al/α-Al_2O_3 composite coatings on AZ91D magnesium alloy. Applied Surface Science. 2009; 256(1): 261–266. DOI: 10.1016/j.apsusc.2009.08.012.

[21] Wu B., Xu B.-S., Zhang B., Lü Y.-H. Preparation and properties of Ni/nano-Al_2O_3 composite coatings by automatic brush plating. Surface and Coatings Technology. 2007; 201(16–17): 6933–6939. DOI: 10.1016/j.surfcoat.2006.12.022.

[22] Cordero-Arias L., Boccaccini A.R., Virtanen S. Electrochemical behavior of nanostructured TiO_2/alginate composite coating on magnesium alloy AZ91D via electrophoretic deposition. Surface and Coatings Technology. 2015; 265: 212–217. DOI: 10.1016/j.surfcoat.2015.01.007.

[23] Garcia I., Fransaer J., Celis J.P. Electrodeposition and sliding wear resistance of nickel composite coatings containing micron and submicron SiC particles. Surface and Coatings Technology. 2001; 148(2–3): 171–178. DOI: 10.1016/S0257-8972(01)01336-6.

[24] Thiemig D., Bund, A. Influence of ethanol on the electroco-deposition of Ni/Al_2O_3 nanocomposite films. Applied Surface Science. 2009; 255(7): 4164–4170. DOI: 10.1016/j.apsusc.2008.10.114.

[25] Aruna S.T., Grips V.K.W., Rajam K.S. Synthesis and characterization of Ni-Al_2O_3 composite coatings containing different forms of alumina. Journal of Applied Electrochemistry. 2010; 40(12): 2161–2169. DOI: 10.1007/s10800-010-0198-3.

[26] Garcia I., Conde A., Langelaan G., Fransaer J., Celis J.P. Improved corrosion resistance through microstructural modifications induced by codepositing SiC-particles with electrolytic nickel. Corrosion Science. 2003; 45(6): 1173–1189. DOI: 10.1016/S0010-938X(02)00220-2.

[27] Malfatti C.F. Elaboração e Caracterização de Nanocompósitos Ni-P-SiC Eletrodepositados [thesis]. Porto Alegre, RS: Universidade Federal do Rio Grande do Sul; 2004. 147 p. Available from: http://hdl.handle.net/10183/4451.

[28] Malfatti C.F., Veit H.M., Menezes T.L., Ferreira J.Z., Rodrigues J.S., Bonino J.P. The surfactant addition effect in the elaboration of electrodepositated NiP-SiC composite coatings. Surface and Coatings Technology. 2007; 201(14): 6318–6324. DOI: 10.1016/j.surfcoat.2006.11.040.

[29] Martins D.F. Estudo de banhos ácidos para substituição de banho alcalino cianídrico na eletrodeposição de zinco sobre pregos [dissertation]. Porto Alegre, RS: Universidade Federal do Rio Grande do Sul; 2009. 142 p. Available from: http://hdl.handle.net/10183/18587.

[30] Lima F.A.S. Eletrodeposição de filmes finos de CdTe para aplicação em células solares fotovoltaicas [dissertation]. Fortaleza, CE: Universidade Estadual do Ceará; 2010. 114 p.

[31] Paunovic M., Schlesinger M. Fundamentals of Electrochemical Deposition. 2nd ed. New York: John Wiley & Sons; 2006. 373 p.

[32] Wolynec S. Técnicas Eletroquímicas em Corrosão. 1st ed. São Paulo, SP: EDUSP; 2013. 176 p.

[33] Neckel I.T. Crescimento e morfologia de ligas CoxFe100-x Eletrodepositadas sobre Si(111) tipo-n [dissertation]. Curitiba, PR: Universidade Federal do Paraná; 2009. 108 p. Available from: http://hdl.handle.net/1884/21180.

[34] Gurrappa I., Binder L. Electrodeposition of nanostructured coatings and their characterization—a review. Science and Technology of Advanced Materials. 2008; 9(4): 1–11. DOI: 10.1088/1468-6996/9/4/043001.

[35] Silva Jr A.I., Filho H.C.A., Silva R.C. Testes de desempenho de eletrodos: Eletrodos de referência. Química Nova. 2000; 23(4): 512–517. DOI: 10.1590/S0100-40422000000400014.

[36] Borkar T., Harimkar S.P. Effect of electrodeposition conditions and reinforcement content on microstructure and tribological properties of nickel composite coatings. Surface and Coatings Technology. 2011; 205(17–18): 4124–4134. DOI: 10.1016/j.surfcoat.2011.02.057.

[37] Shi L., Sun C., Gao P., Zhou F., Liu W. Mechanical properties and wear and corrosion resistance of electrodeposited Ni-Co/SiC nanocomposite coating. Applied Surface Science. 2006; 252(10): 3591–3599. DOI: 10.1016/j.apsusc.2005.05.035.

[38] Sohrabi A., Dolati A., Ghorbani M., Monfared A., Stroeve P. Nanomechanical properties of functionally graded composite coatings: Electrodeposited nickel dispersions containing silicon micro- and nanoparticles. Materials Chemistry and Physics. 2010; 123(2–3): 829–829. DOI: 10.1016/j.matchemphys.2010.04.040.

[39] Sombatsompop N., Sukeemith K., Markpin T., Tareelap N. A new experimental apparatus of electro-codeposited system for Ni-WC composite coatings. Materials Science and Engineering: A. 2004; 381(1–2): 175–188. DOI: 10.1016/j.msea.2004.04.017.

[40] Li J., Sun Y., Sun X., Qiao J. Mechanical and corrosion-resistance performance of electrodeposited titania-nickel nanocomposite coatings. Surface and Coatings Technology. 2005; 192(2–3): 331–335. DOI: 10.1016/j.surfcoat.2004.04.082.

[41] Battisti L.C. Influência do pH e da velocidade de agitação do banho de eletrodeposição no desempenho de revestimentos de zinco e zinco-nanocompósitos [dissertation]. Novo Hamburgo, RS: Universidade Feevale; 2011. 80 p.

[42] Takahashi A., Miyoshi Y., Hada T. Structure of electrodeposited Zn-7 wt% Cr alloy. Journal of the Surface Finishing Society of Japan. 1994; 45(3): 301–306. DOI: 10.4139/sfj.45.301.

[43] Sajjadnejad M., Omidvar H., Javanbakht M., Pooladi R., Mozafar A. Direct current electrodeposition of Zn and Zn-SiC nanocomposite coatings. Transactions of the IMF. 2014; 92(4): 227–232. DOI: 10.1179/0020296714Z.000000000187.

[44] Fustes J., Gomes A., Pereira M.I.D. Electrodeposition of Zn-TiO_2 nanocomposite films-effect of bath composition. Journal of Solid State Electrochemistry. 2008; 12(11): 1435–1443. DOI: 10.1007/s10008-007-0485-z.

[45] Zamblau I., Varvara S., Muresan L.M. Corrosion behaviour of Cu-SiO_2 nanocomposite coatings obtained by electrodeposition in the presence of cetyltrimethyl ammonium bromide. Journal of Materials Sicence. 2011; 46(20): 6484–6490. DOI: 10.1007/s10853-011-5594-5.

[46] Eroglu D., Vilinska A., Somasundaran P., West A.C. Use of dispersants to enhance incorporation rate of nano-particles into electrodeposited films. Electrochimica Acta. 2013; 113: 628–634. DOI: 10.1016/j.electacta.2013.09.113.

[47] Sen R., Das S., Das K. Effect of stirring rate on the microstructure and microhardness of Ni-CeO_2 nanocomposite coating and investigation of the corrosion property. Surface and Coatings Technology. 2011; 205(13–14): 3847–3855. DOI: 10.1016/j.surfcoat.2011.01.057.

[48] Kim S.K., Yoo H.J. Formation of bilayer Ni-SiC composite coatings by electrodeposition. Surface and Coatings Technology. 1998; 108–109(0): 564–569. DOI: 10.1016/S0257-8972(98)00589-1.

[49] Baghery P., Farzam M., Mousavi A.B., Hosseini M. Ni-TiO_2 nanocomposite coating with high resistance to corrosion and wear. Surface and Coatings Technology. 2010; 204(23): 3804–3810. DOI: 10.1016/j.surfcoat.2010.04.061.

[50] Bund A., Thiemig D. Influence of bath composition and pH on the electroco-deposition of alumina nanoparticles and nickel. Surface and Coatings Technology. 2007; 201(16–17): 7092–7099. DOI: 10.1016/j.surfcoat.2007.01.010.

[51] Lekka M., Zendron G., Zanella C., Lanzutti A., Fedrizzi L., Bonora P.L. Corrosion properties of micro- and nanocomposite copper matrix coatings produced from a copper pyrophosphate bath under pulse current. Surface and Coatings Technology. 2011; 205(11): 3438–3447. DOI: 10.1016/j.surfcoat.2010.12.003.

[52] Silva F.L.G., et al. Response surface analysis to evaluate the influence of deposition parameters on the electrodeposition of Cu-Co alloys in citrate medium. Journal of Applied Electrochemistry. 2008; 38(12): 1763–1769. DOI: 10.1007/s10800-008-9630-3.

[53] Lee H.-K., Lee H.-Y., Jeon J.-M. Co-deposition of micro- and nano-sized SiC particles in the nickel matrix composite coatings obtained by electroplating. Surface and Coatings Technology. 2007; 201(8): 4711–4717. DOI: 10.1016/j.surfcoat.2006.10.004.

[54] Stojak J.L., Talbot J.B. Investigation of electrocodeposition using a rotating cylinder electrode. Journal of the Electrochemical Society. 1999; 146(12): 4504–4513. DOI: 10.1149/1.1392665.

[55] Sun K.-N., Hu X.-N., Zhang J.-H., Wang J.-R. Electrodeposited Cr-Al_2O_3 composite coating for wear resistance. Wear. 1996; 196(1–2): 295–297. DOI: 10.1016/0043-1648(95)06860-0.

[56] Roventi G., Bellezze T., Fratesi R. Electrodeposition of Zn-SiC nanocomposite coatings. Journal of Applied Electrochemistry. 2013; 43(8): 839–846. DOI: 10.1007/s10800-013-0571-0.

[57] Daltin D. Tensoativos: Química, Propriedade e Aplicações. São Paulo: Edgard Blucher; 2011.

[58] Hovestad A., Janssen L.J.J. Electrochemical co-deposition of inert particles in a metallic matrix. Journal of Applied Electrochemistry. 1995; 25(6): 519–527. DOI: 10.1007/bf00573209.

[59] Ghorbani M., et al. Electro deposition of graphite-brass composite coatings and characterization of the tribological properties. Surface and Coatings Technology. 2001; 148(1): 71–76. DOI: 10.1016/s0257-8972(01)01322-6.

[60] Iwakura C., Furukawa N., Tanaka M. Electrochemical preparation and characterization of Ni/(Ni + RuO_2) composite coatings as an active cathode for hydrogen evolution. Electrochimica Acta. 1992; 37(4): 757–758. DOI: 10.1016/0013-4686(92)80081-V.

[61] Lima T.G. Eletrodeposição de revestimentos funcionais compósitos Cu/partículas de óxidos de alumínio [dissertation]. Rio de Janeiro, RJ: Universidade do Estado do Rio de Janeiro; 2013. 155 p.

[62] Aruna S.T., Grips V.K.W., Rajam K.S. Synthesis and characterization of Ni-Al_2O_3 composite coatings containing different forms of alumina. Journal of Applied Electrochemistry. 2010; 40(12): 2161–2169. DOI: 10.1007/s10800-010-0198-3.

[63] Guglielmi N. Kinetics of the deposition of inert particles from electrolyte baths. Journal of Applied Electrochemical. 1972; 119(8): 1009–1012. DOI: 10.1149/1.2404383.

[64] Celis J.P., Roos J.R., Buelens C. A mathematical model for the electrolyte co-deposition of particles with a metallic matrix. Journal of Applied Electrochemical. 1987; 134(6): 1402–1408. DOI: 10.1149/1.2100680.

[65] Oliveira R.S., Pinheiro M.A.S. Caracterização de Materiais Compósitos. In: XI CREEM; 30 de agosto a 3 de setembro; Nova Friburgo, RJ. 2004.

[66] Zheng H.-Y., An M.-Z. Electrodeposition of Zn-Ni-Al_2O_3 nanocomposite coatings under ultrasound conditions. Journal of Alloys and Compounds. 2008; 459(1–2): 548–552. DOI: 10.1016/j.jallcom.2007.05.043.

[67] Souza E.A. Avaliação de inibidores de corrosão para sistemas de resfriamento industrial operando com ciclo elevado de concentração [dissertation]. Rio de Janeiro, RJ: Universidade Federal do Rio de Janeiro; 2007. 114 p.

[68] Brandes E.A., Goldthorpe D. Electrodeposition of cermets. Metallurgia. 1967; 76(11): 195–198.

[69] Withers J.C. Electrodepositing cermets. Products Finishing. 1962; 26(11): 62–68.

[70] Martin P.W., Williams R.V. Proc. Interfinish. British Iron and Steel Research Association, London; 1964. 64, p. 182–188.

[71] Foster J., Kariapper A.M.J. Transactions of the IMF. 1973; 51: 27–31.

[72] Tsay P., Hu C.C. Non-anomalous co-deposition of iron-nickel alloys using pulse reverse electroplating through means of experimental strategies. Journal of Electrochemical Society. 2002; 149(10): C492–C497. DOI: 10.1149/1.1504718.

[73] Chang S.-C., Shieh J.M., Dai B.-T., Feng M.-S. The effect of plating current densities on self-annealing behaviours of electroplated copper films. Journal of Electrochemical Society. 2002; 149(9): G535–G538. DOI: 10.1149/1.1500348.

[74] Yoshimura S., Yoshihara S., Shorakashi T., Sato E. Preferred orientation and morphology of electrodeposited iron from iron(II) chloride solution. Electrochimica Acta. 1994; 39(4): 585–595. DOI: 10.1016/0013-4686(94)80105-3.

[75] Zhargami V., Ghorbani M. Alteration of corrosion and nanomechanical properties of pulse electrodeposited Ni/SiC nanocomposite coatings. Journal of Alloys and Compounds. 2014; 598: 236–242. DOI: 10.1016/j.jallcom.2014.01.220.

[76] Praveen B.M., Venkatesha T.V. Electrodeposition and properties of Zn-nanosized TiO_2 composite coatings. Applied Surface Science. 2008; 254(8): 2418–2424. DOI: 10.1016/j.apsusc.2007.09.047.

[77] Dorri-Moghadam A., Schultz B.F., Ferguson J., Omrani E., Rohatgi P.K., Gupta N. Functional metal matrix composites: self-lubricating, self-healing, and nanocomposites-an outlook. Journal of the Minerals, Metals and Materials. 2014; 66(6): 872–881. DOI: 10.1007/s11837-014-0948-5.

[78] Ferguson J., Sheykh-Jaberi F., Kim C.-S., Rohatgi P.K., Cho K. On the strength and strain to failure in particle-reinforced magnesium metal-matrix nanocomposites (Mg MMNCs). Material Science Engineering A. 2012; 558: 193–204. DOI: 10.1016/j.msea.2012.07.111.

[79] Greef R., Peat R., Peter L.M., Pletcher D., Robinson J. Instrumental Methods and Electrochemistry. London: Woodhead Publishing; 1985. 442 p.

[80] Bard A.J., Faulkner L.R. Electrochemical Methods: Fundamentals and Applications. 2nd ed. London: John Wiley & Co; 2000. 864 p.

[81] Brett A.M.O., Brett C.M. Eletroquímica—Princípios, Métodos e Aplicações. 1st ed. Coimbra, Portugal: Almedina Brasil; 1996. 472 p.

[82] Creus J., Mazille H., Idrissi H. Porosity evaluation of protective coatings onto steel through electrochemical techniques. Surface and Coatings Technology. 2000; 130(2–3): 224–232. DOI: 10.1016/S0257-8972(99)00659-3.

[83] Scully J.R., Taylor D.W. Electrochemical Methods of Corrosion Testing. 9th ed. American Society for Metals; 1987; 13. 212 p.

[84] Wang S., Bradford S.A. Potentiodynamic polarization measurement by controlling potential inside a crevice. In: Bronson A., Warren G., editors. Techniques for Corrosion Measurement. Houston: National Association of Corrosion Engineers; 1992.

[85] Grundmeier G., Schmidt W., Stratmann M. Corrosion protection by organic coatings: electrochemical mechanism and novel methods of investigation. Electrochimica Acta. 2000; 45(15–16): 2515–2533. DOI: 10.1016/S0013-4686(00)00348-0.

[86] Olivier M.-G., Poelman M. Use of electrochemical impedance spectroscopy (EIS) for the evaluation of electrocoatings performances. In: Recent researches in corrosion evaluation and protection. Belgium: InTechOpen; 2012. p. 1–26. DOI: 10.5772/1843.

[87] Szczygieł B., Kołodziej M. Composite Ni/Al_2O_3 coatings and their corrosion resistance. Electrochimica Acta. 2005; 50(20): 4188–4195. DOI: 10.1016/j.electacta.2005.01.040.

[88] Helle K., Walsh F. Electrodeposition of composite layers consisting of inert inclusions in a metal matrix. Transactions of the IMF. 1997; 75: 53–58. DOI: 10.1179/0020296713Z.000000000161.

[89] Katamipour A., Farzam M., Danaee I. Effects of sonication on anticorrosive and mechanical properties of electrodeposited Ni-Zn-TiO_2 nanocomposite coatings. Surface and Coatings Technology. 2014; 254: 358–363. DOI: 10.1016/j.surfcoat.2014.06.043.

[90] Bryleva E.Y., Vodolazkaya N.A., Mchedlov-Petrossyan N.O., Samokhina L.V., Matveevskaya N.A., Tolmachev A.V. Interfacial properties of cetyltrimethylammonium-coated SiO_2 nanoparticles in aqueous media as studied by using different indicator dyes. Journal of Colloid Interface Science. 2007; 316(2): 712–722. DOI: 10.1016/j.jcis.2007.07.03.

[91] Lekka M., et al. Mechanical and anticorrosive properties of copper matrix micro- and nano-composite coatings. Electrochimica Acta. 2009; 54(9): 2540–2546. DOI: 10.1016/j.electacta.2008.04.060.

[92] Manahan S.E. Polarographic investigation of the allyl alcohol complex of copper(I) in aqueous solution. Inorganic Chemistry. 1966; 5(3): 482–483. DOI: 10.1021/ic50037a034.

Chapter 9

Parametric Analysis of Electrodeposited Nano-composite Coatings for Abrasive Wear Resistance

Kavian O. Cooke

Additional information is available at the end of the chapter

http://dx.doi.org/10.5772/62153

Abstract

Nano-composite coatings have become the focus of widespread research in recent years due in part to their superior properties when compared to purely metallic films. The benefits of using these types of coatings include high-specific heat, optical non-linearity, novel magnetic properties, enhanced mechanical behavior (large hardness and wear resistance), and good corrosion resistance. This chapter presents a parametric study of electrodeposited nano-composite coatings for improved abrasive wear resistance. The following physical parameters were investigated using a Taguchi L_{18} fractional factorial design of experiments (DOEs): current density, pH, bath temperature, nano-particle concentration, and electrolyte agitation (stir rate). The results were evaluated using the signal-to-noise (S/N) ratio to develop a non-dimensional relationship between the physical parameters and the abrasive wear resistance of the coating. The relationship showed that the abrasive wear resistance of the coating increases as the quantity of nano-particle in the solution and the agitation frequency increase. The analysis of variance (ANOVA) indicated that the particle concentration had the greatest significance to the wear resistance of the coating.

Keywords: Electrodeposition, wear resistance, optimization, Taguchi, nano-composite coating

1. Introduction

Advanced engineering applications often require multifunctional materials with improved performance capabilities, which are usually difficult to fulfill using single-phase materials [1, 2]. The growing demand for improved material performance has led to the development of numerous nano-structured coatings and nano-composite coatings capable of achieving certain technological goals [3–6]. According to Wu et al. [7], these improved properties observed in

nano-coatings have increased their range of application. Currently, these materials find application in medicine, aerospace, automotive, dentistry, electronics, and so on [8–12].

The incorporation of these particles during deposition enables the production of a wide range of composite coatings, which significantly improves the coatings' physical and chemical properties, compared to the pure metallic coatings. These properties are however dependent on the volume of particles that are incorporated in the coating during deposition and the uniformity of the distribution. The amount of incorporated particles is a key parameter for the successful application of the coatings, because it largely determines the properties of composites such as wear resistance, high-temperature corrosion protection, oxidation resistance, and self-lubrication.

The uniformity of the particle distribution within the metal matrix is strongly influenced by the metal matrix morphological and structural characteristics. As such, the co-deposition of a sufficient amount of non-agglomerated particles should lead to production of harder and more wear-resistant coatings. The concentration of particles suspended in solution ranges from 2 g/L up to 200 g/L, producing composites with typically 1–10 vol.% of embedded particles [13].

Particle-reinforced nano-composite coatings based on nickel and alumina are being applied in different technological fields with high demands for wear and corrosion resistance [3]. Lekka et al. [14] show that the co-deposition of SiC nano-particles in copper matrix leads to a more noticeable grain refinement, and therefore, the nano-composite deposits presented a very high micro-hardness, 61% higher than pure copper deposits, and an increase of 58% of the abrasion resistance. Future applications of these materials depend on the ability to produce them with controlled composition and properties, using inexpensive and reliable techniques.

Electrodeposition method satisfies some of these requirements because it is an economical and versatile technique compared to other preparation techniques. Electrodeposited nano-composite coatings are generally obtained by suspending charged ceramic nano-particles in the electrolyte and co-depositing them with the metal. During the electrodeposition process, these insoluble hard particles are suspended in a conventional plating electrolyte and are captured in the growing metal film during deposition. An effective dispersion of inert particles in the electrolyte promotes the adsorption opportunity of inert particles on the cathode and causes a higher volume content of inert particles in the composite coating. The mechanical properties of the composite coating are also promoted by the enhancement of the volume content of inert particles in the coating [15–17].

Two mechanisms have been proposed to describe the process by which ceramic particles are incorporated in the metallic coatings: (1) the first mechanism is known as electrophoresis. The electrophoresis process begins with particles that are well dispersed and are able to move independently in the solvent suspension, and the particles have a surface charge due to electrochemical equilibrium with the solvent. This leads to a migratory attraction of the particles to the deposition electrode [18]. (2) A second mechanism was proposed by Williams and Martin in 1964. In their study, the researchers suggested that the particles were transported to the cathode by a purely mechanical mean due to the agitation of the bath, which leads to entrapment and subsequent embedding of the particles in the growing metal layer [19].

http://dx.doi.org/10.5772/62153

However, the validity of mechanical particle entrapment theory was later challenged by Brandes and Goldthorpe, who suggested that there is some attractive force holding the particles at the cathode long enough to be incorporated by the growing metal layer [20]. Guglielmi proposed a two-step mechanism taking into account electrophoresis and adsorption.

In the first step, particles approaching the cathode become loosely adsorbed on the cathode surface [21]. These loosely adsorbed particles are still surrounded by a cloud of adsorbed ions. In the second step, the particles lose this ionic cloud and become strongly adsorbed on the cathode. This step is thought to be of an electrochemical character; that is, it depends on the electrical field at the cathode. Finally, the strongly absorbed particles are occluded by the growing metal layer [1, 22–25]. One method that has been used to reduce particle coagulation is mechanical stirring [26]. If a particle is strongly adsorbed on the cathode, it will be embedded on the growing metal layer by the electrodeposition of free solvated electro-active ions from the plating bath [3, 23].

According to the scientific literature, the factors that affect the coating properties are directly related to the parameter settings during the deposition process, and as such optimization is an important step in coating development. This chapter presents a parametric study of electrodeposited nano-composite coatings for improved abrasive wear resistance using the Taguchi L_{18} design of experiments (DOEs). The main focus is to evaluate the effects of the coating parameters on its wear resistance, with the objectives being to identify the optimal setting of each parameter and to quantify the contribution of each parameter to the wear resistance of the coating.

2. Experimental Procedure

2.1. Parametric design using Taguchi techniques

In this study, parametric optimization was achieved using Taguchi L_{18} fractional factorial DOE to evaluate the parameters of the electroplating process used for depositing the Ni/Al_2O_3 composite coating for improved hardness and wear resistance. The main process parameters evaluated were cathode current density and agitation/stir rate (A), the pH level of the solution (B), particle concentration (C), and bath temperature (D). The parameter settings used, shown in Table 1, were determined through preliminary investigation and represent three different level settings (levels 1–3). The orthogonal array is presented in Table 2 and shows the parameter combination for each of the 18 experimental runs using the level settings, as shown in Table 1 [27].

The optimization can be achieved by calculating the signal-to-noise (S/N) ratio as a quality tool for evaluating the performance of the coatings produced. The S/N ratio (η) represents the degree of predictable performance of the coatings in the presence of noise factors. To calculate the S/N ratio, the average and variation of the experimental results can be determined using Equation 1 [6].

$$\eta = -10 \log(\text{MSD}), \tag{1}$$

where MSD is the mean square deviation for the output characteristic. As the aim of this study is to minimize the wear loss of the coating, the smaller-is-better quality characteristic was selected and can be calculated using Equation 2 [28].

$$\text{Smaller is better} - \text{MSD} = \frac{1}{n}\sum_{i=1}^{n} y_i^2 \tag{2}$$

Level	Current density (A/mm^2) (A)	Stir rate (rpm) (B)	Bath pH (C)	Al_2O_3 concentration (g/L) (D)	Bath temperature (°C)
1	2.3	440	4.0	10	40
2	2.5	600	4.45	20	50
3	–	800	4.6	30	60

Table 1. Experimental levels used for electrodeposition process.

Experiment	Controlled parameters				
	A	**B**	**C**	**D**	**E**
1	1	1	1	1	1
2	1	1	2	2	2
3	1	1	3	3	3
4	1	2	1	1	2
5	1	2	2	2	3
6	1	2	3	3	1
7	1	3	1	2	1
8	1	3	2	3	2
9	1	3	3	1	3
10	2	1	1	3	3
11	2	1	2	1	1
12	2	1	3	2	2
13	2	2	1	2	3
14	2	2	2	3	1
15	2	2	3	1	2
16	2	3	1	3	2
17	2	3	2	1	3
18	2	3	3	2	1

Table 2. Taguchi L_{18} orthogonal array.

http://dx.doi.org/10.5772/62153

On the other hand, given the relationship between hardness and wear resistance [3], the larger-the-better characteristic was used to optimize the coating for hardness, as shown in Equation 3:

$$\text{Larger is better} - \text{MSD} = \frac{1}{n}\sum_{i=1}^{n}\frac{1}{y_i^2}, \tag{3}$$

where y_i is the value of wear resistance for the ith test; and n is the number of tests.

The average value of the response variable at each parameter level was determined by applying Equation 4 to each parameter level for each factor [24]:

$$m_{A1} = \frac{1}{3}(\eta_1 + \eta_2 + \eta_3). \tag{4}$$

2.2. ANOVA

The analysis of variance (ANOVA) was carried out to examine the influence of each process parameter on quality characteristics. If some parameters do not significantly affect wear rate, they can be fixed to a minimum level and excluded from the optimization process. The percent contribution of each parameter was calculated by determining the total sum of squared deviation and the individual contribution of each parameter to the sum of squared deviations. These variables were calculated using Equations 7:

$$\text{SS}_\text{T} = \frac{1}{n}\sum_{i=1}^{9}(\eta_i - \bar{\eta})^2 \tag{5}$$

$$\bar{\eta} = \frac{1}{9}\sum_{i=1}^{9}\eta_i \tag{6}$$

$$\text{SS}_\text{d} = 3x(\eta_{A1} - \bar{\eta})^2 + 3x(\eta_{A2} - \bar{\eta})^2 + 3x(\eta_{A3} - \bar{\eta})^2 \tag{7}$$

The percentage contribution (ρ) of each factor to the overall response is determined using Equation 8:

$$\rho = \frac{\text{SS}_\text{d}}{\text{SS}_\text{T}} \times 100. \tag{8}$$

2.3. Sample preparation and characterization

The mild steel samples of dimensions 0 × 20 × 15 mm were cut, prepared to 800-grit abrasive paper, and polished to 1-μm diamond suspension, after which they were cleaned in an acetone bath (see Figure 1a). Acid pickling took place in a solution of 15 wt.% HNO_3 and 2 wt.% HF at 50°C for 2 minutes and then rinsed in distilled water. These samples were then used as the cathode in the plating solution.

The electrodeposition of an Ni/Al_2O_3 coating was carried out in a 250-mL glass beaker, as shown in Figure 1(b). The plating solution was prepared by dissolving 250 g/L $NiSO_4$ $6H_2O$, 45 g/L $NiCl_2$ $6H_2O$, 35 g/L H_3BO_3, and 1 g/L saccharin in distilled water. The ceramic particles were added separately to the nickel bath to produce the composite coating. The particles were thoroughly mixed into the solution for 2 hours and kept in suspension in the bath with a magnetic stirrer. The following parameters were adjusted: cathode current density, agitation, and stir rate (A); the pH level of the solution (B); concentration of composite particles (C); and bath temperature (D), as shown in Table 1. The thickness of Ni/Al_2O_3p coatings was controlled by the plating time. The actual amount of Ni/Al_2O_3p electroplated onto a surface was determined by the weight gain after the plating process.

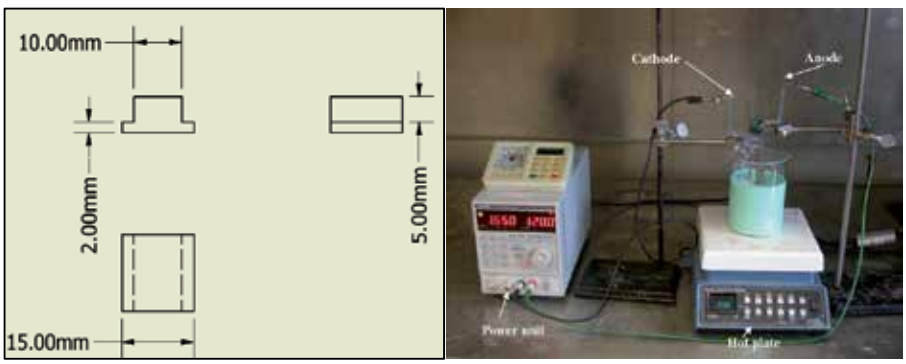

(a) (b)

Figure 1. (a) Specimen size of wear resistance test sample and (b) electroplating equipment and setup.

Coated samples were evaluated for hardness using a Vickers Mitutoyo HM-122 hardness tester with a load of 200 g. Two body abrasive wear tests were conducted using Plint Multi-station Block-on-Ring tester under a load of 20 N at a fixed sliding speed of 3.35 m/s for a sliding distance of 5000 m against steel disc of hardness 500 HV. During sliding, the load is applied on the specimen through cantilever mechanism, and the specimens brought in intimate contact with the rotating disc at a track radius of 100 mm. The samples were cleaned with acetone and weighed (up to an accuracy of 0.01 mg using a Sartorius microbalance) before and after each test. The wear rate was calculated from the weight loss measurement and expressed in terms of volume loss per unit sliding distance.

http://dx.doi.org/10.5772/62153

For each coated sample, three specimens were tested and the average value was used to determine the wear resistance. Examination of the joints microstructure was performed using a Ziess optical microscope, an ASPEX 309 scanning electron microscope (SEM), and a transmission electron microscope (TEM). Quantitative compositional analyses were carried out using wavelength dispersive spectroscopy (WDS) and x-ray diffraction (XRD). Micro-hardness testing was performed on the cross section of the joints according to ASTM E92 standard test method for a Vickers micro-hardness testing. Indentations were made at 100 μm spacing using a diamond tip indenter to which a 0.2 kg load was applied for 15 seconds, after which the length of the diagonals was measured and the hardness number was recorded from tables.

For TEM analyses, sections of the coating were cut to 6 × 5 × 1.5 mm using a thin diamond tip cutter and subsequently mechanically grounded using 600 grit abrasive paper to a thickness of approximately 200 μm. Disc of 3 mm diameter was punched from the 200-μm coating and subsequently mechanically grinded to 25 μm. The grinded samples were thinned by electropolishing method. This was done in a solution containing 150 g/L Na_2CO_3 + 50 g/L Na_3PO_4 + 30 g/L. The solution was maintained at a temperature of 40°C and a voltage of 20 V. All the thinned coatings were examined with a JEOL TEM 2000FX TEM at an accelerating voltage of 200 kV.

3. Results and Discussion

3.1. Microstructure analysis

The TEM micrograph of the Ni/Al_2O_3 coating, as shown in Figure 2(a), revealed the presence of nanosized Al_2O_3 particles embedded in the nickel matrix. The deposition of particle reinforcement during the coating process can be attributed to parameters such as current densities, bath temperature, stir rate, bath pH, and particle concentration [29]. TEM analysis of the as-received powder shown in Figure 2(b) indicated the presence of agglomerated particle clusters. These particle clusters are believed to have been subsequently embedded in the coating during the electrodeposition process. In situations where particle clustering is present, surfactants such as saccharin, hexadecylpyridinium bromide (HPB), and cetyltrimethylammonium bromide (CTAB) are used to improve particle distribution and reduce clustering [4, 30, 31]. In this study, the surfactant saccharin was used to reduce particle clustering; however, particle agglomeration was still present, as shown in Figure 2(a).

An optical micrograph of the nano-composite Ni/Al_2O_3 coating deposited using current density 3.2 × 10^{-4} A/mm^2, stir rate 440 rpm, bath temperature 50°C, pH 4.45, and particle concentration 20 g/L is shown in Figure 3(a). Analysis of the image revealed Al_2O_3 particle clusters consistent with the particle agglomeration observed in the as-received Al_2O_3 powder is shown in Figure 3(b). Similar surface morphology obtained for coatings deposited using current density 5 × 10^{-4}A/mm^2, stir rate 820 rpm, bath temperature 60°C, pH 4.45, and particle concentration 10 g/L was observed to posses large globules that are believed to be agglomerated Al_2O_3 particles embedded into the Ni matrix.

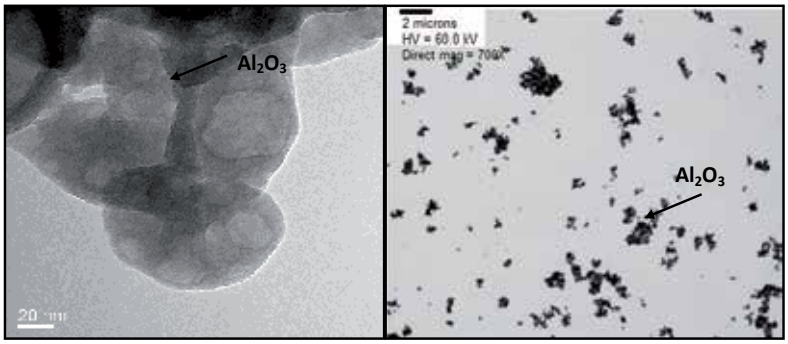

Figure 2. TEM image of the Ni/Al_2O_3coating.

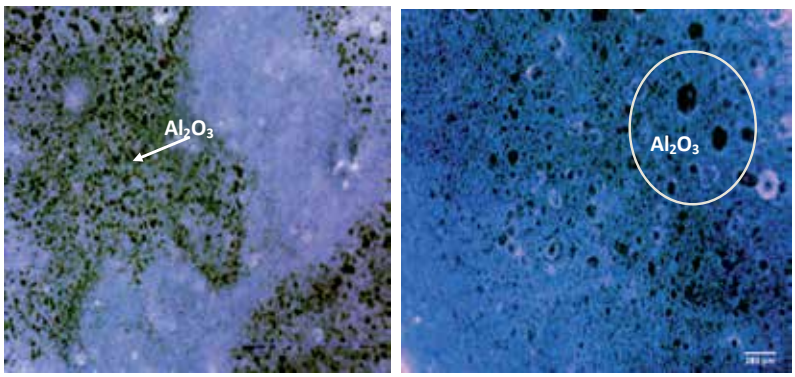

(a) (b)

Figure 3. Optical micrograph of coatings deposited with the parameters outlined in experiment: (a) 2 and (b) 17, as shown in Table 2.

3.2. Micro-hardness

The influence of the process parameters was assessed to maximize the coating hardness. Analysis of the surface hardness revealed that if the parameters were set to current density at level 1 (3.2×10^{-4} A/mm^2), revolutions per minute (RPM) at level 2 (630 rpm), pH at level 2 (4.45), Al_2O_3 concentration at level 3 (30 g/L), and temperature at level 2 (50°C), a surface hardness of 501.5 HV can be achieved. When compared with pure nickel, a surface hardness of 278.82 HV was achieved. The differences observed were attributed to dispersion hardening effects caused by the presence of nanosized Al_2O_3 in the composite coating. According to Lehman et al. [32], the nanosized particles act to restrict/reduce dislocation motion in the nickel matrix, which causes an increase in the surface hardness. The ANOVA test showed that stir rate (RPM), particle concentration, and bath pH had the greatest impact on the hardness of the coatings.

http://dx.doi.org/10.5772/62153

Stir rate (RPM) is used to disperse the nano-particles during the coating process, thus controlling the microstructure produced by keeping particles suspended in the bath solution during coating [33, 34]. It is believed that stirring increases the amount of nano-particles embedded in the coating up to 630 rpm beyond which a reduction in surface hardness is observed.

Similar effects were observed when the concentration of Al_2O_3 particles suspended in the solution increased. The results indicated that particle incorporated into the coating increased with increasing particle concentration in the bath solution until 30 g/L was reached. The microstructure of the coating may also be attributed to the pH of the bath which is believed to control the nucleation and morphology of the coating; as the pH decreases, the grain size of the crystallite also decreases, resulting in an increase in the hardness of the material [35, 36]. The estimated effect of each parameter is shown graphically in Figure 4. Analysis of the data using the larger-is-better characteristics indicated that optimum coating hardness can be achieved if concentration is set to level 3, while all other parameters are set to level 2.

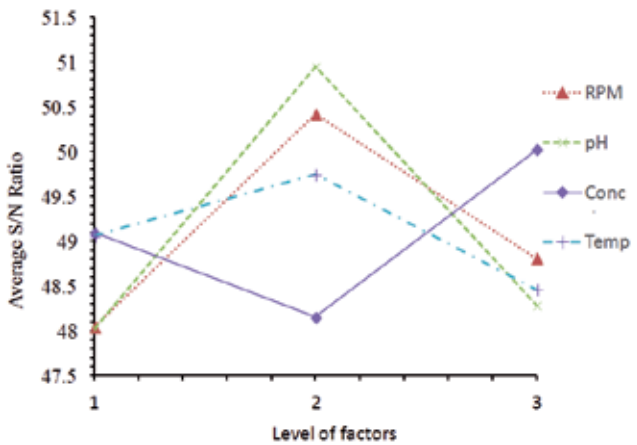

Figure 4. Effect of process parameters on micro-hardness.

3.3. Wear testing

Two-body abrasive wear tests were carried out to evaluate the effects of electroplating parameters on the wear resistance of the deposited coating. Evaluation of the results presented in Table 3 indicated that the wear rate increased from 0.22 kg/s to 2.11 kg/s. The estimated effect of each parameter is shown graphically in Figure 5. Analysis of the data using the smaller-is-better characteristics indicated that the S/N ratio decreased as the stir rate increased from 440 rpm to 630 rpm; however, increasing the stir rate to 820 rpm corresponded to an increase of the S/N ratio; this change can be attributed to achieving suitable particle suspension in the solution at 630 rpm; however, further increase in stir rate caused an increase turbulence in the solution, which can reduce particulate inclusion in the Ni matrix [34]. The impact of bath pH and temperature had similar effects on the S/N ratio [34]. The results indicated that minimal mass loss can be achieved if both pH and temperature are set to level 1 [37].

In addition, the results further revealed that particle concentration had a significant effect on the wear rate, which corresponded to an increase in the hardness of the coatings deposited as the particle concentration increased from 10 g/L to 20 g/L. The reduction in wear rate was attributed to the increase in the Al_2O_3 particles embedded in the Ni matrix during the co-deposition process. The Al_2O_3 nano-particulates co-deposited in the Ni matrix could restrain the Ni grains and the plastic deformation of the matrix under a loading due to dispersion strengthening. The effect is that the coating becomes stronger as the nano-Al_2O_3 particle content increases, thus increasing micro-hardness and wear resistance of the coating. Further increase in the particle content resulted in increase of the brittleness of the coating, which is subsequently reflected as a reduction of the wear resistance of the coating. By utilizing the wear resistance values shown in Table 4, the optimum coating parameters were determined to be A2, B1, C2, and D1.

Experiment	Current density (A)	Stir rate (B)	pH	Concentration (C)	Temperature (D)	Hardness	S/N	Wear rate	S/N
	(A/mm^2; × 10^{-4})	(rpm)		(g/L)	(°C)	(HV)	(η; dB)	(×10^{-6}) (kg/s)	(η; dB)
1	3.2	440	4.3	10	40	208.5	46.38	2.11	116.32
2	3.2	440	4.45	20	50	318.3	50.06	1.00	122.50
3	3.2	440	4.6	30	60	268.3	48.57	0.220	137.44
4	3.2	630	4.3	10	50	357.3	51.06	0.44	131.19
5	3.2	630	4.45	20	60	325.5	50.25	1.10	122.59
6	3.2	630	4.6	30	40	369.4	51.35	0.88	124.32
7	3.2	820	4.3	20	40	300	49.54	0.66	128.05
8	3.2	820	4.45	30	50	363.9	51.22	0.55	129.39
9	3.2	820	4.6	10	60	199.9	46.02	1.00	123.36
10	5	440	4.3	30	60	224.5	47.02	0.66	127.16
11	5	440	4.45	10	40	282.1	49.01	0.33	133.18
12	5	440	4.6	20	50	229.9	47.23	0.55	128.36
13	5	630	4.3	20	60	219	46.81	1.00	122.84
14	5	630	4.45	30	40	449.8	53.06	0.22	136.57
15	5	630	4.6	10	50	582.9	49.99	1.00	122.18
16	5	820	4.3	30	50	279.7	48.93	0.33	133.18
17	5	820	4.45	10	60	403.5	52.12	0.33	132.38
18	5	820	4.6	20	40	178.5	45.03	0.88	124.22

Table 3. Measured results of response variables and S/N ratios.

http://dx.doi.org/10.5772/62153

Factors	Code	Wear rate S/N ratio (dB)			Hardness S/N ratio (dB)		
		1	2	3	1	2	3
Stir rate	A	127.49	126.6	128.43	48.05	50.42	48.81
pH level	B	126.46	129.43	126.65	48.03	50.95	48.29
Al_2O_3 concentration	C	126.44	124.76	131.34	49.1	48.15	50.03
Bath temperature	D	128.47	130.76	129.30	49.06	49.75	48.46

Table 4. Mean S/N ratio of individual levels.

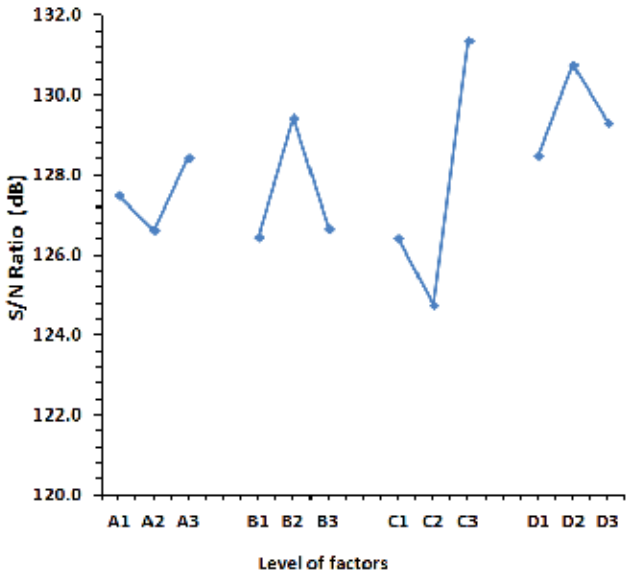

Figure 5. Effect of process parameters on wear resistance.

3.4. Analysis of the level averages

A second analysis using the level averaging technique was also carried out by averaging the experimental results achieved at each level for the respective parameter. A summary of these calculations is shown in Table 5 and is graphically represented in Figure 6. When the effects of stir rate and concentration were evaluated, it was found that the wear rate decreased as both concentration and stir rate increased similar to the results obtained when the S/N ratio was calculated. The optimum wear resistance can be obtained by setting both the stir rate and concentration are set to level 3, whereas bath temperature and pH are set to level 2. Optimization for hardness revealed that all the parameter settings were similar with the only exception being stir rate, which required a level 2 setting (Figure 7). These results are also consistent with literature [34, 37].

Factors	Code	Parameter levels(wear resistance test) × 10^{-7}			Hardness $HV_{0.2\,kg}$		
		1	2	3	1	2	3
Current density		8.84	5.89	0	301.2	287	0
RPM	A	8.12	7.73	6.25	255.3	339.5	287.6
pH	B	7.55	5.88	8.67	260.3	306.2	264.8
Al_2O_3 concentration	C	8.68	8.65	4.77	294.5	261.9	325.9
Bath temperature	D	8.47	6.45	7.18	298.1	310.8	273.5

Table 5. Level averages for each parameter.

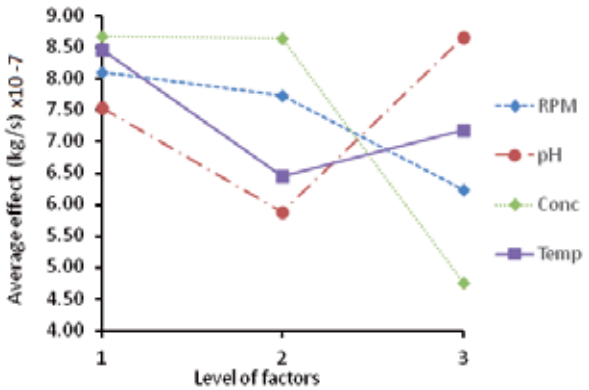

Figure 6. Mean wear rate of each parameter level.

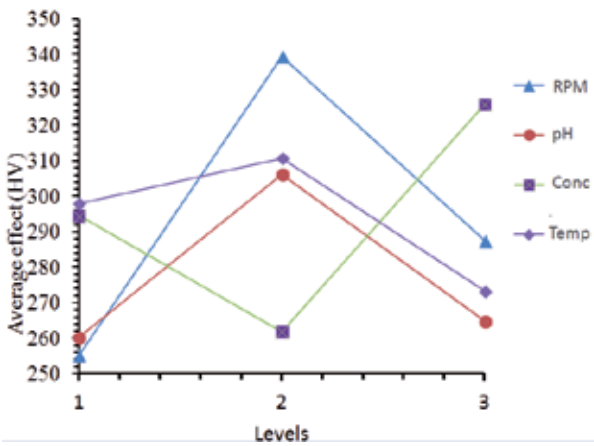

Figure 7. Mean hardness of each parameter level.

http://dx.doi.org/10.5772/62153

3.5. ANOVA

The ANOVA separates the total variability of the response into percentage contribution (P) of each parameter. The higher the percentage contribution, the more important the parameter is to the wear resistance and hardness of the coating. Table 6 shows the ANOVA calculated values and indicates that the greatest contributing factor for wear was the Al_2O_3 particle concentration at 51.68% followed by bath temperature with a contribution of 32.41%, whereas bath pH and stir rate had the lowest impact on the wear resistance of the coating.

Factors	Code	DOF	Sum of squares	Variance	Contribution(%)
Stir rate	A	2.00	5.0	2.48	3.64
pH	B	2.00	16.67	8.33	12.27
Al_2O_3 concentration	C	2.00	70.20	35.10	51.68
Bath t**emperature**	D	2.00	44.03	22.01	32.41
Total		8.00	135.8		100.0

Table 6. ANOVA for wear.

3.6. Selection of the optimum parameters

To select the optimum parameter settings for improved wear resistance, the "smaller-is-better" characteristics were used to select the optimized parameter level, which are shown in Table 7. Table 7 indicates one conflict in the recommended optimized levels: factor A (stir rate). Analysis of the results for both S/N ratio averages and the level averages revealed that the stir rate greater than 630 rpm would result in minimum output; however, analysis of the level-averaged wear rate indicated that a setting at level 2 would be more appropriate. The results suggest that within the parameter levels tested, pH and stir rate had the least effect on the wear rate.

Factors	Code	Optimized levels	
		$\bar{Y}$	S/N ratio
Stir rate	A	3	2
pH	B	2	2
Al_2O_3 concentration	C	3	3
Bath temperature	D	2	2

Table 7. Summary of the factor analysis.

3.7. Confirmation test

Experimental validation of the Taguchi optimization process was necessary to confirm that the minimum wear rate can be achieved using the optimum coating parameters. A conforma-

tional experiment was conducted with the levels of the process parameters (A3, B2, C3, and D2), resulting from the optimization process. Two wear rate values were obtained (4.4E-07 kg/s and 4.1E-07 kg/s), and the average of these values was found to be 4.25E-07 kg/s with an average hardness of 501.5 HV.

An SEM micrograph of the optimized Ni/Al_2O_3 coating as shown in Figure 8(a) revealed the absence of surface defects and interfacial voids; however, agglomerate Al_2O_3 particles were present in the coating.

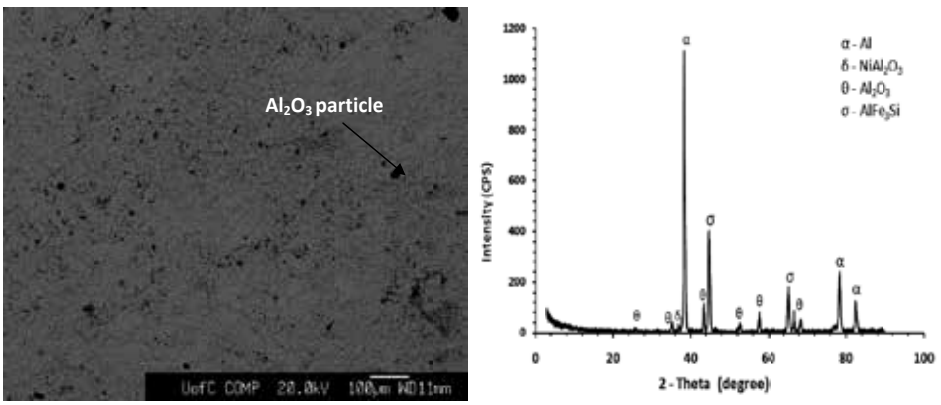

(a) (b)

Figure 8. (a) Surface of Ni/Al_2O_3 coating and (b) XRD spectrum of coated samples.

4. Conclusion

In this chapter, the recent development in the production and utilization of electrodeposited nano-composite coatings was examined. It was found that the tribological application of nano-composite coatings was strongly dependent on their compositional, morphological, and structural characteristics. According to the literature, these properties are directly related to the preparation method and deposition conditions such as current density, substrate, pH, ion concentration, size and quantity of nano-particles, and agitation frequency. Thus, the optimization of the parametric setting is of critical importance to assess the wear resistance of the coating.

The results demonstrated that Taguchi DOEs can be effectively used to optimize the electrodeposition process; however, due to material limitations the experiment was restricted to the use of only two samples per condition. Increasing the temperature and particle concentration caused a reduction in the wear rate of the coating. The results also show that increasing temperature to 50°C caused a reduction in the wear rate of the coatings deposited. Stir rate is the parameter having the least effect on the wear rate of the coatings.

http://dx.doi.org/10.5772/62153

The combination of optimum bonding parameters within the experimental level ranges is found to be a temperature of 50°C, particle concentration 30 vol.%, stir rate 820 rpm, and pH 4.45. Within the experimental level ranges, the most significant influencing parameter is particle concentration, which accounts for 51.68% of the total effect, followed by temperature (32.41), bath pH, and stir rate (12.27% and 3.64%, respectively).

Author details

Kavian O. Cooke

Address all correspondence to: kavian_cooke@yahoo.com

Department of Mechanical Engineering, University of Technology, Jamaica, Kingston, Jamaica

References

[1] Cao, G. Nanostructures and Nanomaterials – Synthesis, Properties and Applications.Published by Imperial College Press, United Kingdom, 2004.

[2] Low, C.T.J. and Walsh, F.C. Self-lubricating metal composite coatings by electrodeposition or electroless deposition. Encyclopedia of Tribology, 3025–3031, ISBN: 978-0-387-92896-8, 2013.

[3] Jung, A., Natter, H., Hempelmann, R. and Lach, E. Nanocrystalline alumina dispersed in nanocrystalline nickel: Enhanced mechanical properties. Journal of Materials Science, 44, 2725–2735, 2009.

[4] Chen, L., Wang, L., Zeng, Z. and Zhang, J. Effect of surfactant on the electrodeposition and wear resistance of Ni–Al_2O_3 composite coatings. Materials Science and Engineering A, 434, 319–325, 2006.

[5] Sheng-Lung, K. Effect of nickel ion concentration on Ni/Al_2O_3 composite coatings. Journal of the Chinese Institute of Engineers, 28(1), 1–8, 2005.

[6] Parida, G., Chaira, D., Chopkar, M. and Basu, A. Synthesis and characterization of Ni–TiO_2 composite coatings by electro-co-deposition, 205 issues 21-22, 4871-4879, 2011.

[7] Wu, G., Li, N., Zhou, D.R. and Mitsuo, K. Electrodeposited Co–Ni–Al_2O_3 composite coatings. Journal of Surface and Coatings Technology, 176, 157–164, 2004.

[8] Moritz, T., Eiselt, W. and Moritz, K. Electrophoretic deposition applied to ceramic dental crowns and bridges. Journal of Materials Science, 41, 8123–8129, 2006.

[9] Hou, K.H., Ger, M.D., Wang, L.M. and Ke, S.T. The wear behaviour of electro-codeposited Ni/SiC composites. Wear, 253, 994–1003, 2002.

[10] Garcia, I., Fransaer, J. and Celis, J.-P. Electrodeposition and sliding wear resistance of nickel composite coatings containing micron and submicron SiC particles. Surface and Coatings Technology, 148, 171–178, 2001.

[11] Bicelli, L.P., Bozzini, B., Mele, C. and D'Urzo, L. A review of nanostructural aspects of metal electrodeposition. International Journal of Electrochemical Science, 3, 356–408, 2008.

[12] Rusu, D.E., Cojocaru, P., Magagnin, L., Gheorghies, C. and Carac, G. Study of Ni–TiO_2 nanocomposite coating prepared by electrochemical deposition. Journal of Optoelectronics and Advanced Materials, 12(12), 2419–2422, 2010.

[13] Stojak, J.L., Fransaer, J. and Talbot, J.B. Review of Electrocodeposition. In Alkire, R.C. and Kolb, D.M. (Eds.), Advances in Electrochemical Science and Engineering, Vol. 7, John Wiley and Sons-VCH Verlag, Germany, 5-30, ISBN: 3-527-29830-4, 2002.

[14] Lekka, M., Koumoulis, D., Kouloumbi, N. and Bonora, P.L. Mechanical and anticorrosive properties of copper matrix micro- and nano-composite coatings. Electrochimica Acta, 54, 2540–2546, 2009.

[15] Foster, J. and Cameron, B. Effect of current density and agitation on the formation of electrodeposited composite coatings. Transactions of the Institute of Metal Finishing, 54(4), 178–183, 1976.

[16] Shao, I., Vereecken, P.M., Cammarata, R.R. and Searson, P.C. Kinetics of particle code-position of nanocomposites. Journal of the Electrochemical Society, 149(11), 610-614, 2002.

[17] Benea, L., Bonora, P.L., Borello, A., Martelli, S., Wenger, F., Ponthiaux, P. and Galland, J. Composite electrodeposition to obtain nanostructured coatings. Journal of the Electrochemical Society, 148(7), C461–C465, 2001.

[18] Whithers, J.C. Electrochemical co-deposition by electrophoresis, Production Finhing. 26, 62, 1962.

[19] Williams, R.V. and Martin, P. W. Electrodeposition and metal finishing, Transactions of the Institute of Metal Finishing, 42, 182, 1964.

[20] Brandes, E.A. and Goldthorpe, Electrodeposition of cermets, D. Metallurgia 76, 195, 1967.

[21] Guglielmi, N. Kinetics of the deposition of inert particles from electrolytic baths. Journal of Electrochemistry Society, 119(8), 1009–1012, 1972.

[22] Gomes, A., Pereira, I., Fernández, B. and Pereiro, R. Electrodeposition of Metal Matrix Nanocomposites: Improvement of the Chemical Characterization Techniques. Intech Open, Croatia, 21–46.

[23] Hunter, R.J. Zeta Potential in Colloids Science. Academic Press, New York, 1981.

[24] Boccaccini, A.R. and Zhitomirsky, I. Application of electrophoretic and electrolytic deposition techniques in ceramics processing. Current Opinion in Solid State and Materials Science, 6, 251–260, 2002.

[25] Kunio, F. and Hideo, M. Dekker Encyclopedia of Nanoscience and Nanotechnology, Editor Cristian Contecu. In Colloidal Nanoparticles: Electrokinetic Characterization, 2nd ed.United States, 773–785, 2009.

[26] Fransier, J., Celis, J.P. and Roos, J.R.Electrochemical preparation of oxide-matrix composites Journal of Electrochemistry Society, 141, 669, 1994.

[27] Belavendram, N. Design by Quality – Taguchi Techniques for Industrial Experimentation. Prentice Hall, London, 1995.

[28] Dobrzañski, L.A., Domaga, J. and Silva, J.F. Application of Taguchi method in the optimization of filament winding of thermoplastic composites.Archives of Material Science and Engineering 28(3), 133–140, 2007.

[29] Goral, A., Beltowska-Lehman, E. and Indyka, P. Structure characterization of Ni/Al_2O_3 composite coatings prepared by electrodeposition. Solid State Phenomena, 163, 64–67, 2010.

[30] Aruna, S.T., Selvi, V.E., Grips, W.V. and Rajam, K.S. Corrosion and wear resistant properties of Ni-Al_2O_3 composite coatings containing various forms of alumina. Journal of Applied Electrochemistry, 41, 461–468, 2011.

[31] Badarulzaman, N.A., Purwadaria, S., Mohamad, A.A. and Ahmad, Z.A. The production of nickel–alumina composite coating via electroplating. Ionics: The International Journal of Ionics: The Science of Technology and Ionic Motion, 15, 603–607, 2009.

[32] Beltowska Lehman, E., Goral, A. and Indyka, P. An electrodeposition and characterization of Ni/Al_2O_3 nanocomposite coatings. Achives of Metallurgy and Materials, 56(4), 919-931, 2011. DOI:10.2478/v10172-011-0101-1.

[33] Ahmad, Y. and Mohamed, A.M. Electrodeposition of nanostructured nickel-ceramic composite coatings: A review. International Journal of Electrochemical Science, 9, 1942–1963, 2014.

[34] Rostami, M., Saatchi, A. and Ebrahimi-Kahrizsangi, R. Influences of bath stiring rate on synetics of nano composite NiSiCGr coatings on St37 via electrodeposition process. Journal of Advanced Materials and Processing, I, 11–19, 2013.

[35] Aruna, S.T., Diwakar, S., Jain, A. and Rajam, K.S. Comparative study on the effect of current density on Ni and Ni–Al_2O_3 nanocomposite coatings produced by electrolytic deposition. Surface Engineering, 21, 209–214, 2005.

[36] Lu, W., Ou, C., Huang, P., Yan, P. and Yan, B. Effect of pH on the structural properties of electrodeposited nanocrystalline FeCo films. International Journal of Electrochemical Sciences, 8218–8226, 2013.

[37] Gopalsamy, B., Mondal, B. and Ghosh, S. Taguchi method and ANOVA: An approach for the process parameters optimization of hard machining while machining hardened steel. Journal of Scientific and Industrial Research, 68, 686–695, 2009.

Chapter 10

Tribological and Corrosion Performance of Electrodeposited Nickel Composite Coatings

Nicholus Malatji and Patricia A.I. Popoola

Additional information is available at the end of the chapter

http://dx.doi.org/10.5772/62170

Abstract

The inclusion of second-phase particles in nickel-based matrix to fabricate composite coatings presents a promising solution to combating corrosion and wear deterioration of materials during service. Composite coatings possess better surface properties such as wear resistance, high microhardness, thermal stability, and corrosion resistance than the traditional nickel coatings. Their excellent properties enable them to be used in advanced industrial applications where they will be constantly exposed to severe and degrading environments. There are various surface modification techniques that are employed to produce these coatings and electrodeposition has received wide range of use in fabrication of nickel matrix composites. This technique is associated with low cost, simplicity of operation, versatility, high production rates, and few size and shape limitations. To produce advanced electrodeposits with better performance during application, the optimization and further developments of the process remain vital. Therefore, this chapter aims to review the electrofabrication and properties of nickel composite/nanocomposite coatings for corrosion and wear applications.

Keywords: Electrodeposition, nickel composite coatings, corrosion resistance, wear resistance, hardness

1. Introduction

Nickel matrix composite/nanocomposite coatings have gained a variety of use in many industrial applications where high wear and corrosion performance are required. The applications where these coatings are employed include automotive, aerospace, electronics, petrochemical, nuclear, marine, and many more [1,2]. The incorporation of nanostructured particles into the matrix imparts special characteristics that are not exhibited by the traditional micro-sized composite coatings. The nanocomposite coatings possess improved properties

such as high hardness, excellent corrosion resistance, thermal stability, wear resistance, and self-lubrication properties [3]. The nanoparticles incorporated into the matrix include those of metal oxides, carbides, nitrides, borides, polymers, and carbon-based materials [4–6].

Electrodeposition is one of the surface modification techniques that are used to fabricate nickel nanocomposite coatings. This technique has several advantages over the other processing methods which include low cost, simplicity of operation, versatility, high production rates, industrial applicability, and few size and shape limitations [7]. However, co-deposition of nanostructured inert particles using electrodeposition has its own challenges. Agglomeration of particles in the electroplating bath, inhomogeneity in the distribution of particles in the matrix, and low content of particles in the coatings are some of the drawbacks associated with this process [8]. These problems compromise the quality of the coatings and result in poor performance during application. Therefore, proper process development and optimization are required to counteract the limitations.

Many researches have been conducted in an attempt to address these limitations. Additions of chemical agents into electrolytic solutions to aid co-deposition of the particles have been found by many researchers to reduce agglomeration of particles and increase their incorporation in the matrix. These additives disturb the electrostatic stabilization of the particles and hence promote their suspension in the solution [9]. Pulse current electrodeposition is another method that has been employed to enhance co-deposition and improve uniform distribution of particles. This type of plating has three independent variables for controlling co-deposition as compared to direct current plating which only has one variable [10]. Ultrasonic energy has also been used to improve the inclusion of particles into the metal matrix. It enhances mass transport of particles to the cathode for co-deposition, reduces the thickness of the diffusion layer, and disperses the particles in the electrolyte [11,12].

2. Electrodeposition of nickel composite/nanocomposite coatings

Electrodeposition of composite coatings has been studied and researched by several scholars over the past few decades. The focus of the research is centred around the development and fabrication of advanced and novel surface coatings that can withstand both physical, chemical, and mechanical deterioration under service conditions. In order to produce these high-quality coatings, the mechanism of co-deposition of reinforcement particles with the matrix, optimization of the process operating parameters, and the properties of the resultant deposits need to be fully understood.

3. Basics of Electroplating of Nickel

Electroplating of nickel involves the passage of current between two electrodes (anode and cathode) immersed in an electrolyte containing nickel salts to cause dissolution of Ni^{2+} ions in the anode to be deposited at the cathode. Equation 1 and 2 show the anodic and cathodic

http://dx.doi.org/10.5772/62170

reactions that take place during nickel deposition. The anode is mainly a nickel plate while the cathode is any metal or material that needs to be protected or decorated. The nickel ions deposited at the cathode are replenished by those formed as the result of the dissolution of the anode. According to Faraday's law of electrolysis, the amount of nickel dissolved at the cathode is equal to the amount of nickel deposited at the cathode, which is directly proportional to the product of current and time [13].

Anodic:

$$Ni \rightarrow Ni^{2+} + 2e^{-} \tag{1}$$

Cathodic:

$$Ni^{2+} + 2e^{-} \rightarrow Ni \tag{2}$$

There are many bath solutions that have been developed for producing different types of nickel deposits. The ones that have gained more usage include the Watts and sulphamate baths. These plating baths are reinforced with surfactants and other additives to improve the quality of the deposits such as brightness, surface morphology, and other functional properties.

4. Mechanism of Co-deposition

Many models have been developed to understand the mechanism of co-deposition of particles into metallic matrix. These models predict the processes that are involved during particle co-deposition and their adsorption rate into the coatings. The processes include electrophoresis, mechanical inclusion, adsorption, and convective-diffusion. One of the most used and accepted model by scholars is Guglielmi's two-step adsorption model. In the first step of particle incorporation, the particles are loosely adsorbed on the cathode covered by a cloud of metal ions. Strong adsorption of particles follows in the second step with current density playing a key role in the particles to be strongly adsorbed on the cathode. The strongly adsorbed particles are embedded into the growing metallic layer [14]. The author related the volume fraction of co-deposited particles (α) to the volume percent of particles suspended in the plating bath (C) with the Langmuir adsorption isotherm as shown in equation 3

$$\frac{C}{\alpha} = \frac{Mi_o}{nF\rho_m v_o} \exp(A - B)\eta \left(\frac{1}{k} + C\right) \tag{3}$$

where is the atomic weight of the electrodeposited metal i_o the exchanging current density, the valence of the electrodeposited metal, F the Faraday constant, ϱ_m the density of electrodeposited metal, the overpotential of electrode reaction, $i = i_o \exp(A\eta)$ and k the Langmuir isotherm

constant, mainly determined by the intensity of interaction between particles and cathode. The parameters v_o and B are related to particle deposition, and both play a symmetrical role with the parameters i_o and A related to metal deposition [15]. Ref. [16] improved Guglielmi's model by using three modes of current density to differentiate the reduction of adsorbed ion on the particles. This new model involved three steps, where in the first step particles are convectively forced to the surface followed by loose adsorption and then irreversible incorporation of particles into the matrix by reduction of adsorbed ions. Ref. [17] incorporated a third-order polynomial equation to further improve Guglielmi's model. This corrective factor will help account for the effects of adsorption and hydrodynamic conditions. Many other models have been developed which involved statistical approach to predict the chances of particles being included into the deposit. However, all these models cannot predict the effect of particles on electrocrystallization and are limited to specific conditions.

The manner of incorporation of particles into metal matrix depends mainly on the electrodeposition process parameters. Some of the most important parameters include the speed at which the bath is stirred, the applied current density, and electrolyte composition. Bath agitation serves as a medium that assists particles to be transported to the cathode, while applied current density and electrolyte composition are responsible for the formation of ionic cloud around the introduced particles. There are three possibilities for particles to be incorporated in to a metal matrix [18]:

- Coatings that are just covered by adsorbed particles on the surface.
- Coatings containing entrapped particles and
- Coatings containing particles truly embedded uniformly into the metal matrix.

A schematic diagram of particle incorporation into a metal deposit is shown in Figure 1. The manner in which particles are incorporated into the coating determines the quality of the resulting deposits. Coatings containing uniformly distributed and truly embedded particles exhibit superior properties than the other manners of incorporation.

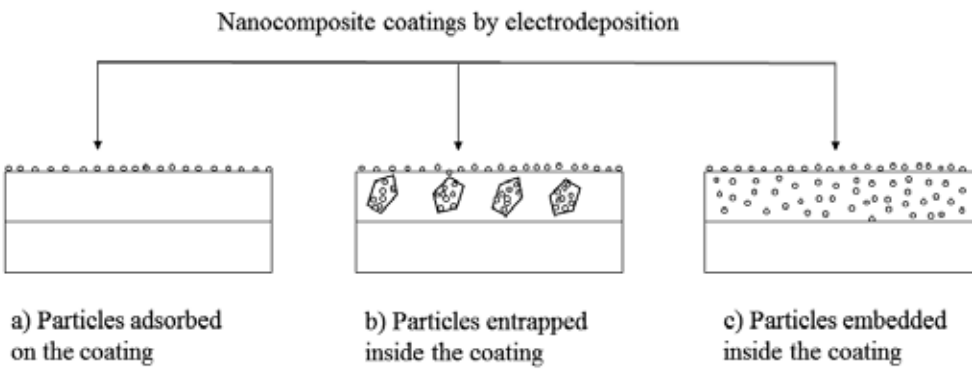

Figure 1. Schematic representation of different co-deposition possibilities

http://dx.doi.org/10.5772/62170

5. Effect of process operating parameters

Electrodeposition of metal matrix nanocomposite coatings is very complex and requires the process operating parameters to be optimized to produce high-quality deposits with improved functional properties. There are several parameters that are very important in fabrication of the composites but only the following will be covered in this review. These include current density, type of current, particle size, particle loading, stirring speed, bath composition, time, and temperature. The typical bath composition and parameters are shown in Table 1.

Bath Composition	**g/l**	**Parameters**	
$NiSO_4.H_2O$	145	Time	2–16 min
NaCl	16.67	Current density	3.75 $mAcm^{-2}$
H_3BO_3	11.11	Temperature	40–80°C
Fe_2O_3	2.37–76	pH	4.6
		Anode	Nickel rod
		Cathode	Mild steel

Table 1. Bath composition and plating parameters [35]

5.1. Current

Current is one of the most important parameters that are used to control the plating process. It is used to reduce dissolved metal cations in solution to form a protective layer on the cathode. The rate in which metal cations are transferred to the cathode for plating determines the amount of second-phase particles that will be incorporated into the metal matrix [14]. Higher current densities enhance deposition rate and thus increasing the chances for the reinforcement of particles to be adsorbed on the cathode. The current density was found to influence the content of alumina particles present in the Ni–P matrix [19]. The increment of current density from 5 to 20 A/dm^2 increased the content of Al_2O_3 particles from 7.75 to 13.65 vol.%. The hardness and phosphorus content of the deposits were also found to be affected by varying the current density. The hardness property of the coatings had direct relationship with the increase in current density while the phosphorus showed an inverse correlation. Ref. [20] obtained similar results when they studied the incorporation of CNT particles into Ni matrix. The CNT content in the coating increased with rising current densities. However, it is not in all cases where increasing current density during plating yields coatings with high microhardness values and particle content. Ref. [21] established an optimum current density of 0.8 A/dm^2 for fabrication of Ni–Cr_2O_3 nanocomposite coatings with excellent mechanical properties. Increasing the current density beyond the optimal conditions had no positive influence on the microhardness values of the resultant deposits. Plating in lower current densities requires time to achieve the desirable thickness and hence gives more time for the particles to be available at the cathode. This increases the chance of the particles to be homogenously incorporated into the matrix, leading to formation of harder surfaces due to dispersion

hardening. Higher current densities increase deposition rate but reduce controllability of the co-deposition process. Ref. [22] obtained similar results when nano-titania particles were added into a nickel electrolyte. At constant pH, increasing current density yielded deposits with low TiO_2 content and increased mean grain size. Table 2 shows the effect of current density on compositional, structural, and mechanical properties of N–W and Ni–W–Al_2O_3. Lower current densities favour good incorporation of tungsten in the matrix, high macro-residual stresses, and small crystallite sizes. However, incorporation of alumina also depends on the type of ceramic phase. Sigma Aldrich alumina particles follow the trend of tungsten, and inclusion of Taimicron alumina shows a deviation. Therefore, it can be concluded that optimization of operating current is required for electrodeposition of nickel composite/ nanocomposites to produce coatings with enhanced surface properties.

j (A/dm^2)	W (wt.%)	Al_2O_3 (%)	(MPa)	k (nm)
Ni-W				
4	44±0.9	-	447±67	8
5	42.4±0.8	-	217±76	10
7	40.5±1.0	-	114±33	10
8	37.6±0.7	-	-209±58	13
Ni-W-Al_2O_3 (SA)				
4	37.0±0.6	1.7±0.2	-	8
5	35.3±0.7	1.8±0.2	1150±46	9
7	31.0±0.6	1.1±0.1	1044±114	11
8	26.6±0.5	0.5±0.3	710±85	12
Ni-W-Al_2O_3 (TA)				
4	35.6±0.7	6.4±0.3	-	6
5	34.4±0.7	5.4±0.2	1360±102	7
7	28.5±0.6	5.6±0.2	1460±80	6
8	23.3±0.5	7.0±0.3	781±186	5

Table 2. The effect of current density on the content of tungsten and alumina in the Ni matrix, macro-residual stresses and crystallite size [23]

Direct current plating had been and is still commonly used for fabrication of thin films. However, this plating technique is associated with slow deposition rates and many defects in

http://dx.doi.org/10.5772/62170

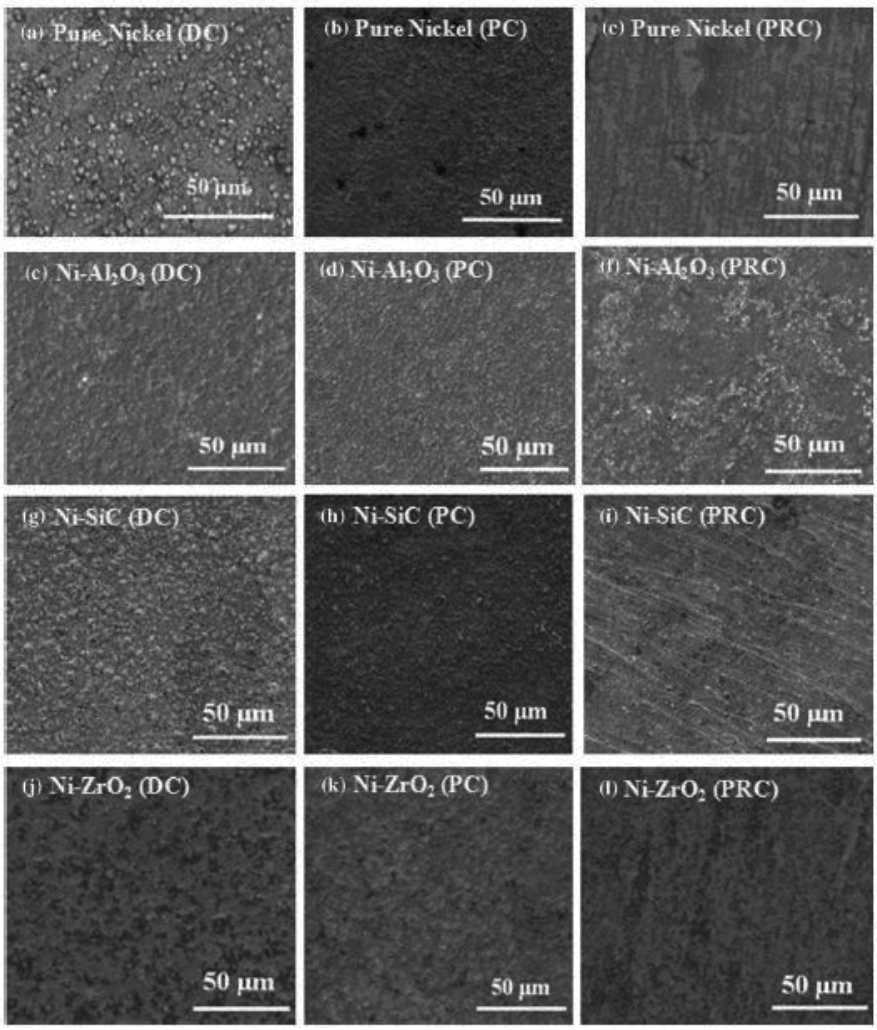

Figure 2. SEM micrographs of the plated samples [24]

the resultant deposits. Pulse current (PC) and pulsed reverse current (PRC) electrodeposition techniques have been developed to address the drawbacks associated with this deposition method. These methods allow better control of the structure and properties of the coatings [25]. The methods have several operating parameters (such as time period in which the pulses are imposed, relaxation time, pulse frequency, and pulse current density) that can be varied and optimized to achieve better deposit with enhanced surface properties as compared to the conventional method. Fine microstructures can be obtained from these plating methods by allowing high overpotential and low surface diffusion which favour the formation of new nuclei and thus perturbing grain growth [9]. Ref. [24] compared the morphologies and mechanical properties of nickel composite coatings produced by different electrodeposition techniques (DC, PC, and PRC). PC and PRC deposits exhibited fine and homogenous micro-

structures more than DC ones (shown in Figure 1). The surface roughness was also reduced and the content of the reinforcement particles in the coatings increased. The high content and uniform Al_2O_3, SiC, and ZrO_2 particles incorporated into the nickel matrix improved the microhardness and tribological properties of the deposits. Ref. [9] obtained similar results when Ni–Al_2O_3 composite coatings fabricated from both DC and PC plating at the same current density were compared. The particle content in the coating increased linearly with increasing current density for PC deposits, while the increase of particle content in DC coatings became negligible in current densities higher than 3 A/dm^2.

5.2. Particle loading

The concentration of the reinforcement particles in the solution to be co-deposited with the matrix has a significant influence on their adsorption rate at the cathode. According to Guglielmi's two-step adsorption model, high particle content in the plating bath increases the adsorption rate of the particles on the cathode [14]. However, when the particle concentration in the bath reaches saturation, agglomeration occurs leading to reduced incorporation or formation of deposits with surface defects [26]. Inclusion of TiO_2 nanoparticles into nickel matrix was found to be dependent on the bath particle loading. The least bath particle loading of 5 g/l of TiO_2 yielded the lowest weight of particles of about 1.8 wt.%, while introducing 15 g/l of the particles increased the particle content in the deposit to be about 3.8 wt.% at the constant current density of 40 mA/cm^2 [7]. Similar behaviour was obtained throughout the experiments when other current densities were used (see Figure 2).

The optimum particle loading for SiC particles into nickel matrix was found to be 20 g/l by ref. [4]. Addition of more particles beyond the optimal levels led to decrease in incorporation of the particles into the coating. The decrease was ascribed to the agglomeration of the SiC particles due to their poor wettability. As much as high content of particles in the bath increases their availability at the cathode, the capturing capacity of the growing metal remains unchanged [27]. Therefore, particle entrapment into the matrix requires conducible conditions to produce high-quality coatings with enhanced surface properties.

5.3. Particle size

Nanoparticles have gained wide use in fabrication of nanocomposite coatings due to their excellent and attractive properties. Their incorporation into metal matrixes is associated with better surface morphologies, improved corrosion resistance, thermal stability, and excellent mechanical properties as compared to their micron and submicron counterparts. However, co-deposition of these particles is associated with many challenges. According to the study conducted by ref. [27], zeta potential of the particles is one of the major driving forces responsible for how micron-, submicron-, or nano-sized particles behave differently in the plating bath. The results showed that micron-sized SiC particles exhibited more negative than the nanoparticles. This indicates that the micron-sized SiC particles are easily adsorbed by the nickel cations. The higher the positive or negative zeta potential the particles possess, the more stable they are in solution since they repel each other and thus limiting the formation of aggregates. Due to the high repulsion forces that exist between the micron-sized particles,

http://dx.doi.org/10.5772/62170

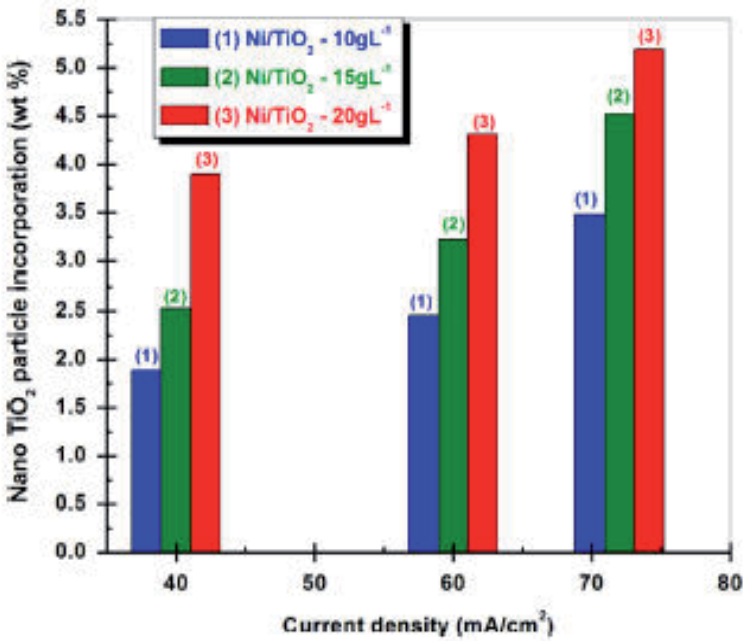

Figure 3. Correlation between TiO_2 content in the deposit with current densities [7]

electrodeposition under high particle loading is possible and thus increasing the chance of more particles to be embedded in the matrix. The authors found that the micron-sized particles were uniformly distributed in the coating as compared to agglomerated nanoparticles. However, these particles were not uniformly distributed along the surface in normal direction which can severely affect the fabricated film properties. Ref. [28] found that particles with average size of 5 μm had lower hardness values than their 10 and 50 nm counterparts. This result can easily be explained by the Hall-Pecth equation (4):

$$\sigma = \sigma_o + A / d^{1/2} \tag{4}$$

where d is the grain size and σ_o and A are constants. According to the equation, it can be seen that smaller grain size has a positive influence on the yield strength since the relationship is inversely proportional. Nanoparticles also has the ability to fill the microholes, gaps, and other surface defects present on the surface of the matrix than micron- or submicron-sized particles [29]. This results in fine microstructures with minimal surface defects and better functional properties. The size of the particles also affects the amount of particles that will be incorporated as shown in Table 3. Finer particles are difficult to incorporate in the matrix than coarser ones. Therefore, the operating parameters such as stirring speed, pH, and current density are very crucial to be optimized to facilitate better uniform distribution and high incorporation rate of fine particles in the deposit.

Particle size	SiC in coating (vol%)	Number density (particles cm^2)	Distant between Particles (nm)
10 nm	15.2	2.89×10^{17}	1.51×10^{1}
50 nm	22.02	3.37×10^{15}	6.67×10^{1}
5 nm	55.24	8.44×10^{9}	4.91×10^{3}

Table 3. Volume percent and number density of SiC particles in composite coatings with the distance between particles [28]

5.4. Bath composition

Electrolyte ionic strength, bath additives, and pH are some of the operating parameters that affect the zeta potential of second-phase particles as explained before. The pH of the bath is a function of bath composition which includes the electrolyte and chemical additives. Strong acid or bases can be added to adjust the pH to be acidic or alkaline. Particles have different zeta potential at different pH depending on their nature. Therefore, various ceramic particles will have more positive or negative charge on either acidic or alkaline conditions. Titania particles were found to exhibit negative zeta potential in acidic solution of pH= 4.3 and positive zeta potential at alkaline conditions with pH of 9.5 [30]. A maximum particle content of 4.3 wt. % was achieved from alkaline baths while 3.3 wt.% resulted from acidic solutions. This shows that the conducible co-deposition of TiO_2 particles with nickel is achievable under high pH values at particle loading of 10 g/l and current density of 1 A/dm^2. A decreasing trend (from 2 to 5) in particle incorporation with increasing pH values was noticed by ref. [22]. At plating conditions of pH=2, particle loading of 100 g/l and current density of 5 A/dm^2, a maximum of 8 vol.% of TiO_2 incorporation was achieved. However, the authors did not study further the behaviour of the particle incorporation in alkaline solutions. The results obtained by the different authors show that particle incorporation depends on several factors than pH of the solution. The electrolyte is the carrier of electroactive species which are responsible for the formation of ionic cloud around the particles to enable their transportation to the cathode for entrapment in the matrix [31]. Variation of nickel sulphate in the bath from 200, 250, and 300 g/l showed significant effect on the incorporation rate of reinforcement particles as reported by ref. [28]. The volume of incorporated SiC particles increased with increasing nickel sulphate content upto 250 g/l and decreased when the concentration was further raised. The effect of electroactive species on SiC particles content present in the coating is shown in Figure 3. Electroactive species to adsorb on the strengthening particles is not sufficient at low nickel sulphate concentration, reducing their entrapment in the coating. Rapid reduction of nickel ions occurs at higher nickel sulphate concentration before the particles can be properly co-deposited, leading to low adsorption rate. High ionic strength of plating solution has also been reported to promote particle agglomeration causing the formation of deposits with defects and low particle content [26].

Chemical additives are added in the bath to serve different functions. These functions include controlling the final appearance of the deposit, altering crystal growth kinetics, and influencing the zeta potential of the second-phase particles. The addition of SDS (sodium dodecyl sulph-

http://dx.doi.org/10.5772/62170

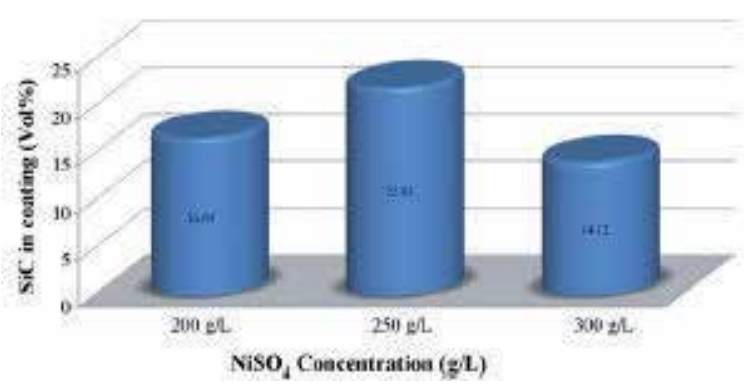

Figure 4. SiC volume percent for various nickel sulphate concentrations in the bath [26]

onate) and saccharine promote smoothening of the Ni coating surfaces [8]. The coatings fabricated from solutions containing the additives exhibited smaller grain sizes. The addition of ethanol (25 and 50 vol.%) into nickel bath solution induced grain refinement resulting in finer microstructure [32]. The effect of ethanol on the crystal size of nickel and nanocomposite coatings is shown in Table 4. The truncated pyramidal crystals were modified to globular grains as a result of the presence of ethanol in the electrolyte. The crystal size of 85 nm of the Ni–Al_2O_3 nanocomposite coating produced from additive free bath was reduced to 25 nm when ethanol was added.

Vol% Ethanol	Pure Nickel	Ni–Al_2O_3
0	131	85
25	70	54
50	39	25

Table 4. Effect of ethanol on the crystal size of pure nickel and Ni–Al_2O_3 nanocomposite coatings

5.5. Stirring speed

Stirring speed is one of the important parameters that control the mechanism of particle incorporation. Mechanical inclusion of particles into the coating forms part of the three processes that are involved in entrapment of particles into a metal matrix [31]. Mechanical agitation aids in the transportation of particles to the cathode to be readily available for adsorption [33]. However, very high or low agitation can have adverse effect on the incorporation rate of the particles. Low stirring speeds offer low energy to break the agglomerate to fine particles and hence reduce their availability for incorporation. High stirring speeds are associated with high impinging velocity of the particles to the cathode and not giving enough retention time for the particles to be adsorbed on the cathode [27]. Particle size has an effect on the required stirring speed since it is easier to keep coarse particles in suspension in solution

than the finer ones. Nanoparticles easily agglomerate when they are added in the plating bath. Therefore, fabrication of nanocomposite coatings requires higher stirring speeds than their composite counterparts. Other forms of agitation have been used in literature and these include the use of ultrasonic energy to keep particles in suspension, enhance mass transport, and reduce diffusion layer thickness [34]. A schematic diagram of electrodeposition cell assisted with ultrasonic energy is shown in Figure 4. The use of ultrasound also helps to modify the surface morphologies of coatings fabricated with conventional DC plating technique [10].

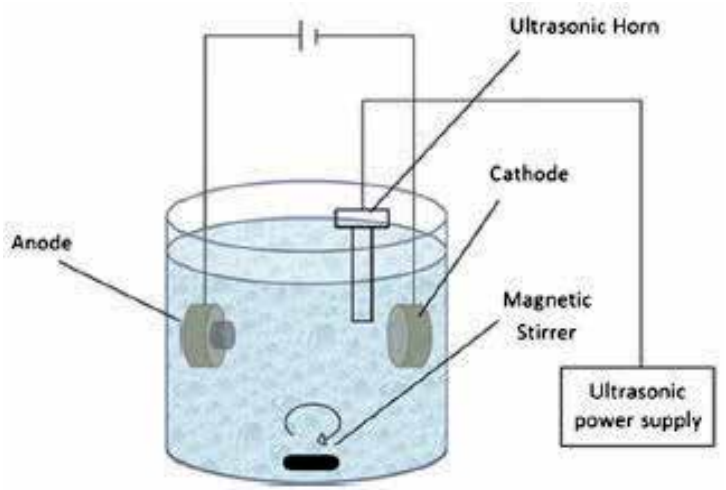

Figure 5. Typical electrodeposition cell assisted with ultrasound energy [34]

5.6. Time and temperature

Particles require time to remain around the cathode to increase the chances of their incorporation. Ref. [35] reported that longer deposition time allows for the formation of thicker and compact coatings with improved microhardness. The highest microhardness values were achieved at a deposition time of 14 min, and beyond this time no adherent spherical globules were formed. Temperature also plays a significant role in co-deposition process. Increase in temperature enhances reaction kinetics, leading to more nickel ions to be transferred to the cathode. The content of SiC particles has been found to be a function of temperature by ref. [36]. Increasing temperature up to 50°C increased the content of the particles in the coating. Above optimal conditions, a decrease in incorporation rate was observed. Thermodynamic movement of ions improves with temperature and the particulates' kinetic energy also increases. This causes rapid deposition, which poses a risk on the control of crystal growth and uniformity in distribution of particles within the matrix. According to ref. [37], increase in temperature reduces adsorpability of the particles and hence decrease in overpotential cathode and electric field. Ref. [35] obtained similar results when Fe_2O_3 nanoparticles were co-deposited with nickel.

http://dx.doi.org/10.5772/62170

6. Nickel composite/nanocomposite coatings and their properties

Nickel composite coatings have been developed to withstand challenging and aggressive conditions during service. These coatings exhibit excellent corrosion resistance, tribological properties, and thermal stability. There are several types of nickel base matrix composite coatings that have been developed over the past few years. These include Ni, Ni–P, Ni–B, Ni–W, and Ni–Co matrix composites. In this topic, the structural and functional properties of these coatings will be discussed.

6.1. Ni composite coatings

The inclusion of second-phase particles into nickel matrix influences the evolution of the coatings surface morphologies. The nickel matrix characterized by pyramidal crystal structure was changed to spherical structure through the addition of inert titanium nanoparticles [38]. The composite coatings also exhibited smaller crystallite sizes than those of the metallic matrix. Particle loading plays a major part in refinement of grains and the smallest grains can be obtained in optimum conditions. Embedment of GNS–TiO_2 nanocomposite into nickel coatings yielded similar results [39]. The reduction in grain size was attributed to the growth-inhibiting ability of reinforcement nanoparticles which are adsorbed on the grain boundaries and thus restricting further growth. The presence of uniformly distributed nanoparticulates in the matrix reduces surface defects (pores, microholes, gaps, crevices, etc.) in the deposits [40]. Coatings with minimal surface defects possess few active sites for chemical attack and thus improve their corrosion resistance. Addition of 50 g/l of nano-SiC particles in a nickel plating bath reduced the current density of nickel coatings from 7.09 to 0.03 $\mu A/cm^2$ [41]. The Tafel plots of pure nickel and Ni–SiC nanocomposite coatings are shown in Figure 5. Improvement in corrosion resistance is depended on the amount of second-phase particles incorporated, and coatings with higher particle content are associated with increased positive potential shift and lower corrosion currents [42]. These nanoparticles also act as inert physical barrier to the initiation and development of defect corrosion.

Ref. [43] incorporated TiCN (titanium carbon nitride) particles into a nickel matrix and the results obtained were similar to those of SiC. The highest volume of 23.9% TiCN yielded coatings which exhibited the highest potential and lowest current density. Addition of ceria particles into electrolytic nickel solution yielded composite coatings which possessed lower potentials, current densities, and corrosion rates [44]. The results obtained by the authors show that these particles cause cathodic protection when incorporated in a nickel matrix. The particles reduce active surface area and cause blockage on the cathode for HER (hydrogen evolution reaction) to occur. Incorporation of ceramic particles into a metallic matrix does not always guarantee improvement in corrosion resistance of the coatings. The inclusion of carbon nanotubes was found to cause negative potential shift and thus increasing the corrosion rate of the matrix on copper substrate [20]. The poor corrosion resistance shown was due to the porous nature of coatings which was dependent on CNT content. However, ref. [45] obtained different results when Ni–CNT coating was electrodeposited on Ti–6Al–4V alloy. The corrosion resistance was notably enhanced by the presence of CNT. These results show that

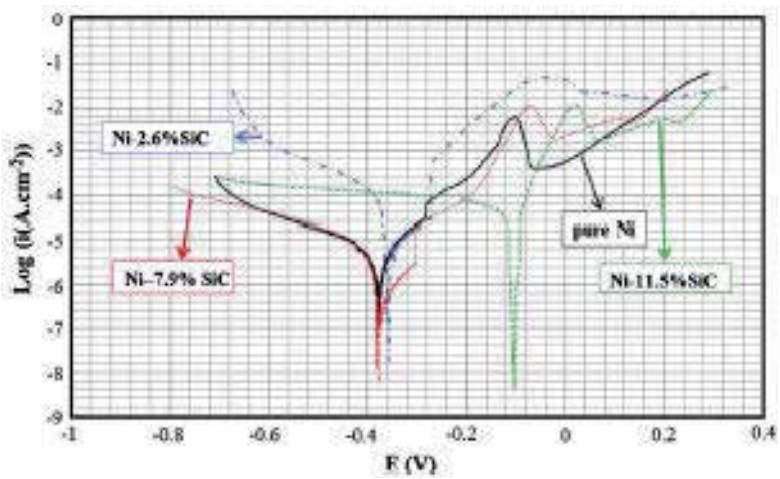

Figure 6. Polarization curves of Ni and Ni–SiC nanocomposite coatings

improvement of functional properties depends not only on incorporated particles but also on different factors such as type of substrate and operating parameters.

Composite	Wear loss mm³	Wear coefficient	Average coefficient of friction
Ni–SiC	10.838×10^{-3}	2.276×10^{-6}	0.798
Ni–Si_3N_4	4.817×10^{-3}	1.282×10^{-6}	0.890
Ni–Al_2O_3	8.304×10^{-3}	1.648×10^{-6}	0.845

Table 5. Tribological properties of Ni–SiC, Ni–Si_3N_4, and Ni–Al_2O_3 composite coatings [46]

Refined microstructures exhibiting small and uniform grains are also characterized by high hardness and excellent wear resistance. The particles have pinning effect allowing little or no movement of dislocations. Co-deposition of nickel with SnO_2 nanoparticles yielded coatings with high hardness, low friction, and better wear resistance [47]. The improvement of mechanical properties was a function of the content of incorporated particles. Samples with the highest ceramic particle content exhibited the highest hardness values, lowest wear volume and friction coefficient. It can be seen from Table 5 that various incorporations yield different results. This is due to the fact that different ceramic materials exhibit their unique properties. Si_3N_4 particles have been reported to exhibit high hardness and self-lubricating properties; hence, their incorporation into a metallic matrix enhances its tribological characteristics [48]. Other particles that have been reported to possess self-lubricating properties include carbon nanotubes and molybdenum sulphide [45, 49]. The deposits that contain these particles exhibit reduced coefficient of friction and high wear resistance as compared to the matrix.

http://dx.doi.org/10.5772/62170

6.2. Ni–P composite coatings

Ni–P alloy coatings exhibit refined microstructure, high hardness, and good corrosion resistance and high wear resistance under moderate conditions [50]. The good properties displayed by these coatings owe to the formation of stable phases such as Ni_3P that leads to precipitation strengthening. However, their exposure to heat treatment conditions makes them brittle and thus rendering the coatings unfit for wear applications. The hardness of the alloy has also been reported to rise with increasing phosphorus content of up to 8 wt.% and decreases beyond that [51]. The incorporation of nano-carbon was reported to induce a positive potential shift of 60 mV to the Ni–P matrix by ref. [50]. The authors also found that the composite coatings possessed higher potentials and low current density after heat treatment than the non-heat-treated Ni–P and Ni–P–C coatings. The formation of thermodynamic stable phases through the recrystallization of rich phosphorus Ni–P alloy is responsible for the super corrosion resistance exhibited by the heat-treated composites. The hardness property of Ni–P–Al_2O_3 was found to be improved when both P and Al_2O_3 content in the deposit were higher [51]. This result obtained by the authors show that phosphorus and second-phase particles content in the deposit have significant influence on the mechanical properties of Ni–P composite coatings. The addition of SiC particles in Ni–P matrix reduced the roughness of the coatings [52].

6.3. Ni–Co composite coatings

The evolution of surface morphology of Ni–Co alloy mainly depends on cobalt content in the coating. This inclusion of the metal induces the formation of fine and compact microstructure with globular crystallites [53]. The presence of cobalt in the nickel coatings enhances their corrosion and mechanical properties which are maintained even when the coatings are exposed to elevated temperatures [54]. The incorporation of nano-Si_3N_4 particles improved the microhardness and lowered the friction coefficient of Ni–Co matrix [48]. The increase in microhardness and reduction in friction coefficient were found to be dependent on the quantity of the reinforcement particles present in the coating. Higher Si_3N_4 content in the deposits gave yield to high microhardness and lower wear loss. Si_3N_4 particles possess self-lubricating properties and reduce the load bearing for the matrix. Variation of normal load and sliding speed has been reported to affect the tribological behaviour of Ni–Co–CNT composite coatings [55]. The friction coefficient decreased with increasing normal load and sliding speed. Carbon nanotubes form lubricious transfer layer on the wearing medium during sliding and thus reducing friction. This lubricious transfer layer forms as the result of wear debris that are generated during sliding and accumulate on the counterpart surface. The rate of transfer and accumulation of the lubricious layer is a function of temperature and rises due to the increasing normal load and sliding speed. The friction coefficients of Ni–Co alloy and Ni–CNT composite coatings are shown in Figure 7. Similar results have been obtained by [56]. Ni–Co–MWCNT films fabricated by DC, PC, and PRC electrodeposition techniques exhibited lower friction coefficient and wear rate at high sliding speed.

The inclusion of micro- and nano-sized SiC particles revealed that the presence of these particles in the deposits has a positive influence on the grain growth of Ni–Co matrix [57]. The micro- and nano-composite coatings exhibited small grain sizes and improved functional

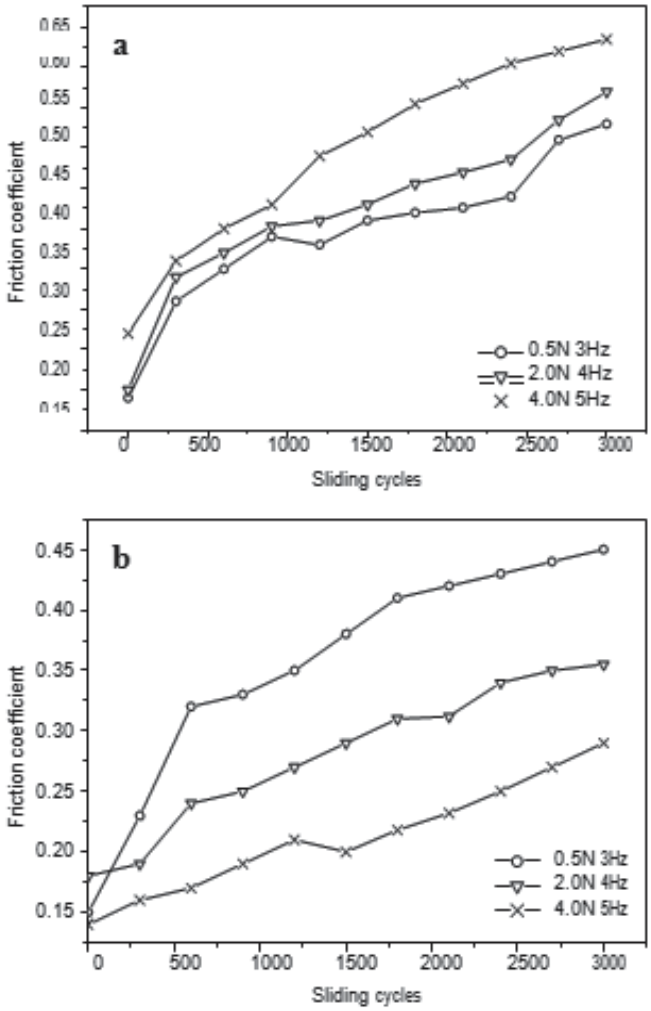

Figure 7. Friction coefficient of (a) Ni–Co alloy and (b) Ni–Co–CNT composite coating under different loads and sliding speeds [55]

properties such as hardness and corrosion resistance. However, the improvement of properties depended also on the size of the particles with nanoparticles strengthened matrixes exhibiting the best enhancement. Incorporation of SiC nanoparticles into Ni–Co matrix also prevents erosion-enhanced corrosion in oils and slurry hydrotransport system [58]. The combined effect of the wear and corrosion resistance of the particles makes it difficult for the turbulence of the flowing slurry to erode the coating and thus minimizing the exposure of the active surface of the substrate to chemical attack. Ref. [59] studied the effect of fly ash on the corrosion resistance of Ni–Co matrix. The inclusion of the fly ash particles yielded deposits with high potentials and low corrosion current. The deposits also exhibited high hardness values as compared to

http://dx.doi.org/10.5772/62170

the Ni–Co matrix, thus proving fly ash to possess better mechanical and electrochemical properties. While reinforcing of Ni–Co matrix with second-phase particles has a positive influence on the resultant deposits, the improvement of functional properties depends on the nature of reinforcement particles and process parameters.

6.4. Ni–B composite coatings

Co-deposition of nickel with boron leads to the formation of stable Ni_3B or Ni_2B phases which improve the hardness, thermal, and tribological properties of nickel coatings. Their exposure to heat treatment further enhances their hardness, resistance to wear degradation, and reduces friction coefficient. During heat treatment, grain coarsening is induced which weakens the hardness of the coatings. The mechanical weakening induced by grain growth is counteracted by the formation of hard and thermodynamically stable Ni_3B particles, hardening the coatings [60, 61]. Increasing boron content favours the improvement of mechanical properties of the coatings, especially hardness and wear resistance [62]. However, Ni–B alloy coatings with high boron content possess corrosion resistance lower than that of the matrix (see Figure 6). Therefore, this effect of boron on the functional properties of the coatings renders alloys to be more suitable for applications where excellent mechanical properties are required.

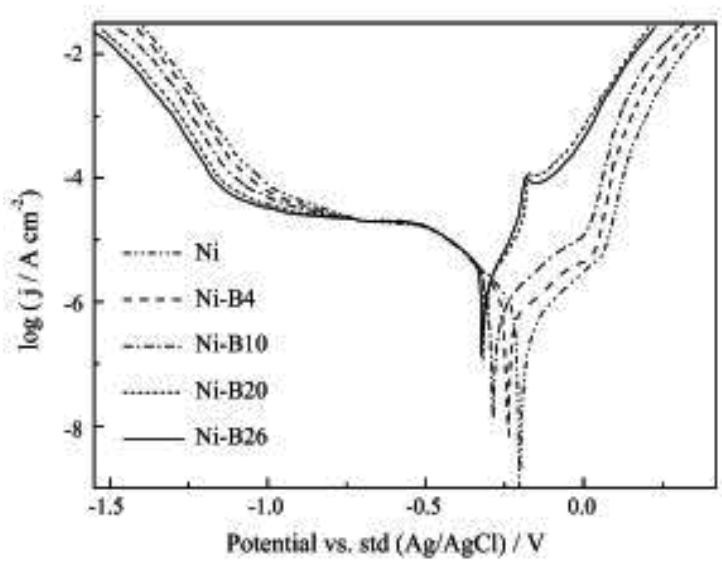

Figure 8. Polarization curves of Ni and Ni–B alloy coatings [62]

The addition of diamond particles modifies the microstructural and hardness properties of Ni–B alloy but has no positive influence on the improvement of its corrosion resistance. However, the combined effects of TMAB (trimethylamine borane) and diamond nanoparticles have significant effect on Ni–B electrochemical behaviour even though it cannot improve the

corrosion resistance of Ni matrix [8]. Sol-enhanced TiO_2 nanoparticles yielded similar behaviour with 12.5 ml/l of the particles increasing microhardness of Ni–B from 677 to 1061 HV. The improvement of hardness was also accompanied by reduction in friction coefficient and low volume wear loss [63]. The TiO_2 sol leads to dispersion strengthening and fining of grains, hence the improvement in hardness and tribological behaviour. Therefore, the incorporation of second-phase particles in Ni–B alloy matrix has not proved to increase nickel coating corrosion resistance, but its mechanical and tribological properties.

6.5. Ni–W composite coatings

The behaviour of Ni–W alloy is similar to that of Ni–B. The presence of tungsten in the nickel matrix improves mainly the mechanical properties of the coatings but not their corrosion resistance [64]. Therefore, research to make Ni–W alloy coatings to possess excellent wear and corrosion resistance has intensified to extend the applications of the coatings. The addition of reinforcement particulates and subjecting the coatings to post-plating heat treatment have been used in an effort to enhance their surface properties. Incorporation of SiO_2 into Ni–W matrix influences the morphology of the coatings and the resultant microstructure is subject to the content of SiO_2 in the coating as shown in Figure 7. The composite coatings are uniform and crack-free. The particles also improved the microhardness and corrosion resistance of the matrix [65]. The lowest particle loading of 2 g/l of SiO_2 yielded coatings with best anti-corrosive properties (see Table 6). The optimum particle concentration of 10 g/l in the bath gave the highest microhardness.

Samples	SiO_2 addition (g/l)	E_{corr}/V	$i_{corr}/\mu A\ cm^{-2}$
A	0	–0.588	13.95
B	2	–0.562	8.76
C	5	–0.580	16.75
D	10	–0.603	24.64
E	15	–0.630	37.43
F	20	–0.672	44.14

Table 6. Corrosion parameters of Ni–W alloy and Ni–W–SiO_2 nanocomposite coatings

Ref. [25] deposited Ni–W–TiO_2 nanocomposite coating using both DC and PC methods. The corrosion resistance for all the deposits increased with the content of TiO_2 in the coating. PC-plated coatings also had superior corrosion resistance than their DC counterparts. However, ref. [66] obtained different results when they plated the nanocomposites using both methods. DC-electrodeposited Ni–W–TiO_2 nanocomposite coatings exhibit inferior corrosion resistance as compared to Ni–W alloy and pulse-plated Ni–W–TiO_2 coatings. Therefore, the current regime and other plating process parameters have significant influence on the improvement

http://dx.doi.org/10.5772/62170

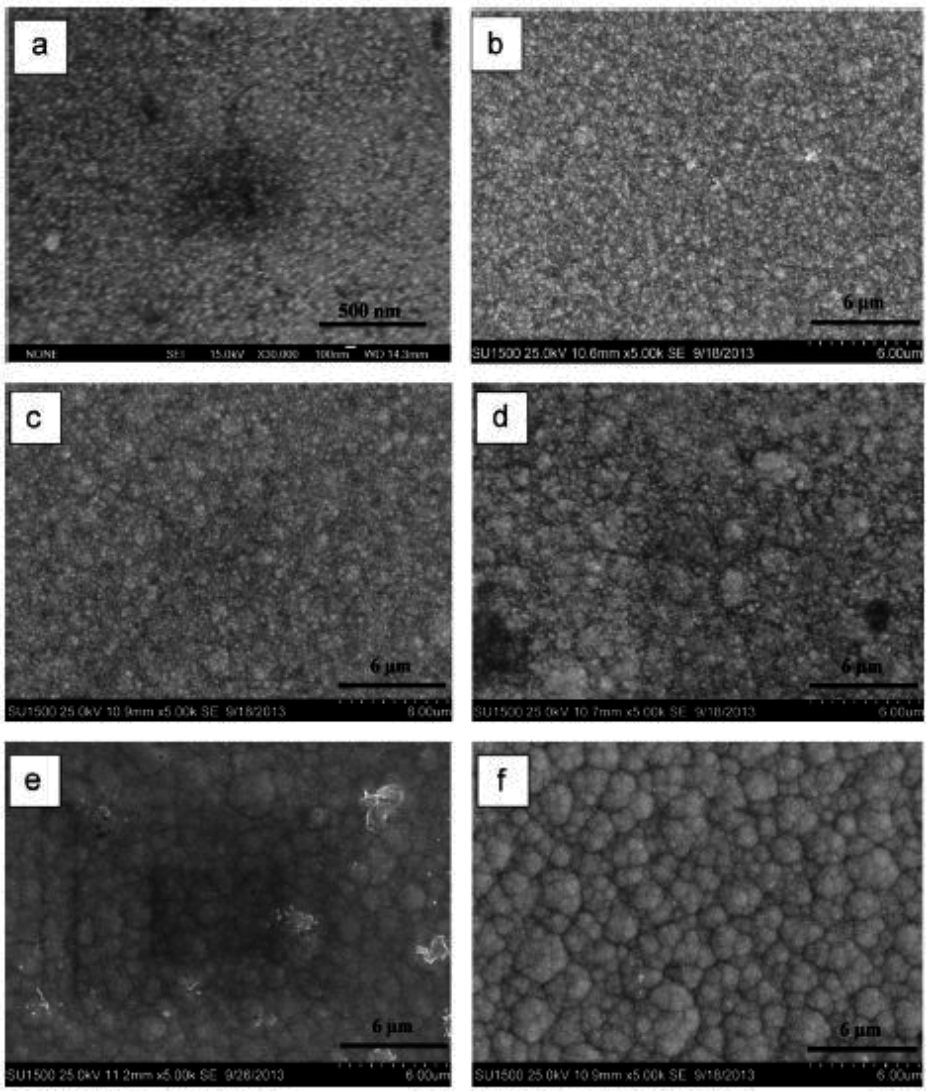

Figure 9. Surface morphologies of Ni–W alloy and nanocomposite coatings [65]

of functional properties. PTFE (polytetrafluoroethylene) particles co-deposited with Ni–W alloy using pulse current electrodeposition showed improvement in morphology, hardness, corrosion resistance, and tribological properties of the deposits [67]. The increase in particle content in the coatings from 0 to 20 g/l had positive influence on the mentioned properties. PTFE particles are chemically inert and possess low coefficient of friction when compared to other polymers. SiC nanoparticles showed similar behaviour when they were incorporated into Ni–W alloy [68]. Boron nitride particles possess excellent self-lubrication properties and reduce the surface roughness of Ni–W alloy, thus decreasing friction of the coatings and improving their wear resistance [69]. The inclusion of the particles also significantly affects the

corrosion resistance of the coatings (30 mV potential shift). Ref. [70] reported MoS_2 particles to lower friction the coefficient of Ni–W matrix and enhance its tribological properties.

7. Applications

Electroplated nickel composite/nanocomposite coatings find applications in machining and finishing of tools requiring excellent corrosion and wear resistance, low friction, and high thermal stability. Wear, friction, and corrosion pose a serious threat to machine lifespan, energy consumption, and performance. These phenomena also compromise the safety of the personnel where the machine is used. Therefore, engineers prefer machines that have long lifespan, save energy, and have better performance throughout its service life. These machines or tools are made of lighter and cost-effective materials such as aluminium and steel, to enhance their quality; materials harder and chemically stable than them are used as coatings to protect them from surface degradation. Nickel, nickel alloy, and composite/nanocomposite coatings are perfect candidates for improving the quality of these materials.

Ni–SiC nanocomposite coatings are used to offer wear protection of aluminium-made engine pistons in automotive industry [70]. These parts operate under high temperatures and wear conditions. Other candidates that perform similar function of lining of cylinders in aluminium engines are Ni–Al_2O_3, TiO_2, WC, Cr_2O_3, etc. [71].

Electrodeposited Ni/diamond coatings have found applications in grinding and cutting tools, such as precision cutting wheels for dicing semiconducting silicon plates [71]. These also include nickel alloy composite coatings such as Ni–W reinforced with diamond nanoparticles. These coatings exhibit high hardness, excellent wear resistance, and elevated thermal stability.

Ni–PTFE composite coatings find use in precise mechanical parts [17]. These possess self-lubricating properties and are convenient for applications that require low friction. Other suitable coatings to perform similar functions are Ni–CNT, MoS_2, graphite, Si_3N_4, Ni–B, and BN composite coatings. They also exhibit high oxidation resistance.

8. Conclusion

This chapter outlines the fabrication of nickel composite/nanocomposite coatings, their properties, and applications. Due to the excellent properties exhibited by these coatings such as high hardness, excellent corrosion resistance and wear resistance, self-lubricating properties, and high thermal stability, the coatings have a good potential to replace chromium-based coatings. Their mechanism of co-deposition and optimization of process parameters need to be understand well to produce better coatings with improved surface properties. This understanding will also enable extension of their applications in the future to serve as alternatives for other coatings fabricated by cost and energy-intensive processes.

Author details

Nicholus Malatji and Patricia A.I. Popoola*

*Address all correspondence to: popoolaapi@tut.ac.za

Department of Chemical, Metallurgical and Materials Engineering, Tshwane University of Technology, Pretoria, South Africa

References

[1] Benea, L., Danaila, E. & Celis, J. 2014. Influence of Electro-Co-deposition Parameters on Nano-TiO_2 Inclusion into Nickel Matrix and Properties Characterization of Nano-composite Coatings Obtained. *Materials Science & Engineering A*, 610,106–115.

[2] Srivastava, M., Grips, V.K.W. & Rajam, K.S. 2009. Influence of Co on Si_3N_4 Incorporation in Electrodeposited Ni. *Journal of Alloys and Compounds*, 469, 362–365.

[3] Aal, A.A. & Hassan, H.B. 2009. Electrodeposited Nanocomposite Coatings for Fuel Cell Application. *Journal of Alloy and Compounds*, 477, 652-656.

[4] Gul, H., Kilic, F., Uysal, M., Aslan, S., Alp, A. & Akbulut, H. 2012. Effect of Particle Concentration on the Structure and Tribological Properties of Submicron Particle SiC reinforced Ni Matrix Composite (MMC) Coatings Produced by Eletrodeposition. *Applied Surface Science*, 258, 4260-4267.

[5] Srivastava, M., Grips, V.K.W. & Rajam, K.S. 2008. Influence of SiC, Si_3N_4 and Al_2O_3 Particles on the Structure and Properties of Electrodeposited Ni. *Materials Letters*, 62, 3487–3489.

[6] Eftekhari, A. & Molaei, F. 2015. Carbon Nanotube-Assisted Electrodeposition. Part I: Battery Performance of Manganese Oxide Films Electrodeposited at Low Current Densities. *Journal of Power Sources*, 274, 1306–1314.

[7] Shakoor, R.A., Kahraman, R., Waware, U.S., Wang, Y. & Gao, W. 2014. Synthesis and Properties of Electrodeposited Ni-B-CeO_2 Composite Coatings. *Materials and Design*, 59, 421–429.

[8] Wang, Y., Wang, S., Shu, X., Gao, W., Lu, W. & Yan, B. 2014. Preparation and Property of Sol-enhanced Ni-B-TiO_2 Nano-composite Coatings. *Journal of Alloy and Compounds*, 617, 472–478.

[9] Monteiro, O.R., Murugesan, S. & Khabashesku, V. 2015. Electroplated Ni–B Films and Ni–B Metal Matrix Diamond Nanocomposite Coatings. *Surface & Coatings Technology*, 272, 291–297.

[10] Gül, H., Uysal, M., Akbulut, H. &Alp, A. 2014. Effect Of Pc Electrodeposition on the Structure and Tribological Behaviour of Ni–Al_2O_3 Nanocomposite Coatings. *Surface & Coatings Technology*, 258, 1202–1211.

[11] Tudela, I., Zhang, Y., Pal, M., Kerr, I., Mason, T.J. & Cobley, A.J. 2015. Ultrasound-assisted Electrodeposition of Nickel: Effect of Ultrasonic Power on the Characteristics of Thin Coatings. *Surface & Coatings Technology*, 264, 49–59.

[12] Katamipour, A., Farzam, M. & Danaee, I. 2014. Effects of Sonication on Anticorrosive and Mechanical Properties of Electrodeposited Ni–Zn–TiO_2 Nanocomposite Coatings. *Surface and Coatings Technology*, 254, 358–363.

[13] Goerge, A. & Di, B. 2010. Modern Electroplating, Fifth Edition. John Wiley and Sons, Inc.

[14] Guglielmi, N. (1972). Kinetics of the Deposition of Inert Particles from Electrolytic Baths *J. Electrochem. Soc.*, 119, 1009–1012.

[15] Wang, S. & Wei, W.J. 2003. Kinetics of Electroplating Process of Nano-ceramic Particle/Ni Composite. *Materials Chemistry and Physics*, 78, 574–580.

[16] Hwang, B.J. & Hwang, C.S. 1993. Mechanism of Codeposition of Silicon Carbide with Electrolytic Cobalt. *Journal of Electrochemical Society*, 140, 979–984.

[17] Bercot, P., Pena-Munoz, E. & Pagetti. 2002. Electrolytic Composite Ni-PTFE Coatings: An Adaptation of Guglielmi's Model for the Phenomena of Incorporation. *Surface Coatings Technology*, 157, 282.

[18] Khan, T.R., Erbe, A., Auinger, M., Marlow, F. & Rohwerder, M. 2011. Electrodeposition of Zinc-silica Composite Coatings: Challenges in Incorporating Functionalized Silica Particles into a Zinc Matrix. *Science and Technology of Advanced Materials*, 12(5), 1–9.

[19] Sheu, H.A., Huang, P.B., Tsai, L.C. & Hou, K. 2013. Effects of Plating Parameters on the Ni–P–Al2O3 Composite Coatings Prepared by Pulse and Direct Current Plating. *Surface & Coatings Technology*, 235, 529–535.

[20] Kim, S. & Oh, T. 2011. Electrodeposition Behaviour and Characteristics of Ni-carbon Nanotube Composite Coatings. *Transactions of Nonferrous Metals Society of China*, 21, 68–72.

[21] Srivastava, M., Balaraju, J.N., Ravishankar, B. & Rajam, K.S. 2010. Improvement in the Properties of Nickel by Nano-Cr_2O_3 Incorporation. *Surface & Coatings Technology*, 205, 66–75.

[22] Spanou, S., Pavlatou, E.A. & Spyrellis, N. 2008. Ni/nano-TiO_2 Composite Electrodeposits: Textural and Structural Modifications. *Electrochimica Acta*, 54, 2547–2555.

[23] Beltowska-Lehman, E., Indyka, P., Bigos, A., Kot, M. & Tarkowski, L. 2012. Electrodeposition of Nanocrystalline Ni–W Coatings Strengthened by Ultrafine Alumina Particles. *Surface & Coatings Technology*, 211, 62–66.

[24] Borkar, T. & Harimkar, S.P. 2011. Effect of Electrodeposition Conditions and Reinforcement Content on Microstructure and Tribological Properties of Nickel Composite Coatings. *Surface & Coatings Technology*, 205, 4124–4134.

[25] Kumar, K.A., Kalaignan, G.P. & Muralidharan, V.S. 2013. Direct and Pulse Current Electrodeposition of Ni-W-TiO_2 Nanocomposite Coatings. *Ceramics International*, 39, 2827–2834.

[26] Beltowska-Lehman, E., Indyka, P., Bigos, A., Szczerba, M.J. & Kot, M. 2015. Ni–W/ZrO_2 Nanocomposites Obtained by Ultrasonic DC Electrodeposition. *Materials and Design*, 80, 1–11.

[27] Lee, H.K., Lee, H.Y. & Jeon, J.M. 2007. Codeposition of Micro- and Nano-sized SiC Particles in the Nickel Matrix Composite Coatings Obtained by Electroplating. *Surface & Coatings Technology*, 201, 4711–4717.

[28] Sohrabi, A., Dolatib, A., Ghorbania, M., Monfared, A. & Stroevec, P. 2010. Nanomechanical Properties of Functionally Graded Composite Coatings. Electrodeposited Nickel Dispersions Containing Silicon Micro-and Nanoparticles. *Materials Chemistry and Physics*, 121, 497–505.

[29] Blejan, D. & Muresan L.M. 2013. Corrosion Behavior of Zn-Ni-Al2O3 Nanocomposite Coatings Obtained By Electrodeposition from Alkaline Electrolytes. *Materials and Corrosion*, 64, 433–438.

[30] Thiemig, D. & Bund, A. 2009. Influence of Ethanol on the Electrocodeposition of Ni/Al_2O_3 Nanocomposite Films. *Applied Surface Science*, 255, 4164–4170.

[31] Sancakoglu, O., Culha, O., Toparli, M., Agaday, B., & Celik, E. 2011. Co-deposited Zn-submicron Sized Al2O3 Composite Coatings: Production, Characterization and Micromechanical Properties. *Materials and Design*, 32, 4054–4061.

[32] Thiemig, D. & Bund, A. 2009. Influence of Ethanol on the Electrodeposition of Ni/Al_2O_3 Nanocomposite Films. *Applied Surface Science*, 255, 4164–4170.

[33] Low, C.T.J., Wills, R.G.A. & Walsh, F.C. 2006. Electrodeposition of Composite Coatings Containing Nanoparticles in a Metal Deposit. *Surface & Coatings Technology*, 201, 371–383.

[34] García-Lecina, E., García-Urrutia, I., Díez, J.A., Morgiel, J. & Indyka, P. 2012. A Comparative Study of the Effect of Mechanical and Ultrasound Agitation on the Properties of Electrodeposited Ni/Al_2O_3 Nanocomposite Coatings. *Surface & Coatings Technology*, 206, 2998–3005.

[35] Haq, I.U., Akhtar, K., Khan, T.I. & Shah, A.A. 2013. Electrodeposition of Ni–Fe_2O_3 Nanocomposite Coating on Steel. *Surface & Coatings Technology*, 235, 691–698.

[36] Vaezi, M.R., Sadrnezhaad, S.K. & Nikzad, L. 2015. Electrodeposition of Ni–SiC Nanocomposite Coatings and Evaluation of Wear and Corrosion Resistance and Electroplating Characteristics. *Colloids and Surfaces A: Physicochememical Engineering Aspects*, 315, 176–182.

[37] SADRNEZHAAD, S.K. 2004. Kinetics Processes in Materials Engineering and Metallurgy, 2nd ed., Amir Kabir Publication Institute, Tehran, Iran, (in Persian).

[38] Zhao, Y., Jiang, C., Xu, Z., Cai, F., Zhang, Z. & Fu, P. 2015. Microstructure and Corrosion behavior of Ti Nanoparticles Reinforced Ni–Ti Composite Coatings by Electrodeposition. *Materials and Design*, 85, 39–46.

[39] Khalil, M.W., Salah Eldin, T.A., Hassan, H.B., El-Sayed, K. & Hamid, Z.A. 2015. Electrodeposition of Ni–GNS–TiO_2 Nanocomposite Coatings as Anticorrosion Film for Mild Steel in Neutral Environment. *Surface & Coatings Technology*, 275, 98–111.

[40] Zhang, H., Zhou, Y. & Sun, J. 2013. Preparation and Oxidation Behaviour of Electrodeposited Ni–CeO_2 Nanocomposite Coatings. *Journal of Rare Earths, 28, 97.*

[41] Wanga, Y., Wang, S., Shu, X., Gao, W., Lu, W. & Yan, B. 2014. Preparation and Property of Sol-enhanced Ni–B–TiO2 Nano-composite Coatings. *Journal of Alloys and Compounds*, 617, 472–478.

[42] Zarghami, V. & Ghorban, M. 2014. Alteration of Corrosion and Nanomechanical Properties of Pulse Electrodeposited Ni/Sic Nanocomposite Coatings. *Journal of Alloys and Compounds*, 598, 236–242.

[43] Özkan, S., Hapçi, G., Orhan, G. & Kazmanli, K. 2013 Electrodeposited Ni/SiC Nanocomposite Coatings and Evaluation of Wear and Corrosion Properties. *Surface & Coatings Technology*, 232, 734–741.

[44] RAMESH BAPU, G.N.K. & JAYAKRISHNAN, S. 2012. Development and Characterization of Electro deposited Nickel-Titanium Carbo Nitride (TiCN) Metal Matrix Nanocomposite Deposits. *Surface and Coatings Technology*, 206, 2330–2336.

[45] Kasturibai, S. & Kalaignan, G.P. 2014, Characterizations of Electrodeposited Ni-CeO_2 Nanocomposite Coatings. *Materials Chemistry and Physics*, 147, 1042–1048.

[46] Lee, C.K. 2012. Wear and Corrosion Behavior of Electrodeposited Nickel–Carbon Nanotube Composite Coatings on Ti–6Al–4V Alloy in Hanks' Solution. *Tribology International*, 55, 7–14.

[47] Srivastava, M., Grips, V.K.W. & Rajam, K.S. 2008. Influence of SiC, Si_3N_4 and Al_2O_3 Particles on the Structure and Properties of Electrodeposited Ni. *Material Letters*, 62, 3487–3489.

http://dx.doi.org/10.5772/62170

[48] Haq, I. & Khan, T.I. 2011. Tribological Behavior of Electrodeposited Ni–SnO_2 Nanocomposite Coatings on Steel. *Surface & Coatings Technology*, 205, 2871–2875.

[49] Shi, L., Sun, C.F., Zhou, F. & Liu, W.M. 2005. Electrodeposited Nickel-cobalt Composite Coating Containing nano-sized Si_3N_4. *Materials Science and Engineering A*, 397, 190–194.

[50] Cardinal, M.F., Castro, P.A., Baxi, J., Liang, H. & Williams, F.J. 2009. Characterization and Frictional Behaviour of Nanostructured Ni-W-MoS_2 Composite Coatings. *Surface and Coatings Technology*, 204, 85–90.

[51] Madram, A.R., Pourfarzad, H. & Zare, H.R. 2012. Study of the Corrosion Behaviour of Electrodeposited Ni-P and Ni-P-C Nanocomposite Coatings in 1M NaOH. *Electrochemica Acta*, 85, 263–267.

[52] Sheu, H., Huang, P., Tsai, L. & Hou, K. 2013. Effects of Plating Parameters on the Ni–P–Al2O3 Composite Coatings Prepared by Pulse and Direct Current Plating. *Surface and Coatings Technology*, 235, 529–535.

[53] Alexis, J., Etcheverry, B., Beguin, J.D. & Bonino, J.P. 2010. Structure, Morphology and Mechanical Properties of Electrodeposited Composite Coatings Ni-P/SiC. *Materials Chemistry and Physics*, 120, 244–250.

[54] Lupi, C., Dell'era, A., Pasquali, M. & Imperatori, P. 2011. Composition, Morphology, Structural Aspects and Electrochemical Properties of Ni-Co Alloy Coatings. *Surface & Coatings Technology*, 205, 5394 – 5399.

[55] Srivastava, M., Grips, V.K.W. & Rajam, K.S. 2009. Influence of Co on Si_3N_4 Incorporation in Electrodeposited Ni. *Journal of Alloys and Compounds*, 469, 362–365.

[56] Shi, L., Sun, C.F., Gao, P., Zhou, F. & Liu, W.M. 2006. Electrodeposition and Characterization of Ni-Co-carbon Nanotubes Composite Coatings. *Surface Coatings and Technology*, 200, 4870–4875.

[57] Karslioglu, R. & Akbulut, H. 2015. Comparison Microstructure and Sliding Wear Properties of Nickel-cobalt/CNT Composite Coatings by DC, PC and PRC Current Electrodeposition. *Applied Surface Science*, 353, 615–627.

[58] Bakhit, B. & Akbari, A. 2012. Effect Of Particle Size and Co-deposition Technique on Hardness and Corrosion Properties of Ni-Co/SiC Composite Coatings. *Surface and Coatings Technology*, 206, 4964–4975.

[59] Yang, Y. & Cheng, Y.F. 2011. Electrolytic Deposition of Ni-Co-SiC Nano-coating for Erosion-enhanced Corrosion of Carbon Steel Pipes in Oils and Slurry. *Surface and Coatings Technology*, 205, 3198–3204.

[60] Panagopoulos, C.N., Georgiou, E.P., Tsopani, A & Piperi, L. 2011. Composite Ni-Co-fly ash Coatings on 5083 Aluminium Alloy. *Applied Surface Science*, 257, 4769–4773.

[61] Liang, Y., Li, Y., Yu, Q., Zhang, Y., Zhao, W. & Zeng, Z. 2015. Structure and Wear resistance of High Hardness Ni-B Coatings as Alternative for Cr Coatings. *Surface and Coatings Technology*, 264, 80–86.

[62] Krishnaveni, K., Narayanan, T.S.N. & Seshadri, S.K. 2006. Electrodeposited Ni-B Coatings: Formation and Evaluation of Hardness and Wear Resistance. *Materials Chemistry and Physics*, 99, 300–308.

[63] Bekish, Y.N., Poznyak, S.K., Tsybulskaya, L.S. & Gaevskaya, T.V. 2010. Electrodeposited Ni-B Alloy Coatings: Structure, Corrosion Resistance and Mechanical properties. *Electrochemica Acta*, 55, 2223–2231.

[64] Wang, Y., Wang, S., Shu, X., Gao, W., Lu, W. & Yan, B. 2014. Preparation and Property of Sol-enhanced Ni-B-TiO_2 Nano-composite Coatings. *Journal of Alloys and Compounds*, 617, 472–478.

[65] Arganaraz, M.P.Q., Ribotta, S.B., Folquer, M.E., Gassa, L.M., Benitez, G., Vela, M.E. & Salvarezza, R.C. 2011. Ni-W Coatings Electrodeposited on Carbon Steel: Chemical Composition, Mechanical Properties and Corrosion Resistance. *Electrochemica Acta*, 56, 5898–5903.

[66] Wang, Y., Zhou, Q., Li, K., Zhong, Q. & Bui, Q.B. 2015. Preparation of Ni–W–SiO_2 Nanocomposite Coating and Evaluation of its Hardness and Corrosion Resistance. *Ceramics International*, 41, 79–84.

[67] Goldasteh, H. & Rastegari, S. 2014. The Influence of Pulse Plating Parameters on Structure and Properties of Ni–W–TiO_2 Nanocomposite Coatings. *Surface & Coatings Technology*, 259, 393–400.

[68] Sangeetha, S., Kalaignan, G.P. & Anthuvan, J.T. 2015. Pulse Electrodeposition of Self-lubricating Ni-W/PTFE Nanocomposite Coatings on Mild Steel Surface. *Applied Surface Science*, 359, 412–419.

[69] Yao, Y., Yao, S., Zhang, L. & Wang, H. 2007. Electrodeposition and Mechanical and Corrosion Resistance Properties of Ni-Co/SiC Nanocomposite Coatings. *Materials Letters*, 61, 67–70.

[70] Sangeetha, S. & Kalaignan, G.P. 2015. Tribological and Electrochemical Corrosion Behaviour of Ni–W/BN (hexagonal) Nano-composite Coatings. *Ceramics International*, 1–10.

[71] Pradeep Devaneyan, S.A. & Senthilvelan, T. 2014 Electro Co-deposition and Characterization of SiC in Nickel Metal Matrix Composite Coatings on Aluminium 7075. *Procedia Engineering*, 97, 1496–1505.

Chapter 11

Electrodeposition of Functional Coatings on Bipolar Plates for Fuel Cell Applications – A Review

Peter Odetola, Patricia Popoola, Olawale Popoola and David Delport

Additional information is available at the end of the chapter

http://dx.doi.org/10.5772/62169

Abstract

The issue of corrosion and degradation has been evaluated as one of the major sources of concern in the history and trend of materials development and their applications in engineering. Design, process, and production consideration of materials hinge on the motive of built-to-last technology in their lifetime applications. The "World Corrosion Organization" has calculated that the direct cost of corrosion worldwide is over 3% of global gross domestic product (GDP)—approximately US $2.2 trillion—every year.

Natural materials tend to return to their original stable states after being conformed through processes into engineering applications. In order to conserve materials' integrity, usability, safety, and performance, the materials have to be subjected to processes that will keep them in its optimal functionalities.

The finishing phase of most materials for engineering applications is usually done with protective barrier in the form of coating, paint, or furnishes to conserve the materials' integrity and inhibit its susceptibility to interact with the environment.

Complete overhauling of a whole corrosion-invaded device is capital intensive. Corrective maintenance through repair work on damaged parts is not economically viable. To minimize or avoid these costs, adoption of functional composite coatings using electrodeposition can be effective.

Bipolar plate of fuel cell is a key performance component with corrosion challenge. This chapter will focus on electrodeposition as one of the corrosion inhibition techniques on bipolar plate of fuel cell [1, 2]. Through electrodeposition, bipolar plate can be protected with appropriate functional coatings to enhance surface quality and impart good surface properties that will prolong lifespan application in fuel cell vehicles.

Keywords: Fuel cell, Bipolar plate, Coatings, Electrodeposition, Corrosion

1. Introduction

The study of fuel cell is highly relevant to solving ongoing worldwide threats of pollution as well as meeting up with the future energy demands for technological advancement. Fuel cells have been proposed for use in automobiles as a replacement of the conventional internal combustion engines. Fuel cells produce power in an entirely different way compared to internal combustion engines and storage batteries. Fuel cell is an electrochemical system that works on reverse electrolysis combining hydrogen from fuel with oxygen from air to produce electric power directly. Heat and non-polluted water vapor are the only by-products of these systems. Internal combustion engines[3] are powered from the combustion of hydrocarbon fuel through the Carnot cycles. The combustion process releases harmful gases such as CO, CO_2, SO_2, etc., into the environment, polluting it and affecting the energy balance of the ecosystem through global warming and damaging the protective ozone layers. Conversely, batteries are chemical energy storage devices that only produce power intermittently, as they must be recharged after being exhausted. The recharging process is always lengthy and inconvenient.

1.1. Timeline for fuel cell development

Fuel cell was first discovered by William Grove in 1839 when he thought it possible to produce electric current through reverse electrolysis by combining hydrogen and oxygen together. This awareness made scientists throughout the 19th century to conduct several studies until Francis Thomas Bacon, a British scientist, worked on developing alkaline fuel cells in 1958. This technology was utilized for NASA Apollo spacecraft program and was licensed to Pratt and Whitney. Through the research work of Thomas Grubb and Leonard Niedrach in 1960, polymer electrolyte membrane (PEM) technology was invented at General Electric (GE). A small fuel cell was further developed in the mid-1960s by General Electric for US Army Signal Corps and US electronic division of the Navy's Bureau of ships. In the year 1970, GE developed a novel water-electrolysis technology for undersea life support leading to the US Navy Oxygen Generating Plant. The British Royal Navy adopted this technology in the early 1980s for their submarine fleet. In the 1990s, Los Alamos National Lab and Texas A&M University researched different ways of reducing platinum load required for PEM cells.

1.2. Definition of fuel cell

A fuel cell is an electrochemical device that converts the chemical energy of a fuel (e.g., hydrogen, methanol, etc.) and an oxidant (air or pure oxygen) in the presence of a catalyst into electricity, heat, and water[4].

Economy benefits of fuel cells are possible as a result of its fantastic flexibility and features over conventional energy sources:

- Fuel cells produce clean energy through electrochemical conversion of the fuel. Therefore, they are environmentally friendly because of the zero or very low emissions.

http://dx.doi.org/10.5772/62169

- Fuel cells are high-power generating system from a few watts to hundreds of kilowatt with efficiencies much higher than conventional internal combustion engine.
- Fuel cells have low noise production because of few moving parts.
- Fuel cells can be used as a power source for mobile applications such as fuel cell vehicles and boats and also in stationary applications such as laptops and phones.

1.3. Component of a fuel cell

The fuel cell assemblage which comprises bipolar plate (BP), membrane electrode assembly (MEA), gas diffusion layers (GDL), catalyst layer (Nafion®), seal, and the end plates function together as heat and electrical generating system[5].

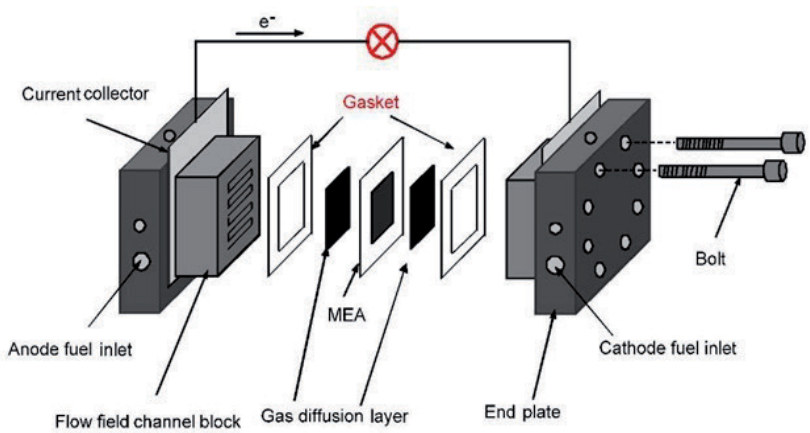

Figure 1. Showing components made up of bipolar plate stacks (www.what-when-how.com)

1.3.1. Membrane electrode assembly

"Membrane Electrode Assembly (MEA)" is the heart of a fuel cell consisting of polymer membrane electrolyte and two electrodes (anode and cathode) that sandwich the polymer membrane. It has three components fused and compressed together by high pressure and temperature. The industry standard of polymer membrane is Nafion developed in the 1970s by DuPont. Nafion consists of polytetrafluoroethylene (PTFE) chains commonly known as Teflon forming the backbone of the membrane. MEA plays the role of separating electrons and protons from fuel and therefore moves the protons (hydrogen ions) to the cathode side where it recombines with the air to form water and heat. It enhances proton conduction and improves stability in terms of chemical, mechanical, and dimensional alteration[6].

1.3.2. Catalyst

"Platinum" is a common noble metallic that acts as a catalyst in the acidic fuel cell environment. The platinum catalyst in the form of tiny particles is deposited on the large surface area of the

carbon cloth for a better reaction. The platinum catalyzes the conversion of hydrogen molecule of the fuel into electrons and protons at the anode side. Moreover, at the cathode side, it helps to split oxygen molecule into two atoms and then combines with the electrons and protons from hydrogen to produce water. Platinum catalyst is extremely sensitive to CO poisoning from the fuel gas derived from hydrocarbon fuel[7].

1.3.3. Gas diffusion layers

"Gas Diffusion Layers (GDL)" is responsible for uniform distribution of the reactants from the bipolar plates into the active catalyst sites. It helps in membrane humidification[8]. It helps in effective current assemblage and water-heat removal as well.

1.4. Fuel cell stack

The amount of power produced by a fuel cell is dependent on several factors, such as the size, type, operating temperature, and pressure of the gas supplied into the cell. However, a single fuel cell produces enough electricity for only the smallest applications. Therefore, to realize sufficient operational power output, individual fuel cells are typically combined in series to form fuel cell stack[4,5,9]. A typical fuel cell stack may consist of hundreds of fuel cells.

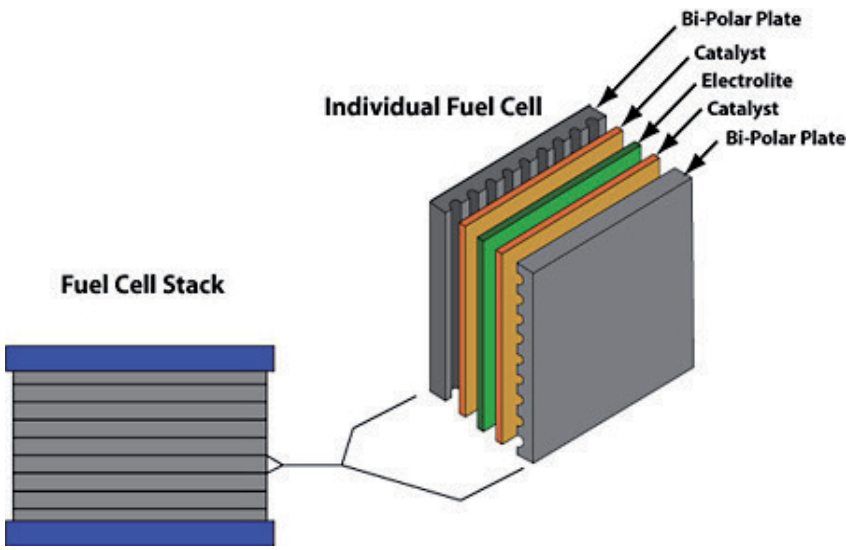

Figure 2. Showing components of fuel cell stack (www.tech-etch.com)

1.5. Types of fuel cell

Fuel cells are broadly classified into the following types:

- Alkaline fuel cell (AFM)

http://dx.doi.org/10.5772/62169

- Direct methanol fuel cell (DMFC)
- Molten carbon fuel cell (MCFC)
- Phosphoric acid fuel cell (PAFC)
- Polymer electrode membrane fuel cell (PEMFC)
- Solid oxide fuel cell (SOFC)

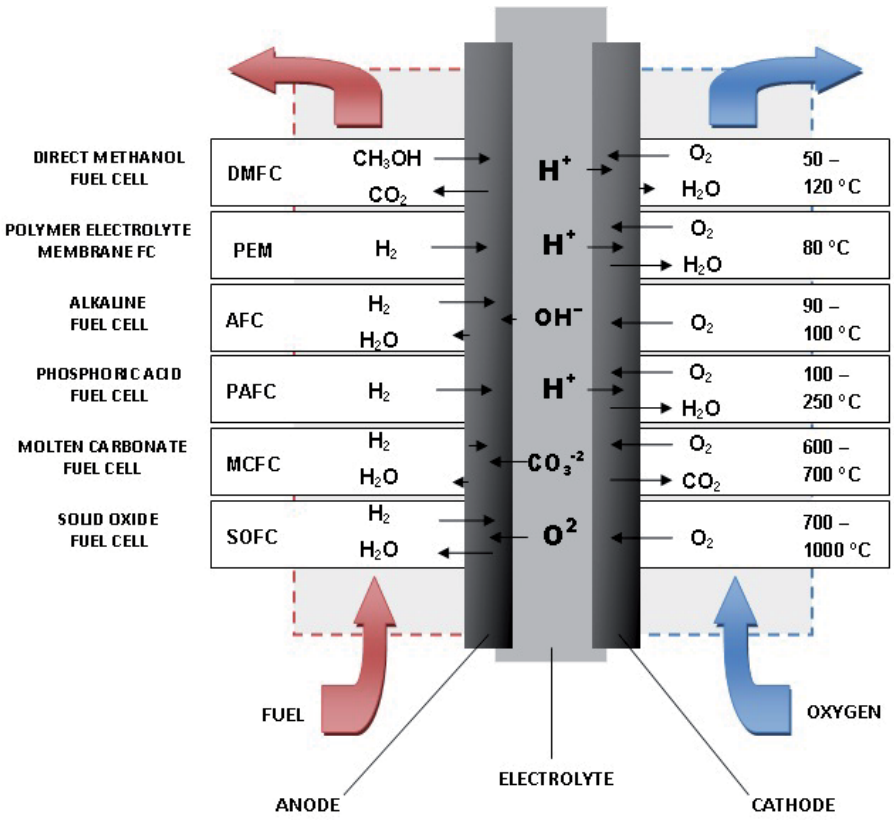

Figure 3. Showing different types of fuel cells (www.fuelcells.org)

1.6. Brief Description of Fuel Cell Type

1.6.1. AFC

"AFC" was one of the first fuel cell technologies developed and was originally used by NASA space shuttle missions to produce electrical energy and water onboard spacecraft. The fuel cell uses a solution of potassium hydroxide as an electrolyte and can use a variety of non-precious metals as a catalyst at the electrodes. This fuel cell has high performance due to the rate at

which chemical reactions take place in the cell. They are also very efficient in space applications with efficiencies up to 60%[10].

The major setback of this fuel cell is carbon dioxide poisoning of the electrolyte. Even little concentration of carbon dioxide in air can adversely affect its operation, making it necessary to purify the hydrogen and oxygen before use. This affects the cell's lifetime and incurs additional cost. AFC stacks have at least 8000 average operating hours and to make it economically viable for large-scale utility operations, operating times exceeding 40,000 hours are needed. This is possibly the most significant hindrance to its commercialization.

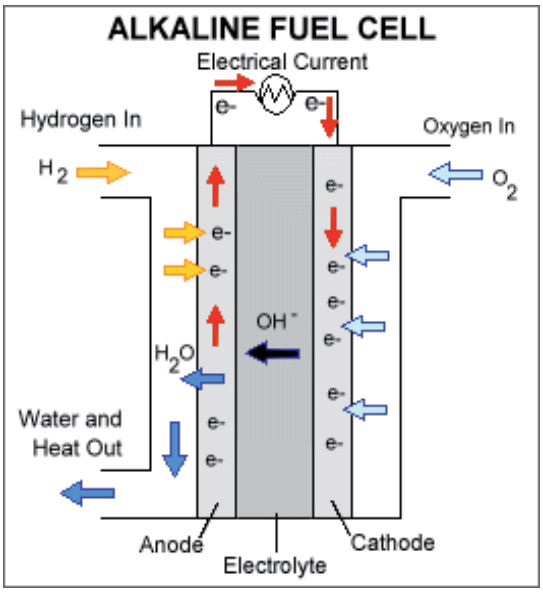

Figure 4. Showing components of alkaline fuel cell (www.fuelcellmarkets.com)

1.6.2. DMFC

"DMFC" uses polymer membrane as an electrolyte such as the polymer electrolyte membrane fuel cells (PEMFC). The distinction lies in the anode catalyst that draws hydrogen from the liquid methanol[11], eliminating the need for reformer. Therefore, pure methanol can be used as fuel.

1.6.3. MCFC

"MCFC" uses molten carbonate salt mixture suspended in a porous, chemically inert ceramic lithium aluminum oxide ($LiAlO_2$) matrix as the electrolyte. In molten carbonate fuel cells, negative ions travel through the electrolyte to generate water and electrons[4]. They operate at extremely high temperatures of about 650°C and beyond. MCFCs offer significant reduction in cost by using non-precious metals as catalysts at the electrodes. The efficiency level is up to

http://dx.doi.org/10.5772/62169

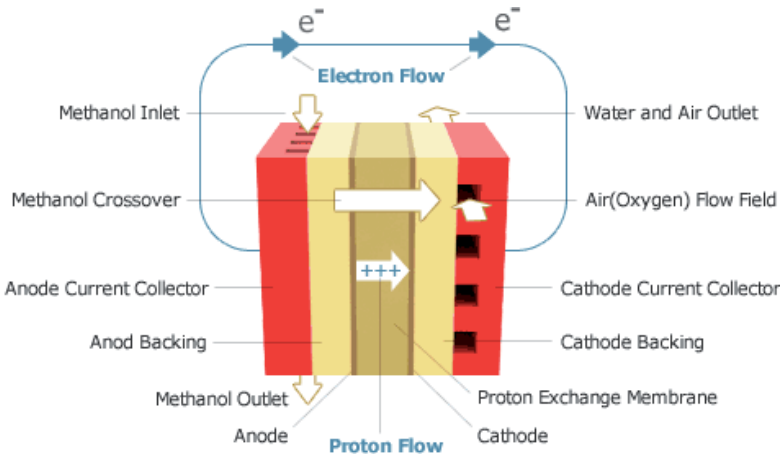

Figure 5. Showing components of direct methanol fuel cell (www.daviddarling.info)

60% which is considerably higher than 35–50% efficiencies of a phosphoric acid fuel cell. Overall, fuel efficiencies mount up to about 85% when the waste heat is captured and used. As a result of the elevated temperature at which it works, the fuels are converted to hydrogen by a process known as internal reforming within the fuel cell. This also makes it economical.

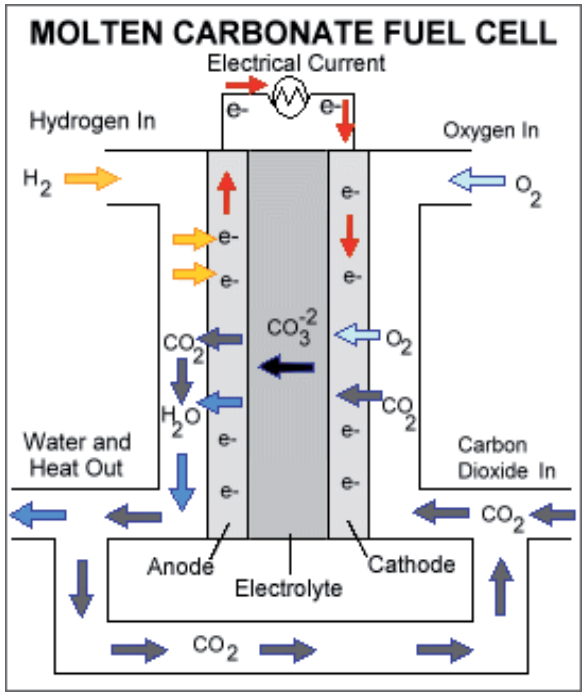

Figure 6. Showing components of molten carbon fuel cell (www.fuelcellmarkets.com)

1.6.4. PAFC

"PAFC" uses liquid phosphoric acid as an electrolyte contained in a silicon carbide matrix bonded in Teflon and has finely dispersed platinum catalyst inside its porous carbon electrodes.

Phosphoric acid fuel cell is considered as the first-generation modern fuel cells. It is the first most commercially developed fuel cell used to power many commercial premises and large buses such as city buses. The major challenge of PAFC is the costly platinum catalyst which makes it uneconomical.

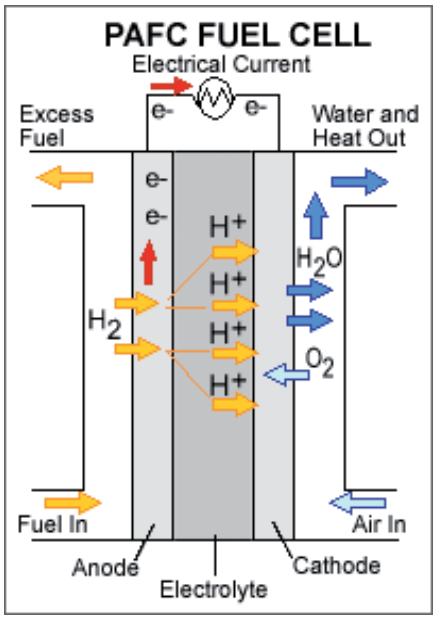

Figure 7. Showing components of phosphorus acid fuel cell (www.fuelcellmarkets.com)

1.6.5. PEMFC

"PEMFC" uses a solid polymeric membrane as the electrolyte and platinum catalyst contained in porous carbon electrodes. Polymer electrolyte membrane fuel cells[2,4& 12]operate at moderately low temperature range of 80°C to 100°C. The low operating temperature range enables them to quick start (short warm-up time) and results in better durability (lesser wear on system components).

PEMFC utilizes the platinum catalyst on its membrane. Platinum catalyst[7]is very expensive even in small quantity and also very sensitive to carbon monoxide poisoning, making application of reactor that will reduce its concentration in hydrogen fuel gas-derived fossil fuel necessary. This adds to the overall cost. In recent times, researchers are exploring platinum/ruthenium catalysts that are more resistant to CO, as better substitutes.

http://dx.doi.org/10.5772/62169

Another significant challenge to suitability of fuel cells for vehicles is low hydrogen storage capacity. Hydrogen is a very light gas with low energy density and will require a very large storage tank to store it onboard to power the fuel cell vehicles over a considerable distance, typically 300–400 miles like the gasoline-powered vehicles before refueling. Higher-density liquid fuels such as methanol, ethanol, natural gas, liquefied petroleum gas, and gasoline cannot be used directly unless they are processed into hydrogen through an onboard reformer unit. This increases costs and maintenance requirements.

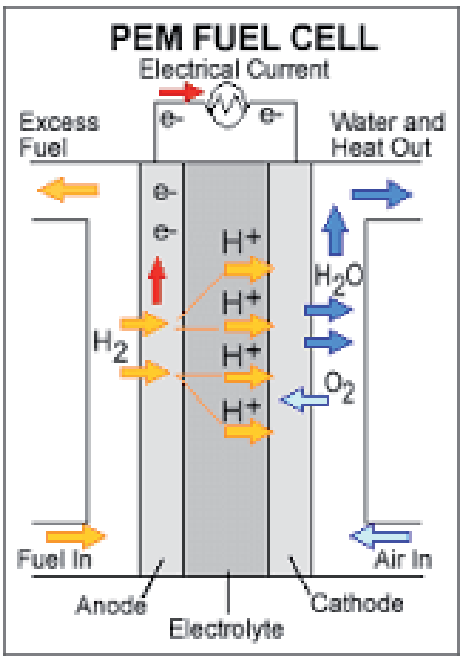

Figure 8. Showing components of polymer electrolyte fuel cell (www.daviddarlin.info)

1.6.6. SOFC

"SOFC" uses a hard, nonporous solid ceramic compound as the electrolyte, such as zirconium oxide stabilized with yttrium oxide, instead of a liquid. It works at a higher temperature range of 800˚C to 1000°C and can attain efficiencies around 60%. This makes it suitable for providing auxiliary power in vehicles and also for industrial electricity and heat generation. The high-temperature operating conditions allow fuels to reform internally and also nullify the need for any precious metal catalyst, thereby saving cost. The high operating temperature results in a slow start-up and requires huge thermal shielding which renders it unsuitable for transportation and small portable applications. The development of moderate cost materials that will be stable under the stringent operating conditions is the major challenge facing this technology. Research and development are currently developing lower-temperature SOFCs operating at or below 800°C with minimal durability problems and lesser cost.

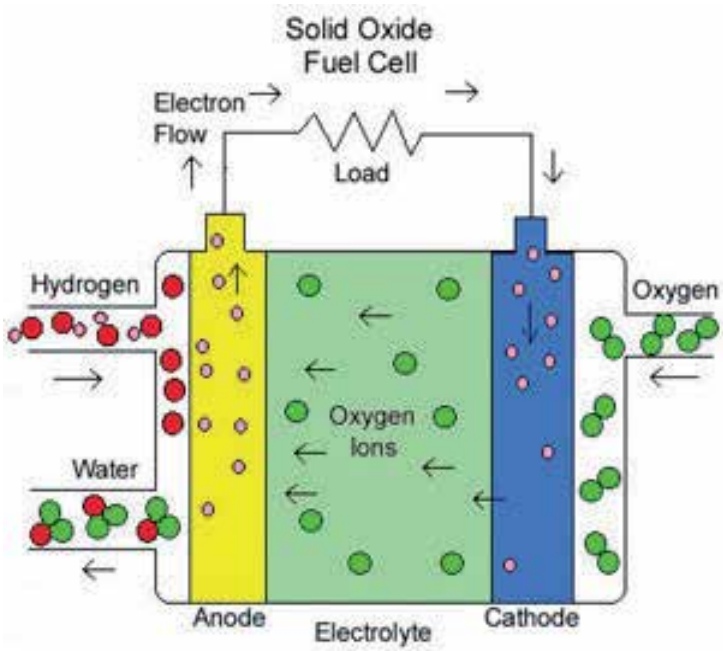

Figure 9. Showing components of molten carbon fuel cell (www.iit.edu)

1.7. Polymer electrolyte membrane fuel cell: A case study

Polymer electrolyte membrane fuel cell also known as proton exchange membrane fuel cell has been proposed to be a suitable candidate for use in fuel cell vehicles[2].

The major portion of the fuel comprises hydrogen (H_2) and oxygen (O_2) from air which together acts as an oxidant. Both react together electrochemically producing electricity and water as by-products.

The different components of PEMFCs are as follows:

- Bipolar plates
- "Anode" is the negative electrode that conducts freed electrons to an external circuit.
- "Cathode" is the positive electrode that distributes oxidant to the surface of the catalyst and it also conducts the electrons back from the external circuit to the catalyst where they can recombine with the hydrogen ions and the oxygen to form water and heat.
- "Catalyst" usually made up of platinum serves the purpose of splitting fuel and oxidant at the anode and cathode interface.
- "The electrolyte" is the proton exchange membrane that is only permeable to hydrogen ions serving as its transport medium.
- Gas diffusion layers (GDL)

http://dx.doi.org/10.5772/62169

1.8. Mode of operation of PEMFC

- Hydrogen gas is fed to the anode side of the fuel cell, while oxygen or air enters through the cathode side of the cell.
- At the anode side, a platinum catalyst causes the hydrogen to split into positive hydrogen ions (protons) and negatively charged electrons.
- The polymer electrolyte membrane allows only the proton to pass through it to the cathode while the electrons are moved away to an external circuit to do useful work.
- At the cathode side, the electrons from the external circuit attract the hydrogen ions through the membrane with an oxygen atom to form water molecule which flows out of the cell.

1.9. Bipolar plates: The key performance component of PEMFC

The successful commercialization of fuel cell for future use and its suitability to compete on economical scale above other energy sources still depend on the performance of the bipolar plates. The bipolar plate accounts for more than 40% of the total stack cost and about 80% of the total weight[13].

As a result of this, there have been significant esearchresearch and evelopmentdevelopment activities in the past few years to lower their cost, reduce their size, and improve their performance and lifetime in applications.

2. Functions of bipolar plates

Bipolar plates perform a number of critical functions simultaneously in a fuel cell stack to ensure acceptable levels of power output and a long stack lifetime[14]as described in the following:

- They collect and transport electrons from the anode to cathode.
- They connect individual fuel cells in series to form a fuel cell stack of the required voltage.
- They separate fuel gas (hydrogen) and oxidant (oxygen or air) feeding hydrogen to the anode and oxygen to the cathode while removing water and unreacted gases. Hence, they are impermeable to gases.
- They contain the gas flow field channels, thereby providing a flow path for gas transport to uniformly distribute the gases over the entire electrode area.
- They provide thermal conduction to help regulate fuel cell temperature and remove heat from the electrodes to the cooling channels or media.
- They provide structural support for the fuel cell stack.

2.1. Bipolar plate materials

The materials [12, 15] required for bipolar plates fall into two categories:

- Non-metallic materials, for example, graphite or polymer-based composites.
- The metallic materials, for example, stainless steel, aluminum, titanium, nickel, copper, etc.

Substrate	Conductivity (S/cm)	Density (g/cm^3)	Thickness (mm)
Aluminum	370,000	2.7	1–2
Stainless Steel	10,000	8.0	1–2
Graphite	110–680	1.8–2	5-6

Table 1. Showing properties variation of bipolar plates materials

2.1.1. Aluminum

It has a relatively low density, good strength, and higher thermal conductivity than stainless steel. Aluminum bipolar plates can be produced by casting, machining, and etching methods. This leads to lower production time and costs when compared to graphite. The major setback of aluminum lies in the formation of an electrically insulating oxide layer which impedes bipolar plate performance.

2.1.2. Stainless steel

Stainless steel has been shown to have the potential to meet all of the requirements for bipolar plates. It has a relatively low cost with high electrical and thermal conductivity, good mechanical properties, and ease of machining. Stainless steel bipolar plates[16] can be rapidly manufactured in large quantities by stamping. In the acidic environment within the fuel cell, stainless steel passivates forming Cr_2O_3 which elevates the interfacial contact resistance.

Most conventional coatings for stainless steel have shown to add to overall cost and also leave surface defects which result in local corrosion, damaging the fuel cell. The development of cost-effective coatings is the most significant research area in metallic bipolar plates. Despite the excellent physical properties and high-volume manufacturing processes available for metal bipolar plates, current technology places the estimated cost at $60–100/kW or 6 to 10 times the current target for transportation[17].

2.2. Bipolar plate DOE performance targets

As defined by the US Department of Energy (DOE), an ideal material for bipolar plates must meet the following requirements[18]:

- Bulk electrical conductivity (in-plain):
- Hydrogen permeability:

http://dx.doi.org/10.5772/62169

- Corrosion rate:
- Interfacial contact resistance: at
- Tensile strength:
- Flexural strength:
- Thermal conductivity:
- Thermal stability: up to for PEMFC
- Cost: 2005,
- Chemical and electrochemical stability in acidic environments
- Low thermal expansion
- Acceptable hydrophobicity
- Rapid and inexpensive manufacture

2.3. Performance control strategies for fuel cell

2.3.1. Corrosion management

Corrosion problem is only associated with metallic bipolar plate materials such as stainless steel, aluminum, nickel, and titanium. The bipolar plate works in an acidic environment and is therefore susceptible to corrosion attack[19, 20] through the electrochemical processes. The corrosion products of the metallic ions from the substrate at first will increase the surface contact resistance, then reduce the ionic conduction of the proton via the membrane electrode, and eventually poison it. Metallic coatings through electroplating can be used to address these problems. It will act as a protective barrier between the substrate and the aggressive acidic environment.

2.3.2. Water management

It has been well established that at the anode interface, the fuel undergoes a splitting process whereby only protons are permitted to pass through the membrane electrode assembly. Fuel cell performance is a function of effectiveness of the Nafion membrane to conduct the protons through it which also depend on the temperature and the level of relative humidity.

The proton conductivity of the Nafion membrane is highly influenced by the quantity of water absorbed in the membrane[21] and the maximum proton conductivity is attained when the membrane is fully saturated with water. Overflooding of water has an adverse effect of blocking the reaction sites of the neighboring electrodes, thereby preventing access of reactant gases into their cell. On the other hand, under low relative humidity, the absorbed water in the membrane vaporizes which remarkably reduces the proton conductivity and drastically increase the ohmic overpotential. To create balance, there is need for incorporation of water retention fillers in the electrolyte membrane such as TiO_2, SiO_2, ZrO_2, and heteropolyacids

which are both hygroscopic and proton conductors. Functionalized one-dimensional carbon nanotubes can also be incorporated into the Nafion membrane to improve the membrane performance operated under low relative humidity and dry conditions [22, 23].

2.4. Surface modification through coating

By definition, coating is a covering that can be applied to the surface of substrate for enhancement, functional, and modification purposes. The major purpose of coating on bipolar plate is to serve as corrosion resistance interface between the substrate and the environment, thereby reducing or eliminating the interfacial contact resistance that affects the overall power output of the fuel cell. They impact special surface properties of hardness, wear control, corrosion, and oxidation resistance without changing the substrate bulk properties. Therefore, improves surface properties.

Coating is mostly needed for application of metallic bipolar plates because of the possible interaction with the stringent acidic fuel cell environments that affects its overall performance. Oxide formation and ion dissolution as a result of metal bipolar plates can be prevented by applications of various coatings. Metallic bipolar plates[24, 25] are often coated with protective coating layers which serve as a barrier between its substrate and the corrosive media thereby preventing corrosion. The coating must be able to satisfy the following important criteria:

- It must have good adhesion to the substrate material without exposing its corrosive media. Proper adhesion of coating to the substrate is achieved by selecting coating materials with thermal expansion coefficients similar to those of the chosen bipolar plate's material to minimize micro- and macro-crack formation.
- It must be impermeable to the fuel cell reactant gases.
- It must be chemically stable or inert and give low contact resistance.
- It must be conductive so as to enhance electron conduction through it to the external circuit.

In the absence of corrosion, there will be no formation of metallic ions poisoning the membrane assembly electrode and reducing its potency for proton transport. Formation of oxide films in stainless steel as a self-protection against progression of corrosion that eventually result into high surface contact resistance will also be eliminated.

Two types of coatings[26–29] that have been investigated over the years as suitable candidates for bipolar plates are as follows:

- Carbon-based coatings: includes conductive polymer, graphite, diamond-like carbon, and organic self-assembled monopolymers.
- Metal-based coatings: comprises metal nitrides, metal carbides, metal oxides, and noble metals like gold, platinum, and ruthenium.

The investigation of metallic bipolar plates is divided into two major parts:

- Stainless steel and their coatings

http://dx.doi.org/10.5772/62169

- Aluminum, nickel, and other non-ferrous alloys and their coatings

2.5. Stainless steel and their coatings

Bare or uncoated stainless steel cannot satisfy DOE criteria for bipolar plate. There are three types of stainless steel with varying chromium contents: austenitic (AISI SS300)[30] has 18–20% Cr, ferritic (AISI SS400)[31, 32] has 17% Cr, and martensitic Cr quantities ≥ 11.5%. Chromium acts to produce a thin layer oxide of Cr_2O_3 which gives it self-surface protection and stop progression of corrosion. The passive layer of the thick oxide film however increases interfacial contact resistance between the bipolar plates and the gas diffusion layers which amount to the overall voltage drop. As a result of this, majority of studies[33, 35] on bipolar plates use measurements of interfacial contact resistance as the main criteria for material suitability.

In the stainless steel group, austenitic stainless steel is the most corrosion resistant due to its high Ni composition coupled with substantial level of chromium that gives it a higher formability at all temperatures from the cryogenic region to the melting point of the alloy.

They are the largest produced stainless steel accounting for about 70%. As a result, the grades 316, 310, and 304 SS have been investigated by many researchers as suitable candidates to replace nonporous graphite bipolar plates.

The primary selection criterion for austenitic stainless steel bipolar plates is the Cr, N, and Mo content that comes in different compositions and therefore makes them to behave differently in various environments. Addition of Mo and N is intended to enhance crevice and pitting corrosion resistance. Nickel and chromium addition is to improve strength and high-temperature oxidation resistance.

Over the years, ferritic stainless steel has been considered as bipolar plate material due to its low nickel content that reduces the overall cost of the material and eliminates the potential problem of Ni ion contamination of the membrane.

2.6. Titanium and their coating

Titanium[33] has been investigated as a suitable material for bipolar plates because of its properties such as low density, good mechanical strength, and high corrosion resistance. Titanium can form an insulating oxide film such as stainless steel. This surface passive film formed significantly increases ohmic losses with the stack resulting in lower power output compared to uncoated 316 SS. To tackle these challenges, further studies on titanium alloys with niobium and tantalum as viable bipolar plate materials showed that the resistivity of their surface oxides were lower than that of pure Ti. It was also found out that INEOS CHLOR patent PEMcoat™ coated on titanium offered an interfacial contact resistance similar to graphite.

2.7. Aluminum and their coating

In terms of cost and density, aluminum offers a better substitute compared to other bipolar plate materials. It also has an inherent problem of developing an oxide film like stainless steel

and titanium. This reduces its surface conductivity and rendered it incompetent as bipolar plate material except used in combination with other metals or with suitable coating blend.

2.8. Nickel and their coatings

Nickel is comparatively inexpensive, and it exhibits good ductility and ease of manufacturing. Pure nickel does not form protective oxide layer like other known bipolar plate materials but is very susceptible to severe corrosion. Therefore, there is need for alloying it with chromium to be very stable at minimum corrosion rate and low electrical resistivity compared to stainless steel alloys.

2.9. Copper and their coatings

Copper emerges as the only bipolar plate material with the highest possible electrical and thermal conductivity. Studies have shown that in a stimulated PEMFC environment, copper beryllium alloy Ce17200 has a corrosion rate of approximately 0.28 μm year at 70°C.

Materials such as Al, Cu, Sn, Ni, and Ni-phosphorous are very susceptible to electrochemical corrosion in acidic solutions that are typical of PEMFC operating conditions. However, gold shows very high resistance to electrochemical corrosion, in comparison to graphite, the traditional bipolar plate material.

In order for its multifunctional roles to be actualized, its material requirement has to be one of excellent electrical and thermal conductivity, good gas permeability, high mechanical strength, high corrosion resistance, and low weight. Having all these required properties locked up in a single material has ever been a challenge facing the research and development community on bipolar plates. As a result, different materials suited for different applications for bipolar plates such as metal, coated metal, graphite, flexible graphite, carbon–carbon composite, and carbon–polymer composites have been adopted over the years. None of these has been able to fulfill at once all the performance requirements and targets set by the US Department of Energy for fuel cell.

3. Electrochemical methods of applying coatings on metals

Techniques here include electrophoretic deposition, electrospray, electrodeposition, and electroless deposition.

3.1. Electrodeposition

This is a technique of using electrochemical processes to apply metallic coatings on metals or other conducting surfaces. Electrodeposition is done for the following purposes:

- Impartation of special surface properties like harness for wear control, toughness for tribology control, surface roughness for frictional control
- Protection and barrier intermediary between a material and the environments of influence

http://dx.doi.org/10.5772/62169

- Appearance as seen in aesthetic outlook and beautification of materials
- Engineering or mechanical properties

Electrodeposition works on the principle of electrolysis. Electroplating utilizes electrolytic cell setup whereby plating metal (anode) and metal to be plated (cathode) are inserted in plating bath containing the solution of a salt of the metal that is to form the coating. The object to be coated is connected to the negative terminal of an electric battery as cathode while the plating metal is connected to the positive terminal of the electric power source as anode. As the electroplating process continues, the metal salts in the bath are used up. If the anode is a bar of the coating metal, the bar dissolves in the bath at the same rate that the bath gives up its metal to the cathode. If the anode is made of another metal, salts of the coating metal must be added to the bath as metal becomes deposited on the cathode. The longer the process continues, the greater the thickness of the coating on the cathode.

3.2. Electroless deposition

Electroless deposition is mainly different from electroplating by not using external electrical power. It is purely chemical or autocatalytic plating that involves a reaction whereby hydrogen is released by reducing agent, normally sodium hypophosphite or thiourea and becomes oxidized, thus producing a negative charge on the surface of the part. The most common electroless plating method is electroless nickel plating, although silver, gold, and copper layers can also be applied in this manner, as in the technique of Angel gilding.

Electroless nickel plating, according to several studies, is a suitable method of coating metallic bipolar plates. Electroless nickel plating layers are known to provide extreme surface adhesion when plated properly.

3.3. Existing literature review on coating of bipolar plates of fuel cell

Corrosion resistance has always been the ultimate goal for bipolar plate of fuel cell. Actualizing this through correct application of surface barrier coating will minimize interfacial contact resistance of the fuel cell. Using electrochemical method TiN has been successfully coated on stainless steel 316L bipolar plate for proton-exchange membrane fuel cell [36]. The result of investigation showed that the TiN-coated 316L exhibits promising interfacial contact resistance and improved corrosion resistance in simulated aggressive PEMFC environments. Slight increase in the ICR was also observed after the potentiostatic polarization. This was due to the formation of stable passive film on the surface of the TiN-coated 316L.

Composite coatings are an excellent corrosion inhibitor and can be suitably formed through electrodeposition. To gain high hardness, good thermal stability, and corrosion resistance, multicomponent TiAlSiN coating has been developed by Li and colleagues using different deposition methods [37]. The authors demonstrated the influence of Al and Si on the electrochemical properties of TiN-coated 316L stainless steel bipolar plate in simulated PEMFC environment. The corrosion inhibiting efficiency was improved by incorporation of the Al and Si in TiN coating.

According to research conducted by Nam and colleagues, electroplating Cr-C coatings on SS304 offers an excellent conductivity and corrosion resistance [38]. The deposition was done under different current densities, and it was discovered that carbon content of the composite coating decreased with increasing current density. The surface roughness of Cr-C plated at current density of was observed to be smooth and crack-free. In addition, the lowest contact resistance was recorded at this value. Beyond this current density was formation of cracks and pinholes in the coating network.

A novel epoxy resin (EP)-based system containing polyaniline (PANI) was developed in the research work carried out by Baldissera and Ferreira [39] The PANI serves as an anticorrosive agent to monitor corrosion behavior of mild steel samples. It was found out that the addition of three different forms of PANI-undoped, sulfonated, and fibers to the epoxy resin increased its corrosion protection capacity. Based on the good outcomes, paints prepared with EP and PANI is able to be used as protective coating to metals even when exposed to aggressive marine environment.

In the study conducted by Hung et al. (2009) [40], coated aluminum and graphite composite bipolar plates were installed in separate single PEM fuel cells and tested under normal operating conditions and cyclic loading. After 1000 hours of operation, samples of both the bipolar plates and the membrane electrode assembly (MEA) were collected and characterized. The purpose was to examine the stability and integrity of the plate's coating and evaluate possible changes of the ionic conductivity of the membrane. The SEM/EDX analysis showed very small variation in the surface composition of the coated aluminum bipolar plate after 1000 hours of operation. Chromium was observed in one of the three cathode samples of the MEA. However, it was confirmed that the released Cr did not react with Pt. The microcracks that were observed in the corrosion resistance coating did not seem to completely penetrate through the substrate layer. Aluminum was also detected in the GDLs that were used in both coated aluminum and graphite composite fuel cell which is believed to come from aluminum oxide carried by the reactant gases from the uncoated back plate and gas manifold.

Conducting polymers as a new type of material have high redox potential complimented with properties of both metals and polymers. Polypyrrole coatings have gained outstanding recognition over the years as one of the most important conductive polymers successfully used in fuel cells, chemical sensors, batteries, anti-corrosion coatings, and drug delivery systems. Graphite-polypyrrole has been successfully coated on SS316L substrate as the bipolar plate for polymer electrolyte membrane electrode [41]. Synergy of graphite and polypyrrole as composite imparts good surface barrier and conductive properties. The polypyrrole enhances good corrosion resistance and electrical conductivity. The graphite further improves the electrical conductivity of the bipolar plate.

4. Summary

It has been shown that metallic bipolar plates are prone to corrosion attack in the fuel cell environment. In addition, the use of precious noble metals is not economical in meeting the

future cost projection of fuel cells to successfully compete with combustion engine vehicles. Though noble metals offer excellent conductivity and good corrosion resistance, they are phased out as viable bipolar plate materials over difficulty in forming them into thin strips. Composite-based bipolar plates are known for brittleness which in the long run may easily fail in operation of the fuel cell.

Metallic bipolar plates were proven to surpass the mechanical strength of graphite composite plates as well as giving acceptable electrical conductivity with minimal production cost on commercial scale. As indicated earlier, metallic plates are prone to corrosion in the fuel cell environment. Considerable research work has been conducted to enhance the material's corrosion resistance and interfacial contact resistance. It is concluded that metallic bipolar plates hold a promising potential as more research and development studies progress on its surface modification through different functional coatings.

Author details

Peter Odetola[1], Patricia Popoola[1*], Olawale Popoola[2] and David Delport[1]

*Address all correspondence to: popoolaapi@tut.ac.za

1 Department of Chemical, Metallurgical and Materials Engineering, Tshwane University of Technology, Pretoria, South Africa

2 Centre for Energy and Electrical Power, Department of Electrical Engineering, Tshwane University of Technology, Pretoria, South Africa

References

[1] Cunningham, B. D., Huang, J. and Baird, D. G. 2007. Review of materials and processing methods used in the production of bipolar plates for fuel cells. *Int. Mater.Rev.,* 52, 1-13.

[2] Hermann, A., Chaudhuri, T. and Spagnol, P. 2003. Bipolar plates for PEM fuel cells: A review. *Int. J. Hydrogen Energy,* 30, 1297-1302.

[3] Hung, Y. 2010. Performance evaluation and characterization of metallic bipolar plates in a proton exchange membrane (PEM) fuel cell.

[4] Fuel Cells 2000. [Online]. www.fuelcells.org/basics/how.html

[5] Viral, M. and Joyce, S. C. 2003. Review and analysis of PEM fuel cell design and manufacturing. *J. Power Sources,* 144, 32-53.

[6] Krishnamurthy, P., Krishnan, R. and Samban, D. K. 2012. Performance of a 1 kW class Nafion-PTFE composite membrane fuel cell stack. *Int. J. Chem. Eng.,* 2012, 7.

[7] Tilquin, J. Y., Cote, R., Guay, D., Dodelet, J. P. and Denes, G. 1996. Carbon monoxide poisoning of platinum-graphite catalysts for polymer electrolyte fuel cells: Comparison between platinum –supported on graphite and intercalated in graphite. *J. Power Sources,* 61, 193-200.

[8] Eckl, R., Zehtner, W., Leu, C. And Wagner, U. 2004. Experimental analysis of water management in a self-humidifying polymer electrolyte fuel cell stack. *J. Power Sources,* 138, 137-144.

[9] Xianguo, L. And Imran, S. Review of bipolar plates in PEM fuel cells: Flow-field designs. *J. Power Sources,* 30, 359-371.

[10] Cifrain, M. And Kordesch, K. 2003. Hydrogen/oxygen (Air) fuel cells with alkaline electrolytes. *Handbook Fuel Cells Fundam. Technol. Appl.,* 1, 267-280.

[11] Amir, F. and Zhen, G. 2005. Challenges and opportunities of thermal management issues related to fuel cell technology and modeling. *Int. J. Heat Mass Transfer,* 48, 3891-3920.

[12] Hermann, A., Chaudhuri, T. and Spagnol, P. 2003. Bipolar plates for PEM fuel cells: A review. *Int. J. Hydrogen Energy,* 30, 1297-1302.

[13] Hermann, A., Chaudhuri, T. and Spagnol, P. 2003. Bipolar plates for PEM fuel cells: A review. *Int. J. Hydrogen Energy,* 30, 1297-1302.

[14] Tsuchiya, H. and Kobayashi, O. 2004. Mass production cost of PEM fuel cell by learning curve. *Int. J. Hydrogen Energy*, 29, 985-990.

[15] Park, J., Dilasari, B., Kim, Y., Kim, K., Lee, C. K. and Kwon, K. 2014. Passivation behavior and surface resistance of electrodeposited nickel-carbon composites. *Electrochemistry,* 82, 561-565.

[16] Wang, Y. and Northwood, D. O. 2008. An investigation into the effects of a nanothick gold interlayer on polypyrrole coatings on 316L stainless steel for the bipolar plates of PEM fuel cells. *J. Power Sources,* 175, 40-48.

[17] Wang, H., Brady, M. P., Teeter, G. and Turner, J.A. 2004. Thermally nitrided stainless steels for polymer electrolyte membrane fuel cell bipolar plates. Part 1.Model Ni–50Cr and austenitic 349TM alloys. *J. Power Sources*, 138, 86-93.

[18] Richie, N. J. 2011. Development of hybrid composite bipolar plates for proton exchange membrane fuel cells. *Scholars' Mine.* Paper 7137.

[19] Karimi, S., Fraser, N., Roberts, B. and Foulkes, F. R. 2012. A review of metallic bipolar plates for proton exchange membrane fuel cells: Materials and fabrication methods.

[20] Lee, S. J., Huang, C. H., Lai, J. J. and Chen, Y. P. 2004. Corrosion-resistant component for PEM fuel cells. *J. Power Sources*, 131, 162-168.

[21] Li, M., Luo, S., Zeng, C., Shen, J., Lin, H. and Cao, C. 2004. Corrosion behavior of TiN coated type 316 stainless steel in simulated PEMFC environments. *Corros. Sci*., 46, 1369-1380.

[22] Eckl, R., Zehtner, W., Leu, C. and Wagner, U. 2004. Experimental analysis of water management in a self-humidifying polymer electrolyte fuel cell stack. *J. Power Sources*, 138, 137-144.

[23] Ketpang, K., Shanmugam, S., Suwanboon, C., Chanunpanich, N. and Lee, D. 2015. Efficient water management of composite membranes operated in polymer electrolyte membrane fuel cells under low relative humidity. *J. Membr. Sci,* 493, 285-298.

[24] Ous, T. and Arcoumanis, C. 2013. Degradation aspects of water formation and transport in proton exchange membrane fuel cell: A review. *J. Power Sources,* 240, 558-582.

[25] Borup, R. L. and Vanderborgh, N. E. 1995. Design and testing criteria for bipolar plate material for PEM fuel cell application. *Mater. Res. Soc. Symp. Proc., 393*, 151-155.

[26] Wind, J., Spah, R., Kaiser, W. and Bohm, G. 2002. Metallic bipolar plates for PEM fuel cells. *J. Power Sources*, 105, 256-260.

[27] Mehta, V. and Cooper, J. S. 2003. Review and analysis of PEM fuel cell design and manufacturing. *J. Power Sources*, 114, 32-53.

[28] Woodman, A. S., Anderson, E. B., Jayne, K. D. and Kimble, M. C. Development of-Corrosion-Resistant Coatings for Fuel Cell Bipolar Plates, in *American Electroplaters and Surface Finishers Society 1999, AESF SUR/FIN '99 Proceedings*, June 1999.

[29] Hermann, A., Chaudhuri, T. and Spagnol, P. 2005. Bipolar plates for PEM fuel cells: A review. *Int. J. Hydrogen Energy*, 30, 1297-1302.

[30] Wind, J., Spah, R., Kaiser, W. and Bohm, G. 2002. Metallic bipolar plates for PEM fuel cells. *J. Power Sources*, 105, 256-260.

[31] Tian, R.J., Sun, J.C. and Wang, J.L. 2006. Surface stability and conductivity of a high Cr and Ni austenitic stainless steel plates for PEMFC. *Rare Met*., 25, 229.

[32] Wang, H. and Turner, J. A. 2004. Ferritic stainless steels as bipolar plate material for polymer electrolyte membrane fuel cells. *J. Power Sources*, 128, 193-200.

[33] Ravi Narayan, L. 2012. Forming of ferritic stainless steel bipolar plates. *Electronic Theses and Dissertations.* Paper 205.

[34] Wang, Y., Chen, K. S., Mishler, J., Cho, S. C. and Adroher, X. C. 2011. A review of polymer electrolyte membrane fuel cells: Technology, applications, and needs on fundamental research. *Appl. Energy*, 88, 981-1007.

[35] Tawfik, H., Hung, Y. And Mahajan, D. 2007. Metal bipolar plates for PEM fuel cell—a review. *J. Power Sources*, 163, 755-767.

[36] Wang, S. H., Peng, J. and LUI, W. B. 2006. Surface modification and development of titanium bipolar plates for PEM fuel cells. *J. Power Sources,* 160, 485-489.

[37] Li, M., Luo, S., Zeng, C., Shen, J., Lin, H. and Cao, C. N. 2004. Corrosion behavior of TiN coated type 316 stainless steel in simulated PEMFC environments. *Corrosion Sci.,* 46, 1369-1380.

[38] Nam, N. D., Vaka, M. and Tran Hung, N. 2014. Corrosion behavior of TiN, TiAlN, TiAlSiN-coated 316L stainless steel in simulated proton exchange membrane fuel cell environment. *J. Power Sources,* 268, 240-245.

[39] Hsiang, C. W., Kung, H. H., Che, E. L. and Ming, D. G. 2014. The study of electroplating trivalent CrC alloy coatings with different current densities on stainless steel 304 as bipolar plate of proton exchange membrane fuel cells. *Thin Solid Films,* 570, 209-214.

[40] Baldissera, A. F. and Ferreira, C. A. 2012. Coatings based on electronic conducting polymers for corrosion protection of metals. *Prog. Org. Coatings,* 75, 241-247.

[41] Hung, Y., Tawfik, H. and Mahajan, D. 2009. Durability and characterization studies of polymer electrolyte membrane fuel cell's coated aluminum bipolar plates and membrane electrode assembly. *J. Power Sources,* 186, 123-127.

[42] Li, J. Y., Hai, J. Y., Li, J. J., Lei, Z., Xu, Y. J. and Zhong, W. 2011. Graphite-polypyrrole coated 316L stainless steel as bipolar plates for proton exchange membrane fuel cells. *Int. J. Minerals Metallurgy Mater*, 18, 53.

Chapter 12

Pulse Electrodeposition of Lead-Free Tin-Based Composites for Microelectronic Packaging

Ashutosh Sharma, Siddhartha Das and Karabi Das

Additional information is available at the end of the chapter

http://dx.doi.org/10.5772/62036

Abstract

This chapter provides a detailed overview of the various Sn-based composites solders reinforced with ceramic nanoparticles. These solders are lead free in nature and are produced by various process like powder metallurgy, ball milling, casting as well as simple and economic pulse co-electrodeposition technique. In this chapter, various electrodeposited composite solders, their synthesis, characterization, and evaluation of various properties for microelectronic packaging applications, such as microstructure, microhardness, density and porosity, wear and friction, electrochemical corrosion, melting point, electrical resistivity, and residual stress of the monolithic Sn-based and (nano)composite solders have been presented and discussed. This chapter is divided into the following sections: such as introduction to microelectronic packaging, synthesis routes for solders and composites, various nanoreinforcement, and the mechanism of incorporation in solder matrix, the pulse co-electrodeposition technique, the various factors affecting composite deposition, and the improved properties of composite solders over monolithic solders for microelectronic packaging applications are also summarized here.

Keywords: Composite, lead free, plating, double layer, zeta potential

1. Introduction

1.1. Microelectronic packaging

Microelectronic packaging is a multidisciplinary branch of materials engineering that deals with the study of various interconnecting materials, electronic components packaging from chip level to final board level, for example, computers, cellphones, notebooks, laptops, and iPads. It also includes a method of joining various components to the respective substrates, as well as reducing their weight/volume for faster processing, multifunctionality, and portability.

In olden times, various wires and cables are used to connect the different components into an electric box. With the passage of time, printed circuit boards (PCB), or printed wire boards (PWB) invented near 1950s as a great revolution among electronics industries. Moreover, the invention of transistors and integrated circuits (ICs), analog-to-digital electronics in 1947 made luxurious life style of the common public. This technology of interconnecting various IC's and other electronic component devices like transistors, capacitors, inductors, and resistors within circuits over a PCB substrate to form a compact electronic device is known as microelectronic packaging.[1, 2] The common packages in a personal computer are shown below (Fig. 1).

Figure 1. Micropackaging assemblies inside a personal computer.

1.2. Microelectronic packaging materials

Since the civilization, the most commonly used solder is lead–tin (Sn–Pb) solder in electronic packaging. However, the toxicity of Pb is a serious concern among the electronic manufacturers. Pb containing solders are in use so far due to their indispensable properties. The effect of Pb contamination on human beings is a serious threat nowadays. Therefore, Pb and its compounds in electronic devices are now being restricted on account of the bans and regulation imposed by European organizations such as restriction of hazardous substances and waste electrical and electronic equipments.[3–5] It is also to be noted that, though Pb is cost effective, available in abundance, and provides no undesirable reaction with the substrate, yet it shows some technical problems like inferior bonding strength which is important for microjoining.[1–6] Therefore, composites solders are now being regarded as an alternative to conventional Sn–Pb solders and developed to resolve these concerns.

1.3. Lead free packaging materials

Large number of Pb-free solder alloys have been developed and studied where Sn is the major fraction. The most popular Pb-free alloy system candidates are narrated in detail in a review

http://dx.doi.org/10.5772/62036

paper in Ref. [7]. In the present state, the advanced solders that have been developed so far are mostly Sn coupled with other elements like Cu, Ag, Zn, Bi, Sb, Ni.[8–14] Among all the binary eutectic Pb-free alloys, Sn–Ag, Sn–Zn, and Sn–Cu are considered to be the potential candidates to replace Sn–Pb. For ternary alloys, the most commonly used system is Sn–Ag–Cu which is proved the most effective due to its lower melting temperature and superior mechanical properties compared to the other combinations.[15] However, there exist some issues of reliability such as the formation of brittle/needle type intermetallics of Ag_3Sn and Cu_6Sn_5 in ternary alloys which damages the mechanical and soldering properties.[5, 16] These Sn-rich alloys are sensitive to tin whisker growth if prolonged for a long time which is known to cause short circuiting in electronic devices. The major driving force for tin whisker growth is known to be the internal residual stresses due to the inherent compounds like Cu_6Sn_5, Cu_3Sn with time.[5]

2. Synthesis of nanocomposites solders

Although enormous amount of research activities are being done all around the world for a better lead-free solder alloy, no solder alloy is able to completely replace the conventional Sn–Pb solder in terms of performance, economy, availability, solderability, simplicity, mechanical strength, and substrate reaction.[4, 17]

In current research scenario, the development of solder alloys reinforced with nanoceramic particles is being paid more attention toward designing a lead-free solder. Such reinforced solder alloys are generally termed as nanocomposite solders. Nanocomposite solders have shown excellent solderability and reliability. Most of the solder matrix composites are reinforced with ceramic particles like ZrO_2, Al_2O_3, TiO_2, SiC, Cu_2O, SnO_2, La_2O_3.[7, 18, 19, 21–25] The reinforcing particles suppress growth of intermetallic compounds (IMC) and provide uniform stress distribution in the matrix.[8, 18, 19] This method of nanotechnology would provide high strength and reliable solders for microelectronic packaging devices.[18, 20]

Various processing routes like melting and casting, powder metallurgy, high-energy ball milling/mechanical alloying, physical vapor deposition, sol–gel, plasma sprayed deposition, chemical methods, and electroplating have been employed to produce solder materials.[9–10, 26–31] Powder metallurgy and mixing methods have been often used to fabricate the lead-free solders reinforced with nanoparticles: Cu, SiC, ZrO_2, Al_2O_3, SnO_2, Y_2O_3, TiB_2, carbon nanotube (CNT), rare earth.[9, 21–22, 25, 32–36] There is also a limit on the amount of nanoreinforcement addition in the solder matrix; otherwise, it will deteriorate the solderability and strength. In literature, there is a limited research on solders produced by electrodeposition with a few studies on Sn–CNT and Sn–Bi–SiC solders.[37, 38] Electrodeposition has been already shown to improve reliability of microelectronic devices in 3D Through Silicon Via interconnection packaging.[39, 40] Recently, Sharma *et al*. developed CeO_2 nanoparticle reinforced Sn–Ag alloy by pulse co-electrodeposition technique and found a great enhancement in strength, microstructure, and successfully manipulated the residual stress to mitigate of dangerous tin whiskers.[41]

3. Pulse co- electrodeposition of Sn based composites

Initially, the pulse electrodeposition was used for decorative and jewellery applications to improve the surface appearance and shine, wear and friction, fretting corrosion resistance.[42] Recently, more attention has been paid to incorporate different nanoparticles to obtain much improved properties. There are various processing parameters in electrodeposition that affect the particle incorporation in composite deposits, such as (1) particle type, size, and shape; (2) bath pH, constituents, additives, and aging; (3) deposition variables, such as particle concentration in bath, current density, agitation, pulsing methods, and temperature.[42–44]

Composite system	Methodology	Improved properties	Reference
Sn-reinforced with CNT	Electrodeposition	Improved shear properties	[37]
Sn-Pb reinforced with Cu and TiO_2 nanoparticles	Blending and solidification	Improved microhardness	[47]
Sn-Cu reinforced withAl_2O_3 nanoparticles	Powder Metallurgy	Improved mechanical performance	[21]
Sn-Cu reinforced with Si_3N_4	Powder Metallurgy	Improved wetting	[48]
Sn-Bi reinforced with SiC nanoparticles	Electro Deposition	Improved shear properties	[38]
Sn-Bi reinforced with Yttrium oxide nanoparticles	Powder Metallurgy	Improved shear strength	[33]
Sn-Ag reinforced with ZrO_2 nanoparticles	Casting and solidification	Improved mechanical performance	[22]
Sn-Ag reinforced with SnO_2 nanoparticles	Powder Metallurgy	Improved mechanical performance	[25]
Sn-Ag reinforced with Cu_6Sn_5, Ni_3Sn_4, $FeSn_2$ nanoparticles	In situ methods	Creep resistant	[46]
Sn-Ag reinforced with CeO_2 nanoparticles	Pulse electroplating	Whisker resistant	[41]
Sn-Ag-Cu reinforced with SiC nanoparticles	Mixing and solidifying	Improved mechanical performance	[22]
Sn-Ag-Cu reinforced with Multiwalled CNT	Powder Metallurgy	Improved mechanical performance	[34]
Sn-Ag-Cu reinforced with TiO_2 nanoparticles	Melting route	Improved mechanical performance	[23]
Sn-Ag-Cu reinforced with TiB_2 nanoparticles	Powder Metallurgy	Improved mechanical performance	[49]

Table 1. Nanocomposite solder produced by various routes

http://dx.doi.org/10.5772/62036

The different nanocomposite solders produced in literature are shown in Table 1. The composite approach has been developed mainly to improve the strength and reliability of solder joints. Nano-sized reinforcement particles in conventional solder matrices due to their effectiveness in improving the reliability by spreading the stress uniformly in the matrix.[19, 45, 46]

In this chapter, an effort has been made to discuss the strength related concerns by incorporating the reinforcement nanoparticles within the solder matrix using co-electrodeposition process.

3.1. The co-electrodeposition mechanisms

Guglielmi demonstrated the mechanism of codeposition for the first time in 1972. The mechanism provides a fundamental insight of codeposition theory.[50] According to this model the entrapment of particles is based on various adsorption processes. This is a mathematical formulation of the influence of particle content and current density on the particle codeposition rate into the metal matrix excluding particle characteristics and hydrodynamic conditions.

3.1.1. Guglielmi model

The first step involves the loose adsorption of the particles onto the electrode surface. This is a physical adsorption process. However, in the second step, the particles are attracted towards the electrode under electric field and causes a stronger adsorption of particles onto the electrode, as shown in Fig. 2.

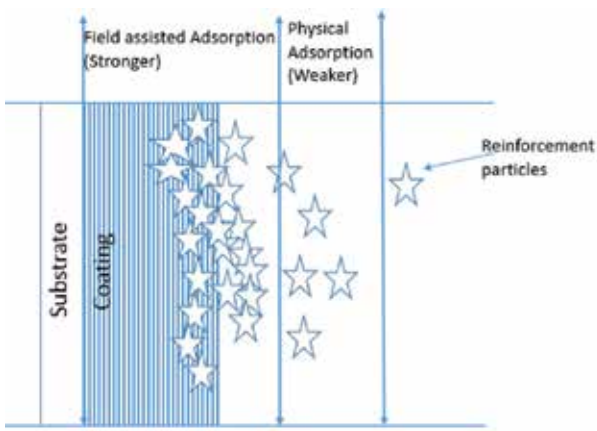

Figure 2. Codeposition mechanism into a metal matrix.[50, 51]

As a result of strong adsorption, the particles are incorporated in the deposit and form a composite layer. This model is the simplest and is adopted for various composite systems, however, it does not account for hydrodynamic effects, particle size, type and shape in detail.

3.1.2. Celis model

Guglielmi model triggered the development of other codeposition theories by Celis, and his co-workers. They predicted the co-deposited particles content in the matrix. According to the Celis model the inert particles approach towards the cathode in a specific sequence: (1) the adsorption of ionic cloud surrounding the particle surface, (2) the force of convection currents in electrolyte also supports the particles incorporation partly, (3) the diffusion kinetics of particles across the electric double layer, (4) the adsorption of the inert particles and the absorption of ionic cloud onto the cathode, and (5) the decrease in adsorbed ionic content and their embedment in the metal coating (Fig. 3).

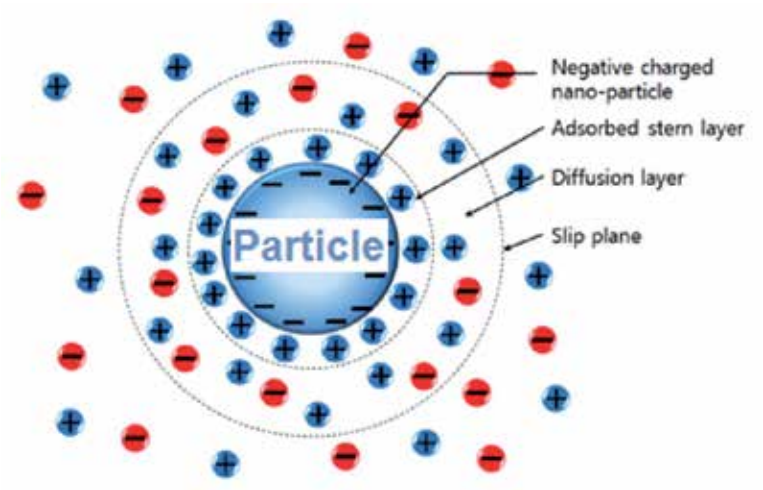

Figure 3. Electric double layer around the ceramic particle showing the ionic concentration and generated potential difference as a function of the distance from the charged particle suspended in electrolyte.[51]

There are various other codeposition models such as for non-Brownian motion of particles in the bath.[52, 53] Although the various developed codeposition models are important tools in the nanocomposite fabrication yet. these models are not perfect for the understanding the influences of process parameters on the codeposition rate in the metal matrix without any experimental data.

4. Factors affecting composite co-electroplating

4.1. Deposition current density

The deposition rate in electrodeposition process plays a vital role in the fabrication of nano-composites. The number density of particles approaching the cathode surface depends on the applied electric potential, and the thickness of the growing metal is determined by the deposition current density. The rate determining step in the co-electrodeposition is when the

strong adsorption of particles on the cathode surface occurs. A strong adsorption of particles is always difficult and is improved by applying current or feeding the corresponding overpotential in the electrolyte. As a consequence, the particle incorporation in the coating increases continuously. However, at a sufficiently high current density, the codeposition rate of the coating decreases drastically. This may be caused by the limited supply of the metal ions toward cathode leading to the decrease in the particle amount.[54] The embedded particle density as a function of current density has been studied for different particle concentrations in the bath in Ref. [55]. It has been reported that at lower current densities (0.5 A dm-2), the embedded particle density is poor due to a weaker adsorption of nanoparticles on the cathode. In few reports, there is a negligible effect of current density on the particle density in the matrix. [42, 56] In other cases, various optimum particle concentrations have been detected in the current density versus particle concentration graph.[51, 57–59] It is also noteworthy point that the current density not only influences the codeposition rate, but the particles present in the electrolyte also modify the current density and hence the morphology of the deposits.[60, 61]

4.2. Zeta potential

The zeta potential is a parameter used to measure surface charge of the particle in the solution, and it indicates the stability of the colloidal suspensions. A higher zeta potential means a lower degree of particle agglomeration in the electrolyte.[62] From electrodeposition point of view, the stability of the nanoparticles is an important factor for a better embedded particle density in the matrix. It has been found that for the nickel matrix composites, when the electrostatic repulsion within the dispersed particles increases, particle agglomeration decreases, and the embedded particle density increases uniformly in the nickel matrix.[62] Uniform dispersion of nanoparticles shows higher attraction toward cathode and thus produces strong adsorption. [63] The zeta potential depends on the various factors, i.e., size of particles (nano or micro), addition of surfactants, electrolyte composition, the particle shape, the bath pH, and the energy of hydration.[64–66] Bund and Thiemig reported that negatively charged particles are highly attracted when there is an excess plus charge on the electrical double layer. This observation works for various composite systems. However, in case of electrophoresis, the negatively charged particles have been successfully deposited into the nickel matrix.[68] This might be correlated to not only the zeta potential but the absolute value of the zeta potential too in addition.

4.3. Bath temperature and pH

Generally, effect of temperature is always to increase the metal grain growth rate. There are different results of the effect of temperature on various codeposition systems. For example, the nickel matrix composite reinforced with Al_2O_3 shows no increment of the volume fraction of particles with temperature.[60, 69] On the contrary, the Ni–Co alloy matrix composite shows a significant increment in the reinforced TiO_2 as a function of temperature up to 45 °C.[70] Similar behavior was shown by the nickel matrix composite reinforced with SiC at 50 °C. [71] Several reports are also available that show a linear decrease in the mass fraction of copper matrix composites as described in Ref. [42].

The bath pH is directly related to the surface charge density of the nanoparticles in the electrolyte. The surface charge density is generally related to the parameter termed as zeta potential. Zeta potential is a measure of the colloidal stability. The nickel matrix reinforced with the Al_2O_3 shows no effect on incorporation rate when bath pH >2. When the bath pH is increased beyond 2, the incorporation rate declines.[60] This result is consistent with those of Verelst and his co-workers.[69] Similarly, Wang et al. observed that nickel matrix reinforced with SiC nanoparticles shows an improvement in particles incorporation rate beyond a bath pH of 5.[72] Park and his co-workers also investigated the effect of pH on nickel matrix composites reinforced with SiO2 and TiO2 nanoparticles. They found that the dispersion of SiO_2 is better at alkaline pH (~ 8) values rather than in acidic pH values. Moreover, for the dispersion of TiO_2, the acidic pH (~3.5) provided better results.[73] The particle content in the composite also behaved in the similar way. They correlated this to the fact that SiO_2 has a negative zeta potential from pH 2–11. It is not clear if these effects are accompanied by a decrease of particle content below pH 2, because the SiC content of the deposits is not investigated. However, in the case of Ni–TiO_2, the TiO_2 particles experience a point of zero charge around pH<5 in the plating bath and particle content increases.

4.4. Bath agitation

Electrolyte agitation is always required to avoid the settling of the particles in electrolyte and to improve their movement toward the cathode. Vaezi and his co-workers observed that increasing the stirring rate up to 120 rpm increases the amount of SiC nanoparticles in the matrix but falls at a higher stirring rate. At a higher stirring rate, the flow is turbulent and not only the metal ions but the SiC particles are washed away on the cathode surface quickly.[74] A similar trend was observed by Baghery *et al*.[75] in the electrodeposition of Ni–TiO_2 nanocomposite. Sen. *et al*.[76] also studied the effect of stirring rate on the microstructure of Ni–CeO_2 nanocomposite and found that fraction of CeO_2 particles increases up to stirring rate of 450 rpm, whereas at higher stirring rates the incorporation of CeO_2 decreases. The coelectrodeposition of ultrafine WC into Ni matrix on a rotating disk electrode with various rotation velocities in the range of 200–1200 rpm under pulse and direct current (DC) conditions is performed in Ref. [77]. This study also verified the fact that the increase in rotation speed has a beneficial effect up to a certain limit. In some studies, the ultrasound waves have been utilized in an attempt to avoid the formation of agglomerated nanoparticles in the plating bath due to the generation of large pressure causing breakdown of agglomerates. Kuo *et al*.[63] reported that the diameter of the agglomerated alumina particles may be refined by ultrasound energy, but the result of particle incorporation is not reasonable.

4.5. Particle concentration and size

Generally, the smaller particles possess higher van der Waals force of attraction or repulsion. It has been reported that the volume fraction of nanoparticles in nickel matrix increases with increasing particle concentration in the electrolyte.[60] The dependence of particle content in the deposit and consequently on the microstructure and surface properties has been studied by many authors.[78–80] In all studies, the volume fraction of the incorporated particles in the coatings with increase in the particle concentration in the plating bath up to an optimum value

http://dx.doi.org/10.5772/62036

and decreases again. The particle shape affects the adsorption of the particles on the cathode by varying the charge on the particle surface and the suspension stability. Regarding the effect of particle size on codeposition, different results have been reported. Such as for Ni–Co/SiC[80], an increase in the fraction of embedded particles was reported for micron-sized SiC compared to nano-SiC, while a negligible influence of particle size is observed for Ni–$A1_2O_3$ composite.[69] It can be explained as when two particles come closer, agglomeration occurs as the force of attraction exceeds the force of repulsion between them. The magnitude of the net forces thus produced depends on the bath parameters and the processing conditions of the system.[41]

4.6. Bath types and surfactants

The type of plating baths also affects the co-electrodeposition process. For example, few studies have been conducted on non-aqueous plating baths and organic solvents. In some cases, water has been used partially or completely mixed with organics to avoid hydrogen embrittlement and to obtain a wider processing window.[82] Shrestha *et al*. studied the codeposition of nickel matrix composite using ethyl alcohol base in nickel bath and succeeded to achieve maximum amount of particle incorporation in the Ni matrix. They also found superior wear properties of the composite coatings prepared from ethanol electrolyte compared to those obtained from Watts's type plating bath.[83] Singh *et al*. also investigated the electrodeposition of Ni–TiC composite in acetate bath using *n*-methyl formamide as non-aqueous solvent and found better composite properties.[78]

Surfactants also enhance the rate of particle incorporation in composite electrodeposition. The choice of a given surfactant depends on their charge or polarity. Cationic surfactants are widely used for increasing the particle incorporation rate in the metal matrix. They impart positive charge to the particle surface and prevent the agglomeration in the plating bath.[84] It has been observed that the cationic adsorption is more effective if the particle size is in the nanoscale.[85] According to one report, cationic surfactants can increase the particle content up to 5 times for nickel matrix composites.[57] In another study, the content can be SiC content increased up to 50 volume percent with a fluorocarbon surfactant.[42] Similar study shows that azo-cationic surfactant improved the incorporation rate up to 62.4 volume percent.[86] However, it is always recommended to use surfactants in a minute concentration in the plating bath to avoid carbon compounds in the coating.

4.7. Plating mode

Various electrodeposition modes utilizing pulsing waveforms like pulsed current (PC), pulsed reverse current, and DC have been used to improve the embedded particles density into composite matrix.[87] The application of PC technique in nickel electroplating has been shown to improve mechanical properties, wear and friction, and more uniform distribution of the particles compared to DC technique.[77]

At a given average current density, a decrease in t_{on} time induces a fine crystallite size and increases nucleation rate have been reported.[88] In addition, a longer t_{off} promotes the grain growth and the arrival of more particles near the cathode. Therefore, pulse plating is impor-

tant for co-electrodeposition of nanocomposites. For example, in Ni–SiC deposition, the application of PC results in the production of composite coatings with higher fraction of particles, and better properties than obtained with DC plating.[89] In another technique of pulse reversing, the pulsed-reverse current (PRC) technique, a stripping time is also applied to the pulse waveform, during which the surface projections are dissolved and produce more smooth deposit.[90] The Zn matrix nanocomposite reinforced with the TiO_2 nanoparticles using the PRC technique has been shown to improve the embedded TiO_2 particle density in the matrix.[91]

5. Properties of electro-composites

The original driving force for the preparation of nanocomposite solders was to improve the mechanical, thermal, and corrosion resistance of the solder alloys to utilize them in high temperature, harsh service conditions. The properties that are improved compared to the conventional Pb–Sn solder are summarized as follows:

5.1. Density

The density of a microelectronic device is very important for developing portable electronic goods. There are various reports which show a reduction in density values in nanoparticle reinforced composites. [18, 21, 41] Zhong *et al.* reported that the Al_2O_3 reinforced Sn matrix composite is lighter compared to monolithic matrix, while Babaghorbani *et al.* found that SnO_2 reinforced Sn–3.5Ag matrix did not show any change in density. This may be due to the fact that the matrix and reinforcement have the similar values of density.[21, 25]

5.2. Electrical conductivity

The electrical conductivity of a metal matrix is a function of various factors like fraction of secondary reinforcement phase, fraction of pores, size and shape, and the metal matrix. [92, 93] Nai *et al.* observed that the dispersion of CNT in the Sn based matrix does not decrease the conductivity of the matrix.[94] They correlated this fact with the low volume fraction of pores as well as reinforcement in the solder matrix. This type of behavior has been also observed by Sharma *et al*. for Sn–CeO_2 and Sn–Ag/CeO_2 nanocomposites.[41, 95] Babaghorbani *et al.* studied the electrical properties of nanocomposite solders in detail and reported that nano-sized reinforcements is advantageous in not degrading the electrical conductivity of the device, while micron sized particles can degrade the conductivity values .[96] This further confirms the unique properties of nanocomposite solders for electromigration property microelectronic packaging devices. Recently, it has been demonstrated the nanoparticles reinforced solders can be promising candidates for preventing electromigration failure in electronic packaging devices.[97]

5.3. Melting point

There is wide distribution of results on the thermal behavior of solders.[18, 22, 23, 41, 95, 98, 99] The melting points of the nanocomposite solders generally decreases with an increase in

http://dx.doi.org/10.5772/62036

the fraction of the nanoparticles in the matrix. Liu *et al.* reported that Sn–Ag–Cu/nano-SiC showed a reduction in melting point compared to monolithic Sn-Ag-Cu alloy. They correlated this observation to the increase in the interface surface instabilities after the addition of SiC nanoparticles. Similarly Kumar *et al.* also observed a slight depression in the melting point in CNT reinforced solder matrix. However, Nai *et al.* did not observe any significant drop in the melting point.[98, 99] Shen *et al.* while working on ZrO_2 reinforced solder the reinforcement particles, i.e., ZrO_2 nanoparticles behave as a nucleating agents and promote the nucleation of the matrix during solidification. Therefore, more nucleating sites results in grain refinement and a drop in melting point could be noticed. [22] Recently, Sharma *et al.* have found a decreased melting point of Sn–CeO_2 and Sn–Ag/CeO_2 nanocomposites and explained this behavior to the refinement of matrix grains after addition of nanoparticles.[41, 95]

5.4. Solderability

During soldering, in order to form a proper metallurgical bond between two materials, wetting must take place. There is an increase in solder wetting onto the metallic substrates after addition of the nanoparticles in the solder matrix. The high surface energy nanoparticles decrease the surface tension and wetting angle and results in the improved solderability. However, too much addition of nanoparticles in the solder may degrade the wetting properties due to the increase in agglomeration of nanoparticles in the molten alloy.[35] Additions of metallic additives also have been shown the similar behavior where the wetting decreases due to the increase in surface tension and oxidation of the reinforcing phase.[100] Recently, Sharma *et al*. investigated the solderability of Sn–Ag–Cu alloy reinforced with La_2O_3 nanoparticles in terms of spreading ratio and wetting balance measurements. They also found that the wetting is improved up to an optimum amount of La_2O_3 nanoparticles and decreases beyond that due to the increase in surface tension and melt viscosity.[19]

5.5. Microhardness

The nanocomposite solders developed have better microhardness as required for the electronics packaging industry. It has been reported that the addition of ceramic oxides or inert nanoparticles [19, 21–23, 34–37, 41, 95] can improve the mechanical performance, tensile strength, elongation and creep properties of nanocomposite solders. Moreover, the additions of nanoparticles refine the grains of the matrix as well as are adsorbed on the intermetallic to refine them. In general, there is an enhancement at the cost of ductility of the solder which is undesirable. Recently, Sharma *et al*. have produced Sn–Ag–Cu/La_2O_3 solder with an improved tensile strength as well as ductility. They explained this due to the mechanism of slip mode transition of dislocation when interacting with the La_2O_3 nanoparticles in the solder matrix.[19]

5.6. Wear and friction behavior

In various microelectronic devices and assemblies, Sn based connectors such as press fit plugs and sockets, separable interconnects in consumer electronic appliances are gaining popularity

nowadays. Gold and silver based contacts provide optimum wear resistance in sliding contacts but they are not economical. Therefore, the sliding wear and tear are important for Sn based solders may limit their applications. [101] Tin based contacts are generally susceptible to fretting wear which is a prime concern in automobile applications.[102, 103] Sn based connectors are very ductile and more sensitive to fretting wear. Hammam *et al*. investigated the wear and frictional properties of various Sn coating prepared hot dipping, electroplating, and reflow processes. They suggested that the different processing routes for Sn deposition produce different thickness of the Sn coatings and hence the intermetallic compounds on a metallic substrates. [104] In case of nanocomposite solders, Jun *et al*. reported that tin bronze reinforced with carbon fibers improves the resistance against the fretting wear appreciably.[105] Sharma *et al*. have recently found a significant enhancement on the wear resistance of Sn and Sn–Ag matrices reinforced with CeO_2 nanoparticles.[41, 95]

5.7. Electrochemical corrosion

Electrochemical behavior of Sn based coatings is important in microelectronic packaging devices. The corrosion of Sn base coatings may deteriorate the microstructural properties of the solder joints and ultimately lead to entire failure of the device. For example, in marine applications, the chlorides ions from the sea can dissolve the solder joints by forming soluble compounds.[106] There are various forms of corrosion such as pitting, crevice, and/or galvanic corrosion of solder and substrate material. Therefore the corrosion of electronic devices may impose a serious threat among microelectronics community to produce corrosion resistant solder materials. However, there is a scarcity of information of electrochemical corrosion of the solder joints.[107, 108] It has been shown that presence of Bi in Sn–Bi solder can increase the dissolution of Sn slightly in sulfuric acid solution and vigorously in nitric acid solution compared to that of pure tin.[108, 109]. It has been noticed that lead-free solders are highly corrosion resistant towards chloride ion attack compared to conventional Sn-Pb solder. [110] Recently, Sharma *et al.* proposed that use of nanoparticles is better idea to avoid the localized dissolution of Sn coatings. If the nanoparticles are added in an optimum concentration in the solder matrix, the corrosion resistance of the solder matrix can improve significantly by setting up of homogeneous corrosion instead of preferential and sudden damage. The high surface energy nanoparticles in the solder matrix reduce the corrosion potential, corrosion current, and diffusion capacitance, thus increasing passivity of the solder coating.[111]

5.8. Whisker growth mitigation

Tin whisker growth in the Sn based coatings is a serious issue in microelectronic packaging devices. The driving force of these whisker growth is the generation of compressive stresses in the coatings on storage for a long time. When plated on a metallic substrate like copper, the Cu-Sn interdiffusion across the interface may give rise to the formation of Cu6Sn5, Cu3Sn etc., IMCs and grow with time causing a volume expansion of the interface. The expansion of the interface causes the setup of compressive stress in the coatings. Recently, it has been identified by various researchers that addition of nanoparticles may suppress the growth of IMCs and restrict the formation of whiskers in the matrix. Generally, the ceramic nanoparticles are very

http://dx.doi.org/10.5772/62036

smaller compared to size of IMCs. Therefore they can easily attach with the growing IMC in the molten metal and restrict the growth of IMCs during solidification as predicted by the surface adsorption theory.[18, 19, 22, 41]

6. Summary

Addition of nanoparticles in the solder matrix improves the microstructural properties due to the refinement in the grain size as well as the thickness of the IMC (Cu_6Sn_5, Ag_3Sn) in the solder matrix. Wettability is improved due to the decrease in interfacial energy in presence of high surface energy nanoparticles. The higher hardness of nanosolder composites as compared to monolithic alloys can be attributed not only to the grain size and dispersion strengthening effect, but also to the refinement of the IMCs such as Cu_6Sn_5, Ag_3Sn by ceramic nanoparticles. The melting point of the solders is minimum form an optimum reinforcement amount in the matrix, which indicates its possibility to use without any change in the existing soldering procedures. There is a rise in the resistivity of the composite matrix compared to the monolithic materials. However, the resistivity of the composites falls within the usable limits as reported for other Sn and Sn–Ag-based composites, used for electrical contact applications. The nanoscale reinforcements are added in minute concentrations and do not degrade the resistivity much if their distribution is uniform and electromigration phenomena in the composite solders. The addition of reinforcement in the Sn matrix also improves the wear resistance, which ultimately increases the coating life for application. The wear resistance of the composite coatings is better than that of the monolithic materials, and it is associated with an enhancement in the microhardness of the composite. It is also observed that composite solders possess the better corrosion resistance as compared to monolithic ones. The presence of fine Ag_3Sn compounds in composite increases the passivation of the matrix which acts as a noble barrier in addition to ceramic reinforcements against corrosion propagation. It is also observed that an incorporation of CeO_2 nanoparticles in the composite matrix reduces the compressive stresses developed in the coatings. The residual stresses of monolithic materials are negative, i.e., compressive in nature. A decline in residual stress indicates that the driving force for whisker growth can be minimized by choosing an optimum concentration of ceria, and thus, the coating life can be improved.

Author details

Ashutosh Sharma[1*], Siddhartha Das[2] and Karabi Das[2]

*Address all correspondence to: stannum.ashu@gmail.com

1 Department of Materials Science and Engineering, University of Seoul, South Korea

2 Department of Metallurgical and Materials Engineering, Indian Institute of Technology, Kharagpur, India

References

[1] Tummala, R.R.. Fundamentals of Microsystems Packaging. McGraw-Hill; 2000. p. 185–210.

[2] Alam, M.O. Study of Interfacial Reactions in Ball Grid Array (BGA) Solder Joints for Advanced Integrated Circuits (IC) Packaging, PhD Thesis, City University of Hong Kong; 2004.

[3] Puttlitz, K.J.; Gaylon, G.T. Impact of RoHS Directive on High Performance Electronic Systems. Journal of Materials Science: Materials in Electronics. 2007; 18: 347–365.

[4] Subramanian, K.N. Lead Free Electronic Solders. A Special Issue of the Journal of Materials Science: Materials in Electronics. New York: Springer Science; 2007. p. 55–76.

[5] Suganuma, K. Lead Free Soldering in Electronics – Science, Technology and Environmental Impact. New York: Marcell Dekker, Inc.; 2004.

[6] Puttiltz, K.J.; Stalter, K.A. Handbook of Solder Technology for Microelectronic Assemblies. New York: Marcell Dekker, Inc.; 2004. p. 51–55.

[7] Abtew, M.; Selvaduray, G. Lead Free Solders in Microelectronics. Materials Science and Engineering R. 2000; 27: 95–141.

[8] Guo, F. Composite Lead-Free Electronic Solders, Lead free electronics solders, A Special Issue of the Journal of Materials Science: Materials in Electronics. 2006; 129–145.

[9] Alam, M.E.; Nai, S.M.L.; Gupta, M. Development of High Strength Sn–Cu Solder Using Copper Particles at Nanolength Scale. Journal of Alloys and Compounds. 2009; 476: 199–206.

[10] Lai, L.H.; Duh, J.G. Lead-Free Sn–Ag and Sn–Ag–Bi Solder Powders Prepared by Mechanical Alloying. Journal of Electronic Materials. 2003; 32: 215–220.

[11] El-Daly, A.A.; Hammad, A.E. Elastic Properties and Thermal Behavior of Sn–Zn Based Lead-Free Solder Alloys. Journal of Alloys and Compounds. 2010; 505: 793–800.

[12] Miao, H.-W.; Duh, J. Microstructure Evolution in Sn–Bi and Sn–Bi–Cu Solder Joints Under Thermal Aging. Materials Chemistry and Physics. 2001; 71: 255–271.

[13] Nogita, K.; Nishimura, T. Nickel-Stabilized Hexagonal $(Cu, Ni)_6Sn_5$ in Sn–Cu–Ni Lead-Free Solder Alloys. Scripta Materialia. 2008; 59: 191–194.

[14] Lin, K.L.; Shih, P.C. IMC Formation on BGA Package With Sn–Ag–Cu and Sn–Ag–Cu–Ni–Ge Solder Balls. Journal of Alloys and Compounds. 2008; 452: 291–297.

[15] [15]Wu, C.M.L.; Yu, D.Q.; Law, C.M.T.; Wang, L. Properties of Lead-Free Solder Alloys With Rare Earth Element Additions. Materials Science and Engineering R. 2004; 44: 1–44.

[16] Suganuma, K. Advances in Lead-Free Electronics Soldering. Current Opinion in Solid State and Materials Science. 2001; 5: 55–64.

[17] Coombs, C.F. Printed Circuits Handbook. USA: McGraw Hill; 2001. p. 45.1–45.9.

[18] Shen, J.; Chan, Y.C. Research Advances in Nano-Composite Solders, Microelectronics Reliability. 2009; 49: 223–234.

[19] Sharma, A.; Baek, B.G.; Jung, J.P. Influence of La_2O_3 Nanoparticle Additions on Microstructure, Wetting, and Tensile Characteristics of Sn–Ag–Cu Alloy. Materials and Design. 2015; 87: 370–379.

[20] Jin, S.; McCormack, M. Dispersoid Additions to a Pb-Free Solder for Suppression of Microstructural Coarsening. Journal of Electronic Materials. 1994; 23: 735–739.

[21] Zhong, X.L.; Gupta, M. Development of Lead-Free Sn–0.7Cu/Al_2O_3 Nanocomposite Solders With Superior Strength. Journal of Physics D: Applied Physics. 2008; 41: 095403.

[22] Shen, J.; Liu, Y.C.; Han, Y.J.; Tian, Y.M.; Gao, H.X. Strengthening Effects of ZrO_2 Nanoparticles on the Microstructure and Microhardness of Sn–3.5Ag Lead-Free Solder. Journal of Electronic Materials. 2006; 35: 1672–1679.

[23] Liu, P.; Yao, P.; Liu, J. Effect of SiC Nanoparticle Additions on Microstructure and Microhardness of Sn–Ag–Cu Solder Alloy. Journal of Electronic Materials. 2008; 37(6): 874–879.

[24] Tsao, L.C.; Chang, S.Y. Effects of Nano-TiO_2 Additions on Thermal Analysis, Microstructure and Tensile Properties of Sn3.5Ag0.25Cu solder. Materials and Design. 2010; 31: 990–993.

[25] Sivasubhramaniam, V.; Bosco, N.S.; Janczak-Rusch, J.; Cugnoni, J.; Botsis, J. Interfacial Intermetallic Growth and Strength of Composite Lead Free Solder Alloy Through Isothermal Aging. Journal of Electronic Materials. 2008; 37: 1598–1604.

[26] Babaghorbani, P.; Nai, S.M.L.; Gupta, M. Development of Lead-Free Sn–3.5Ag/SnO_2 Nanocomposite Solders. Journal of Materials Science: Materials in Electronics. 2009; 20: 571–576.

[27] Miller, C.M.; Anderson, I.E.; Smith, J.F. A Viable Tin Lead Solder Substitute: Sn–Ag–Cu. Journal of Electronic Materials. 1994; 23: 595–601.

[28] Aggarwal, A.O.; Abothu, I.R.; Raj, P.M.; Sacks, M.D.; Tummala, R.R. Lead-Free Solder Films Via Novel Solution Synthesis Routes. IEEE Transactions on Components and Packaging Technologies. 2007; 30: 486–493.

[29] Conway, P.P.; Fu, E.K.Y.; Williams, K. Precision High Temperature Lead-Free Solder Interconnections by Means of High-Energy Droplet Deposition Techniques. CIRP Annals – Manufacturing Technology. 2002; 51: 177–180.

[30] Hsiao, L.-Y.; Duh, J.-G. Synthesis and Characterization of Lead Free Solders With Sn–3.5Ag–xCu (x=0.2, 0.5, 1.0) Alloy Nanoparticles by the Chemical Reduction Method. Journal of Electrochemical Society. 2005; 159(9): J102–J109.

[31] Hsiung, C. K.; Chang, C. A.; Tzeng, Z. H.; Ho, C. S.; Chien, F. L. Study on Sn–2.3Ag Electroplated Solder Bump Properties Fabricated by Different Plating and Reflow Conditions. 9th Electronics Packaging Technology Conference. 2007; pp. 719–724.

[32] Ruythooren, W.; Attenborough, K.; Beerten, S.; Merken, P.; Fransaer, J.; Beyne, E.; Hoof, C.V.; Boeck, J.D.; Celis, J.P. Electrodeposition for the Synthesis of Microsystems. 200; 10: 101–107.

[33] Wang, X.; Liu, Y.C.; Wei, C.; Gao, H.X.; Jiang, P.; Yu, L.M. Strengthening Mechanism of SiC-Particulate Reinforced Sn–3.7Ag–0.9Zn Lead-Free Solder. Journal of Alloys and Compounds. 2009; 662–665.

[34] Fouzder, T.; Gain, A.K.; Chan, Y.C.; Sharif, A.; Yung, W.K.C. Effect of Nano Al_2O_3 Additions on the Microstructure, Hardness and Shear Strength of Eutectic Sn–9Zn Solder on Au/Ni Metallized Cu Pads. Microelectronics Reliability. 2010; 50: 2051–2058.

[35] Liu, X.; Huang, M.; Wu, C.M.L.; Wang, L. Effect of Y_2O_3 particles on microstructure formation and shear properties of Sn-58Bi solder. Journal of Materials Science: Materials in Electronics. 2010; 21: 1046–1054.

[36] Nai, S.M.L.; Wei, J.; Gupta, M. Lead-Free Solder Reinforced with Multiwalled Carbon Nanotubes, Journal of Electronic materials. 2006; 35(7): 1518–1522.

[37] Nai, S.M.L.; Wei, J.; Gupta, M. Influence of Ceramic Reinforcements on the Wettability and Mechanical Properties of Novel Lead-Free Solder Composites. Thin Solid Films. 2006; 504: 401–404.

[38] Chen, Z.; Shi, Y.; Xia, Z.; Yan, Y. Properties of Lead-Free Solder SnAgCu Containing Minute Amounts of Rare Earth, Journal of Electronic materials. 2003; 32(4): 235–243.

[39] Choi, E.K.; Lee, K.Y.; Oh, T.S. Fabrication of Multiwalled Carbon Nanotubes-Reinforced Sn Nanocomposites for Lead-Free Solder by an Electrodeposition Process. Journal of Physics and Chemistry of Solids. 2008; 69: 1403–1406.

[40] Shin, Y.S.;, Lee, S.; Yoo, S.; Lee, C.W. Mechanical and Microstructural Properties of SiC-Mixed Sn–Bi Composite Solder Bumps by Electroplating. Proceedings of Electronics Packaging Technology Conference. 2009; 1–4.

[41] Jung, D.H.; Sharma, A.; Kim, K.H.; Choo, Y.C.; Jung, J.P. Effect of Current Density and Plating Time on Cu Electroplating in TSV and Low Alpha Solder Bumping. JMPEG. 2015; 24: 1107–1115.

[42] Roh, M.H.; Sharma, A.; Lee, J.H.; Jung, J.P. Extrusion Suppression of TSV Filling Metal by Cu–W Electroplating for Three-Dimensional Microelectronic Packaging. Metallurgical and Materials Transactions A. 2015; 46: 2051–2062.

[43] Sharma, A.; Bhattacharya, S.; Das, S.; Das, K. Fabrication of Sn–Ag/CeO_2 Electro-Composite Solder by Pulse Electrodeposition. Metallurgical and Materials Transactions A. 2013; 44: 5587–5601.

[44] Hovestad, A.; Janessen, L.J.J. Electrochemical Co-Deposition of Inert Particles in a Metallic Matrix. Reviews in Applied Electrochemistry. 1995; 40: 519–527.

[45] Kedward, E.C.; Wright, K.W.; Tennett, A.A.B. The Development of Electrodeposited Composites for Use as Wear Control Coatings on Aero Engines. Tribology. 1974; 7(5): 221–227.

[46] Stankovic, V.D.; Gojo, M. Electrodeposited Composite Coatings of Copper With Inert, Semiconductive and Conductive Particles. Surface and Coatings Technology. 1996; 81: 225–232.

[47] Liu, J.P.; Guo, F.; Yan, Y.F.; Wang, W.B.; Shi, Y.W. Development of Creep-Resistant, Nanosized Ag Particle-Reinforced Sn–Pb Composite Solders. Journal of Electronic Materials. 2004; 33(9): 958–963.

[48] Choi, S.; Lee, J.G.; Guo, F.; Bieler, T.R.; Subramanian, K.N.; Lucas, J.P. Creep Properties of Sn–Ag Solder Joints Containing Intermetallic Particles. JOM. 2001; 53: 22–26.

[49] Lin, D.C.; Liu, S.; Guo, T.M.; Wang, G.X.; Srivatsan, T.S.; Petraroli, M. An Investigation of Nanoparticles Addition on Solidification Kinetics and Microstructure Development of Tin–Lead Solder. Materials Science and Engineering A. 2003; 360: 285–292.

[50] Mohd Salleh, M.A.A.; Mustafa Al Bakri, A.M.; Kamarudin, H.; Bnhussain, M.; Zan@Hazizi, M.H.; Flora, S. International Conference on Physics Science and Technology (ICPST 2011). In: Physics Procedia. 2011; 22: 299–304.

[51] Wei, J.; Nai, S.M.L.; Wong, C.K. Gupta, M. Enhancing the Performance of Sn–Ag–Cu Solder with the Addition of Titanium Diboride Particulates. SIMTech technical reports. 6(1), pp. 29–32.

[52] Guglielmi, N. Kinetics of Deposition of Inert Particles From Electrolytic baths, Journal of Electrochemical Society. 1972; 119(8): 1009–1012.

[53] Celis, J.P.; Roos, J.R., Buelens, C. A Mathematical Model for the Electrolytic Codeposition of Particles With a Metallic Matrix. Journal of Electrochemical Society. 1987; 134(6): 1402–1408.

[54] Fransaer, J.; Celis, J.P.; Roos J.R. Analysis of the Electrolytic Codeposition of Non-Brownian Particles With Metals. Journal of Electrochemical Society. 1992; 139(2): 413–425.

[55] Vereecken, P.M.; Shao, I.; Searson, P.C. Particle Codeposition in Nanocomposite Films. Journal of Electrochemical Society. 2000; 147(7):2572–2575.

[56] Guo, D.; Zhang, M.; Jin Z.; Kang R. Effects of Chloride Ion on the Texture of Copper and Cu–ZrB_2 Coatings Electrodeposited from Copper Nitrate Solution in Different Plating Modes. Journal of Materials Science and Technology. 2006; 22: 643–646.

[57] Gay, P.A.; Bercot, P.; Pagetti, J. (2001). Electrodeposition and characterisation of Ag–ZrO_2 electroplated coatings. Surface and Coatings Technology. 2001; 140: 147–154.

[58] Graydon, J.W.; Kirk, D.W. Suspension Electrodeposition of Phosphorus and Copper, Journal of Electrochemical Society. 1990; 137: 2061–2066.

[59] Chang, Y.S.; Lee, J.Y. Wear Resistant Nickel Composite Coating from Bright Nickel Baths with Suspended Very Low Concentration Alumina. Materials Chemistry and Physics. 1988; 20: 309–321.

[60] Celis, J.P.; Roos, J.R. Kinetics of the Deposition of Alumina Particles from Copper Sulfate Plating Baths. Journal of Electrochemical Society. 1977; 124: 1508–1511.

[61] Rudnik, E. Influence of Surface Properties of Ceramic Particles on Their Incorporation into Cobalt Electroless Deposits. Applied Surface Science. 2008; 225: 2613–2618.

[62] Sautter, F.K. Electrodeposition of Dispersion-Hardened Nickel–Al_2O_3 Alloys. Journal of Electrochemical Society. 1963; 110: 557–560.

[63] Watson, S.wW. Electrochemical Study of SiC Particle Occlusion during Nickel Electrodeposition. Journal of Electrochemical Society. 1993; 140: 2235–2238.

[64] Simunkova, H.; Pessenda-Garcia, P.; Wosik, J.; Angerer, P.; Kronberger, H.; Nauer G.E. The Fundamentals of Nano- and Submicro-scaled Ceramic Particles Incorporation into Electrodeposited Nickel Layers: Zeta Potential Measurements. Surface and Coatings Technology. 2009; 203: 1806–1814.

[65] Kuo, S.-L.;Chen, Y.-C.;. Ger, M.-D.; Hwu, W.-H. Nano-particles Dispersion Effect on Ni/Al_2O_3 Composite Coatings. Materials Chemistry and Physics. 2004; 86: 5–10.

[66] Morterra, C.; Cerrato, G.; Ferroni, L. Surface Characterization of Yttria-stabilized Tetragonal ZrO_2 Part 1. Structural, Morphological, and Surface Hydration Features. Materials Chemistry and Physics. 1994; 37: 243–257.

[67] Wernet, J.; Feke, D.L. Effects of Solids Loading and Dispersion Schedule on the State of Aqueous Alumina/Zirconia Dispersions. Journal of the American Ceramic Society. 1994; 77: 2693–2698.

[68] Kim, S.K.; Yoo H.J. Formation of Bilayer Ni–SiC Composite Coatings by Electrodeposition. Surface and Coatings Technology. 1998; 108–109: 564–569.

[69] Bund, A.; Thiemig D. Influence of Bath Composition and pH on the Electrocodeposition of Alumina Nanoparticles and Nickel. Surface and Coatings Technology. 2007; 201: 7092–7099.

[70] Low, C.T.J.; Willis, R.G.A.; Walsh, F.C. Electrodeposition of Composite Coatings Containing Nanoparticles in a Metal Deposit. Surface and Coatings Technology., 2006; 201: 371–383.

[71] Verelst, M.; Bonino, J.P.; Rousset, A. Electroforming of Metal Matrix Composite: Dispersoid Grain Size Dependence of Thermostructural and Mechanical Properties. Materials Science and Engineering A. 1991; 135: 51–57.

[72] Abed, F.A. Deposition of Ni–CO/TiO_2 Nanocomposite Coating by Electroplating. International Journal of Advanced research. 2015; 3: 241–246.

[73] Hamal, K..; Gyawali, G..; Rajbhandari (Nyachhyon), A.; Lee, S.W. Effect of Bath Temperature on Electrochemical Codeposition of Nickel Silicon Carbide Composite. International Journal of Chemistry and Pharmaceutical Sciences. 2014; 2: 777–782.

[74] Wang, S.C.; Wei, W.C.J. Kinetics of Electroplating Process of Nano-sized Ceramic Particle/Ni Composite. Materials Chemistry and Physics. 2003; 78: 574–580.

[75] So-Yeon, P.; Myung-Won, J.; Jae-Ho, L. Nano Oxide-Dispersed Nickel Composite Plating. Electronic Materials Letters. 2013; 9: 801–804.

[76] Vaezi, M.R.; Sadrnezhaad, S.K.; Nikzad, L. Electrodeposition of Ni–SiC Nano-composite Coatings and Evaluation of Wear and Corrosion Resistance and Electroplating Characteristics. Colloids and Surfaces A: Physicochemical and Engineering Aspects. 2008; 315: 176–182.

[77] Baghery, P.; Farzam, M.; Mousavi, A.B.; Hosseini, M. Ni–TiO_2 Nanocomposite Coating with High Resistance to Corrosion and Wear. Surface and Coatings Technology. 2010; 204: 3804–3810.

[78] Sen, R. Synthesis and Characterization of Pulse Electrodeposited Ni–CeO_2 Nanocomposite Coatings. PhD Thesis. IIT Kharagpur; 2011.

[79] Stroumbouli, M.; Gyftou, P.; Pavlatou, E.A.; Spyrellis, N. Codeposition of Ultrafine WC Particles in Ni Matrix Composite Electrocoatings. Surface and Coatings Technology. 2005; 195: 325–332.

[80] Singh, D.K.; Singh, V.B. Electrodeposition and Characterization of Ni–TiC Composite Using *N*-Methylformamide Bath. Materials Science and Engineering A. 2012; 532: 493–499.

[81] Ramesh Bapu, G.N.K.; Jayakrishnan, S. Development and Characterization of Electro Deposited Nickel–Titanium Carbo Nitride (TiCN) Metal Matrix Nanocomposite Deposits. Surface and Coatings Technology. 2012; 206: 2330–2336.

[82] Shrestha, N.K.; Takebe, T.; Saji, T. Effect of particle size on the co-deposition of diamond with nickel in presence of a redox-active surfactant and mechanical property of the coatings. Diamond and Related Materials. 2006; 15:1570–1575.

[83] Bakhit, B; Akbari, A. Effect of Particle Size and Co-deposition Technique on Hardness and Corrosion Properties of Ni–Co/SiC Composite Coatings. Surface and Coatings Technology. 2012; 206: 4964–4975.

[84] Gores, H. J.; Barthel, J. M. G. Nonaqueous Electrolyte Solutions: New Materials for Devices and Processes Based on Recent Applied Research. Pure and Applied Chemistry. 1995; 67: 919–930.

[85] Shrestha, N.K.; Saji, T. Non-aqueous Composite Plating of Ni-ceramic Particles Using Ethanol Bath and Anti-wear Performance of the Coatings. Surface and Coatings Technology. 186 (2004) 444.

[86] Pompei, E.; Magagnina, L.; Lecis, N.; Cavallotti, P.L. Electrodeposition of Nickel–BN Composite Coatings. Electrochimica Acta. 2009; 54: 2571–2574.

[87] Ewa, R.; Lidia, B.; Łukasz, D.; Maciej, M. Electrodeposition of Nickel/SiC Composites in the Presence of Cetyltrimethylammonium Bromide. Applied Surface Science. 2010; 256: 7414–7420.

[88] Shrestha, N.K.; Kobayashi, G.; Saji, T. Electrodeposition of Hydrophobic Nickel Composite Containing Surface-Modified SiO2 Particles under the Influence of a Surfactant with an Azobenzene Moiety. Chemistry Letters. 2004; 33(8): 984–985.

[89] Jung, A.; Natter, H.; Hempelmann, R.; Lach E. Nanocrystalline Alumina Dispersed in Nanocrystalline Nickel: Enhanced Mechanical Properties. Journal of Materials Science. 2009; 44: 2725–2735.

[90] Bicelli, L.P.; Bozzini, B.; Mele, C.; D'Urzo, L. A Review of Nanostructural Aspects of Metal Electrodeposition. International Journal of Electrochemical Science. 2008; 3: 356–408.

[91] Gyftou, P.; Pavlatou, E.A. & Spyrellis N. Effect of Pulse Electrodeposition Parameters on the Properties of Ni/nano–SiC Composites. Applied Surface Science 2008; 254: 5910–5916.

[92] Chandrasekar, M.S.; Pushpavanam, M. Pulse and Pulse Reverse Plating—Conceptual, Advantages and Applications. Electrochimica Acta. 2008; 53: 3313–3322.

[93] Fustes, J.; Gomes, A.; da Silva Pereira, M.I. Electrodeposition of Zn–TiO_2 Nanocomposite Films—Effect of Bath Composition. Journal of Solid State Electrochemistry. 2008; 12: 1435–1443.

[94] Chang, S.Y.; Chen, C.F.; Lin, S.J.; Kattamis, T.Z. Electrical Resistivity of Metal Matrix Composites. Acta Materialia. 2003; 51: 6191–6302.

[95] Weber, L.; Dorn, J.; Mortensen, A. On the Electrical Conductivity of Metal Matrix Composites Containing High Volume Fractions of Non-Conducting Inclusions. Acta Materialia. 2003; 51: 3199–3211.

[96] Nai, S.M.L.; Wei, J.; Gupta, M. Effect of Carbon Nanotubes on the Shear Strength and Electrical Resistivity of a Lead-Free Solder. Journal of Electronic Materials. 2008; 37(4): 515–522.

[97] Sharma, A.; Bhattacharya, S.;, Das, S.; Fecht, H.-J.; Das, K. Development of Lead Free Pulse Electrodeposited Tin Based Composite Solder Coating Reinforced with *Ex Situ* cerium Oxide Nanoparticles. Journal of Alloys and Compounds. 2013; 574: 609–616.

[98] Babaghorbani, P.; Nai, S.M.L.; Gupta, M. Reinforcements at Nanometer Length Scale and the Electrical Resistivity of Lead-Free Solders. Journal of Alloys and Compounds. 2009; 478: 458–461.

[99] Sharma, A.; Xu, D.E.; Chow,.; Mayer, M.; Sohn, H.-R.; Jung, J.P. Electromigration of Composite Sn–Ag–Cu Solder Bumps. Electronic Materials Letters. In press, DOI: 10.1007/s13391-015-4454-x.

[100] Kumar, K.M.; Kripesh, V.; Tay, A.A.O. Influence of Single-Wall Carbon Nanotube Addition on the Microstructural and Tensile Properties of Sn–Pb Solder Alloy. Journal of Alloys and Compounds. 2008; 455: 148–158.

[101] Nai, S.M.L.; Wei, J.; Gupta, M. Improving the Performance of Lead-Free Solder Reinforced With Multi-Walled Carbon Nanotubes. Materials Science and Engineering A. 2006; 423: 166–169.

[102] Lee, H.Y.; Sharma, A.; Kee, S.H.; Lee, Y.W.;, Moon, J.T.; Jung, J.P. Effect of Aluminium Additions on Wettability and Intermetallic Compound (IMC) Growth of Lead Free Sn (2 wt. % Ag, 5 wt. % Bi) Soldered Joints. Electronic Materials Letters. 2014; 10:997–1004.

[103] Baumann, W.; Degner, W.; Fiedler, J.; Horn, J.; Richter, G.; Weissmantel, C. A Study of Frictional, Wear and Contact Resistance Performance of Tin Alloy Coatings. Thin Solid Films. 1983; 105: 305–318.

[104] Wu, J.; Pecht, M. Fretting Corrosion Studies for Lead Free Alloy Plated Contacts. Electronics Packaging Technology Conference. 2002; pp. 20–24.

[105] Sankara Narayanan, T.S.N.; Park, Y.W.; Lee, K.Y. Fretting-Corrosion Mapping of Tin-Plated Copper Alloy Contacts. Wear. 2007; 262: 228–233.

[106] Hammam, T. The Impact of Sliding Motion and Current Load on the Deterioration of Tin-Coated Connectors. Proceedings of the Fourty Fifth IEEE Holm conference on Electrical contacts. 1999; pp. 203–212.

[107] Jun, Z.; Jincheng, X.; Wei, H.; Long, X.; Xiaoyan, D.; Sen, W.; Peng, T.; Xiaoming, M.; Jing, Y.; Chao, J.; Lei, L. Wear Performance of the Lead Free Tin Bronze Matrix Composite Reinforced by Short Carbon Fibers. Applied Surface Science. 2009; 255: 6647–6651.

[108] Song, F.; Lee, S.W.R. Corrosion of Sn–Ag–Cu Lead-free Solders and the Corresponding Effects on Board Level Solder Joint Reliability. Proceedings of 56th Electronic Components and Technology Conference. 2006; pp. 891–898.

[109] Rosalbino, F.; Angelini, E.; Zanicchi, G.; Carlini, R.; Marazza, R. Electrochemical Corrosion Study of Sn–3Ag–3Cu Solder Alloy in NaCl Solution. Electrochimica Acta. 2009; 54: 7231–7235.

[110] Mohanty, U.S.; Lin, K.L. Electrochemical Corrosion Study of Sn–XAg–0.5Cu Alloys in 3.5% NaCl Solution. Journal of Materials Research. 2007; 22: 2573–2581.

[111] Wu, B.Y.; Chan, Y.C.; Alam, M.O.; Jillek, W. Electrochemical Corrosion Study of Pb-Free Solders. Journal of Materials Research. 2006; 21: 62–70.

[112] Li, D.; Conway, P.P.; Liu, C. Corrosion Characterization of Tin–Lead and Lead Free Solders in 3.5 wt.% NaCl Solution. Corrosion Science. 2008; 50: 995–1004.

[113] Sharma, A.; Das, S.; Das, K. Electrochemical corrosion behavior of CeO_2 nanoparticle reinforced Sn–Ag based lead free nanocomposite solders in 3.5 wt.% NaCl bath. Surface and Coatings Technology. 2015; 261:235–243.

Edited by Adel M. A. Mohamed and Teresa D. Golden

Nanocomposite coatings have various properties that can be utilized for corrosion protection and tribological improvements. Synthesis of the nanocomposite coatings using an electrodeposition method allows unique control of the experimental parameters. By fine tuning the experimental parameters, various compositions and properties can be obtained for the nanocomposite coatings. This book covers some of the electrochemical methods used for nanocomposite coating deposition as well as discusses in detail examples of several nanocomposite coating. The corrosion and tribological performance of the nanocomposite coatings are also covered and some nanocomposite coatings are discussed for specific technological areas, such as fuel cells and microelectronics.

ISBN 978-953-51-4205-8

Photo by tiero / DollarPhoto

IntechOpen